



TOGETHER
for a sustainable future

OCCASION

This publication has been made available to the public on the occasion of the 50th anniversary of the United Nations Industrial Development Organisation.



TOGETHER
for a sustainable future

DISCLAIMER

This document has been produced without formal United Nations editing. The designations employed and the presentation of the material in this document do not imply the expression of any opinion whatsoever on the part of the Secretariat of the United Nations Industrial Development Organization (UNIDO) concerning the legal status of any country, territory, city or area or of its authorities, or concerning the delimitation of its frontiers or boundaries, or its economic system or degree of development. Designations such as “developed”, “industrialized” and “developing” are intended for statistical convenience and do not necessarily express a judgment about the stage reached by a particular country or area in the development process. Mention of firm names or commercial products does not constitute an endorsement by UNIDO.

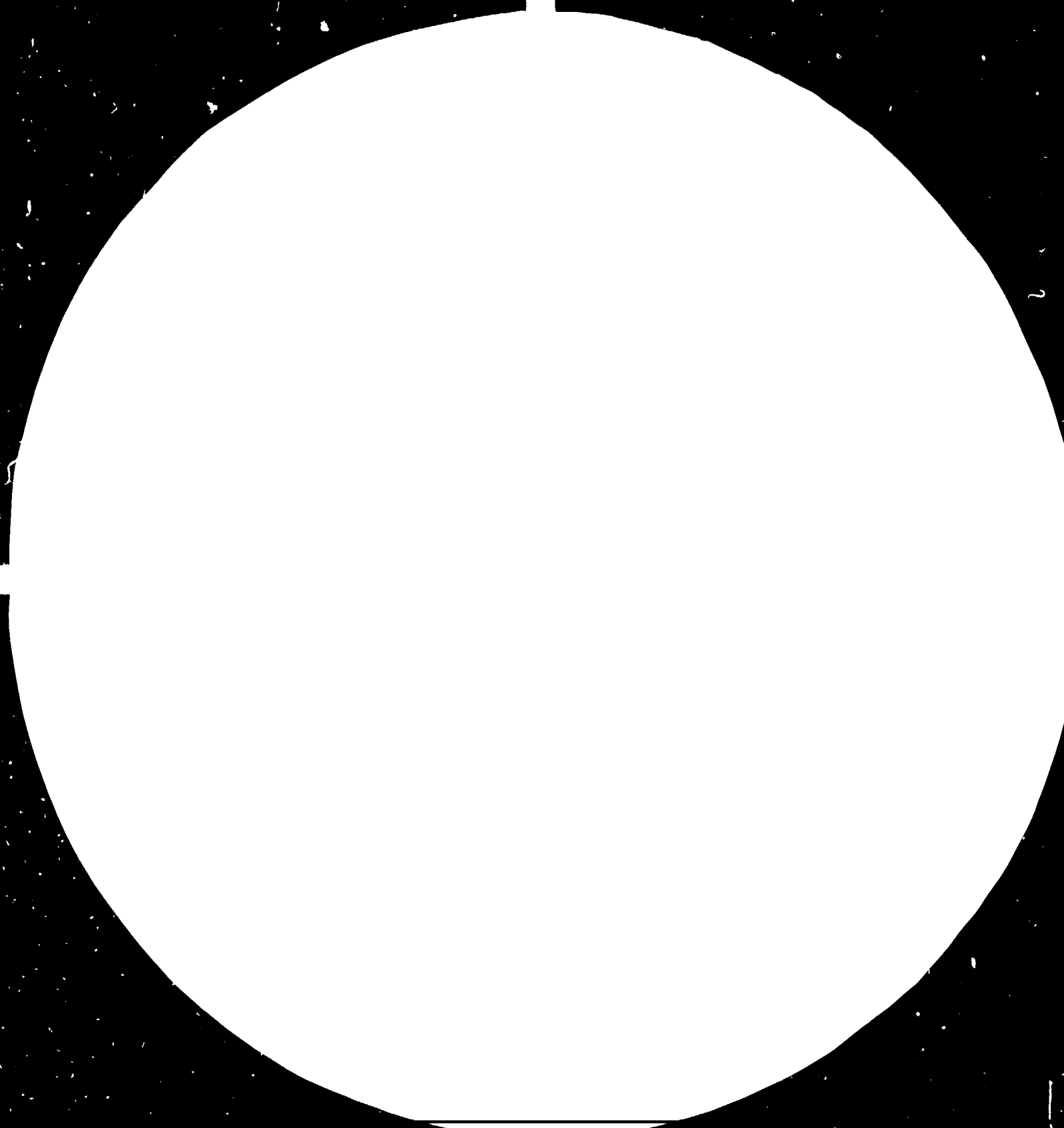
FAIR USE POLICY

Any part of this publication may be quoted and referenced for educational and research purposes without additional permission from UNIDO. However, those who make use of quoting and referencing this publication are requested to follow the Fair Use Policy of giving due credit to UNIDO.

CONTACT

Please contact publications@unido.org for further information concerning UNIDO publications.

For more information about UNIDO, please visit us at www.unido.org





1.0 25

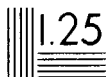
1.25 22

1.5 20



1.1 20

1.1 18



Resolution test charts are available in a variety of sizes and quantities.

For more information, contact your nearest Nikon representative or write to:

Nikon Resolution Test Charts, P.O. Box 1000, Princeton, NJ 08542

or call (609) 981-2000, ext. 2000. A charge card is also available.

© 1987 Nikon Corporation. All rights reserved. Nikon is a registered trademark.

DISTR. RESTRICTED

UNIDO/IG

ENGLISH

NOVEMBER 1984

India

→ Pembleton

APPLICATION OF ALTERNATIVE FUELS FOR
INTERNAL COMBUSTION ENGINES, IIP, DEHRA DUN.

DP/IND/82/001

INDIA

14245

TECHNICAL REPORT *

Prepared for the Government of India,
by the United Nations Industrial Development Organization,
acting as Executing Agency for the United Nations Development Programme

✓
Based on the work of Anton Cernei
Expert in fuel introduction in internal combustion engines
under the post 11-02

FROM
DI Ms. Neumann
Room No. / No de bureau | Extension/Poste / Date
01170 | 1582

UNITED NATIONS INDUSTRIAL DEVELOPMENT ORGANIZATION

* This document has been reproduced without formal editing.

TOPICS REQUIRED

1. Proposals concerning methyl fuel use in vehicular 4-stroke engines. Power outputs range 75 + 110 kW NA-DI version only. Piston dia's range $\varnothing 95 + 105$ mm with open bowls:
 - ω typ
 - cylindrical DB bowl typThe most interesting aspects:
 - ignition
 - performances
 - outputs
2. Dual fuel operations with mixed $D2-CH_3OH$ composition. Here the mixing procedure is required as well as proposals for approach.
3. HP injection related to methyl-fuel diesel engine operation. The benefits and potential improvements using DB-IHM-KHD-TAM new results.
4. Piston engine mechanics and balance. Approach to calculations.
5. Approach to piston bowl design for DI-diesel engine taking into account: injection performances swirl, squish as well as geometrical relations.
6. Needle lift measurements and practical approach to fuel injection calculations.
7. Experimental approach to fuel atomization in bench test experiments. Screening effects and differences between Sauter mean droplet dia's defined by calculation and by practical bench test experiments.
8. Comment and proposal pertinent IIR (7 Pages) Report worked out by D.Kumar and F.P.Purdin.

9. NOx, THC-THCC measurements.

Topics point 2 and Point 5 were as more urgent selected by IIP for the beginning of the common work.

Topic 2

Up to 30 % neat CH_3OH may be added to diesel oil without addition of a combustion improver (Hexanolnitrat, Amylnitrat). However, because of water presented, starting, warm-up period, idling, long term low-load operation in city-drive application, stops intervals and transients the above cited percentage may be reduced on 20 %. Thus for vehicular engines, combining other fuel saving techniques with 20 ÷ 25 % methyl fuel doping, 20 ÷ 25 % diesel oil in-field consumption rate may be reduced.

Practically for vehicular application, without: glow plug assistance combined with ceramic comb. chamber isolation (ATI) or spark ignition assistance, only 20 ÷ 25 % of methyl fuel may be considered as a max. amount, which may be mixed with D2 without ignition improver. Glow plug-ceramic isolation - and spark plug techniques will be discuss in TOPIC 1. Here, dual fuel injection technique was omitted because of a high first cost. MWM pressure distributor technique will be once again touched in TOPIC 1 (See the first report, Černej A., 1983.). One new approach with glow plug ignition and methyl fuel doping control in dependence of the HP pump control rod position will be shortly explained in TOPIC 1, as well.

According to the forementioned in the TOPIC 2, the attention will be paid to dual mixing technique only. Thus, up to 25 % by volume methyl fuel mixed with diesel oil is considered.

1. The system for supplying methyl fuel/gasoil

Fig.1 shows a diagrammatic sketch of fuel mixing system proposed.

Potential problems:

- 1.1 - relatively modest decrease of diesel oil consumption
- 1.2 - first cost increase
- 1.3 - because of methyl fuel tank, dead box increase and two different fuel to tank in.
- 1.4 - unknown reaction of specified engine (CI, swirl, bowl ..)
- 1.5 - unknown methyl fuel water content
- 1.6 - vapour formation (cavities) in fuel pump (pump gallery) and in low pressure system may produce injection irregularities
- 1.7 - starting (see pos.5+6 or/and JX) and warm-up periods
- 1.8 - service life of HP pump
- 1.9 - fuelling increase for the power output given
- 1.10 - turbo-charged version is omitted
- 1.11 - THC and THCO exhaust emission increase
- 1.12 - Vapour lock between fuel tank and LPP (Fig.1)

Because of very short time on desposal only, it's the best way to start with the problem denoted under 1.4.

Problem 1.4 - unknown reaction of specified engine (related to points 1.2, 1.5, 1.6, 1.7, 1.9, 1.11 also)

For the engine selected, when burning methyl fuel - diesel oil blends, its reactions have to be investigated at first. It is not because of obtaining ideas about the best blending rations only. Moreover, in order to decrease the lab- and the engine first cost (what must be changed ?) as well as to save the research time, preliminary organized engine test bench experiments may not be omitted.

For the sake of forementioned we need:

- a - simple prepared fuel blends
- b - on test bench experimental programme
- c - selected instrumentation on desposal
- d - evaluation criterions

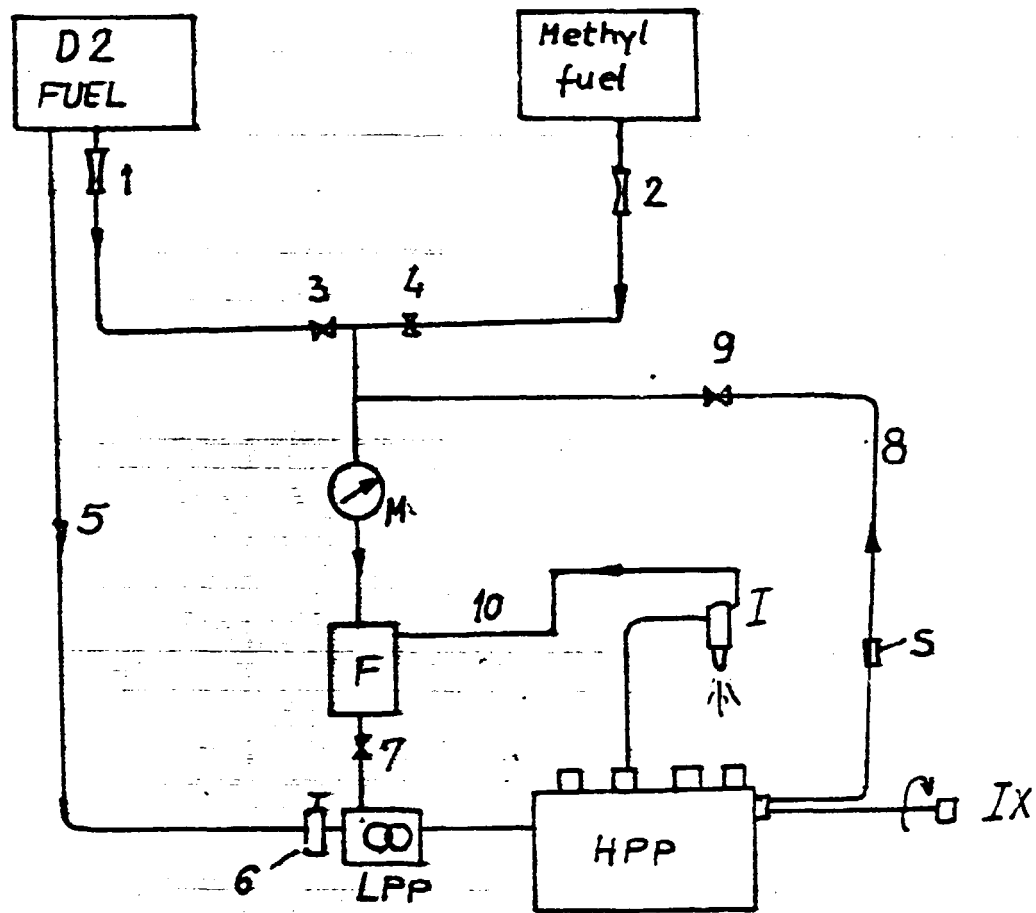


Fig.I Diagrammatic sketch of dual fuel mixing and injection system

- 1,2 - flow control
- 3,4,7,9 - single direction flow valve
- 5 - D2 fuel supply line for starting (alternatively)
- 6 - existed small hand pump
- 8 - mixing line
- 10 - injector leakage overflow line
- M - pressure gauge (during experiments needed only)
- S - sample checking (during experiments needed only)
- F - fuel filter
- LPP - existed low pressure pump
- HPP - high pressure injection pump
- I - injector
- IX - mixer (alternative for Pos.5)

Point 1.4-a. Provisional blends preparation

In a simple fuel container (see Fig.2) selected components to be blended, have to be tanked. The amounts of the single "fuels" mixed is recommended as follows:

	CH ₃ OH % by vol	DIESEL OIL % by vol.	WATER % by vol
Group A	20	75	5
	20	70	10
	20	65	15
Group B	30	65	5
	30	60	10
	30	55	15

Unfortunately, it is very well established fact that CH₃OH will not go into solution with diesel fuel, especially not in the presence of water. However, an on-board emulsifier can produce unstabilized methyl fuel - diesel oil blend (Fig.2).

Emulsifier (Pos.2, Fig.2) use normally chemists in their lab's and it may be borrowed for short time. The fuel in the tank (Pos.4, Fig.2) must be kept at reasonable temperature, what can be done with water cooling flow (Pos.1, Fig.2). Just a narrow plastic tube (Pos.5, Fig.2) serves as a vent pipe stretching out of the lab. To prevent (vapour) cavities the distance between low pressure pump (Pos.9, Fig 2) if existed, and fuel tank (Pos.4) has to be short.

Fuel temperature in the pump sump can be high as 65 °C and because of known phenomenon during spilling and fuel flowing into the barrel (Fig.3), the pressure fluctuations may produce cavities, thus injection irregularities and the measurements in error. For the information Fig 4 shows CH₃OH vapour saturation pressure vs. temperature as well as for gasoline. Only to mention, Fig 4 demonstrate also clearly, the cold start problem when convert to methyl fuel.

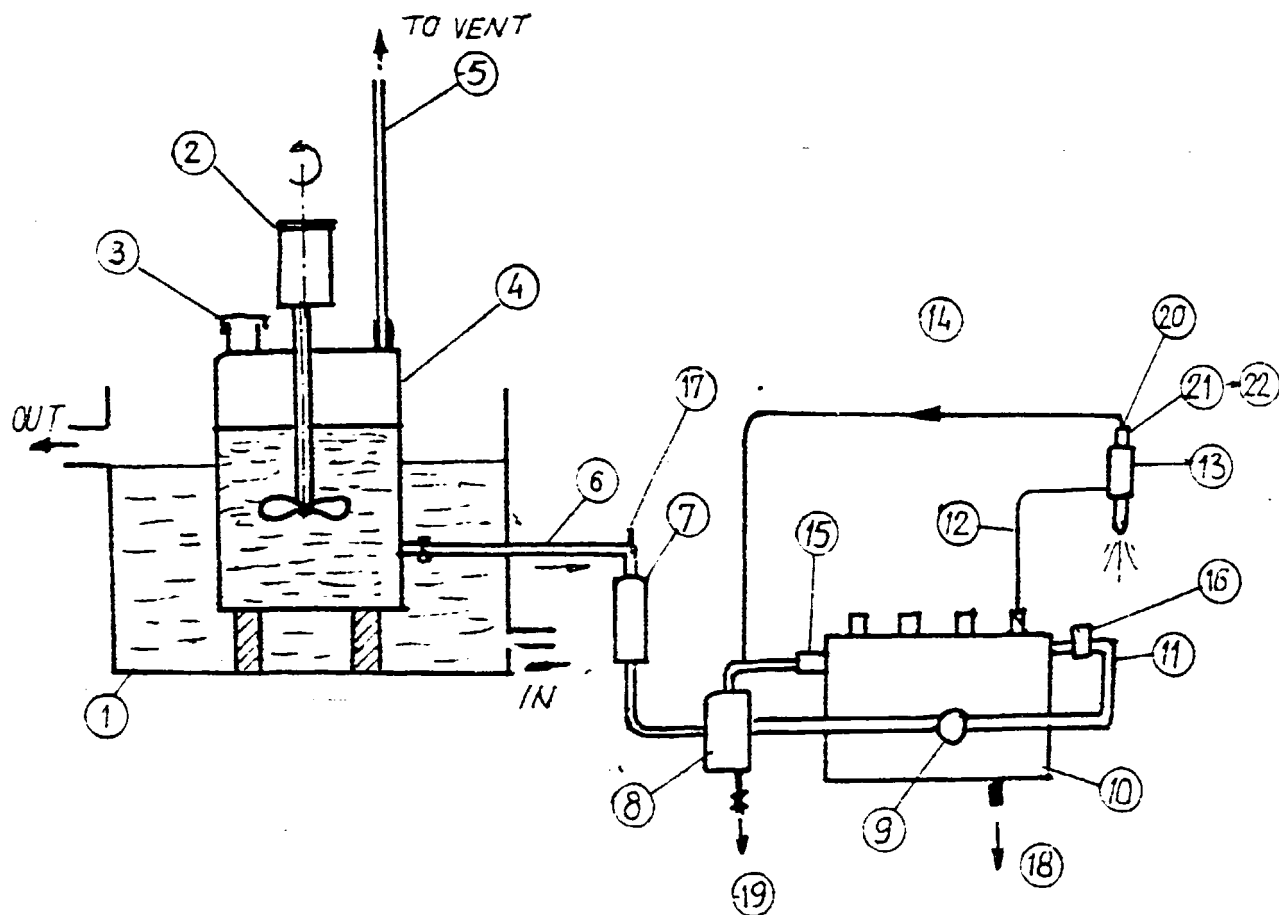


Fig 2 Diagrammatic sketch of
on-board emulsifier

- | | |
|--|---|
| 1 - water tank | 14 - overflow leakage tube |
| 2 - emulsifier | 15 - pressure control valve |
| 3 - sealling cap | 16 - pressure gauge |
| 4 - fuel tank | 17 - thermometer |
| 5 - plastic tube $\varnothing 8$ | 18 - oil sample |
| 6 - tube | 19 - fuel sample |
| 7 - fuel consumption
measur. device | 20 - inductive needle lift
measurement |
| 8 - fuel filter | 21 - induct. bridge |
| 9 - low pressure pump | 22 - registration |
| 10 - high pressure pump | |
| 11 - tube | |
| 12 - HP tube | |
| 13 - injector | |

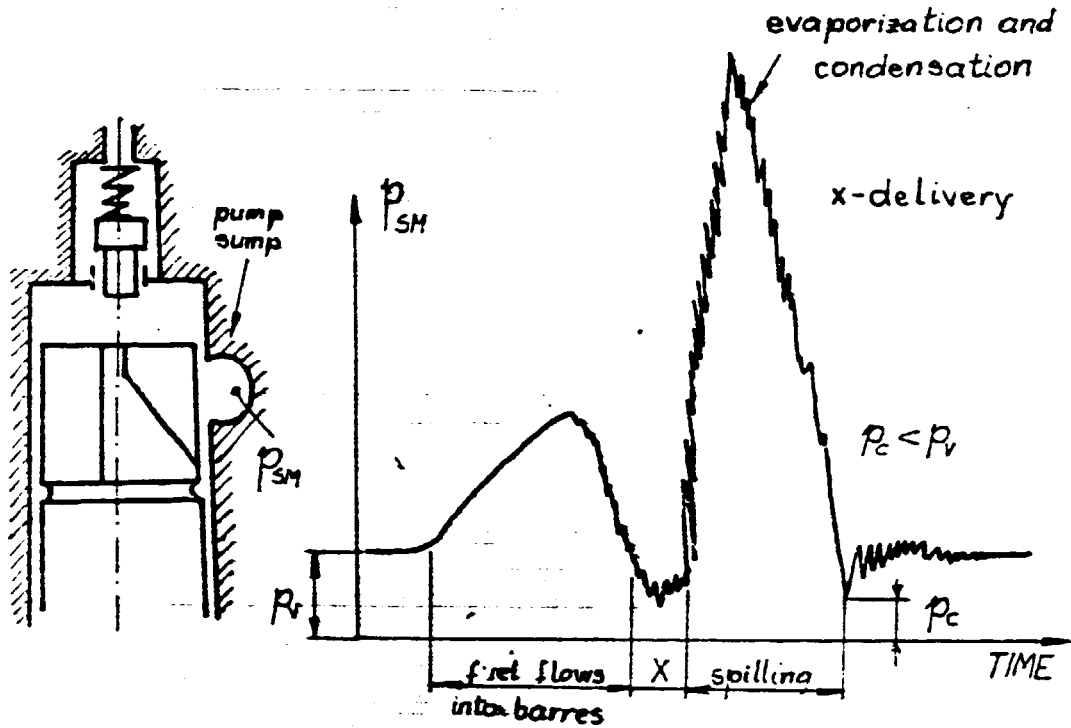


Fig 3 Effect of spilling and filling on cavities formations in the sump, vs. time

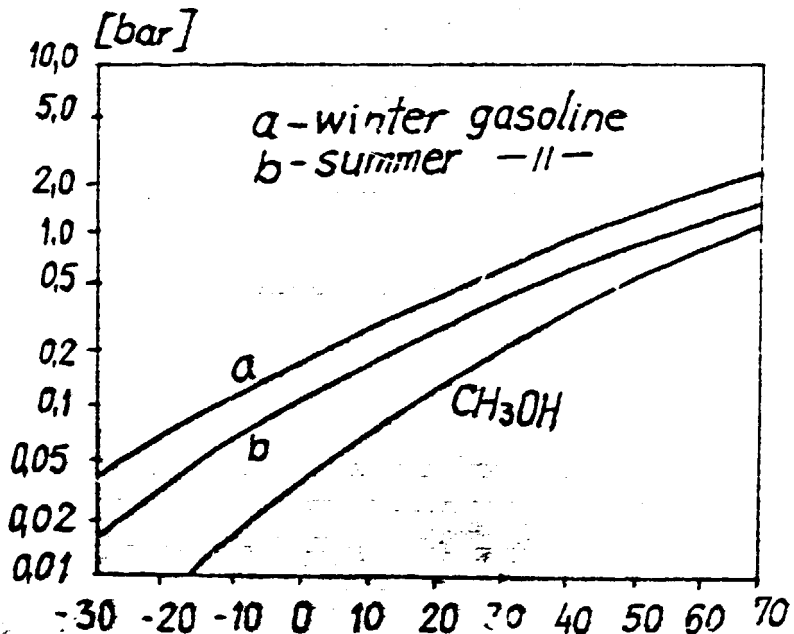


Fig 4 Vapour saturation pressure vs. temperature

Fig 4 explains very clearly, that the valve (Pos.15, Fig 2) may not be omitted, but its opening pressure has to be adjusted at $p_v=0,15 - 0,7$ bar above the ambient one. On the contrary, if the low pressure pump does not exist the supply pressure valve (Pos.15) could not be installed and provisional measure must be undertaken to cool the sump body from outside or to press fuel air. In the later case is the best way to compress the fuel tank (Pos.4, Fig2) taking into account the fuel measurement device.

To the HP pump (Pos.10, Fig 2) and to the injector (Pos.13) special attention must be paid. At first to be sure, that fuel mixture tested corresponds exactly to the wanted one, therefore the fuel sample checking (Pos.19). To have idea about leakage (in order to avoid expensive redesign) sample (Point 18, Fig 2) is very useful. Fuel consumption measuring device (Pos.2) must be of high accuracy with error of repeatability less than 1 % (under all testing conditions).

The HP pump and injector itself, must have surplus of capacity in order to ensure a reasonable duration of injection and satisfied fuel atomization for the all fuel mixture tested. The later can be done by readjustings or, if need, by changing the components of injection equipment.

With the first fuel chosen the injection parameters have to be investigated but with the fuelling changed. It can be done on the engine in operation under next conditions:

- needle lift registered
- TDC marking
- pressure before injector
- accurate measur. of fuel consumption rate
- pump rod position measur. for loads and rotational speeds given.

The later way is recommended. Namely, the afore dted measurements accomplished with in-cylinder pressure diagrammes can enable the later unavoidable analysis on the whole. Besides that, we have the possibility to avoid the missmeasurements, for example: afterinjection, if happend, we change retracting delivery valve at once.

It is also very useful some precalculations, to obtain the idea about the fuelling and other injection parameters.

For precalculations approach we need:

- supposing the same engine efficiency we calculate the fuelling for our mixtures chosen. Here, for outputs given D2 fuel consumption rate must be known
- D2 calorific value must be known, per example in the Europe D2-G. ranges 42750 - 42500 kJ/kg.
- neat methanol has lower CV than D2

	kJ/kg	kJ/m ³	<u>kg air stoichiometric</u> <u>kg fuel</u>
CH ₃ OH	19600	15490	6,46
D2	42600	35600	14,3

If we are going to add 15 % water to methanol we decrease the calorific value. Per example, adding 15 % water to CH₃OH we have:

	kJ/kg	kJ/m ³
CH ₃ OH + 15% H ₂ O (methyl fuel)	16510	13640

(It is assumed in Germany that the water content in methyl fuel in dependence of the production, may reach (till) 15 % by volume).

Thus we can now calculate the fuelling for every mixture given.

- Using short programmes for fuel injection calculations (Programme I and II given IIP) we may traced the potential errors in before hand.

Point 1.4 - b. On test bench experiments programme

It may be suggested the bellow programme presented:

Starting

Calorific value per volume of diesel oil is 2,2 times per volume higher than the value of CH_3OH . Relative to diesel fuel one liter of neat methanol requires 4,4 times more heat of vaporisation. Since the large fuel flow and high vaporization heat figures, methanol needs 9,8 times more heat than diesel fuel to evaporate. Besides that in the presence of water ignition temperature increases onward. Thus, neat methanol (latest data) approaches Cet.No 3 but adding water 10% by vol. to CH_3OH Cet.No ranges about 1,5 ÷ 2. Ignition temperature increases with water content increased:

CH_3OH	ignition temperature (stoichiometric)	478 °C
$\text{CH}_3\text{OH} + 5\%$ water by vol.	"	480 °C
$\text{CH}_3\text{OH} + 10\%$ water by volume	"	485 °C
$\text{CH}_3\text{OH} + 20\%$ water by volume	"	490 °C
$\text{CH}_3\text{OH} + 30\%$ water by volume	"	510 °C

All above mentioned effects drastically the starting process in CR engine. One of the important goal, dealing with CH_3OH , in ERD noted:

increase of self ignition property.

Thus in our experiments we may not neglected this fact. It means we have to compare the ignition quality for the specific engine, when fuelled with D2 and with our mixture selected.

One of the approaches to study starting is more time consuming but enables very deep insight into the whole process. Moreover for the friction analysis such approach may not be omitted (not our subject). For IIP as a scientific institute is to be recommended (perhaps for the next future). Forementioned is the reason to show the whole procedure shortly.

To study starting. Approach 1.

Instantaneous effective torque may be written as follows:

$$M_e = M' - (M'' - M''' - M''')$$

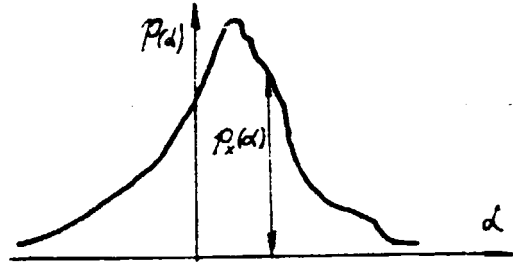
where:

m_l' - instantaneous gas pressure torque

$$m_l' = \frac{\pi \cdot D^2}{4} \cdot p_x(\alpha) \cdot \dot{x}$$

$$\dot{x} = r \cdot \omega \cdot \left[\sin \alpha + \frac{\lambda}{2} \sin 2\alpha \right]$$

$$\lambda = \frac{r}{L}$$



ω - instantaneous angular velocity

During start period engine is disconnected, it means $m_e = 0$

$m'' \approx 0$ instant. potential energy torque

Thus:

$$m''' = m_l' - m'' \quad \text{inst. frictional torque}$$

$$m'' = \frac{1}{2} \omega^2 \bar{R}' \sin 2\alpha + \dot{\omega} \left[\bar{R} + \frac{1}{2} \bar{R}' (1 - \cos 2\alpha) \right]$$

$$\bar{R} = k^2 m + r^2 \left(1 - \frac{s'}{L} \right) \cdot m' \quad ; \quad \bar{R}' = r^2 \cdot \left(\frac{s'}{L} \cdot m' + m'' \right)$$

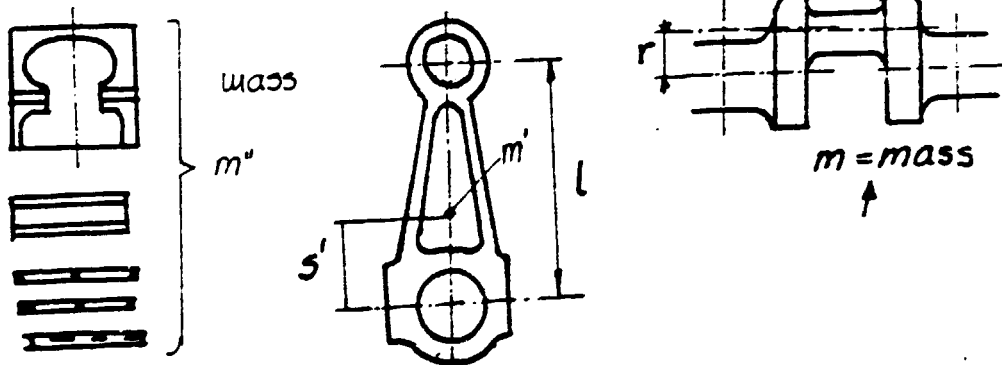


Fig 5 Notation

Storing $p_x(\alpha)$, ω and $\dot{\omega}$ for every cycle during starting we may:

- follow the ignition stability
- follow firing fouling
- to adjust properly advancing

- follow effect of switch-on diesel fuel starting
- calculate the frictional instant. losses

(For much more information see TOPIC 4).

To study starting. Approach 2.

Comparable starting period measurements with D2 fuel and mixture selected under the same ambient - and adjusting conditions. When reached rated speed the start period is accomplished. The best way for such measurements is the pen recorder trace registration of engine rotational speeds.

However, for different fuels may not be avoided:

- the advance readjusting
- start fuelling change

to find out the shortest start period. In the case of too high $dp_x(\alpha)/d\alpha$ or/and p_{max} in-cylinder the selected advance of injection may be kept during starting and warm-up periods only. The solution for changing the beginning of injection in engine operation may not be difficult. However, the first price increases.

To study warm-up period

During warm-up period may be recommended:

- to observe in-cylinder pressure diagrams to follow p_{max} or irregularities
- to measure THC exhaust emission (when possible equivalent C_3H_8 diluted by air during calibration). Here to be mentioned: dealing with CH_3OH in warming-up period the next correction is valid:
every C-atom in THCO produces error in reading by factor $2/3$

Again comparable measurements are needed.

The best way is to find out, by means of startings and warming-up periods, the max possible CH_3OH content or/and to analyse for potential improvements. For example: swirl ratio decrease may help to improve starting, change in nozzle orifices distribution or/and dia's may control the rate of evaporation and with this, the rate of temperature decrease before ignition,

here is no doubt that the compression ratio (CR) increase may help to greater extent for better startings. Moreover, with CR increase we only compensate the "lost" because of CH_3OH doped. CR = 16 may not be applied with CH_3OH content of 30 % by volume. Probably CR=18 - 19 with swirl decreased is more promising way for higher CH_3OH + water contents and engine may benefit from high compression, assuming reasonable max in-cylinder pressures. (Before ignition neat methanol/air stoichiometric mixture drops in-cylinder temperature for 122 °C. It means that we have to increase CR up to 25 which produces a high in-cylinder pressure).

Max. in-cylinder pressure may be diminished by prolonged injection and with this decreases the temperature drop of combust. mixture as well.

Combining:

- increases CR
- decreased SR (swirl ratio)
- prolonged injection period

we may increase methyl fuel content without first cost increase.

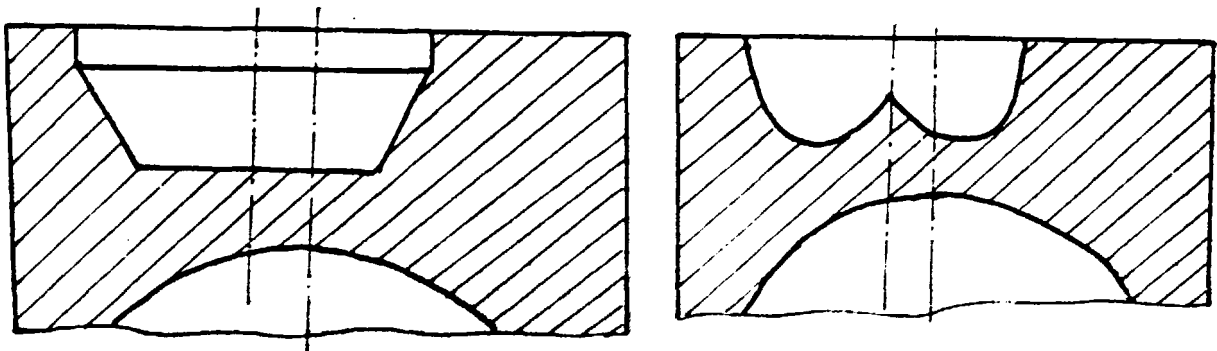
Starting and warm-up period are turning points for ahead investigations. However, in the case of low possible content of methyl fuel because of starting (warm-up satisfactory), some other means are also on desposal, per example, diesel oil start, but it complicate the operation via switching-on technique.

To study engine performancies

Programme related performancies is stringent dependent on engine application. Thus, the same programme could not be applied for vehicular engine and for engine coupled with water pump.

IIP intends to apply CH_3OH + water + D2 mixture on the next two vehicular engines:

Make	A	B
Combustion chamber	open	open
Bore x stroke [mm]	Ø92x120	Ø105,58x120,65
Swept volume [dm ³]	4,78	6,075
In row	6 cyl.	6 cyl.
Compression ratio	1 : 17	1 : 16
Rated power [kW]	82,35	80,88
Typ	NA	NA
Rated speed [rpm]	2800	2400
Mean eff. pressure at rated power [bar]	7,58	6,66
Minimum fuel consumption rate [g/kWh]	<u>265</u>	<u>279</u>
Minimum fuel consumption rate at [rpm]	<u>2400</u>	<u>2400</u>
Fuel consumption rate (calculated) [g/kWh]	<u>283</u>	<u>298</u>
Lowest loading (calculated) [rpm]	<u>1400</u>	<u>1200</u>



Comb. chamber A
(old version Daimler-benz)

Comb. chamber B
(old version Lyland)

Fig 6

Injection pump MICO
(BOSCH - Typ A)
Injector 4 holes MICO
(BOSCH DLLA 150S 187)

Injector 4 holes

Looking at the data collected it could not be avoided to mention, engines selected are remained behind in development. Moreover, the fuel consumption figures look very disappointing. It seems to be reasonable at first to reduce the fuel consumption rate in diesel oil operation. For example:

engine A has 4 piston rings

engine B has even 5 piston rings

Piston may be also changed related to its height. Applying 3 piston rings, reducing the piston height and changing the skirt ovality, the both, first cost and fuel consumption rate may be decreased. It is especially truth at higher piston velocities (than 9 m/s), having in mind that 75% of the neat friction losses is related to piston group.

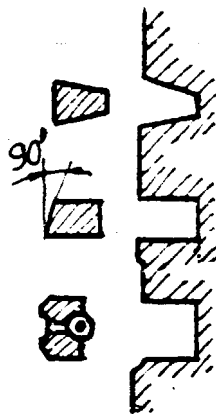


Fig 7

Fig 7 shows the ring set which may be recommended.

Here is only one very small subject touched but certainly must be more than one. Just comparing with other up-to-date engines may be concluded that fuel consumption rate is to be reduced up to 15 %, turbocharging and speed decrease out of consideration.

However,

- rotational speed decrease with piston stroke increased
- turbo-charging
- swirl and squish decrease with injection pressure increase and less dependent of rotational speed

are characteristics of the modern vehicular engines. Moreover, dealing with vehicular engines, better matching to the vehicle demands may save still more fuel.

With above cited potential fuel reduction in mind, may not be exaggerated to put the question about the course of investigation. To save 10 ÷ 15 % D2 fuel with mixing technique with first cost increase or at first to reduce the high diesel oil consumption rate and to obtain more modern competitive engine?

In any case to obtain performances - for decision - the next programme may be proposed:

1. Full load characteristic
2. 75 % of full load characteristic
3. 50 % of full load
4. Idling stability

Besides standard data measured, THC and soot measurements have to be included.

Evaluation criterions. Point 1.4-d

The most important criterion is to estimate the benefit of the quantity of diesel oil saved via blending and compare it with:

- first cost increase
- complications with dual fuel system in practical service
- potential diesel oil using other techniques
- possibility and troubles related to methyl fuel tank location to existed vehicles
- reasonable fair engine characteristics matched to vehicle operation demands (startability, pollution, fuel consumption, transients, torque back up, stability, oil degradation and change interval of the oil, service life, reliability in operation).

For the information:

1. Investigations of DFG (IHM), BMVI (see AIF - No5074) showed that up to 10 - 30 % of CH₃OH (engine dependent) may be added to diesel oil, the larger quantity may produce starting, misfiring and knock problems. (See also MTZ 45, 1984).
2. Ricardo News "World wide Engine and Fuel Relationship" reported:

"Up to, say, 30% could be used by blending with diesel fuel or in a dual fuel engine where the alcohol was carbureted into the cylinder and the mixture was ignited by an injection of diesel fuel. Alternatively, ignition improvers additives, such as isopropyl nitrate may be used, but the quantities required, up to say 20 % make the process prohibitively expensive. The best solution would seem to be a multi-fuel

engine such as MAN EM which, on an energy basis, when operating on pure alcohol fuel, would give a thermal efficiency equivalent to that of an IDI diesel engine"

3. "Istituto di Macchine e Tecnologie Meccaniche" Trieste (Italy) reported:

"Test have been made on a serial truck engine running on a gas-oil/methanol mixture containing up to 30% methanol, with and without the addition of a combustion improver. Max. ranged 35% CH_3OH by volume..

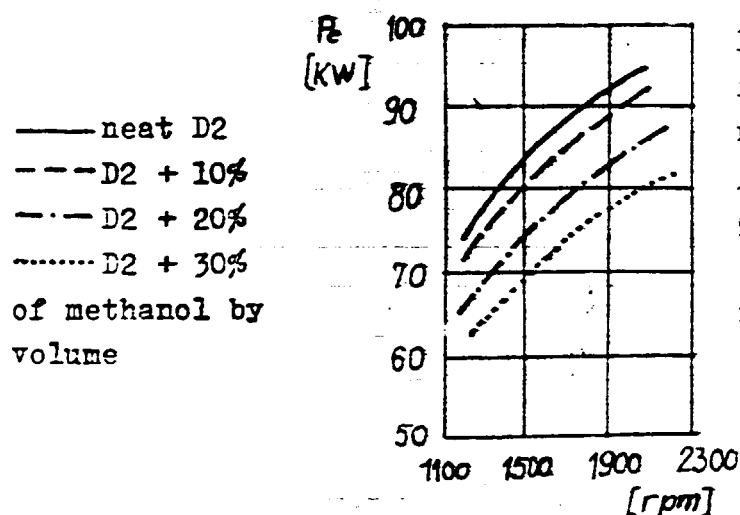


Fig 8 Performance of the four-cylinder engine running on different gas-oil/ CH_3OH mixtures (truck engine in regular production). Data obtained without fuelling increase.

Conclusions of "Istituto di M. e T.M.":

- without fuelling increase, addition of CH_3OH produces power output drop and specific thermal consumption increase
- adding ignition improver and more than 35% of CH_3OH by volume, the results obtained showed that besides of fuel cost increase, the startability was not improved because of a very high CH_3OH cooling effect. Thus, ignition improver effect was canceled by cooling
- additional reason for higher specific thermal consumption rate when mixing methanol was its cooling effect, which does not increase the volumetric efficiency in CI-NA engine.

(See also MTZ 44 (1983) 1)

(Using turbo-charged version CH_3OH may be used for air cooling and in this way to increase the volumetric efficiency.

Moreover, charge-air cooler may be omitted which produces: the first cost decrease and also box volume may be reduced).

- ceramic components are still our future

However, we must confess, that the method A is less expensive related to the first cost and may be more reliable in the services.

Forementioned depicts that the both A and B method have to be considered. B for the first neat methanol use in diesel engine application and A method as a following one.

Is to be mentioned, the suggestions given in the ECFC 1 are restricted related to:

- IIP considers NA version only
- only single fuel, neat CH_3OH has to be tanked
- the attention will be paid to the aforementioned method B

Point 1

The net heat of vaporization of methanol approach 1110 kJ/kg and that of diesel fuel 250 kJ/kg only. In order to ignite neat methanol in diesel DI engine, our experimental results showed, that CR ratio must be at the least 25 supposing cold-starting ability at reasonable low ambient temperatures also. We apply λ combustion chamber and CR=17 in diesel fuel operation with NA version.

It means that up to 8 units the compression ratio has to be increased. To apply CR=25-26 the main drawbacks is a high mechanical loading.

However, to support the ignition some compensation of temperature drop is still desirable. Moreover, the net compression pressure will not be increased although the geometrical CR ratio becomes higher. As was yet recommended in the first report (1983) CR may be enhanced for up to 2 units without mech. loading increase.

Point 2

To decrease the heat transfer in the preignition period, the next may be suggested:

- swirl ratio (SR) decrease (it was also yet recommended in the first report)
- light designed cast-iron piston

It is no doubt, that converting to neat methanol, SR ratio has to be decreased. Doing that, results in:

- reduced air motion save more heat of compression into combustion chamber and with this the temperature before ignition increases
- the ignition stability will be improved
- with SR reduced volumetric efficiency increase in NA version, more power output and higher compression temperature because of more air introduced
- less thermal loading of the parts formed the combustion chamber
- better control via injection

However, the rate of SR decrease must be considered with POINT 3 together. It is not reasonable to decrease to much SR ratio with spark plug supported, but still in this case related to diesel fuel operation, SR ratio may be reduced for at the least 15 ÷ 20 %.

It is well established fact that cast iron posses less thermal conductivity than that of Alu alloy, and with this before the ignition more heat may be saved. Light modern design of cast iron piston with cut-non thrust skirt sides and with three piston rings set (1st keystone-and 2nd tapered 90° compression rings, spring loaded elastic oil ring) may not be much heavier than of Alu-alloy one.

Point 3

Methanol prevaporization control means to control the fuel quantity-injected into combustion chamber on/and evaporated before ignition.

It may be done by means of fuel film dispersion on combustion chamber wall, discontinued needle lift (still in development), and modified cam shape of HPP camshaft.

Point 3.1 and Point 6

Fuel film deposition on combustion chamber wall is well known method initiated by MAN with M-process. Further development of M-process and its modifications are well known till

now also, thus no need for a background.

The fuel deposition on in-piston bowl wall is connected with spark-plug ignition. This is the reason, that in this point the spark-plug ignition procedure may not be omitted.

Fig 9 shows well known MAN combustion chamber of FM engine.

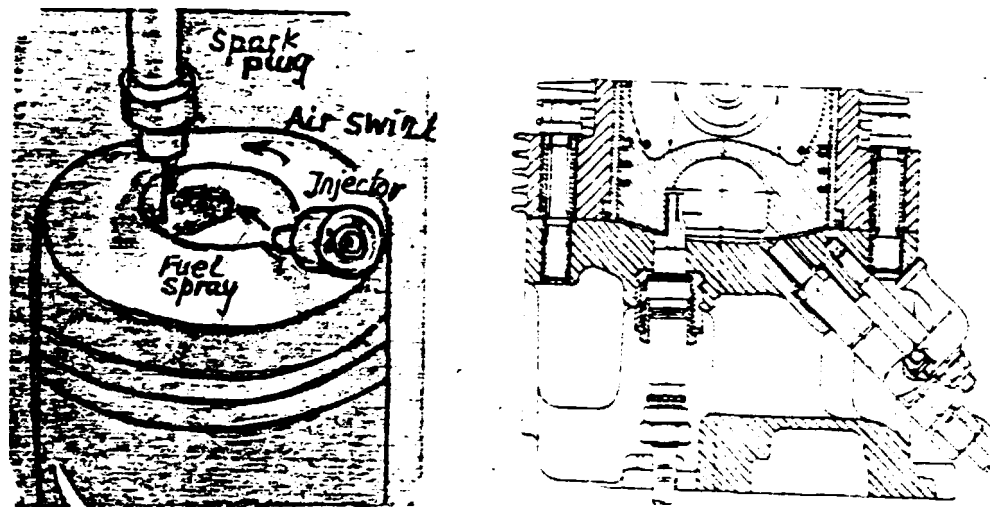


Fig 9 Combustion chamber of engine
L 9204 FM

MAN-FM combustion system has been derived from the diesel engine and is excellently suited for operation on methanol or other alcohols, because this hybrid system benefits from high diesel compression, direct injection and nonthrotling output control while ignition of the mixture is ensured by spark-plug as in the otto-cycles Fig 9 (Method B in this report).

The control mechanism in the proposed method B is projected on separation between injection- and mixture formation functions. To do this (during injection) fuel was deposite in the wall of the spherical chamber. The spark-plug is situated on the opposite side of the injector and its electrodes reach the fuel film zone.

The most important features of method B may be the follows:

- CR ratio as for diesel engine
- direct injection with single hole injector
- wall fuel deposition

- spark plug ignition
- range of piston dia. $\varnothing 85 \div \varnothing 130$

One part of the heat of evaporation is taken from combustion chamber wall in engine operation. It means that one part of the heat transferred to the wall comes back in the process increasing its efficiency. Thus, converting to methanol, brake thermal efficiency must be better than in diesel fuel operation. To support this statement the Fig's 10 and 11 are shown.

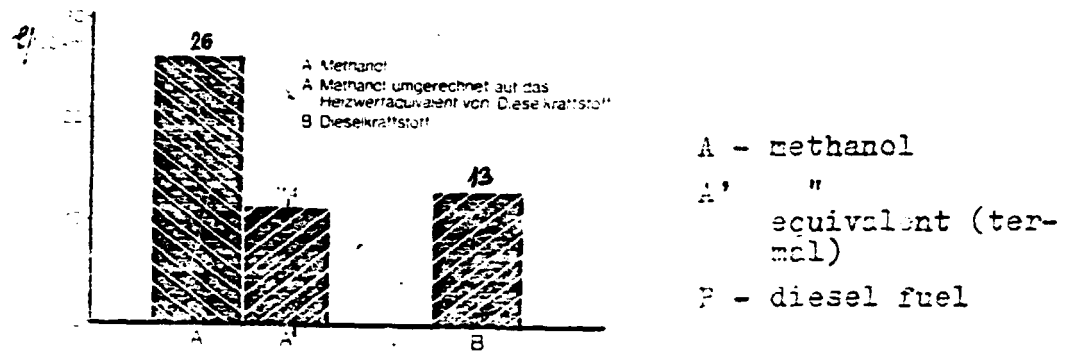


Fig 10 Fuel consumption of 2,1 tone vehicle with methanol engine I9204 FM compared with diesel engine I9204 M, constant speed 60 km/h. Methanol thermal equivalent fuel consumption decreased for 14 %.

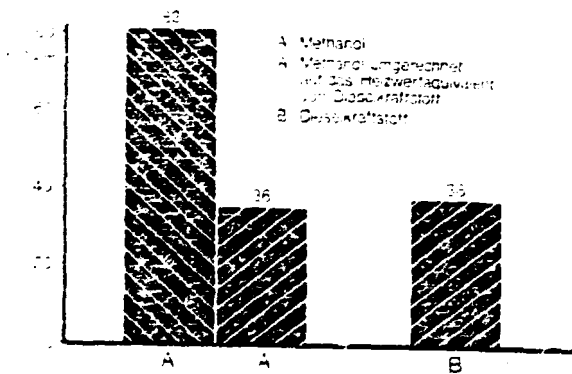


Fig 11 Fuel consumption of MAN city Bus with methanol engine D2⁶⁶FMUH compared with diesel engine D2⁶⁶MUH, urlem cycle. Methanol thermal equivalent fuel consumption decreased for 46,5 %.

The above Figures depict:

1. At higher loading more fuel saving with methanol. Its conclusion supported the heat come-back in the cycle.
2. Converting to methanol fuel, saving may reach up to 10% in general application.

The heat drop cause by methanol vaporization may be used for mean effective pressure increase or/and for better matching to the vehicle demands.

Fig 12 support this statement.

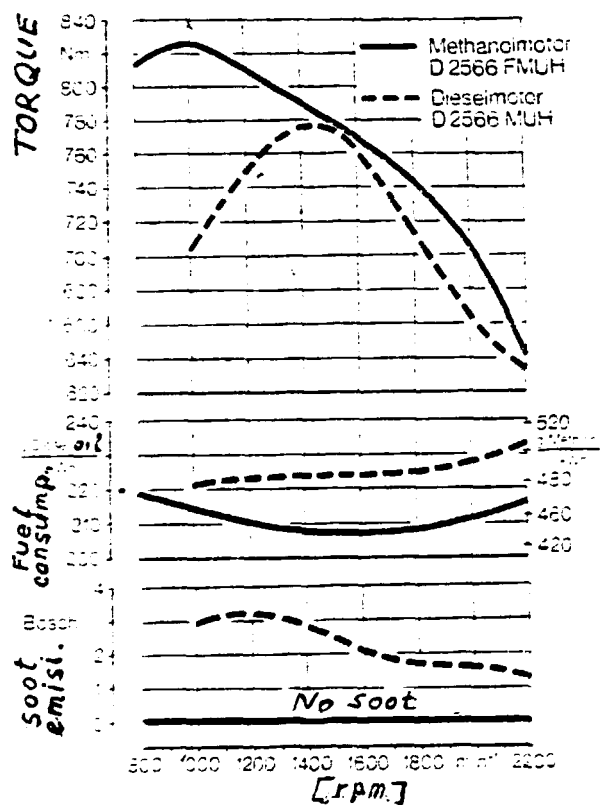


Fig 12 Full-load characteristics of methanol engine D 2566 FMUH compared with diesel engine D 2566 MUH

Fig 12 depicts:

1. Converting to methanol max. torque increases up to 6,5 % but its speed position is much more improved by 42 %.

2. Torque back-up in methanol operation reaches 50 % and in diesel fuel operation 22 %.
3. Sootless exhaust in methanol operation, still one support more, for torque back up increase.

Moreover, converting to methanol the parts forming combustion chamber are less loaded, thus the service life of spark plug electrodes will be extended. Spark-plug is of specific design but all other ignition system is normal transistorized high-tension ignition system, used in automobiles.

The bellow cited may be recommended:

1. Combustion chamber is spherical with small gaps for injector and spark-plug. For given piston dia. and CR=18 all other proportions are very simple to obtain.
2. Ignition system is normal as for modern engines used in automobiles.
The exeption is the spark-plug which maybe purchased from BOSCH.
3. Single hole injector
4. Using the programme sent last year (1985, see the first report) fuel injection may be very accurately calculated. Moreover, fuel spray - combustion chamber wall contact in the programme enables to follow the fuel deposition.

Point 3.2

In order to decrease the fuel quantity in the combustion chamber before the ignition needle lift event may be modified, Fig 12.

During injection at high loads, using system in Fig 12, the nozzle discharge areas may be changed, Fig 15.

In the preignition period the discharge area a and time b may be accomodated to the specific demands. In our case we may control the injection quantity before the ignition changing a and b, Fig 13. It means we control the temperature drop before the ignition also.

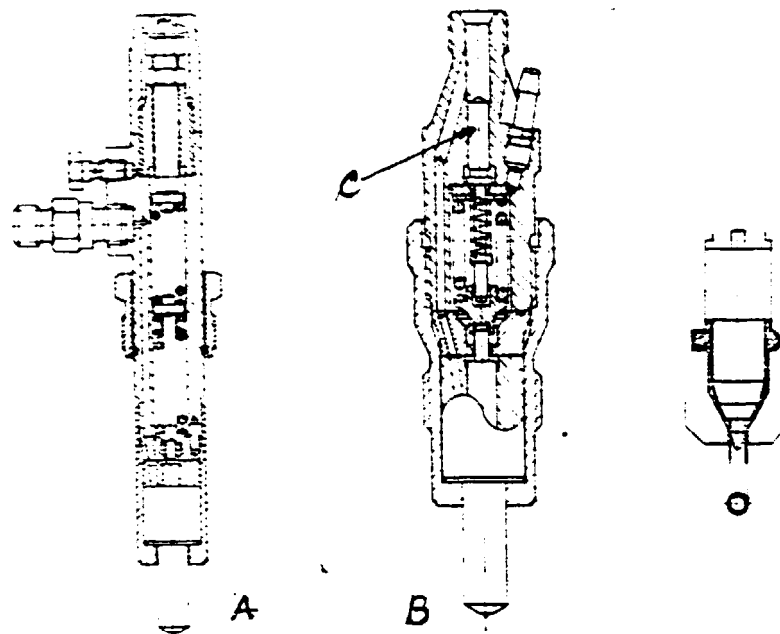
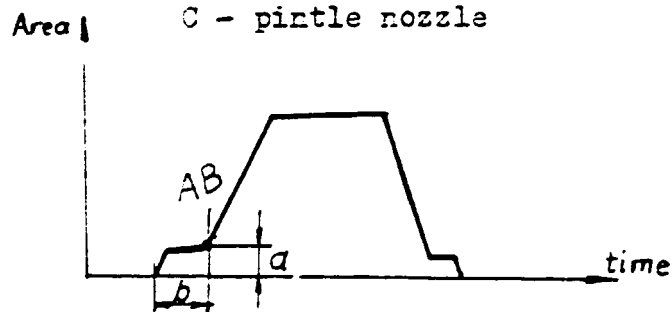


Fig 12 A - Two-spring injector, B - Bosch injector with control plunger ,
C - pintle nozzle



Nozzle discharge area change
during injection

Fig 13 Nozzle discharge area change
during injection

In the system A, Fig 12 the bottom spring control the opening pressure, at AB point, Fig 13 the upper spring starts with compression. This system was developed by MAN. Bosch used other approach, B Fig 12, here a small piston C controls the point AB in Fig 13. The diameter of piston C is smaller than needle dia, thus the fuel acting on the both, controls with pressure the needle lift.

Moreover, the system shown is very useful in low-load operation. Over-fuelling or inertia-supported fuelling is prevented. Because of low pressure levels nozzle discharge area remains small and the injection period becomes prolonged. At low-loads and low speeds the system shown in Fig 12 may be solution to avoid misfiring.

The same events may be followed by single nozzle.

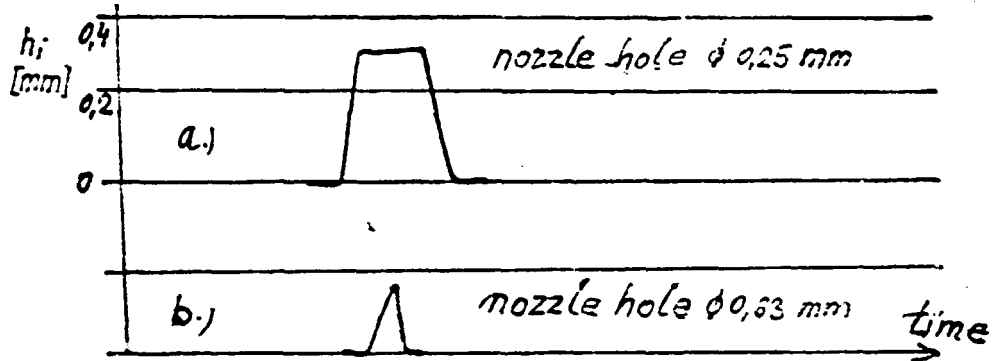
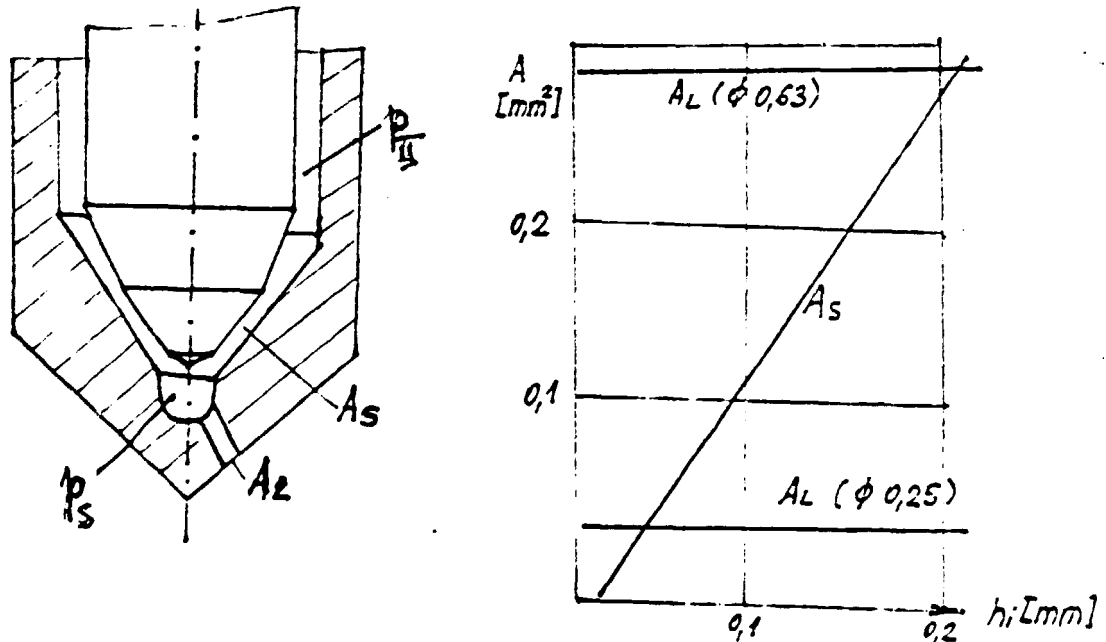


Fig. 14 Idling speed, fuelling $15 \text{ cm}^3/\text{cycle}$
 a) simple-hole nozzle $\phi 0,25 \text{ mm}$
 b) simple-hole nozzle $\phi 0,63 \text{ mm}$
 h_i - needle lift

The reason for the needle lift change may be explained in Fig 15.



Taking into account Fig 15 and Fig 16 the self control HP pump - HP line - injector may be clearly observed.

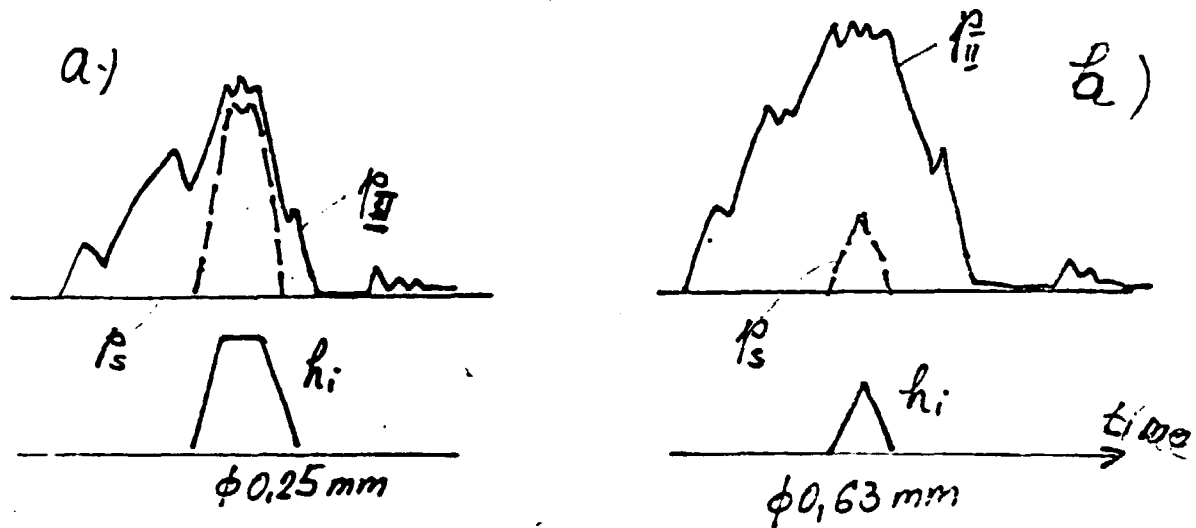


Fig 16 Self-control between p_{III} , p_s and h_i (see Fig 15). Note p_{IIIb} p_{IIIa} , thus p_{III} events a - b could not be compared related to amplitudes in Fig 16

The next expression shows:

$$p_{AS} + \frac{\rho \cdot w_{AS}^2}{2} = p_s + \frac{\rho \cdot w_s^2}{2}$$

where:

p_{AS} , p_s - are instantaneous pressures in the cross-sectional area AS and before the nozzle hole respectively

w_{AS} , w_s - are instantaneous velocities respectively

ρ - fuel density

Following the expression given the philosophy about needle lift control and fuel deposition may be explained.

Dealing with spray tip - comb chamber wall contact control via injector, the injector springs have to be adapted (Fig 12) to our demands:

- X1 - injection period
- X2 - area of fuel film deposition
- X3 - history of fuel film deposition
- X4 - preignition fuelling
- X5 - injection pressure

(Points X1 ÷ X5 may be calculated only using Programme 1, sent IIF, see the 1st Report)

In the first Programme sent, relations related to spring are omitted. Therefore the additional informations are given bellow (see also the book Cernej-Dobovisek).

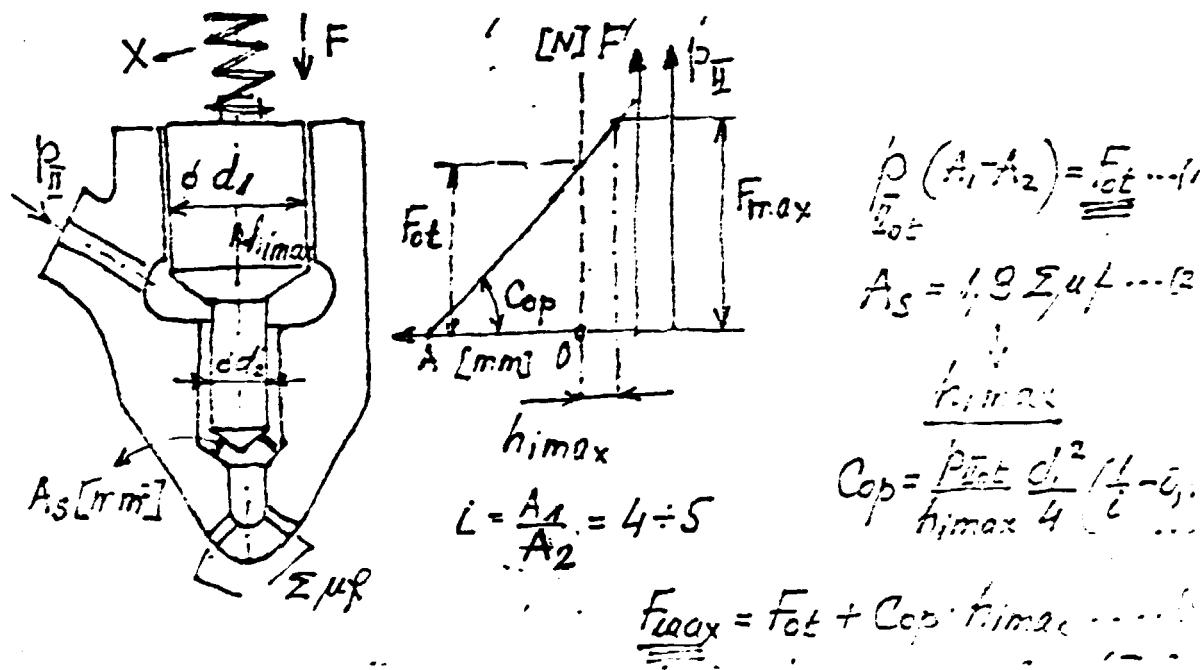


Fig 17 F - spring force, F_{ot} - spring opening force
 - effective flow-cross-sectional nozzle holes area
 P_{ot} - injection opening pressure
 C_{op} - spring rate, A - area
 i - hydraulic injector ratio

$$A_1 = \frac{\pi \cdot d_1^2}{4} \quad ; \quad A_2 = \frac{\pi \cdot d_2^2}{4}$$

F_{ot} - spring force at opening press.

F_{max} - spring force at max. needle lift

h_0 - spring lenght compressed at F_{ot}

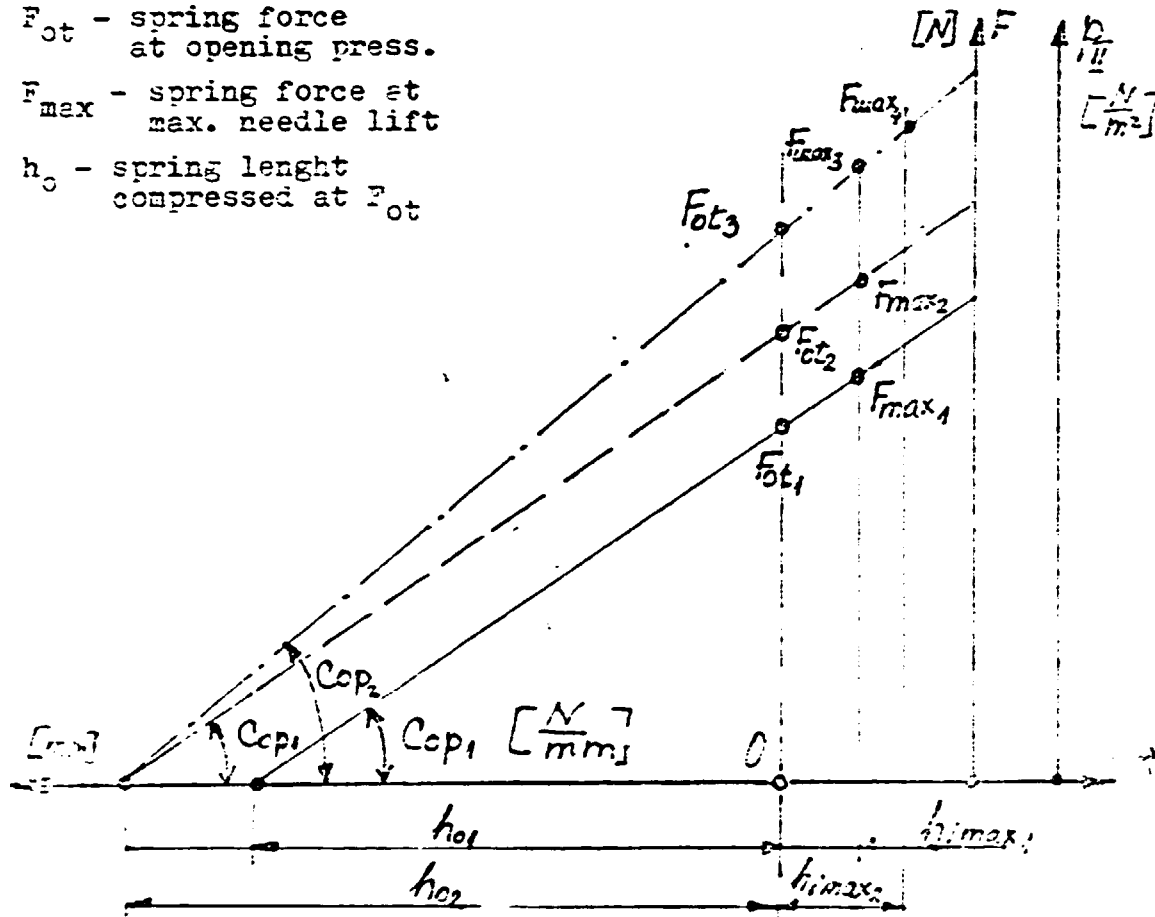


Fig 18 Spring force accomodation

Fig 18 shows:

- in order to change the opening pressure we change the spring precompression

$$F_{ot2} - F_{ot1}, \quad F_{max2} - F_{max1}$$

- in order to change the both, opening pressure and spring rate increasing the needle lift also we have:

$$F_{ot3} - F_{ot1}, \quad F_{max4} - F_{max1}$$

Injector spring design.

Fig 19 shows Smith-diagramme for the spring wire steel of middle quality. Today max. quality approaches:

$$\tau_{\max} = 65000 \text{ N/cm}^2 \text{ and } \tau_w = 35000 \text{ N/cm}^2$$

Using the max. steel quality but middle quality in production we calculate:

$$\tau_{\max} = 50000 \text{ N/cm}^2 \text{ and } \tau_w = \frac{\tau_{\max}}{2}$$

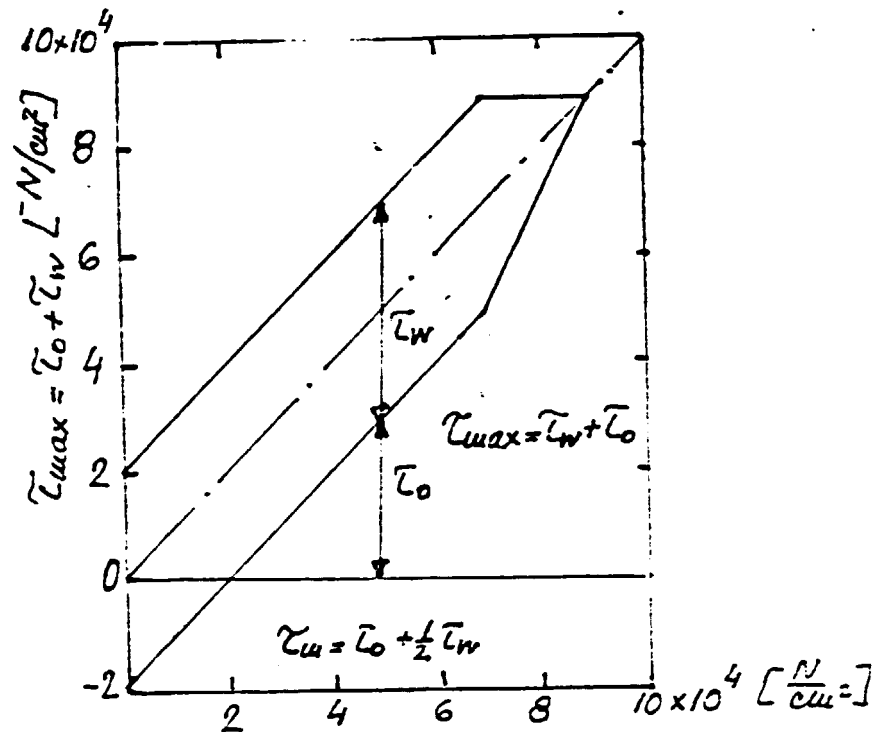


Fig 19 Middle spring steel quality

Defining h_0 and $h_{i,\max}$ we have the next expressions:

$$h_0 + h_{i,\max} = h_{i,\max} \frac{\tau_{\max}}{\tau_w} \quad (1)$$

$$d = \sqrt[3]{\frac{8 \cdot F_{\max} \cdot D \cdot \psi}{\pi \cdot \tau_{\max}}} \quad (2)$$

d - spring wire dia.

D = see Fig 20

$$\psi = 1 + \frac{5}{4} \left(\frac{d}{D} \right) + \frac{7}{8} \left(\frac{d}{D} \right)^2 \quad (3)$$

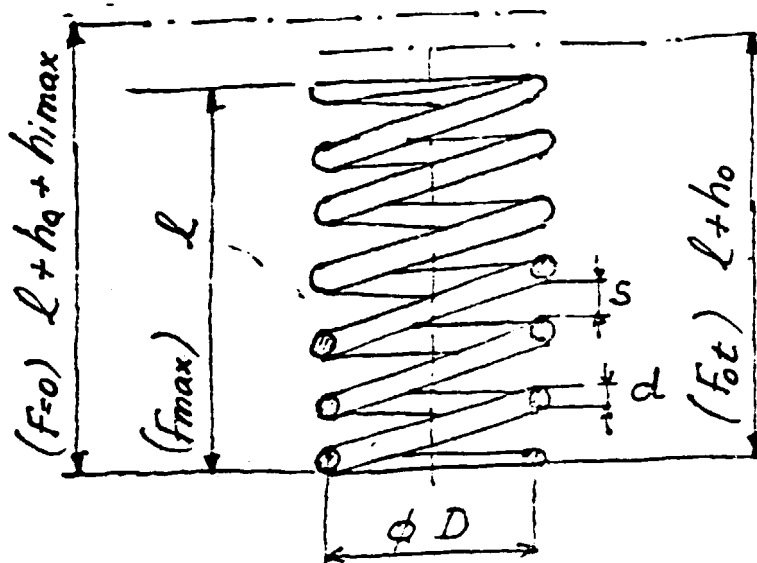


Fig 20 Injector spring proportions

The active coil number may be calculated as follows:

$$h_o + h_{i,max} = \frac{8 \cdot z \cdot D^5 \cdot F_{max}}{G \cdot d^4} \quad (4)$$

where:

$$G = 8,5 \cdot 10^6 \text{ N/cm}^2$$

$$\psi_1 = 1 - \frac{3}{16} \left(\frac{d}{D} \right)^2 \quad (5)$$

The whole coil number z_u as:

$$z_u = z + 1,5 \quad (6)$$

The spring length at max load:

$$l = (z_u + 1) \cdot d + z_u \cdot s \quad (7)$$

where: $s = (0,15 \div 0,3) d$ (9)

The first eigen frequency as:

$$\tau_e = 0,8178 \cdot \frac{\tau_w}{\psi \cdot h_{i \max}} \quad (9)$$

$$\tau_w \left[\frac{N}{cm^2} \right] \quad , \quad h_{i \max} [cm]$$

Taking into account oscillations of the spring results in:

$$\tau_{wD} = \tau_w + 4,5 \cdot 10^6 \cdot \psi \cdot \xi_x \quad (10)$$

where:

$\xi_x [cm]$ - the amplitude of the first harmonic

The penetration of the spray tip is directly dependent on Δp (pressure drop at nozzle hole) and indirectly on p_{II} (measured pressure before injector).

$$\Delta V_c = \mu \cdot A \cdot \sqrt{\frac{2}{\rho}} \cdot \sqrt{\Delta p} \cdot \Delta t$$

The pressure drop Δp may be calculated using one of three programmes given to IIP. However, to get idea about relations between Δp and p_{II} Fig 21 is presented (se W. Dall-Ricardo)

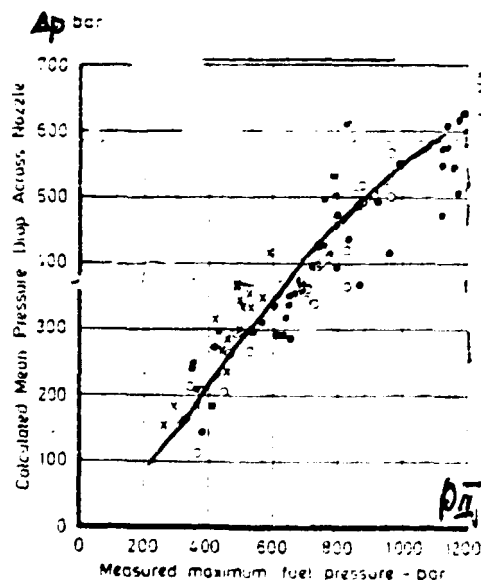


Fig 21 The relation between Δp calculated and p_{II} measured

Note: Before the needle lift control according Fig 12 we may analyse the pump-injector self-control.

$A_k v_k$ delivery pulse of HP pump influenced by connecting channel (HP tube) reach the injector area deformed. Two Eq's control the fuelling events at injector:

$$\dot{V} = \mu \cdot A \cdot \sqrt{(\rho_1 - \rho_2) \cdot \frac{2}{\rho}}$$

$$m \cdot \ddot{h}_i + F_0 + c \cdot \dot{h}_i + F_{tr} = \rho_1 \cdot A_x$$

(see book Černej-Dobovišek) but only are at the pump:

$$A_k \cdot v_k = \frac{\pi \cdot d_k^2}{4} \cdot (v_0 + \beta \cdot \varphi) \cdot n = C_1 \cdot d_k^2 \cdot (v_0 + \beta \cdot \varphi)$$

d_k - plunger dia.

v_0 - defined velocity at geometrically defined start of delivery (prelift setting)

β - defined cam shape

φ - angle

It means according to above Eq's that injector possesses a very high influence on the whole process being represented by two Eq's. It was the reason for needle lift control application

Point 3.3

Modified cam shape of HPP camshaft

In the past as well as still nowadays the people are trying to control the preignition fuelling by means of modified cam shape.

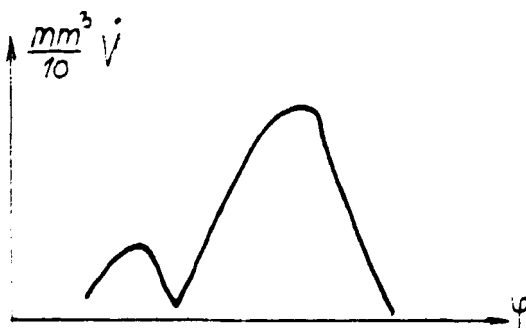


Fig 22 devided fuelling

To do this cam shape has to be modified according to Fig 23.

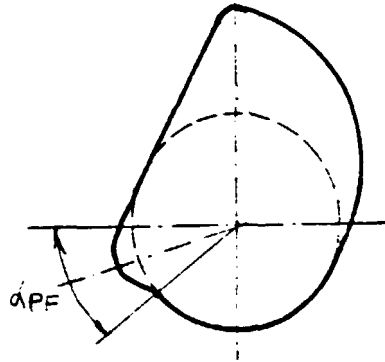


Fig 23 modified cam for divided fuelling

The shape in the region α_{PP} defines the prefuelling. However, still today no practical applications of the cam shown in Fig 23, thus this way may not be recommended.

Point 4

To start injection in more favourable ambient for ignition

Retarding the timing fuel starts to penetrate in combustion chamber later, when the temperature of compressed air becomes higher and therefore the in-combustion chamber ambient more favourable for ignition. It means that the ignition delay becomes shorter as well as fuelling injected till TDC smaller.

The aforementioned said supposes:

- late combustion and knocking are avoided under all operational condition
- product

$$\int \dot{x} \cdot p(\alpha)$$

during expansion stroke reached reasonable high level in full load operation

- conventional in-cylinder peak pressures
- reasonable high pressure rate increase
- exhaust gaseous emission figure better or the same as for diesel fuel operation

- fair fuel consumption figure in low load operation also.

The above cited in neat methanol operation is possibly to reach only applying:

- spherical combustion chamber
- single hole nozzle or pintle nozzle
- spark plug ignition control
- matched SR
- matched CR
- matched injection events

To improve engine performances is to be completed with:

- investigations concerning injector controlled prefuelling
- retarded timing
- optimization of fuel deposition

Still one benefit from the proposal given may be a modest demand related to fuel system power capacity. Thus, the both, fuel consumption and first cost may be reduced. However, the both have to be investigated, low pressure and high pressure injection. It can be done by calculation at first and then optimised solution can be applied.

Topic 6

One inductive transducer of a high sensitivity 50 kHz for needle lift measurements was given to IIP as well as the sketch for appropriate bridge.

Unfortunately IIP not disposes of an appropriate bridge which as well as various transducers may be purchased by us.

The inductive transducer given was suitable for injector selected. Min. transducer which may be produced in the lab. conditions is $\varnothing 4$ mm outside dia. It should be taken into account that 600 coils in one direction and 600 coils in another one have to be put in, as well as outside and inner isolation.

Last year we trained pressure measurements before the injection and this the both, pressure and needle lift. In this way the main parameters of injection may be recorded. In the first report rig test bench for (μA) of injection was suggested, and completing that all calculations can be made.

Moreover, the needle lift measurements are unavoidable tool for accurate calculations.

Based on Woschni results Dr Ivan Filipović developed before 7 years two practical programmes for simple fuel injection calculation.

MODEL I

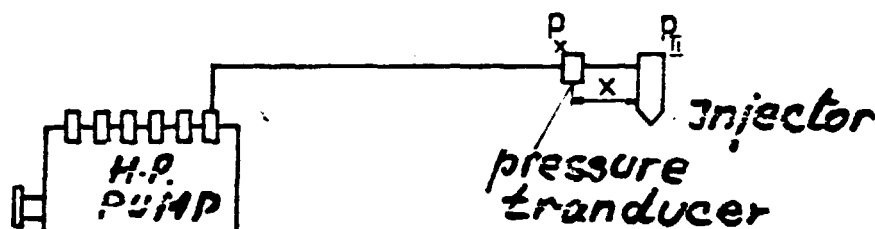


*Fig. 1 Sketch of HP system.
 p_x at distance x .*

As for input data, the total transient pressure p_x (Fig 1) at defined distance x must be registered (or stored). But also for the system given we collected the next input data:

- effective cross-sec. injector flow area vs. needle lift ($\mu_r A_b$)
- fuel properties
- in-injector dead volume V_t
- forces and geometrical proportions of injector (see nomenclature).

The whole calculation is based on the well known d'Alembert solution for the pressure wave transport:

$$P = P_0 + P_v + P_r \quad (1)$$

It means, the total transient pressure measured at distance x may be written as sum of: forward directed pressure wave p_{vx} , receding pressure wave p_{rx} and residual pressure p_0 .

$$P_x = P_0 + P_{xv} + P_{xr} \quad (2)$$

pressure at the injector inlet:

$$P_{II} = P_0 + P_{IIv} + P_{IIr} \quad (3)$$

The same may be drawn as shown in Fig 2.

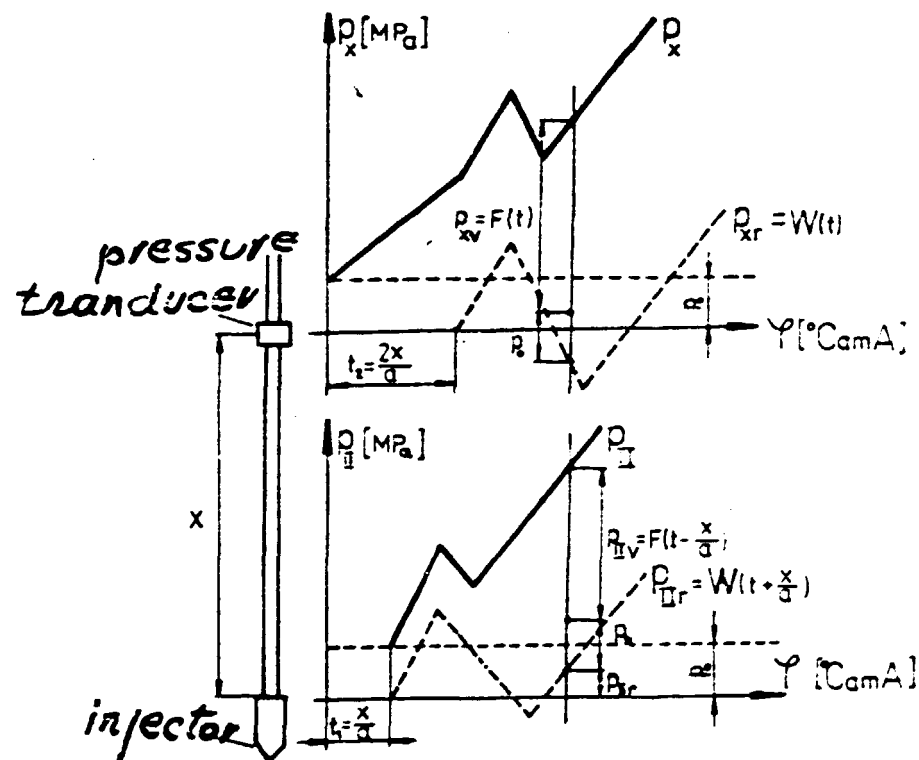


Fig 2 The sketch of pressure events at measuring distance x and at injector inlet

Pased upon the Fig 2 and afore cited the next eqs. for calculation of injection events, may be written:

- mass continuity equation describes the injection function:

$$\frac{d\rho_x}{dt} = \left[A_c \cdot W_x - (\mu_b A_b) \cdot \sqrt{\frac{2}{\rho} (\rho_x - \rho_x)} - A_2 \cdot v_i \right] \cdot \frac{1}{\alpha V_b} \quad (4)$$

- based upon the equation of needle motion (inertia due to mass of the injector moving parts (m_i), forces due to control spring (F_{ob} , h , C_{ob}) and fluid pressures are included), we may write the next two eqs.:

$$\frac{dv_i}{dt} = \left[(A_2 - A_x) \cdot \rho_x - F_{ob} + A_x \cdot \rho_B - h_i \cdot C_{ob} \right] \cdot \frac{1}{m_i} \quad (5)$$

$$\frac{dh_i}{dt} = v_i \quad (6)$$

- where ρ_B may be calculated as follows (Fig 3)

$$\rho_B = \frac{(\mu_b A_b)^2}{(\mu A)_B^2} \cdot (\rho_x - \rho_x) + \rho_x \quad (7)$$

- total transient velocity at II - II (see Fig 3)

$$W_x = \frac{1}{\alpha \rho} \cdot \left[\rho_0 - \rho_x + 2 \cdot F \left(t - \frac{x}{\alpha} \right) \right] \quad (8)$$

- receding pressure wave

$$W \left(t + \frac{x}{\alpha} \right) = \rho_0 - \rho_x + F \left(t - \frac{x}{\alpha} \right) \quad (9)$$

where is:

$$F \left(t - \frac{x}{\alpha} \right)_t = F(t)_{t - \frac{x}{\alpha}} \quad (10)$$

- forward directed pressure wave measured at distance x may be written as follows:

$$\rho_{rx} = F(t) = \rho_x - \rho_0 + W(t) \quad (11)$$

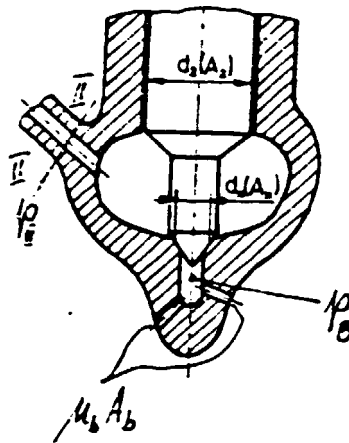


Fig 3 Sketch of injector

where is:

$$W(t)_t = W(t + \frac{x}{a})_{t - \frac{x}{a}} \quad (12)$$

- law of injection as:

$$\dot{q}_c = u_b A_b \cdot \frac{1}{6 \cdot \eta} \cdot \sqrt{\frac{2}{5} (p_2 - p_2)} \quad \left[\frac{\text{mm}^3}{\text{s}} \right] \quad (13)$$

- integrated law of injection as:

$$q_c = \int_{\varphi_p}^{\varphi_k} \dot{q}_c d\varphi \quad (14)$$

The unknown values in eqs. 4-14 of model I are:

p_{II} , V_1 , h_1 , p_B , w_{II} , $W(t)$, $W(t + x/a)$, $F(t)$, $F(t - x/a)$, q_c , q_c .

Solution of above system of eqs. $y' = f(x, y)$ may be found using Runge Kutta approximation (4-step) and variable time step.

MODEL II

For the system where the residual pressure tends to drop below the fuel vapor pressure Model I could not give satisfactory results. Here, the Model II was developed in which the both: the total transient pressure p_x at distance \underline{x} and needle lift h_1 were registered and used as input data .

- needle velocity may be written as follows:

$$v_i = \frac{h_{im} - h_{iv}}{2 \Delta \varphi} \cdot 6n \quad (15)$$

- mass continuity equation in injector

$$\frac{d\rho_x}{dt} = [A_c \cdot w_x - (\mu_b \cdot A_b) \cdot \sqrt{\frac{2}{\rho} (\rho_x - \rho_0)} - A_2 \cdot v_i] \cdot \frac{1}{\alpha \cdot V_b} \quad (16)$$

- the total transient injector inflow velocity is:

$$w_x = \frac{1}{a \cdot \rho} [\rho_0 - \rho_x + 2 \cdot F(t - \frac{x}{a})] \quad (17)$$

- receding pressure wave may be written as follows:

$$W(t + \frac{x}{a}) = \rho_0 - \rho_x + F(t - \frac{x}{a}) \quad (18)$$

- where is:

$$F(t - \frac{x}{a})_t = F(t)_{t - \frac{x}{a}} \quad (19)$$

- the relation for forward directed pressure wave at distance x may be written as:

$$F(t) = \rho_x - \rho_0 + W(t) \quad (20)$$

- where is:

$$W(t)_t = W(t + \frac{x}{a})_{t - \frac{x}{a}} \quad (21)$$

- law of injection:

$$\dot{q}_c = \mu_b \cdot A_b \quad (22)$$

- fuel quantity injected per cycle:

$$q_c = \int_{\varphi_p}^{\varphi_k} \dot{q}_c d\varphi \quad (23)$$

The unknown values in eqs. 15 ÷ 23 of model II are:

v_i , P_{II} , w_{II} , $W(t)$, $W(t+x/a)$, $F(t)$, $F(t-x/a)$, q_c , q_c .

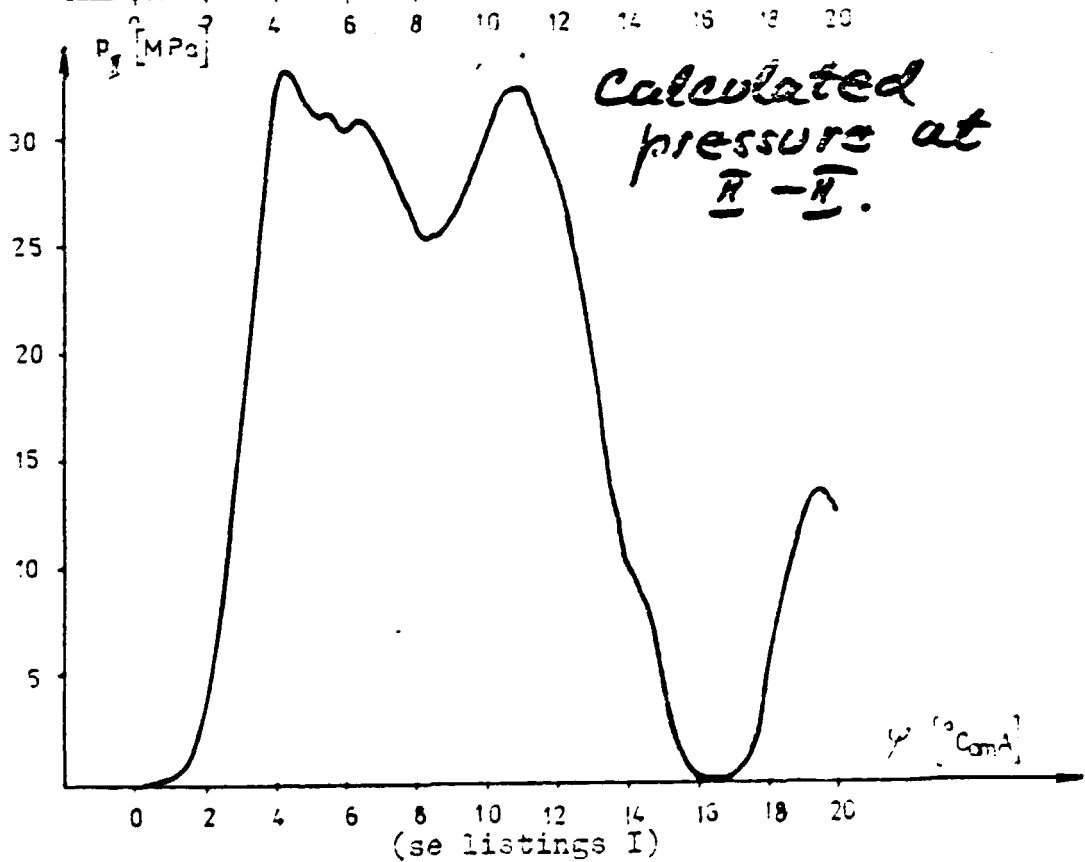
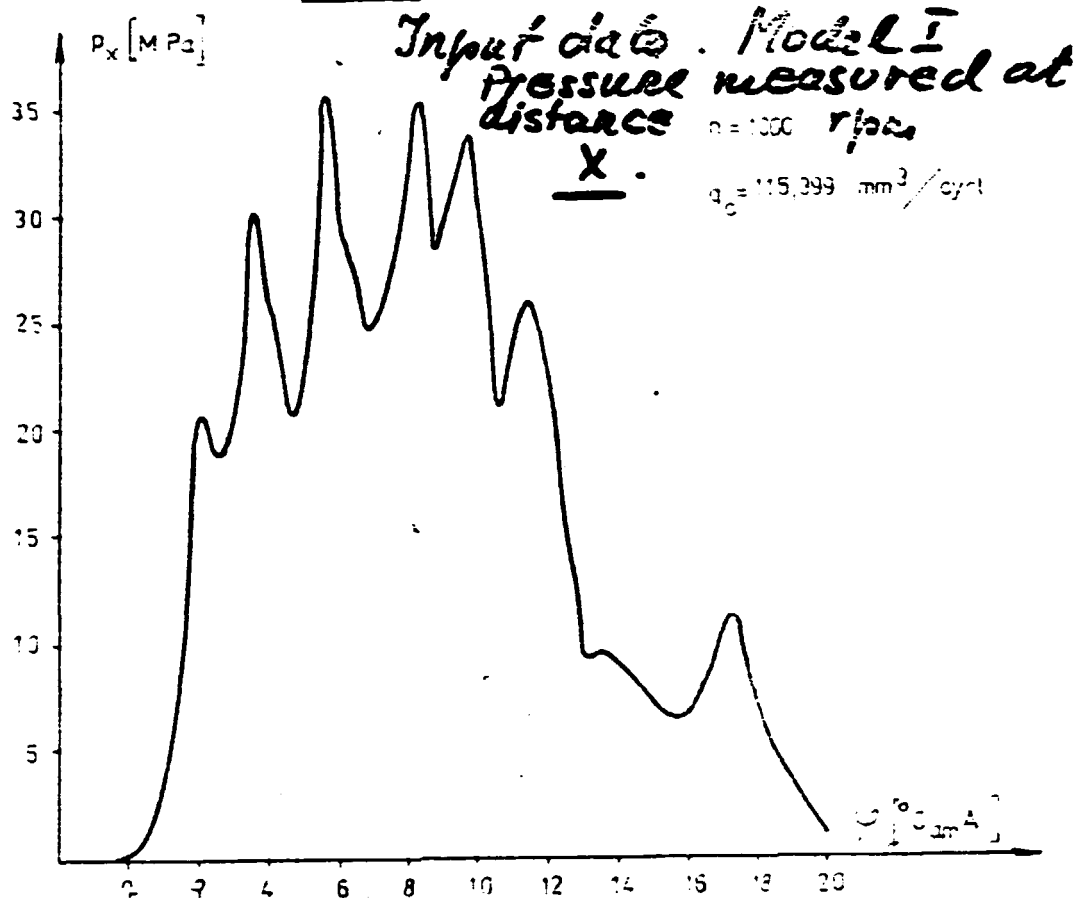
For numerical solution of above system of eqs. a 4-step Runge-Kutta approximation may be applied using variable time step (see listings II appended).

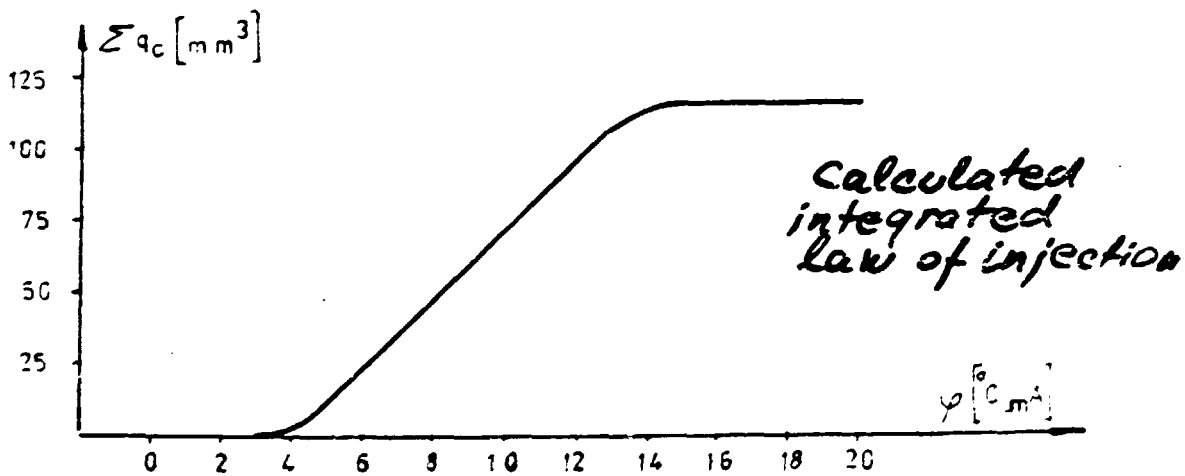
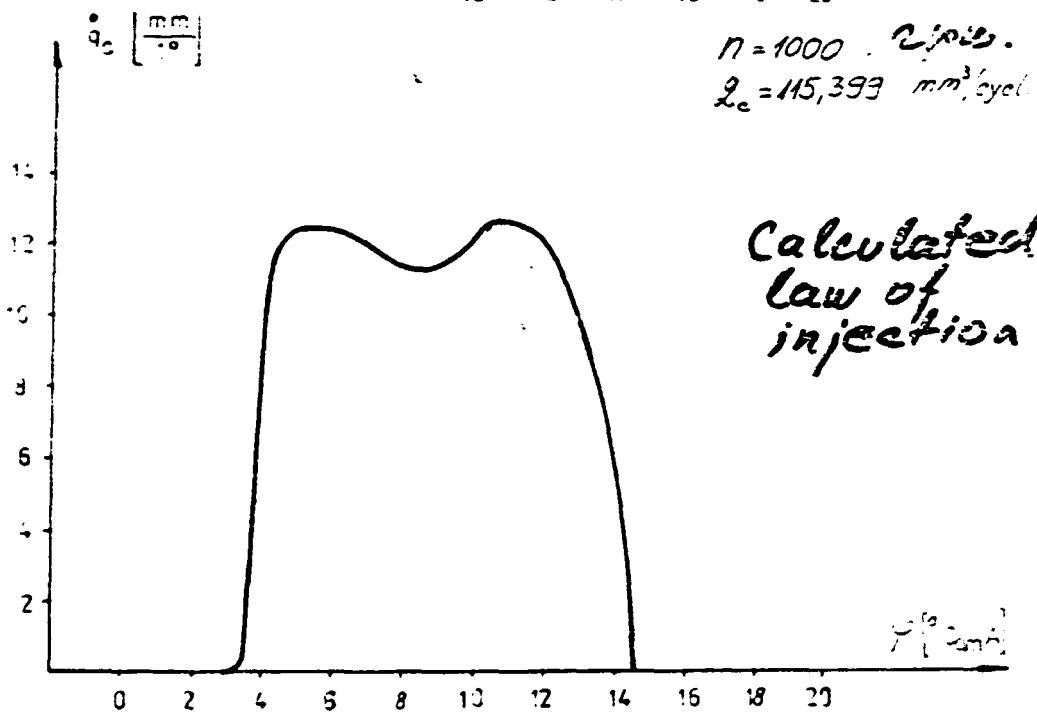
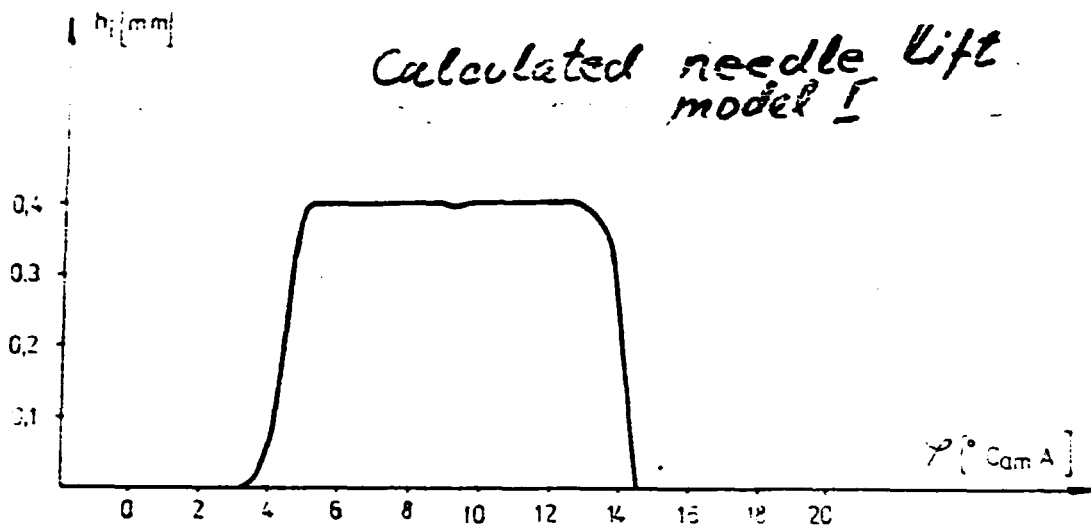
Nomenclature

a (A)	- velocity of sound
A_c (AC)	- high pressure tube cross-sect. flow area
A_x (AX)	- needle cross-sect area (see Fig 3)
A_2 (A2)	- " " " "
C_{of} (COF)	- spring rate
F_{of} (FCF)	- opening force of the injector spring
h_i (Y(3), HIX)	- needle lift
m_i (MI)	- mass of the injector moving parts
n (AI)	- pump rotational speed
p	- pressure
p_E (PE)	- pressure in the injector sack volume
p_o (PO)	- residual pressure
p_r	- receding pressure wave
p_v	- forward directed pressure wave
p_x (PX)	- pressure at measuring distance x
p_z (PZ)	- in-cylinder pressure
$p_{xr}, W(t)$ (WT, PRQ)	- receding press-wave at measuring distance x
$p_{xv}, F(t)$ (FT, PVX)	- forward directed pressure wave at dist. x
P_{II} (Y(1))	- total transient pressure at II - II (at injector inlet)
$P_{IIr}, W(t+x/a)$ (WTL, PDR)	- receding pressure wave at II - II
$P_{IIv}, F(t-x/a)$ (FTL, PDV)	- forward directed pressure wave at II - II
q_c (QC)	- flow of injection
t, t_1, t_2	- time
v_i (Y(2), V)	- needle velocity
V_b (VB)	- injector dead volume
w_{II} (WII)	- total injector inflow fuel velocity

- x - distance between press. tr. and inject. (see Fig 1)
 $E=1/$ (EMOD) - bulk modul of elasticity
 ${}_b A_b$ (AMBAP) - effective injector flow area
 $A)_P = {}_b A_b)_{max}$
 (AMAP) - max. effective injector flow area
 (RC) - fuel density
 (Y) - instanteneous value

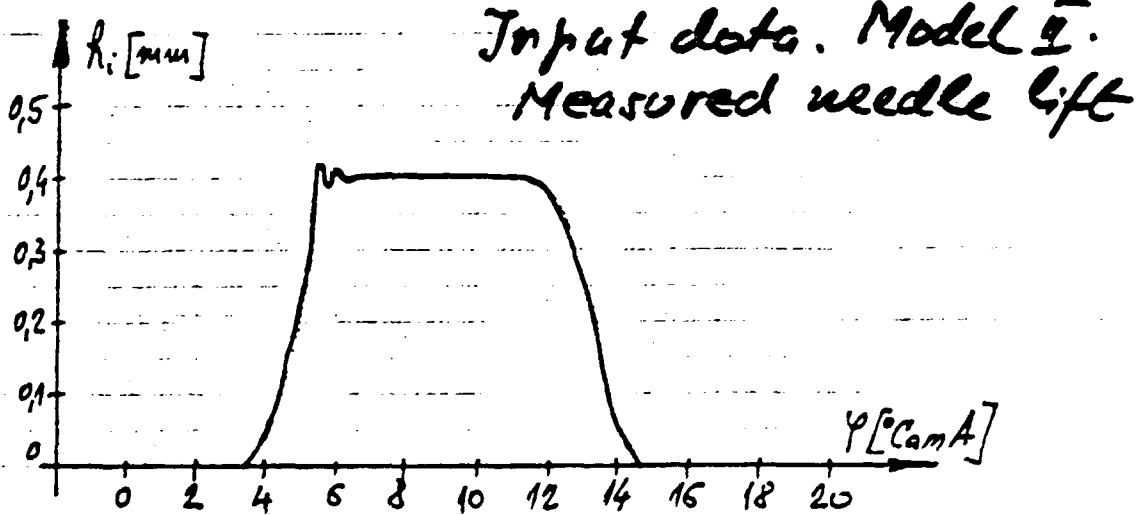
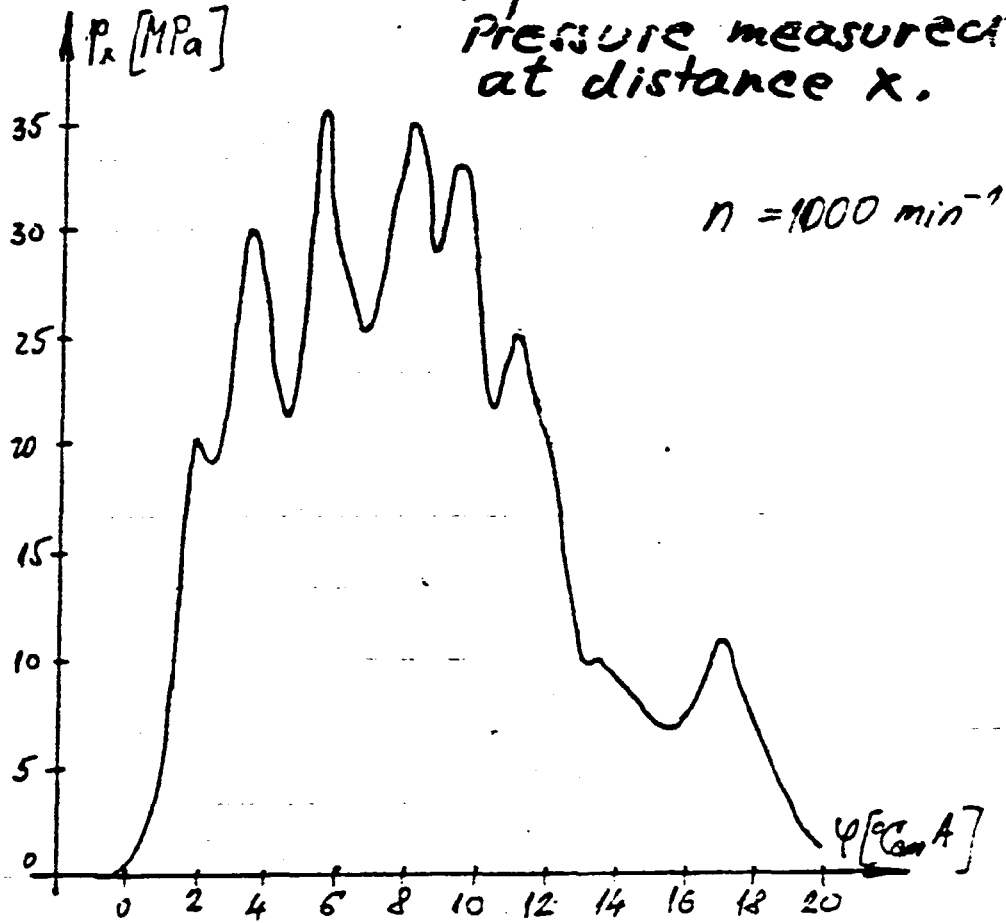
RESULTS





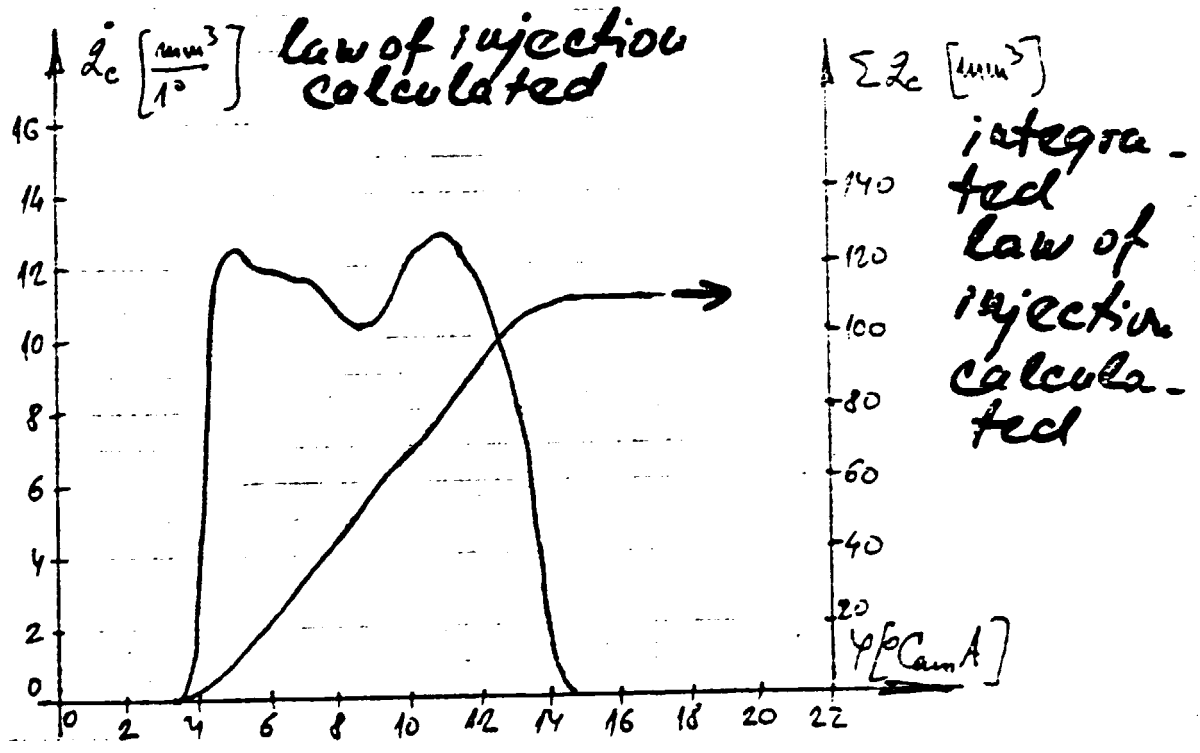
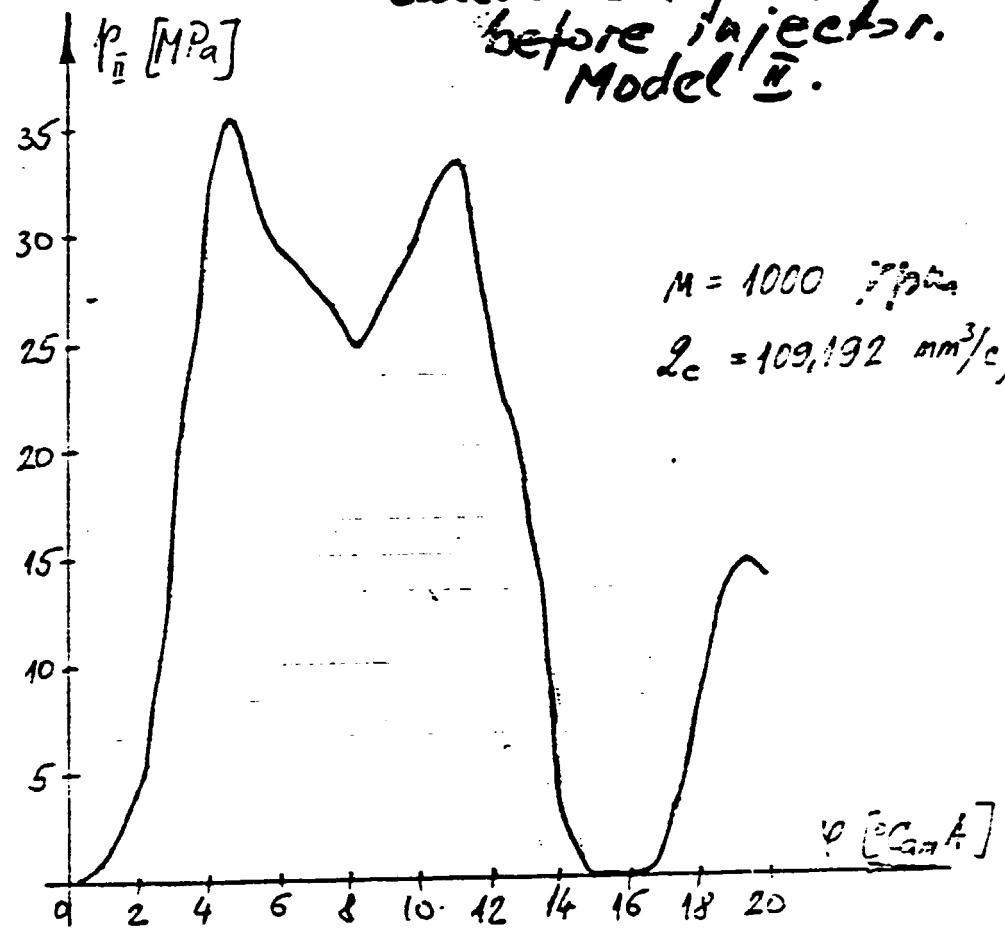
(se listings I)

Input data, Model II
Pressure measured
at distance x .



(see listings II)

Calculated pressure before injector.
Model II.



(see listings II)

Topic 7

Laser doppler effect (LDE) may be applied only by accomplishing:

- the correct selection of optical depth
- the calibration

According to the principle LDE enables to define:

- the range of droplet velocities in the spray
- the degree of turbulence
- velocity change of the spray investigated
- spray penetration time -
- density of droplets per unit volume
- droplet mean dia
- droplet distribution
- droplet shape

For the nozzle hole d_2 , in-cylinder pressure p_2 and pressure before the injector p_{II} given we define the next dimensionless parameters:

- the velocity at the nozzle hole exit

$$V = \sqrt{\frac{2}{\rho_2} (\rho_{II} - p_2)}$$

- Weber number

$$We = \frac{\rho_g \cdot v^2 \cdot d_s}{\sigma_g}$$

- Laplace number

$$L_p = \frac{\rho_g \cdot d_s \cdot \sigma_g}{\mu_g^2}$$

- density ratio

$$M = \frac{\rho_2}{\rho_g}$$

where:

ρ_g - fuel density

ρ_2 - in-cylinder air density

μ_g - fuel viscosity [Ns/m²]

σ_g - fuel surface tension [N/m]

$$m_1 = 1,2 \text{ for } p_2 \gg 0,7 \text{ ata}$$

$$m_1 = 0,6 \text{ for } p_2 < 0,7 \text{ ata}$$

where:

(7)

$$\frac{d_p}{d_0} = N_1 \cdot \left(\frac{x}{d_0}\right)^{1,38} \cdot L_p^{-0,14} \cdot M^{-0,55} \cdot m_1$$

for $x < x_{gr}$

may be given as:

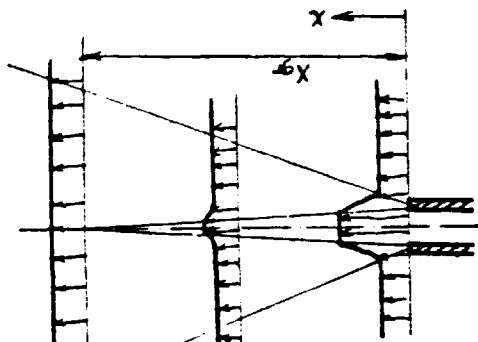
The expression for the mean specific fuel flow at distance x

$$\text{and its volume as } V_x = d_p^3 \cdot \pi / 6$$

(8)

$$d_p = d_0 \cdot 2,21 \cdot (M \cdot W_0)^{-0,266} \cdot L_p^{-0,073}$$

Mean volume droplet dia. $d_{30} = d_p$ may be expressed as:



$$q_1 = 3,85; q_2 = 0,6 \text{ for } p_2 \gg 0,7 \text{ ata}$$

$$q_1 = 46,9; q_2 = 0,24 \text{ for } p_2 < 0,7 \text{ ata}$$

where:

(9)

$$x_{gr} = C \cdot d_0 \cdot W_0^{0,25} \cdot L_p^{-0,4} \cdot M^{-0,8}$$

The end of the potential core of the spray may be expressed as:

$$D_1 = 0,0112 \quad m_1 = 0,5 \text{ for } p_2 \gg 0,7 \text{ ata}$$

$$D_1 = 0,00364 \quad m_1 = 0,26 \text{ for } p_2 < 0,7 \text{ ata}$$

where:

(1)

$$L_p \frac{d}{z} = D_1 \cdot W_0^{0,32} \cdot L_p^{0,07} \cdot M^{m_1}$$

as follows:

To estimate the spray cross-sectional area at the distance of the nozzle hole x : the cone angle of the spray may be written

For $x > x_{gr}$

$$\frac{a_m}{a_0} = 0,125 \cdot F_1^{-2,0} \cdot \left(\frac{d_g}{x}\right)^{2,0} \cdot L_p^{-0,2} \cdot We^{-0,6} \cdot M^{-2 \cdot n_1} \quad \dots\dots\dots (5)$$

where: $F_1 = 0,019$; $n_1 = 0,8$ for $p_2 \geq 0,7$ MPa

$F_1 = 0,003$; $n_1 = 0,4$ for $p_2 < 0,7$ MPa

The coefficient N_1 in Eq (4) may be calculated as follows:

For $p_2 < 0,7$ MPa

$$N_1 = 138,88 \left(\frac{d_g}{x_{gr}}\right)^{0,62} \cdot L_p^{-0,06} \cdot We^{-0,05} \cdot M^{-0,2} \quad \dots\dots\dots (6)$$

For $p_2 \geq 0,7$ MPa

$$N_1 = 347 \left(\frac{d_g}{x_{gr}}\right)^{0,62} \cdot L_p^{-0,06} \cdot We^{-0,05} \cdot M^{-0,4} \quad \dots\dots\dots (7)$$

The mean droplet velocity at distance x may be approximately expressed as follows:

For $x < x_{gr}$

$$V_m = 0,7 \cdot A_i \cdot v \cdot \left(\frac{d_g}{x}\right)^{0,43} \cdot We^{0,24} \cdot L_p^{-0,114} \cdot M^{-0,43 \cdot n_1} \quad \dots\dots\dots (8)$$

where: $n_1 = 0,5$ for $p_2 \geq 0,7$ MPa

$n_1 = 0,225$ for $p_2 < 0,7$ MPa

For $x > x_{gr}$

$$V_m = \frac{1}{2\sqrt{2} \cdot D_1} \cdot v \cdot \left(\frac{d_g}{x}\right) \cdot We^{0,21} \cdot L_p^{0,16} \cdot M^{-m_1} \quad \dots\dots\dots (9)$$

where: $D_1 = 3$; $m_1 = 1$ for $p_2 \geq 0,7$ MPa

$D_1 = 0,22$; $m_1 = 0,45$ for $p_2 < 0,7$ MPa

Coefficient A_i in the Eq (8) may be calculated as:

$$A_i = K_1 \cdot \left(\frac{d_g}{x_{gr}}\right)^{0,57} \cdot We^{-0,03} \cdot L_p^{-0,046} \cdot M^{-b_1} \quad \dots\dots\dots (10)$$

where: $K_1 = 0,17$; $b_1 = 0,285$ for $p_2 \geq 0,7$ MPa

$K_1 = 2,295$; $b_1 = 0,13$ for $p_2 < 0,7$ MPa

Fuel concentration may be expressed as:

$$C_m = \rho_m / V_m, \quad \rho_m / \text{kg/m}^2\text{s}; \quad C_m / \text{kg/m}^3 /$$

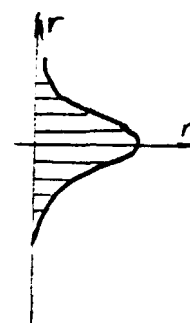
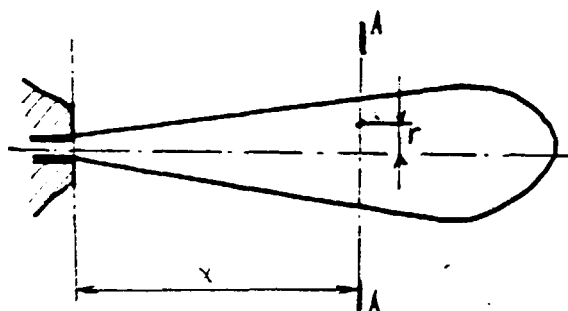
and the mass of one droplet:

$$P_k = \rho_g \cdot V_k; \quad V_k = d_k^3 \cdot \pi / 6$$

and finally:

$$m_m = C_m / P_k \quad / \quad \frac{\text{number of droplet}}{m^3} /$$

The concentration expressed in number of droplet per unit volume may be obtained at any distance x of the spray axis also.



$$n = n_m \cdot \exp\left[-\frac{1}{6 \cdot a_c^2} \left(\frac{r}{x}\right)^2\right] \quad \dots\dots\dots(11)$$

where:

$$a_c = F_i \cdot We^{0,3} \cdot L_p^{0,1} \cdot M^{n_1} \quad \dots\dots\dots(12)$$

where:

$$n_1 = 0,8 \text{ for } p_z \geq 0,7 \text{ MPa}$$

$$n_1 = 0,4 \text{ for } p_z < 0,7 \text{ MPa}$$

The possibility of application of LDE in connected with poly-dispersed spray. At the same time in the optical direction we have abatement and dissipation of emission. Therefore, the degree of influence of heterogeneous dispersed spray on the measurements has to be estimated at first. For purpose of estimation of spray influence the optical depth may be used, expressed as follows:

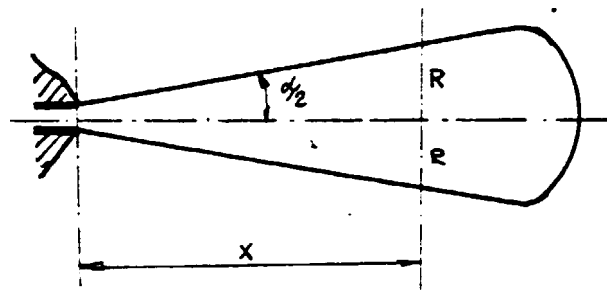
$$\gamma = \frac{a^2 \cdot L}{l^3} \quad \dots\dots\dots(13)$$

where: a =radius of droplet
 L =length of optical depth
 l =mean distance between droplets

Dissipation is too large for $\tau \gg 1$, thus LDE method could not be applied or the large error of the results of measurement has to be tolerated.

The prerequisite related to a small error of measurements supposes:

$$\tau \ll 1 \dots\dots\dots(14)$$



$L=2R=2x \cdot \text{tg } \alpha/2$ - length of optical depth.

Using the Fig. shown and Eq (13) results in:

$$\tau = 1,5 \cdot \frac{C_m \cdot x \cdot \text{tg } \frac{\alpha}{2}}{P_g \cdot \pi \cdot d_{32}^2} \dots\dots\dots (15)$$

where:

Sauter mean dia. $d_{32} = 1,48 d_k$

Fig.3 shows an example of optical depth obtained by experiments.

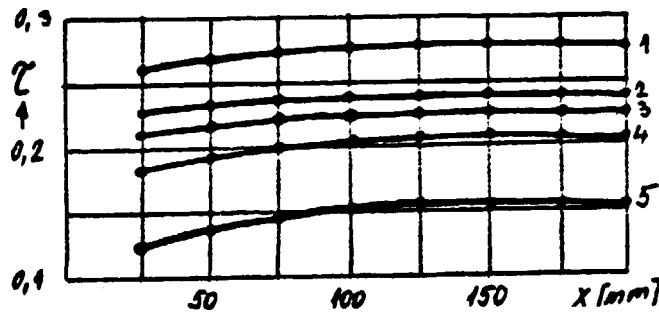


Fig.3 Optical depth by measurement vs. distance x for various nozzle holes d_B and pressures
 1- $p_{II}=5$ MPa , $p_z=0,5$ MPa , $d_B=0,3$ mm
 2- $p_{II}=20$ MPa , $p_z=2$ MPa , $d_B=0,2$ mm
 3- $p_{II}=20$ MPa , $p_z=2$ MPa , $d_B=0,3$ mm
 4- $p_{II}=20$ MPa , $p_z=0,5$ MPa , $d_B=0,3$ mm
 5- $p_{II}=80$ MPa , $p_z=0,5$ MPa , $d_B=0,3$ mm

Approaching to $\tau=1$ the informations of the movement of some droplets may be lost because of a large optical depth. Optical depth shown in Fig 3 was calculated but also checked indirectly.

Spray tip velocity along x axis is shown in Fig 4. Max. velocity equals fuel out-flow one at the nozzle hole exit. At large distances x and low pressure p_{II} , droplet velocity approaches zero.

It's well established fact, that our attention must be paid to the spray characteristics in the period of ignition delay. At the end of ignition delay period the tip velocity or "velocity of mean Sauter droplet" may be reduced till 20 m/s. Therefore, the application of LDE method is important for low spray velocities also.

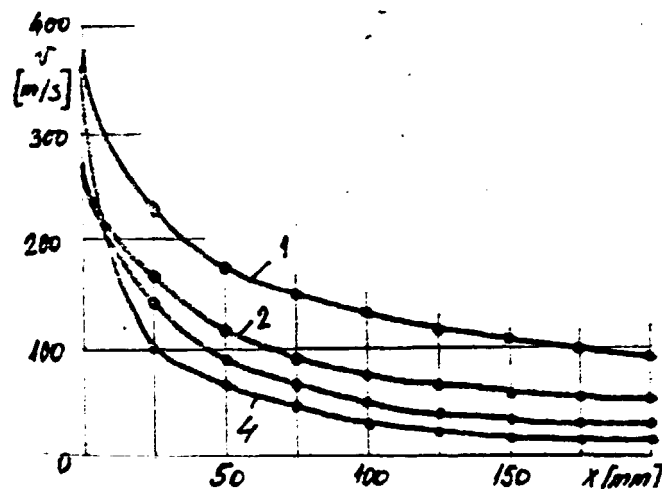


Fig.4 Spray tip velocity vs. distance x

- 1- $p_{II}=80$ MPa , $p_z=0,5$ MPa , $d_B=0,5$ mm
- 2- $p_{II}=40$ MPa , $p_z=0,5$ MPa , $d_B=0,5$ mm
- 3- $p_{II}=40$ MPa , $p_z=0,5$ MPa , $d_B=0,3$ mm
- 4- $p_{II}=80$ MPa , $p_z=2,0$ MPa , $d_B=0,5$ mm

Droplet concentrations characteristics-n vs. length of spray-x are shown in Fig 5. It may be seen that the concentration changes in a quite large proportion. However, LDE method is effective for relatively small droplet number per unit volume.

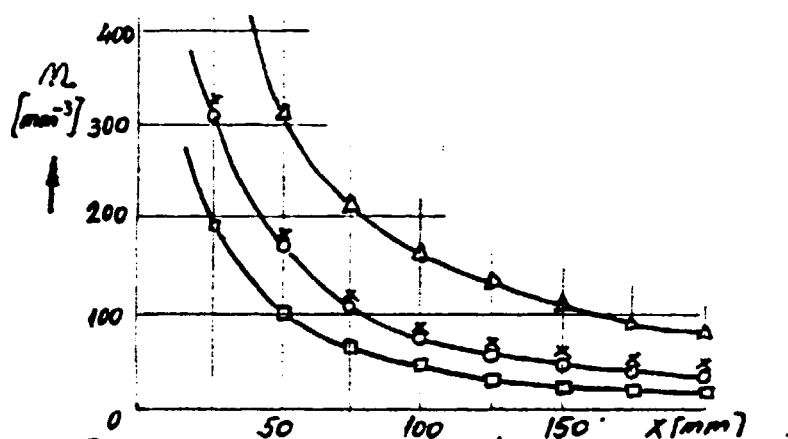


Fig.5 Droplet concentration vs. distance x

- Δ - $p_{II}=60$ MPa, $p_z=2,0$ MPa, $d_k=20$ μm, $d_B=0,3$ mm
- x - $p_{II}=60$ MPa, $p_z=2,0$ MPa, $d_B=0,3$ mm, $d_k=28$ μm
- - $p_{II}=20$ MPa, $p_z=2,0$ MPa, $d_B=0,3$ mm, $d_k=40$ μm
- - $p_{II}=60$ MPa, $p_z=0,5$ MPa, $d_B=0,3$ mm, $d_k=40$ μm

The min. volume for analysis approaches $0,002-0,0025$ mm³ and the max. concentration ranges $400-500$ droplets/mm³. The later said supposes rig test experiments under pressurized ambient. Fig. 5 shows, that the above requirement related to concentration was reached at:

$$x \geq 35+40 \text{ mm}$$

TAM approach for $x < 40$ mm may be explained as follows:

- measurements at $x=50$ mm and at $x=70$ mm
- analysis
- using the data measured, calculation may be applied for shorter x distances.

The volume mean dia. of droplet for diesel oil D2 ranges $20+100$ μm. Therefore, the range of $5-500$ μm of dispersed droplets is of interest. For the purpose of calibration helps disperser producing monodispersed spray of about 5 μm droplets dia.

Fuel spray applied in diesel engine is unsteady with duration of about $2+5$ ms, but the pressure range increase (dp_{II}/dt) may reach $60+70$ MPa/1 ms effecting very drastically all characteristics of the spray.

LDE method may be applied in rig test experiments for fuel spray investigations, supposing the bellow cited characteristics of it instrumentation :

- velocity range 20+400 m/s
- max. droplet concentrations of about 400 droplets/mm³
- droplet dia.'s of 5+500 μm
- spherical droplet shape
- period of measurements 10+15 ms
- max. velocity of changing of parameters investigated 300%/lms.

LDE may not be applied for spray analysis at $x < 40$ mm.

Examples of calculation

1. Diesel oil D2

Fuel density $\rho_g = 840$ kg/m³

" viscosity $\mu_g = 2,1 \cdot 10^{-3}$ Ns/m²

" surface tension $\sigma_g = 0,028$ N/m

Nozzle hole dia. $d_B = 0,4$ mm

Pressure before nozzle hole $p_{II} = 600$ bar

"In-cylinder" pressure $p_z = 40$ bar

"In-cylinder" temperature $T_z = 1100$ K

Air "in-cylinder" density $\rho_z = 12,67$ kg/m³

Spray angle:

$$\tan \frac{\alpha}{2} = D_1 \cdot We^{0,32} \cdot L_p^{0,07} \cdot M^{0,1}$$

$$We = \frac{\rho_g \cdot v_g^2 \cdot d_B}{\sigma_g} = \frac{840 \cdot \left(\sqrt{\frac{2}{840} \cdot (600 - 40)} \right)^2 \cdot 0,4 \cdot 10^{-3}}{0,028} = 1,6 \cdot 10^6$$

Laplace number:

$$L_p = \frac{\rho_g \cdot d_B \cdot \sigma_g}{\mu_g^2} = \frac{840 \cdot 0,4 \cdot 10^{-3} \cdot 0,028}{(2,1 \cdot 10^{-3})^2} = 2133,3$$

Density ratio:

$$M = \frac{\rho_z}{\rho_g} = \frac{12,67}{840} = 0,0155$$

Thus:

$$\tan \frac{\alpha}{2} = 0,0112 \cdot (1,6 \cdot 10^6)^{0,32} \cdot (2133,3)^{0,07} \cdot 0,0155^{0,5} = 0,2305 \rightarrow \alpha = 25,96^\circ$$

Potential core end: $X_{gr} = C_1 \cdot d_B \cdot We^{0,25} \cdot L_p^{-0,4} \cdot M^{-2,1} =$

$$= 8,85 \cdot 0,4 \cdot 10^{-3} \cdot (1,6 \cdot 10^6)^{0,25} \cdot (2133,3)^{-0,4} \cdot 0,0155^{-2,1} = 71,487 \text{ mm}$$

Volume mean droplet dia.:

$$d_k = 2,21 \cdot d_B \cdot (M \cdot We)^{-0,266} \cdot L_p^{-0,073} =$$

$$= 2,21 \cdot 0,4 \cdot 10^{-3} \cdot (0,0155 \cdot 1,6 \cdot 10^6)^{-0,266} \cdot 2133,3^{-0,073} =$$

$$= 34 \mu m$$

Sauter mean dia.:

$$d_{32} = 1,48 \cdot d_k = 50,32 \mu m$$

Specific dimensionless flow at distance $x = 90 \text{ mm}$ ($x > x_{gr}$) may be calculated as follows:

$$\frac{q_m}{q_0} = 0,125 \cdot F_1^{-2} \left(\frac{d_B}{x}\right)^2 \cdot L_p^{-0,2} \cdot We^{-0,6} \cdot M^{-2n_1} =$$

$$= 0,125 \cdot 0,019^{-2} \cdot \left(\frac{0,4 \cdot 10^{-3}}{0,09}\right)^2 \cdot 2133,3^{-0,2} \cdot (1,6 \cdot 10^6)^{-0,6} \cdot 0,0155^{-2 \cdot 0,8} =$$

$$= 2,212 \cdot 10^{-4}$$

Spray tip velocity at distance $x = 90 \text{ mm}$ is calculated as:

$$V_m = \frac{1}{2\sqrt{2} \cdot D_1} \sqrt{\frac{2}{\rho} (\rho_1 - \rho_2)} \cdot \left(\frac{d_B}{x}\right) \cdot We^{0,21} \cdot L_p^{-0,16} \cdot M^{-n_1} =$$

$$= \frac{1}{2 \cdot 1,41 \cdot 3} \cdot \sqrt{\frac{2}{840} (600 - 40) \cdot 10^5} \cdot \left(\frac{0,4 \cdot 10^{-3}}{0,09}\right) \cdot (1,6 \cdot 10^6)^{0,21} \cdot 2133,3^{-0,16} \cdot 0,0155^{-1} =$$

$$= 72,03 \text{ m/s}$$

2. Methanol

CH₃OH density $\rho_g = 774 \text{ kg/m}^3$
 " viscosity $\mu_g = 0,4 \cdot 10^{-3} \text{ Ns/m}^2$
 " surface tension $\sigma_g = 0,021 \text{ N/m}$

All other data as for the aforegiven example with diesel oil

Weber number:

$$We = \frac{774 \left(\sqrt{\frac{2}{774} (600 - 40) \cdot 10^5}\right)^2 \cdot 0,4 \cdot 10^{-3}}{0,021} = 2,13 \cdot 10^6$$

Laplace number:

$$L_p = \frac{774 \cdot 0,4 \cdot 10^{-3} \cdot 0,021}{(0,4 \cdot 10^{-3})^2} = 4,06 \cdot 10^4$$

Density ratio:

$$M = \frac{12,67}{774} = 0,0164$$

Spray angle:

$$\tan \frac{\alpha}{2} = D_1 \cdot W^{0,32} \cdot L_p^{0,07} \cdot M^{n_1} =$$

$$= 0,0112 \cdot (2,13 \cdot 10^6)^{0,32} \cdot (4,06 \cdot 10^4)^{0,07} \cdot 0,0164^{0,5} = 0,319 \rightarrow \alpha = 35,4^\circ$$

The end of potential core:

$$x_{gr} = C_1 \cdot d_B \cdot We^{0,25} \cdot L_p^{-0,4} \cdot M^{-2,1} =$$

$$= 8,85 \cdot 0,4 \cdot 10^{-3} \cdot (2,13 \cdot 10^6)^{0,25} \cdot (4,06 \cdot 10^4)^{-0,4} \cdot (0,0164)^{-2,1} =$$

$$= 22,8 \text{ mm}$$

Volume mean droplet dia.:

$$d_k = 2,21 \cdot d_B \cdot (M \cdot We)^{-0,266} \cdot L_P^{-0,073} = 2,21 \cdot 0,4 \cdot 10^{-3} \cdot (0,0164 \cdot 2,13 \cdot 10^6)^{-0,266} \cdot (4,06 \cdot 10^4)^{-0,073} = 25 \mu\text{m}$$

Sauter mean dia.:

$$d_{32} = 1,48 \cdot d_k = 37 \mu\text{m}$$

Specific dimensionless flow at distance $x=90 \text{ mm}$ ($x > x_{gr}$) may be calculated as follows:

$$\frac{g_m}{g_0} = 0,125 \cdot F_1^{-2} \left(\frac{d_B}{x}\right)^2 \cdot L_P^{-0,2} \cdot We^{-0,6} \cdot M^{-2,71} = 0,125 \cdot 0,019^{-2} \cdot \left(\frac{0,4 \cdot 10^{-3}}{0,09}\right)^2 \cdot (4,06 \cdot 10^4)^{-0,2} \cdot (2,13 \cdot 10^6)^{-0,6} \cdot 0,0164^{-2,71} = 9,45 \cdot 10^{-5}$$

Spray tip velocity at distance $x=90 \text{ mm}$ is calculated as:

$$V_m = \frac{1}{2,12 \cdot D_1} \sqrt{\frac{2}{\rho} (\rho_E - \rho_2)} \cdot \left(\frac{d_B}{x}\right) \cdot We^{0,21} \cdot L_P^{-0,16} \cdot M^{-0,11} = \frac{1}{2,12 \cdot 3} \sqrt{\frac{2}{774} \cdot (600 - 60) \cdot 10^5} \cdot \left(\frac{0,4 \cdot 10^{-3}}{0,09}\right) \cdot (2,13 \cdot 10^6)^{0,21} \cdot (4,06 \cdot 10^4)^{-0,16} \cdot 0,0164^{-0,11} = 47,54 \text{ m/s}$$

Note: All expressions derived serve for the both, experimental arrangement and avoidance of measurement in error.

For methanol let's calculate the parameters related to LDE experimental application.

g_0 (see Eq 4) may be calculated as:

$$g_0 = \rho_g \cdot V$$

$$V = \sqrt{\frac{2}{\rho} (\rho_E - \rho_2)} = \sqrt{\frac{2}{774} (600 - 60) \cdot 10^5} = 373 \frac{\text{m}}{\text{s}}$$

$$\rho = 774 \text{ kg/m}^3$$

$$g_0 = 373 \cdot 774 = 2,88702 \cdot 10^5 \frac{\text{kg}}{\text{m}^2 \text{s}}$$

$$g_m = 9,45 \cdot 10^{-5} \cdot 2,88702 \cdot 10^5 = 27,28 \frac{\text{kg}}{\text{m}^2 \text{s}}$$

$$C_m = \frac{g_m}{V_m} = \frac{27,28}{47,54} = 0,57388 \frac{\text{kg}}{\text{m}^3}$$

$$n_m = \frac{C_m}{\rho_k}$$

$$\rho_k = \rho \cdot V_k = 774 \cdot \frac{1}{6} \cdot 25^3 \cdot \pi \cdot 10^{-18} = 6,33 \cdot 10^{12} \text{ kg}$$

$$n_m = \frac{C_m}{\rho_k} = \frac{0,57388}{6,33 \cdot 10^{12}} = 90,6 \frac{\text{droplets}}{\text{mm}^3}$$

(Note $\text{m}^3 = 10^9 \text{ mm}^3$)

It means that we have less than 400 droplets/mm³, thus related to n_m LDE for the distance 90 mm selected, may be applied.

Optical depth

$$\tau = \frac{d_k^2 L}{\lambda^3}$$

$$L = 2 \cdot x \cdot \operatorname{tg} \frac{\alpha}{2} = 2 \cdot 90 \cdot 0,319 = 57,42 \text{ mm}$$

To define l we calculate:

$$90 \cdot \left(d_k + \frac{l}{2}\right)^2 \cdot \frac{\pi}{4} = 1 \text{ mm}^2 = 10^6 \mu\text{m}^2$$

$$\left(25 + \frac{l}{2}\right)^2 \cdot 90 \cdot \frac{\pi}{4} = 10^6 \rightarrow l = 188 \mu\text{m}$$

$$\tau = \frac{25^2 \cdot 57,44 \cdot 10^3}{188^3} = 5,36$$

Some disturbances caused by screening effect may be expected. However, because of low C_m some corrections may be applied.

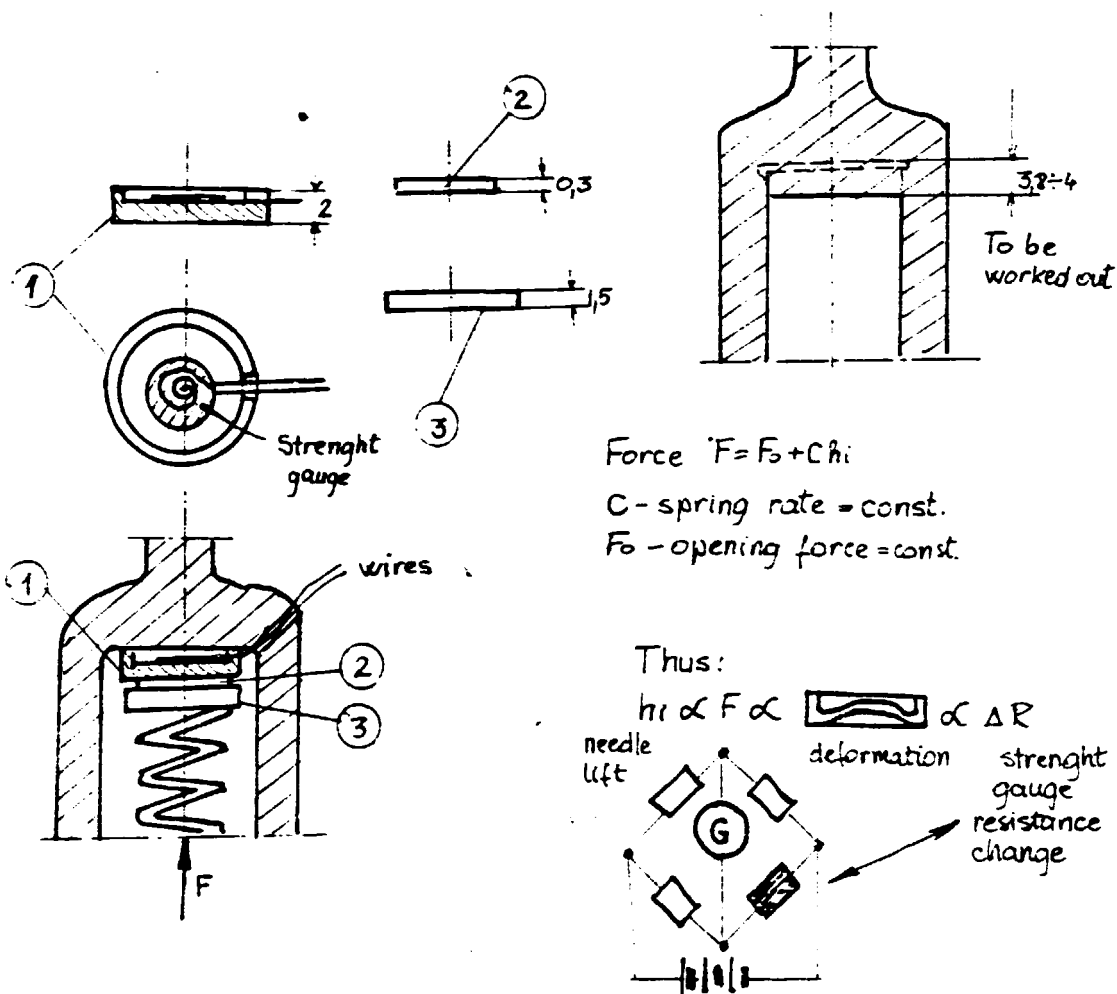
In order to define the optical depth we have to equal $\tau=1$
This calculation gives $L=10,7 \text{ mm}$

Auxiliary needle lift measurement technique

Needle lift measurements may be performed using streight gauge technique also. If one appropriate bridge and a small membrane streight gauge exist the other arrangements are very simple.

However, the needle lift diagraphes recorder suffer from:

- some nelinearity (what is also not important)
- some other oscillations may be noticed in needle lift diagraphes at the end



Force $F = F_0 + Ch_i$
 C - spring rate = const.
 F_0 - opening force = const.

Thus:
 $h_l \propto F \propto \Delta R$
 needle lift, deformation, streight gauge resistance change

The Fig's shown explain the arrangement

How to calculate injector holes ?

Fuel injected per one cycle or fuelling may be expressed as follows:

$$G = b_e \frac{P_e}{3600 \cdot n_M \cdot z \cdot i_2} \left[\frac{g}{\text{cycle cylinder}} \right] \dots(1)$$

where:

- b_e /g/kWh/ -fuel consumption rate
- P_e /kW/ -power output
- n_M /s⁻¹/ -rotational engine speed
- $z = 0,5$ - 4 stroke eng. , $=1$ -2 stroke engine

iz - cylinder number

Substituting Eq (1) into expression of the injection law results in:

$$\mu_0 F_0 = \frac{G}{4472 \cdot \rho_k \cdot \tau_E} \cdot \sqrt{\frac{\rho_k}{\rho_{avo} - \rho_G}} \quad [cm^2] \quad \dots\dots(2)$$

where:

ρ_k /g/cm³/ -specific fuel mass

τ_E /s/ -injection time

$P_{EVD} = P_{III}$ /MPa/ -fuel pressure before injector

P_G /MPa/ -in-cylinder pressure

F_0 /cm²/ -geometrical cross-sectional flow area of the injector holes

A_D /-/-coefficient of discharge (ranges 0,6+0,8).

Distance of the spray tip vs. time (or angle) is a factor for fuel system matching to the combustion chamber and piston movement (see x in "Dynamic").

Moreover, depending on the comb. process in development and fuel used the importance of ignition delay may be very high. Thus, quantity of the fuel injected and spray tip history could'nt be neglected.

At first we calculate the angle of ignition delay (α_{zv}); per example for D2 fuel acc. Sitkei as follows:

$$\alpha_{zv} = 0,36 \cdot \eta_m \left[0,5 + \left| \frac{0,0256}{P_c^{0,7}} - \frac{0,0735}{P_c^{1,6}} \right| e^{\frac{19,32}{T_c}} \right] [KW] \quad \dots\dots(3)$$

or by time:

$$\tau_{zv} = \frac{\alpha_{zv}}{360 \cdot n_m} \quad [s] \quad \dots\dots(3')$$

Eq (3) was derived for diesel fuel but the same influencing factors with have with other fuels also. With CH₃OH, acc. to Eq (3), the both, the pressure- and the temperature of compression are dropping down, because of excess cooling. The above results in: knocking or misfiring. Therefore, retarded injection as well as controlled

injection quantity in τ_{zv} -time ,may help significantly.

Siegfried and Ahmed developed the formule for spray tip penetrati-
on as:

$$\Delta S_{st} = 0.027 \frac{d_d}{(\Sigma \Delta T)^{0.85}} \cdot H_o^{0.48} \cdot R_e^{0.3} \cdot \left(\frac{\rho_k}{\rho_L}\right)^{0.15} \quad [cm] \quad \dots\dots(4)$$

where: ΔT -increment of time /s/

$$H_o = \frac{w_o \cdot T}{d_d} \quad ; \quad R_e = \frac{w_o \cdot d_d}{\nu_k} \quad ; \quad \rho_L \text{ - air density } \left[\frac{g}{cm^3}\right]$$

Eq (4) was derived recently, where only in-cylinder pressure but without air motion was respected.

From Eq (4) nozzle hole dia. may be obtained:

$$d_d = \left[\frac{20827 \cdot 10^5 \cdot S_{st} \cdot \nu_k^{0.3} \cdot \Delta T^{0.37}}{w_o^{0.79} \left(1 + \frac{1}{2^{0.85}} + \frac{1}{3^{0.85}} + \frac{1}{j^{0.85}}\right)} \cdot \left(\frac{\rho_L}{\rho_k}\right)^{0.15} \right]^{1.22} \quad [cm] \quad \dots\dots(5)$$

The fuel velocity at the exit of the nozzle hole may be calculated by:

$$w_o = 4.4721 \cdot 10^3 \cdot \mu_D \cdot \sqrt{\frac{P_{cvo} - P_c}{\rho_k}} \quad \left[\frac{cm}{s}\right] \quad \dots\dots(6)$$

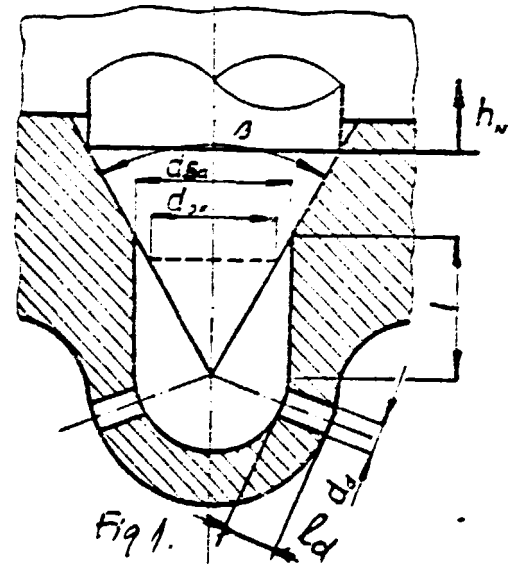
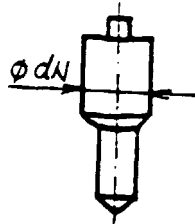
From Eq.'s (2) and (5) we obtain the number of the nozzle holes as:

$$i = \frac{\mu_D F_D}{\mu_D \frac{\pi d_D^2}{4}} \quad \dots\dots(7)$$

Dia ϕd_{sa} (see Fig 1) may be calculated by:

$$d_{sa} \approx \frac{2}{\pi} \cdot d_d \cdot i \quad [cm] \quad \dots\dots(8)$$

The simple approach shown, may be useful by CH_3OH application also.



After aforeshown calculation the choice related to needle seat dia (d_{si}) or needle opening pressure (P_0) has to be done.

When the bellow cited data are known:

- d_N needle dia (Fig 1)
- p_z max in-cylinder pressure
- d_{SA} sack hole dia (Fig 1)
- p_0 needle opening pressure
- p_s needle closing pressure

needle seat dia. (d_{si}) may be calculated as follows:

$$d_{si} = \sqrt{\frac{d_w^2 (p_0 - p_s) + 0.5 \cdot d_{sa}^2 (p_s - p_s)}{p_0 + 0.5 (p_z - p_s)}} \quad [cm] \quad \dots(9)$$

Sometimes is more convenient to use an accustomed hydraulic ratio (see the book Černej-Dobovišek, "Injection"). Doing that, seat dia. d_{si} known and the needle closing pressure may be defined as:

$$p_s = \frac{(d_w^2 - d_{si}^2) p_0 - (d_w^2 - d_{sa}^2) 0.5 \cdot p_s}{d_w^2 - 0.5 (d_{si}^2 + d_{sa}^2)} \quad [MPa] \quad \dots(10)$$

However, injector hole dia. (d_g) must be examined related to cavitation also.

Thus minim. (d_{dmin}) nozzle hole dia. to prevent cavitation may be defined as:

For $l_d/d_d > 3$ (see Fig 1)

$$d_{dmin} = 0,0053 \sqrt{\frac{b_e \cdot P_e \cdot K_{\bar{u}}}{\rho_k \cdot l_z \cdot \frac{l_e}{2} \cdot i}} \sqrt{\frac{\rho_k}{M_d} \left(\frac{2 - 2M_d - M_d \cdot \lambda \cdot l_e/d_d}{p_s - p_0} \right)} \quad [cm] \dots(11)$$

For $l_d/d_d \leq 3$

$$d_{dmin} = 0,00634 \sqrt{\frac{b_e \cdot P_e \cdot K_{\bar{u}}}{\rho_k \cdot l_z \cdot \frac{l_e}{2} \cdot i}} \sqrt{\frac{\rho_k}{M_d} \left(\frac{1 - M_d}{p_0 - p_0} \right)} \quad [cm] \dots(12)$$

where:

$K_{\bar{u}}$ /-/- coefficient of overloading (1,1+1,12)

\mathcal{L}_E /°CA/ -duration of injection

Supposing the avoidance of cavitation phenomenon, the max. velocity at the nozzle hole may be calculated as:

$$W_{2max} = 3152,4 \sqrt{\frac{p_2 - p_0}{\rho_2 \left(\frac{1}{\mu_2} - 1 - \frac{\lambda}{2} \frac{l_2}{d_2} \right)}} \left[\frac{cm}{s} \right] \dots\dots(13)$$

where:

λ = coefficient of friction in the nozzle hole ($\lambda = 0,02$)

To obtain the effective cross-sectional nozzle hole area in dependence of needle lift two locations must be considered:

- flow area at needle seat
- flow area at nozzle holes

The both types of needle tip will be considered:



Geometrically defined cross-sectional flow area of the nozzle holes:

$$F_d = i \frac{d_0^2 \cdot \pi}{4} \quad [cm^2] \dots\dots(14)$$

For the cross-sectional flow area of the needle seat (see Fig 1) the next expression may be derived:

$$F_{si} = h_n \cdot \pi \left(d_{sa} - \frac{h_n}{2} \sin \beta \right) \sin \frac{\beta}{2} \quad [cm^2] \dots\dots(15)$$

The expression (15) may be applied for the both needles, Type 1 and Type 2 under condition:

$$\text{respectively} \quad d_{of} \leq d_{sa} - \frac{h_n}{2} \sin \beta \quad h_n \leq \frac{2(d_{sa} - d_{of})}{\sin \beta}$$

$$F_{si} = h_n \cdot \pi \left(d_{of} + \frac{h_n}{2} \sin \beta \right) \sin \frac{\beta}{2} \quad [cm^2] \dots\dots(16)$$

The expression (16) may be applied for needle Type 2 under condition:

$$d_{of} > d_{sa} - \frac{h_n}{2} \sin \beta$$

respectively

$$h_n > \frac{2(d_{sa} - d_{of})}{\sin \beta}$$

Discharge coefficient of the needle cone-seat area (Fig 1) depends on quality of surfaces and ranges 0,77-0,9. Discharge coefficient of nozzle hole may be calculated, as shown bellow.

Ratio of geometrical flow areas of nozzle holes and sack hole (see Fig 1- ϕd_{sa}) may be expressed as:

$$m = \frac{F_d}{F_{sa}} \quad \dots\dots\dots (17)$$

and pressure ratio as:

$$X = \frac{P_{sa} - P_G}{P_G} \quad \dots\dots\dots (18)$$

where: P_{sa} - instanteneous fuel pressure in sack hole

P_G - instanteneous in-cylinder pressure

X value is limited related to cavitation, thus ($X_{max} = X_{grenz}$):

$$X_{grenz} = \frac{1 - \psi^2 m^2 + 2\psi^2 - 2\psi}{-2\psi^2 + 2\psi} \quad [-] \quad \dots\dots\dots (19)$$

Coefficient ψ may be found by means of Tabeles in dependence of m and rims.

Furthermore discharge coefficient of nozzle hole may be calculated as:

$$\mu_d = \sqrt{\frac{1 - \psi^2 m^2}{1 - \psi^2 m^2 + 2\psi^2 - 2\psi}} \quad [-] \quad \text{for } X \leq X_{grenz} \quad \dots\dots\dots (21)$$

or in other case:

$$\mu_d = \psi' \sqrt{1 + \frac{1}{X}} \quad [-] \quad \text{for } X > X_{grenz} \quad \dots\dots\dots (22)$$

where:

$$\psi' = \frac{\psi}{\sqrt{1 - \psi^2 m^2}} \quad \dots\dots\dots (20)$$

The pressure in the sack hole may be expressed as follows:

at first the mean flow rate to be defined:

$$\dot{V} = \frac{G}{\gamma_E \cdot \rho_k} \quad \left[\frac{\text{cm}^3}{\text{s}} \right] \quad \dots\dots\dots(23)$$

The pressure in the sack hole:

$$P_{sa} = \frac{50 \cdot \dot{V} \cdot \rho_k}{10^9 \cdot (\mu_d F_d)^2} + \frac{P_2 + P_e}{2} \quad \dots\dots\dots(24)$$

And effective flow area of the injector holes:

$$\mu_d F_d = \sqrt{\frac{(\mu_d F_d)^2 \cdot (\mu_{si} F_{si})^2}{(\mu_d F_d)^2 + (\mu_{si} F_{si})^2}} \quad [\text{cm}^2] \quad \dots\dots\dots(25)$$

Sack volume of injector may be calculated as:

$$V_{sa} = \frac{d_{sa}^2 \pi}{4} \cdot \left(l - \frac{d_{sa}}{6 \tan \frac{\beta}{2}} + \frac{d_{sa}}{3} \right) + \frac{1}{6 \tan \frac{\beta}{2}} \cdot \left(\frac{d_{df}^2 \pi}{4} d_{df} \right) [\text{cm}^3] \quad \dots\dots\dots(26)$$

Expression (26) is valid for:

- $d_{df} > d_{sa}$
- for nozzle Type 1 and 2 (for Type 1 $\rightarrow d_{df}=0$) (see Fig 1)

7.1 Controlled singl-hole nozzle (CSEHN)

The function of controlled nozzle as improvement related to ignition was jet explained in the section-neat methanol use in diesel engine. However, pintle nozzle suggested may not be used because of cylinder head. Existed cylinder head to operate with CH_3OH can not be replaced so easily. This is the reason to show one different approach for the use in lab. experiments.

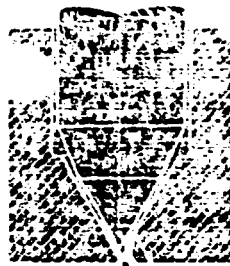
Controlled singl hole nozzle has not the aforementioned drawback, namely, fuel spray may be directed fairly independent of nozzle, holder axis. Thus, existed cylinder head may be used and fuel spray deposition area on the wall of piston bowl may be optimized.

In experiments with CSEHN, MAN tryed four goals to reach:

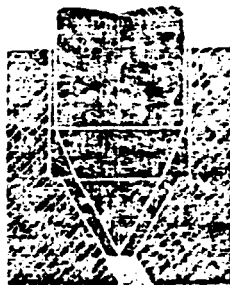
- cylinder head of methanol diesel engine must be the same as for diesel oil operation
- controlled effective flow area
- at low partial loads more fuel dispersed in air
- at higher loads more fuel deposited on the wall

Fig 2 shows the idea.

Difference between one conventional nozzle and CSEHN may be explained by:



partially open hole



fully open hole

Fig 2 - 338H

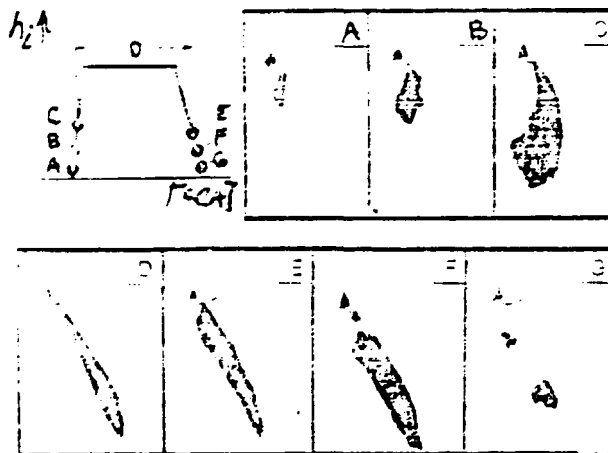


Fig 3 Fuel jet patterns of a controlled single hole nozzle at different positions of nozzle needle (h_1)

- no sack hole
- short toward needle axis directed single hole emerging in nozzle seat surface
- needle tip immersed into nozzle hole

With (CSHN) small needle lifts, seat flow area becomes smaller than that of nozzle hole, thus, fuel spray obtaining a high velocity in the seat area unhampered penetrates more toward the center of the piston bowl, being dispersed more in air.

With fully open injector, hole flow area becomes smaller than seat area, thus, directed dense fuel spray follows hole angle designed.

By means of spray patterns in Fig 5 MAN demonstrated the above cited. With CSHN some decrease in fuel consumption figure as well as better startability of engine were observed.

Defining hole and seat area conversion of more potential energy into kinetic form, before seat area, may produce unwanted pressure losses as well as uncontrolled fuel spray direction. To have idea about above said, by black colored surface demonstrates Fig 4 the relation of kinetic energy converted.

black colored
part of kinetic
energy

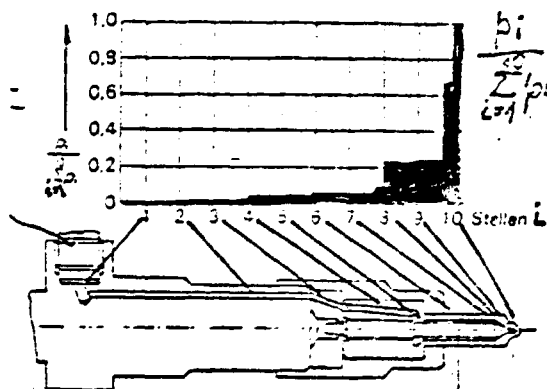


Fig 4

Is to be mentioned, that at position x (see Fig 4) some fillers (fuel filters) convert to much potential energy into kinetic one. It may happen converting to methanol because of fuelling increased. In any way, before seat area only small pressure drop may be permitted.

To obtain more informations about ratios of flow areas, Fig 5 is presented.

When before the needle seat slope of any free area vs. needle lift becomes smaller than that of line a (see Fig 5), injector holder must be corrected.

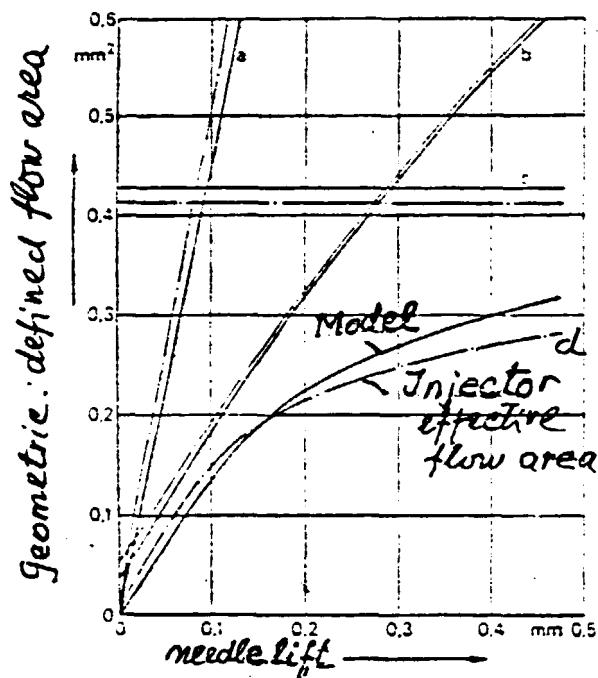


Fig 5 Flow areas vs. needle lift

- a - needle seat flow area
- b - entrance flow area of sack hole
- c - nozzle holes flow area
- a,b,c - geometrically defined
- d - effective flow area of assembled injector

Coefficient of discharge μ_D vs. Reynolds number is presented in Fig 6. As parameter fuel pressure and relative needle lift h/h_{\max} were used.

h/h_{\max} means: measurements were performed without nozzle, thus this data are valid for nozzle holder.

For seat area given coefficient of discharge decreases with nozzle hole dia. increased. The later said has to be considered charging the fuel also. Fig 7 demonstrates the aforementioned. Fig 7 demonstrates also, that for test bench measurements of injector effective flow area is no use the increase the pressure drop over 100 bar (as well jet recommended in the 1st report).

With controlled single hole nozzle seat area must be seriously considered. To give more information about it Fig 8 is presented. Fig 8 demonstrates a high conversion of potential energy into kinetic form of the needle seat area, when low needle lift was set. In other words, lowering the needle lift fuel velocity incre-

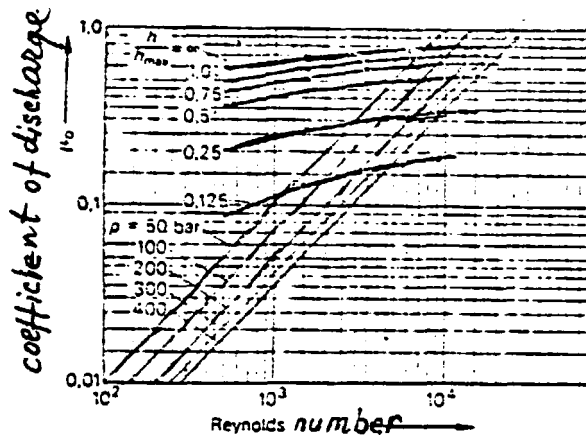


Fig 6 Coefficient of discharge μ_D vs. Reynolds number
DLIA 150 S 186 - injector

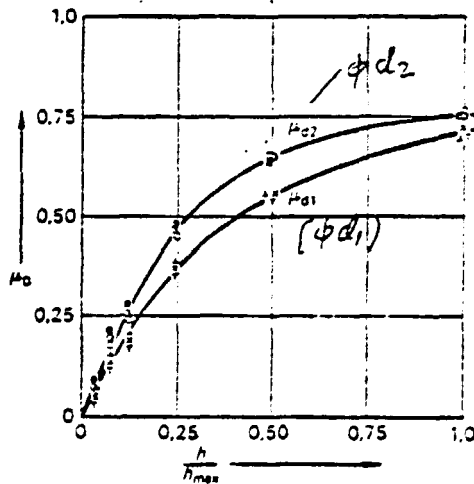
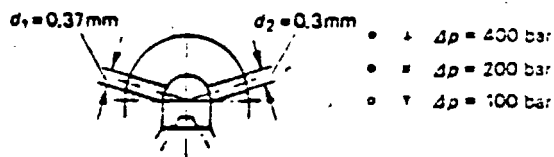


Fig 7 Coefficient of discharge μ_D vs. relative needle lift with nozzle hole dia. and pressure drop (Δp) at nozzle hole as parameters

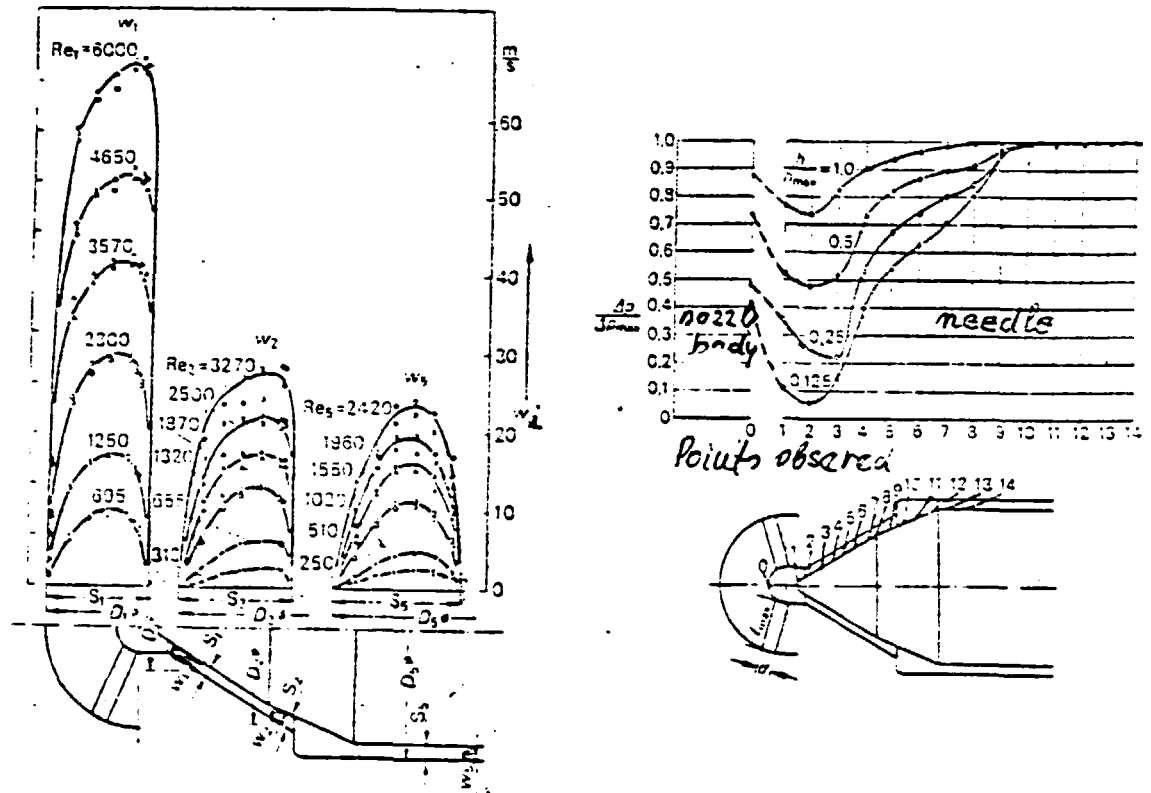


Fig 8 Velocity change along seat area for various pressure drops (on the left) and pressure change at various points in dependence of relative needle lift (on the right). The later measurements mentioned are valid for : nozzle hole dia. ϕ 0,365 mm, $\Delta p_{max}=400$ bar, $h_{max}=0,4$ mm, $l=1,5$ mm.

ases drastically, but in seat flow area. This is the reason that controlled single hole injector was suggested by KAM.

For most practical cases:

$$2,5 \leq l/d \leq 4,5$$

$$\mu_D \approx 0,8 \quad \text{if} \quad \text{seat flow area} \geq 1,7 \cdot \text{nozzle flow area} \\ \text{and} \quad Re_e \geq 10^4$$

Under above conditions the penetration of fuel spray can be obtained from the following equation:

$$S = 13,6 \left[\left(\frac{\Delta p}{\rho_s} \right)^{1/2} \cdot t \cdot d \right]^{1/2} \cdot \left(\frac{530}{T_g} \right)^{1/4}$$

where:

s - penetration distance of jet /in/

Δp - mean effective pressure drop across injector/lb_l/sq.in/

ρ_g - density of gas in bomb or engine cylinder /lb_l/cu.in/

t - injection time /sec/

d - injector orifice diameter /in/

T_g - mean temperature of gas in bomb or engine cylinder /R/

The above Eq. was derived for diesel fuel injected in quiescent compressed air. However, calculating the fuel velocity and replacing the fuel next expression may be used:

$$S = \left[8 \cdot v_{jet} \cdot t \cdot d \cdot \left(\frac{\Delta p}{\rho_g} \right)^{1/2} \right]^{1/2}$$

The both expression given for spray penetration may be considered as very approximative ones. The reason to show them was, first coarse estimation of spray-piston bowl relations.

With:

- book translated, explained and given
- training : theory and praxis
- practical measurements
- first report
- additional material sent as appendices
- three programmes for calculation given
- needle lift measurement completed
- second report

may be considered the engineers being dealing with fuel introduction are fearly well informed related to diesel fuel as well as methanol use.

7.2 Injector wear

Although injector wear was not included in the topics, during subsequent discussion related to lubrication and wear, some recommendations about injector wear were wanted. Thus HP-pump and - tube out of considerations.

Locations of injector wear (see Fig 9)

1. Needle seat
2. Nozzle holes
3. Needle-body sliding area of nozzle

- 4. Injector spring-seat area
- 5. Sealing surfaces on injector holes-nozzle body
- 6. Sack hole
- 7. Needle lift upper seat
- 8. Stem (b)-needle contact surface

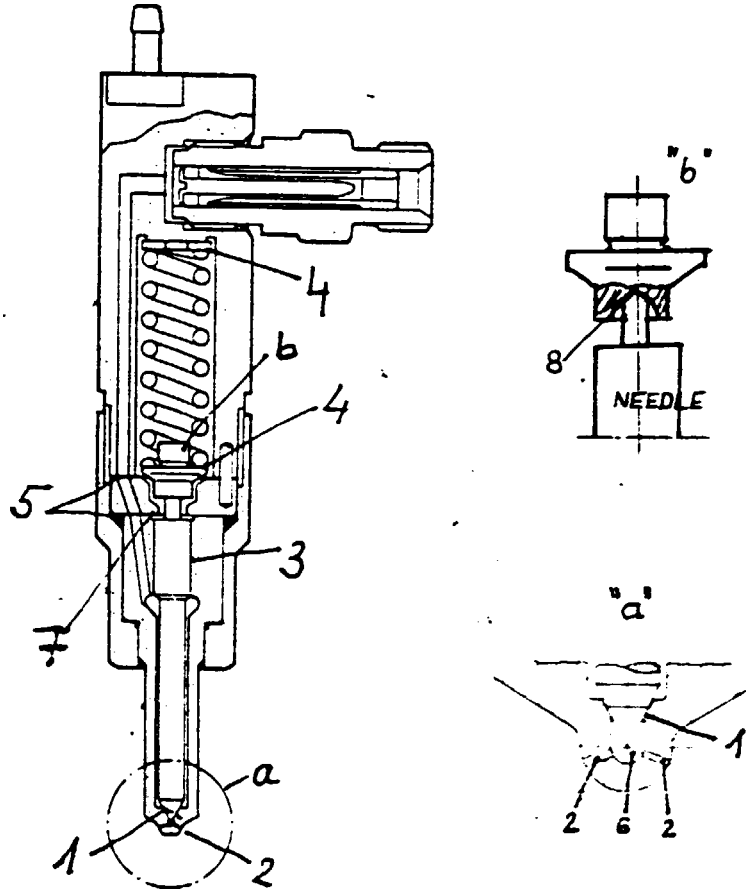


Fig 9 Locations of injector wear

1. Needle seat

- A. Hammering of surface layer accompanied by wear
- B. Contact corrosion
- C. Erosion
- D. Cavitation (in specific case only)
- E. Chemical corrosion

2. Nozzle hole

- A. Cavitation
- B. Erosion
- C. Chemical corrosion (Cacking out of consideration)

3. Nozzle needle-body sliding area

- A. Wear cause by sliding friction
- B. Corrosion

4. Injector spring seat area

- A. Contact corrosion
- B. Chemical corrosion

5. Sealing surfaces on injector holder-nozzle body

- A. Chemical corrosion

6. Sack hole

- A. Cavitation

7. Needle lift upper seat

- A. Fanning of surface layer accompanied by wear

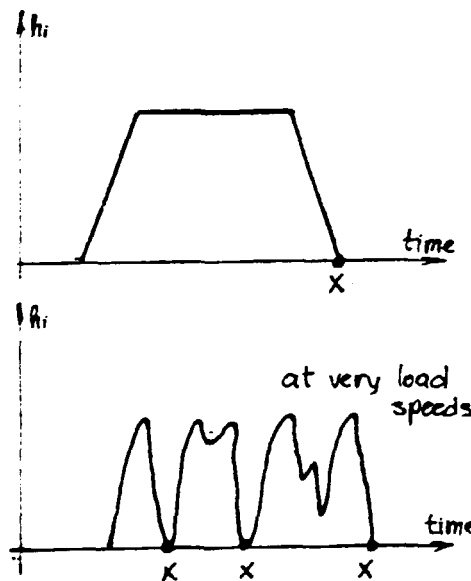
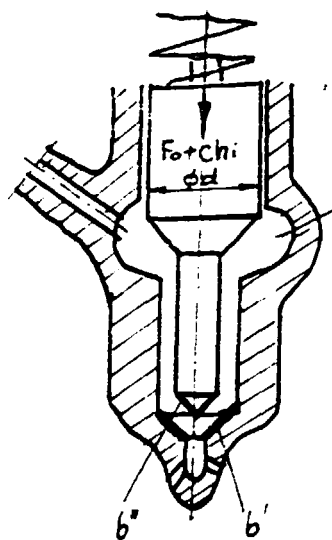
8. Stem needle contact surface

- A. Contact corrosion

1A Fanning of surface layer accompanied1B by wear and contact corrosion

a) Forces effecting needle movement may be balanced as :

$$\underbrace{m \cdot \ddot{h}_i}_{\text{inertia force}} + \underbrace{F_0 + c \cdot h_i}_{\text{spring force}} \pm \underbrace{F_{tr}}_{\text{friction}} = \underbrace{P_{II} \frac{\pi d^2}{4}}_{\text{fuel pressure}}$$



at full load
and higher speeds

at very load
speeds

Fig 10

The both surfaces b' and b'' may be hommersed.

At closing (point x , Fig 10) masses of needle, stem and ^{one} half of spring have been accelerating toward the seat. Needle velocity becomes largest at point x (see Fig 10). Although, max. needle lift with high speed engines amounts $0,25 \pm 0,5$ mm, the hit force is quite high. The impact of the both surfaces,

Depending on thermal treatment of the steels used, caused some small dislocation of the surface layer. At the same time contact corrosion attended as a small high cycle relative movements between two metallic surfaces. The latter said is the main reason of seat wear.

With greater masses, higher speeds and lower stiffness of nozzle body seat area, contact corrosion may produce a very short service life of injector, especially when dirtiness in oil and bad surface texture in production are attended (see Fig 11).

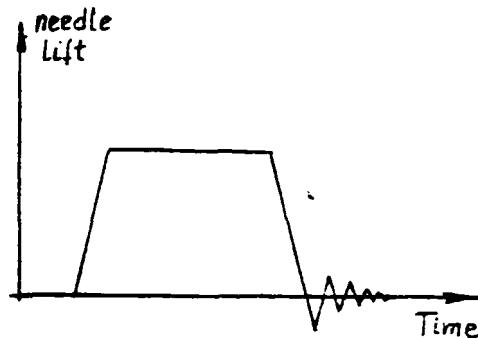


Fig 11 High cycle oscillation at seat area

13.3.3 Erosion, Cavitation and Chemical Corrosion

Fig 12 explains, cavitation wear in seat area may appear very rarely.

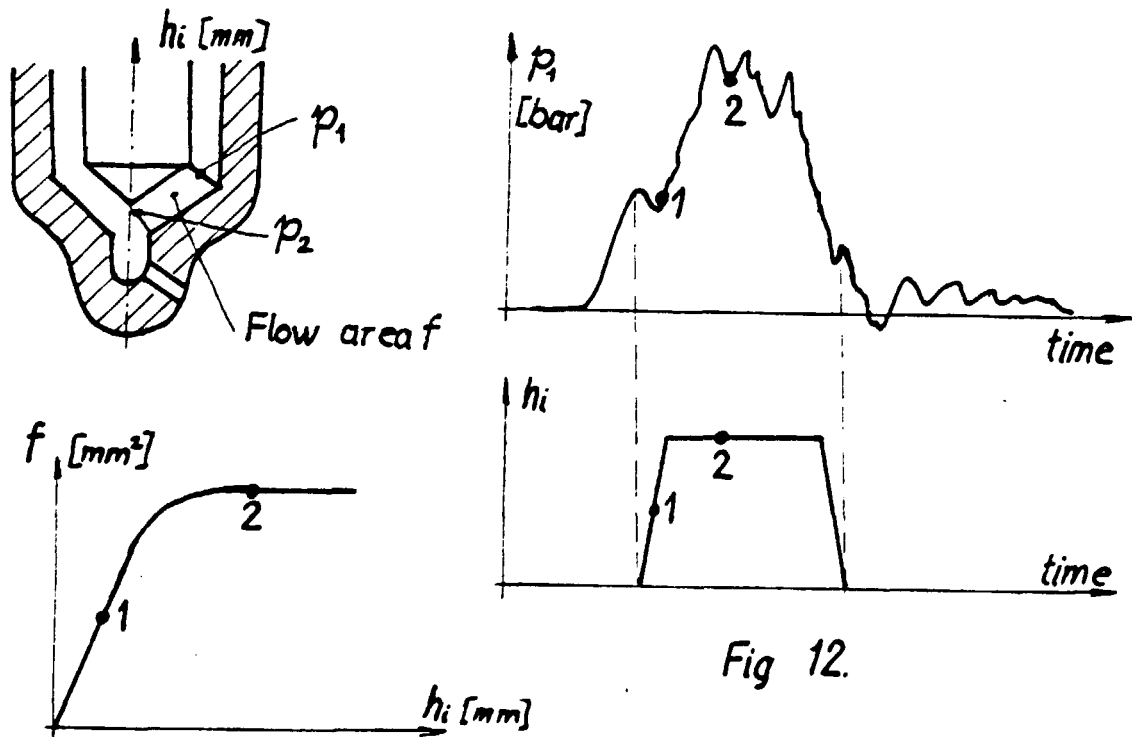


Fig 12.

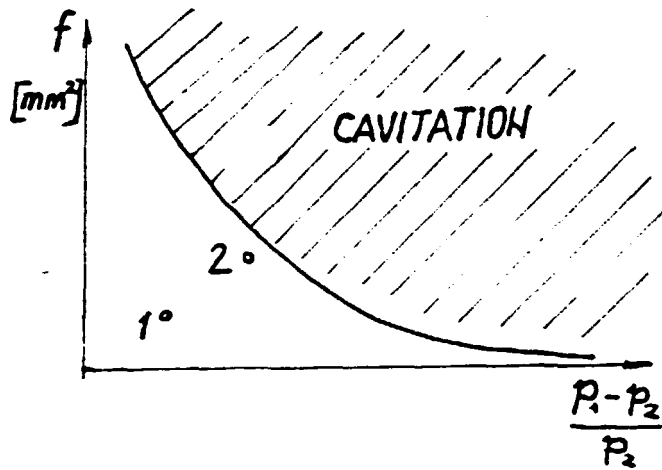


Fig 12

The reason for cavitation is very well known, thus we are not going into details. Erosion becomes higher with dirtiness in oil and is getting higher through time. Chemical attack with diesel oil is mostly promoted if water presented.

Shortcomings

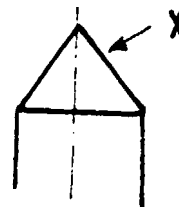
The main drawback is lost of sealing at needle seat. Some increased max. needle lift is not important but accompanied decrease of nozzle opening pressure may be of influence.

Lost of sealing may produce :

- increased soot emission
- increased THC emission
- increased fuel consumption
- increased thermal loading
- increased cylinder-piston-rings wear
- decreased power output
- nozzle hole cocking

Inspection

1. Comparing the surface x of injector tested with new one
2. Increasing opening pressure of injector - p_0 for 10 bar at first, then with constant oil



pressure - no checking if any droplet or leakage may be noticed at nozzle hole exit.

The same procedure should be done with increased ρ , till 350 bar. Now at 300 bar checking, very small wetting on the tip of nozzle body may be allowed.

2. Nozzle hole wear

2 A Cavitation

Cavitation wear will be considered for the both, nozzle holes and sack hole. Fig 13 depicts the cavitation wear of

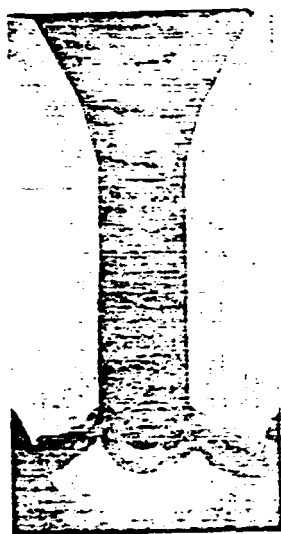


Fig 13 Cavitation wear in nozzle holes after 1000 h of operation.

Phase 0
Before injection
Sack volume filled with gas

Phase 1
First opening phase of needle
Wear at the bottom of sack
----- ZONE ATTACKED

Phase 2
Flow cavitation narrowst
cross-sec. seat area
Cavitation attack at sack
circumference

Phase 3
Total pressure drop in
nozzle holes. Flow cavitation
in nozzle holes

p_{II} - fuel pressure
 h_i - needle lift

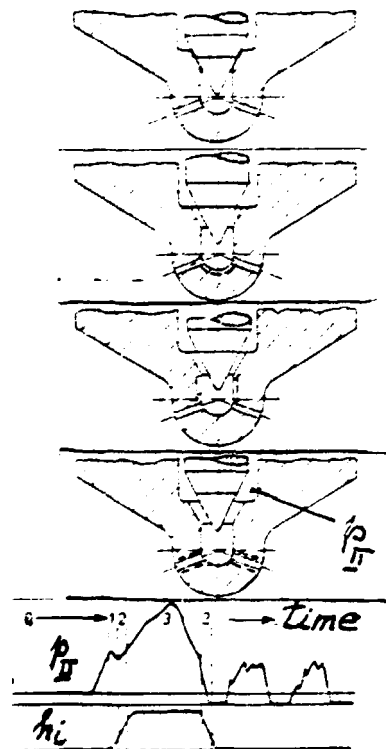


Fig 14

nozzle holes after 1000 h operation. Measured effective cross-sectional flow area of nozzle holes increased by factor 1,67. Unfortunately cavitation wear of nozzle holes may be experienced with some diesel engines. Converting to methanol cavitation wear may increase noticeably.

To give more insight in the cavitation wear of nozzle holes, Fig 14 is presented. Fig 14 clearly demonstrates the locations of potential wear of cavitation. Related to injection wear in nozzle holes is much more important than in sack hole.

Erosion in the nozzle hole increases with impurities content (in fuel) increase.

Concerning chemical corrosion must be taken into account the temperature also as well as gas attacking.

Shortcomings

The main drawbacks:

- decrease of fuel injection pressure
- decrease of atomization intensity
- decrease of injection period
- decrease residual pressure
- increase in fuelling
- change in fuel spray penetration history

The above cited results in:

- increased soot emission
- increased THC emission
- increased CO emission
- increased fuel consumption
- decreased power output
- piston damages
- late combustion and thermal overloading
- increase of noise.

Inspection

1. Before testings, if any change, the new injector has to be checked related to cavitation in nozzle hole. The same must be done converting to methanol.

Fuel pressure in injector has to be determined. It may be done by calculation or by measurements. By measurements or by calculation needle lift diagramme has to be accomplished also.

Having the both: pressure-and needle lift diagramme it's possible to determine three positions according to Fig 14.

On rig test bench (see drawing given in the first report) $Q=f(h_i)$ measurements may be performed. However, here pressure drop must be accommodated to corresponding pressure diagram.

$$\Delta Q = \underset{\substack{\uparrow \\ \text{measured} \\ \text{usually} \\ 2 \text{ - } 4 \text{ dm}^3}}{\mu f} \cdot \overset{\substack{\uparrow \\ \text{TO} \\ \text{CALCULATE}}}{\sqrt{\frac{2}{\rho}}} \cdot \sqrt{\rho_1 - \rho_2} \cdot \overset{\substack{\uparrow \\ \text{measured /s/}}}{\Delta t}$$

ρ - fuel density

$\rho_1 - \rho_2 = \Delta \rho$ - pressure drop

μf - may be determined for any pressure drop $\Delta \rho$ wanted
Doing that, results in diagram shown in Fig 15. Marked points A' indicate the beginning of decrease in effective nozzle hole flow area (μf).

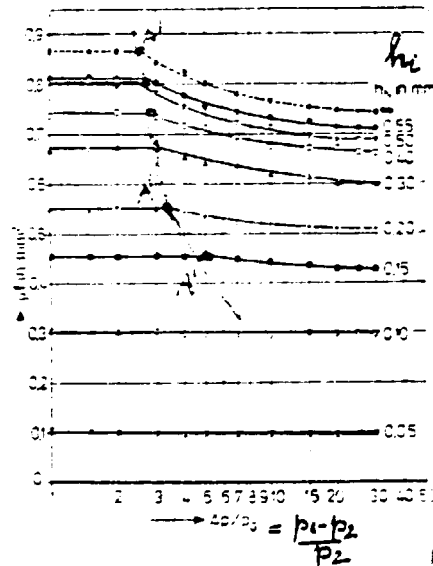


Fig 15 Marked points A' depict start of cavities formation in the nozzle hole

p_1 - pressure in injector
 p_2 - simulated in-cylinder pressure (for measurements only $p_2 = \text{ambient}$)
 μf - eff. cross-sectional flow area of nozzle holes

In order to avoid some uncertainties related to cavities formation in seat area, the additional measurements have to be performed.

Cutting the bottom part of nozzle body (by grinding only) μf area of needle seat can be measured, acc. to Fig 16. For the diagram Fig 16 shown, μf seat area is not critical related to cavitation up to $h_i \approx 1$ mm. Comparing the both, Fig 15 and Fig 16, may be concluded, that nozzle holes are much more inclined to cavitation wear than needle seat area.

2. With injector tested the best inspection may be measurements at $h_{i \max}$ with $\Delta \rho = 100 \text{ bar} = \text{const.}$, supposing that

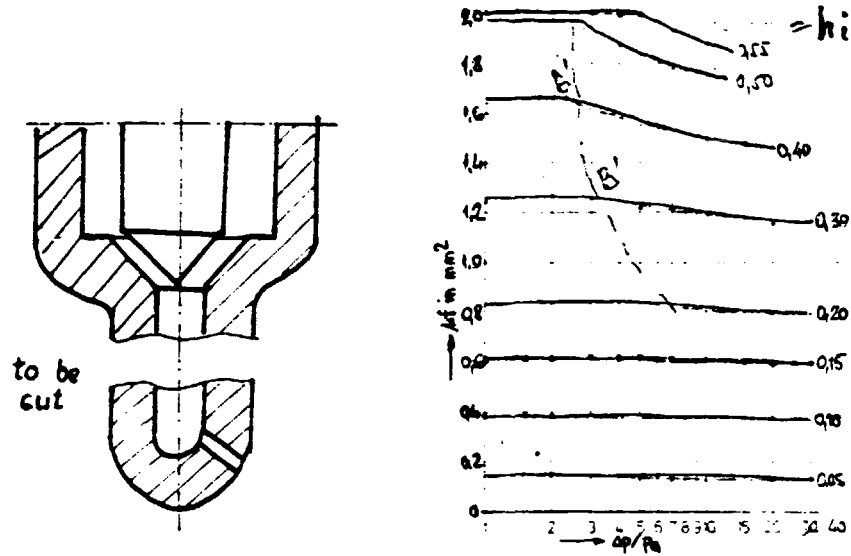


Fig 16

such data before testing existed also. By comparison wear of cavitation may be estimated. It's useful during testings, via μf measurements to follow cavitation wear vs. time (if existed). μf measurements mentioned are yet explained in Report 1.

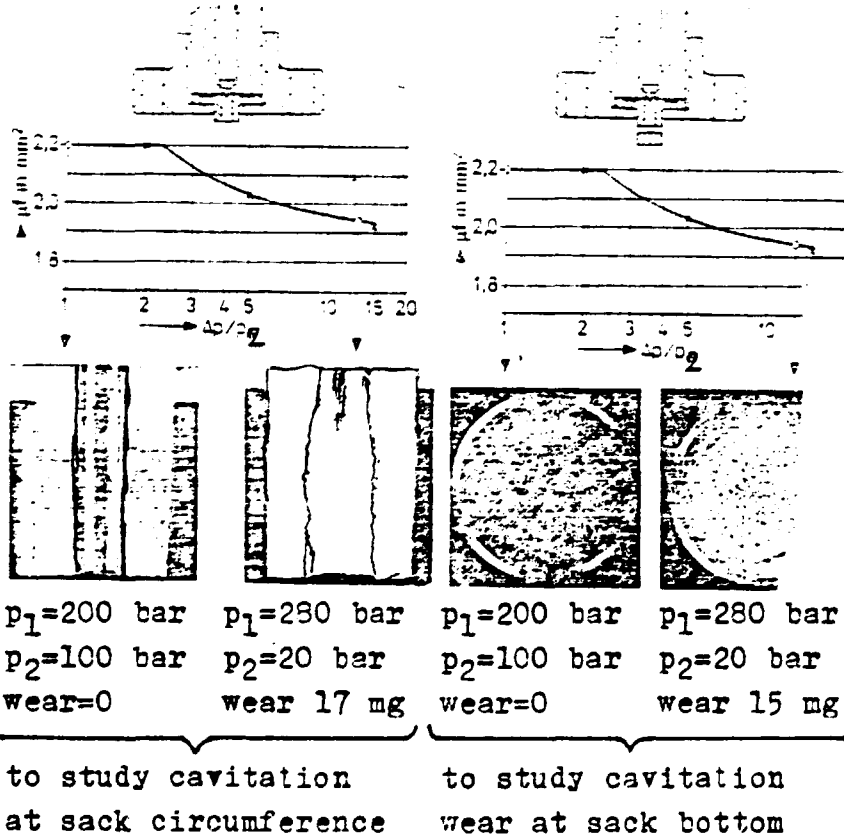


Fig 17

Fig 17 explains the procedure how to study cavitation at sack circumference and sack bottom.

3. Needle - nozzle body sliding area

Here wear of sliding friction will be considered only. However, some negotiations must be made at first:

1. It's impossible to measure the clearance between needle and nozzle hole (sliding hole) at various positions in order to calculate mean effective one. Moreover, so defined says nothing about the leakage and reaptibility of measurements is very poor.

To solve this problem the bellow shown method may be suggested.

Again
$$Q = \mu f \sqrt{\frac{2}{\rho}} \sqrt{\Delta p} \Delta t$$

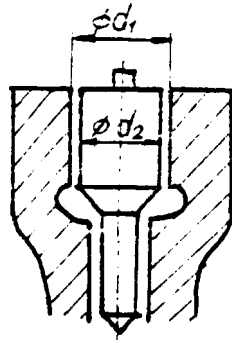
substituting $\mu=1$ results in

$$f = \frac{Q}{\sqrt{\frac{2}{\rho}} \sqrt{\Delta p} \Delta t} = \Delta d (2d_1 - \Delta d) \frac{\pi}{4}$$

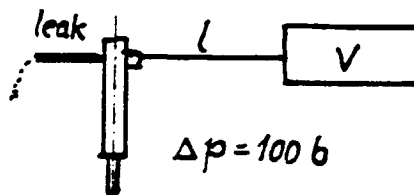
d_1 - producers nominal value let say $d_1 = 6 \text{ mm}$.

This Δd may be defined more effective and easily measured as follows:

Q - overflow leakage quantity in time Δt at defined pressure drop Δp ($\Delta p \approx p_1$ because of $p_2=1$).



2. For every type of injector leakage time must be accomplished.



$$t_{min} = \dots [s]$$

$$t_{max} = \dots [s]$$

Volume V , line l as well as p must be the same as for engine producer. Time observation of leakage is not only because of too much overflow. Moreover, the danger comes from too low leakage. Leakage overflow, although unwanted related to injection, is unavoidable related to cooling and to lubrication of sliding parts. Many stickings and seizures of injector needle are known because of too small overflow leakage.

3. One must be sure (or to check) that heat treatment of hardening was completed with very deep cooling ($-55^{\circ}\text{C} \pm 5^{\circ}\text{C}$). This is important treatment for the both: needle and nozzle body. The reason for that is rest-austenite which by increased heating may be transformed into martensite. This process is accompanied (per example) by increase of needle dia., which may produce total loss of gap ($\Delta d=0$). If happened, extreme high friction produces overheating and seizure.

A high needle wear had occurred in one type of vehicular diesel engine with new injector supplier. The inspection had performed acc. to Fig 18. Measurements gave evidence about doubtful heat treatment of needle (see Fig 18, b) although the diameter of nozzle body was "stable" during heating up period (Fig 18, a). Thus needle - nozzle body gap may decrease in operation (see Fig 18, c) what in the praxis at random occurred. The reason for above investigations were:

- two needle seizure in servis operation
- unstable idling with about fifty engines accompanied with increased fuel consumption rate in low load operation.

4. Any kind of deformation of nozzle body or needle increases friction accompanied with wear increased.

a) The cap x in Fig 19 must be tighten carefully with order torque. The same may be recommended when fasten injector - cylinder head. A high friction may be noticed with many injectors acc. Fig 20.

The reason for that, is to high torque by fastening in cylinder head or by injector assembling.

b) Any overheating may produce increased friction and inversly increased friction produces higher heating in sliding area.

Poor cooling of cylinder head, etc., may produce overheating but with increased wear of sliding part especially at low speed and low load operation, overheating may occur because of hot gas penetration in the space y (see Fig 21). When instantaneous fuel pressures drop under in-cylinder gas pressures (see Fig 21) for any time (or angle α_k), hot gases penetrate into space y accompanied by: overheating, needle "colouring" and in the end, by nozzle hole cocking. (Till now 17 reasons are known related to nozzle hole cocking).

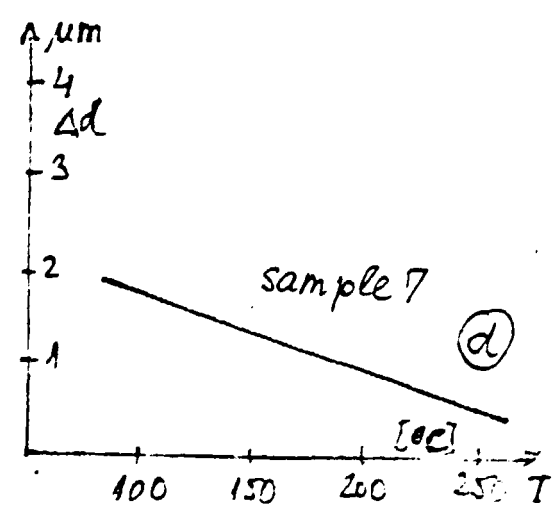
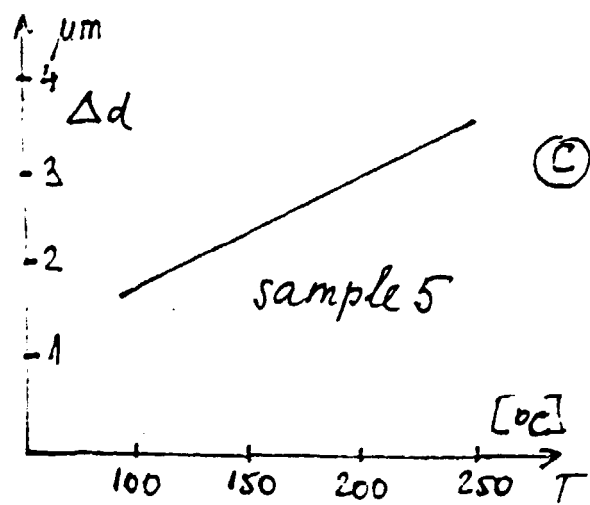
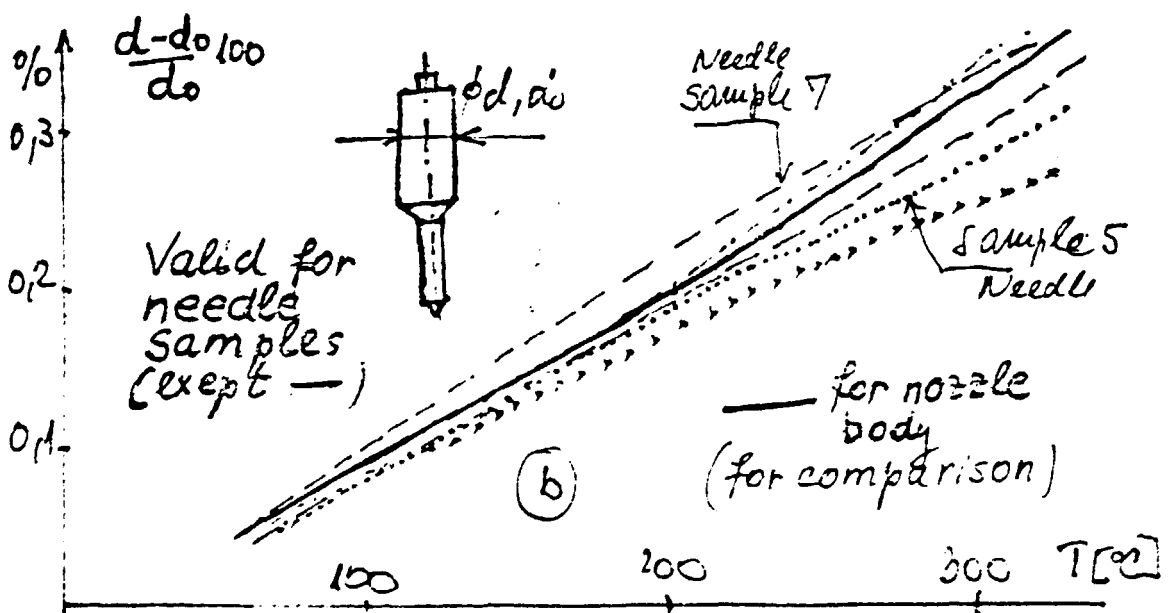
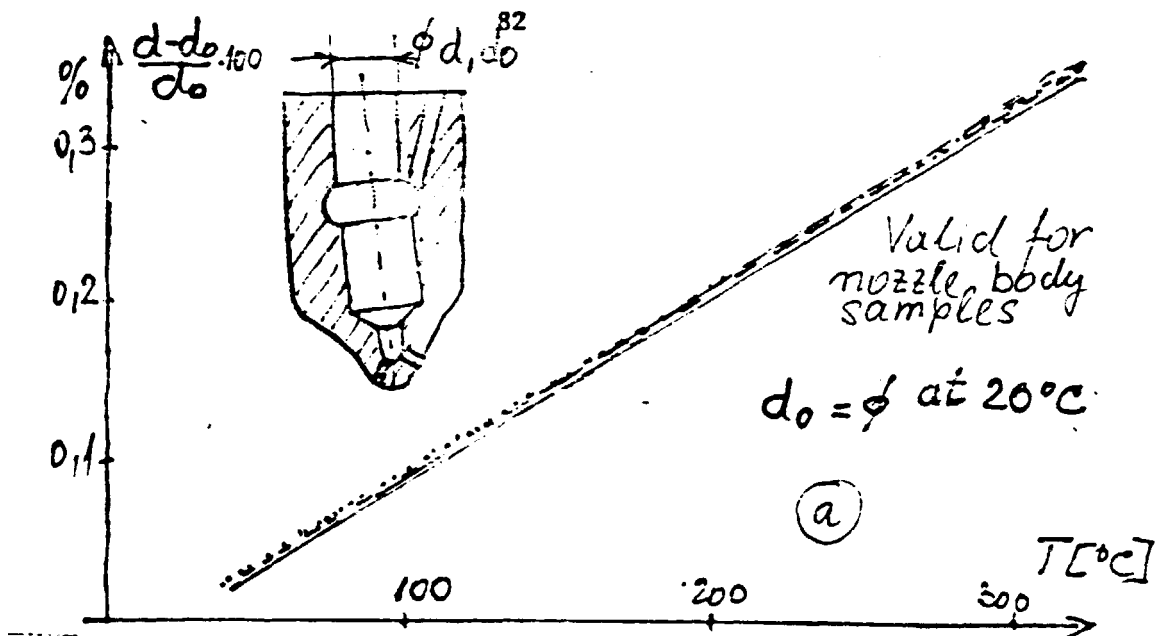


Fig 18

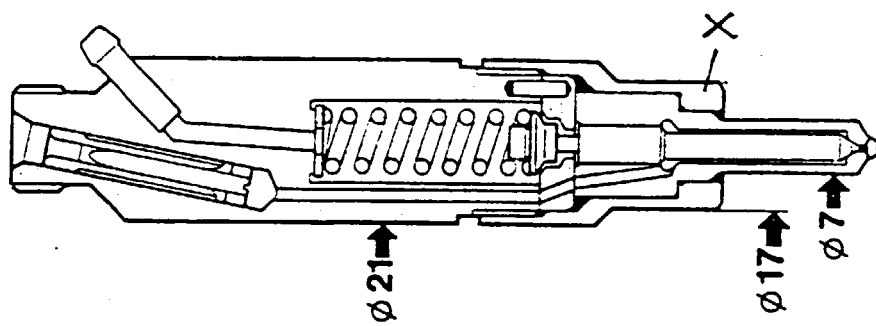


Fig 19

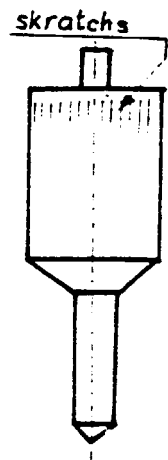


Fig 20

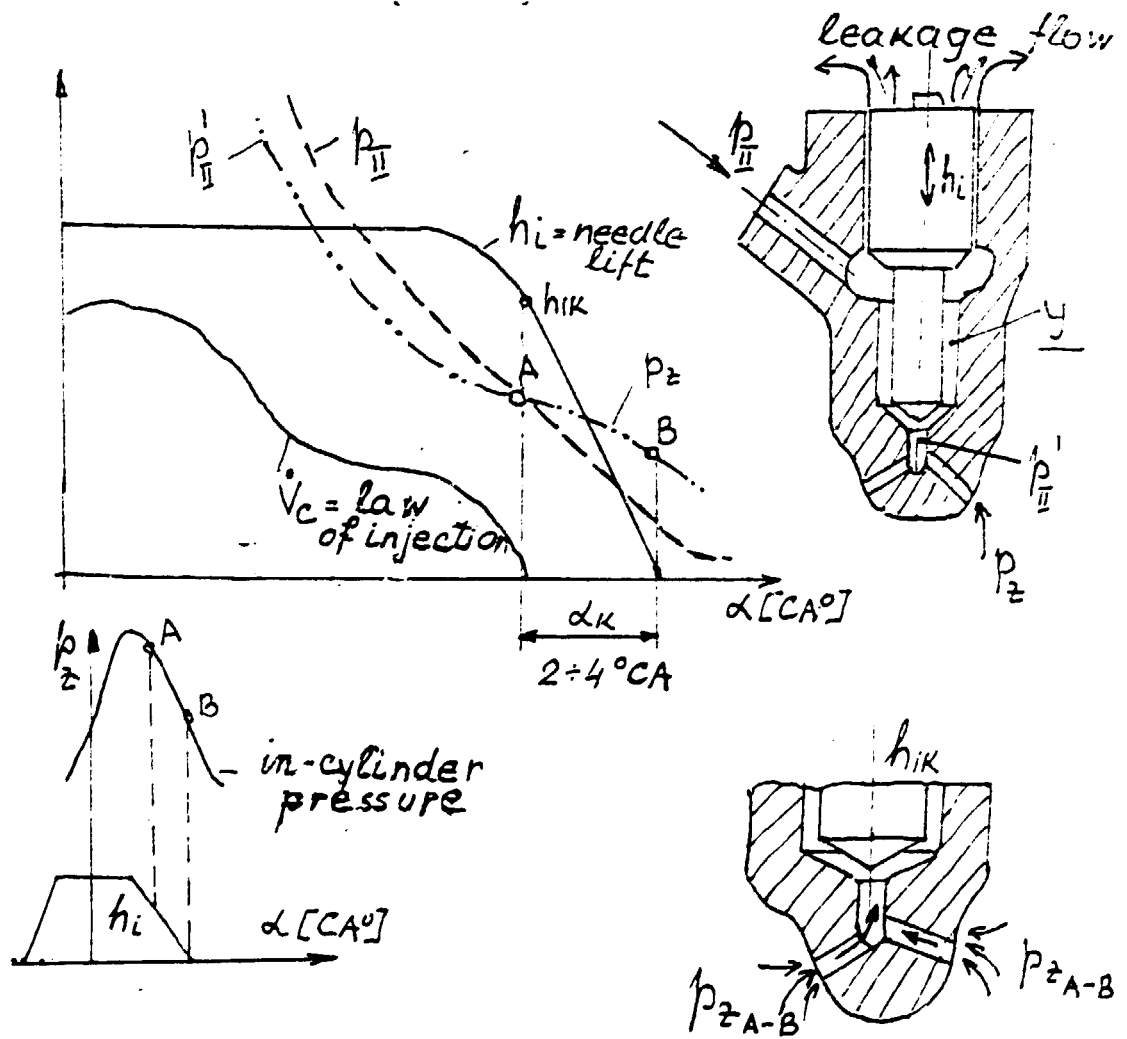


Fig 21

5. According to Fig 22, injection fuel system is coupled hydraulically. During injection, leakage flow although very small, is

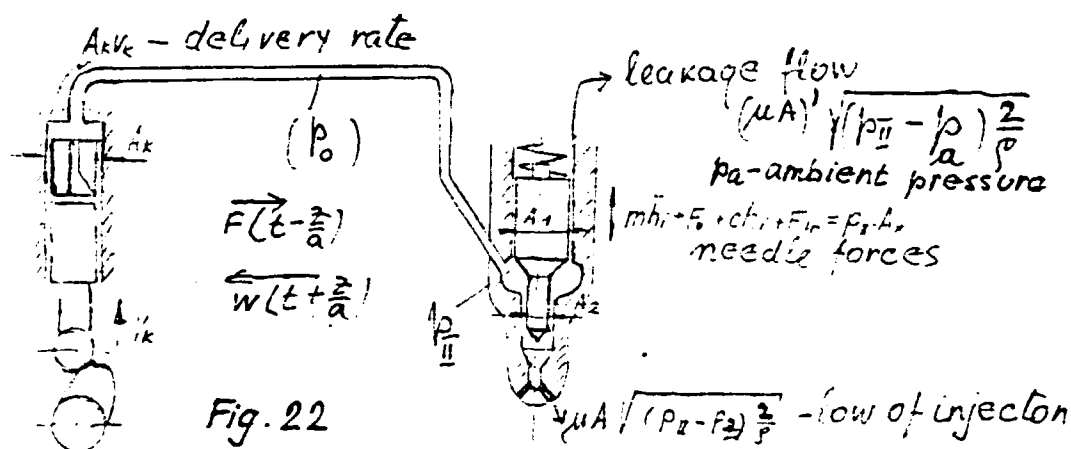


Fig 22

only one connection of HP system with ambient. When leakage flow increases:

$$\int (\mu A)' \sqrt{(P_I - P_a) \frac{2}{\rho}}$$

fuelling decreases $\rightarrow v_c = \int \mu A \sqrt{(P_I - P_a) \frac{2}{\rho}}$

Although, leakage flow rate must be higher at higher speeds related to higher pressures p_{II} , the fuelling corrected will be lower because of time (see Fig 23).

Residual pressure p_0 will be influenced also and unwanted corrected. The time between two cycles is a long period and the closed HP system has still connection with ambient via leakage flow. It may have a high influence in methanol application as was (in the first Report) yet explained. A high wear and lower fuel density, accompanied with CH_3OH evaporation in the upper part of sliding area, may produce leakage flow, at low speed-low load operations, more than 20 % of corresponding fuelling.

To avoid the above cited leakless injector may be the solution (still in development). Fig 24 shows diag. sketch of leakless injector. The first results have been encouraging (soot emission decreased, torque back up increased, injector is getting smaller, higher injector closing pressure, less expensive system). However, retraction volume of the retraction valve must be matched to the demands of the closed system as well as the volume V_A (see Fig 24). When matching was poor (Fig 24, a and b

dated lines) resulted in after injection and needle blocking.

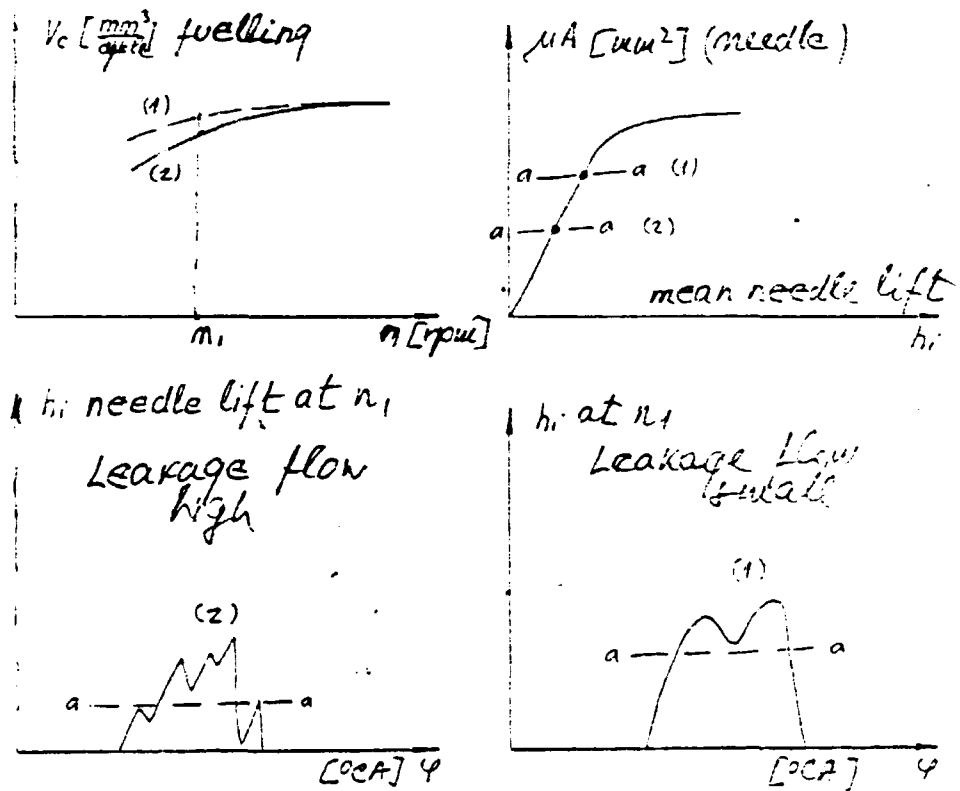


Fig 23

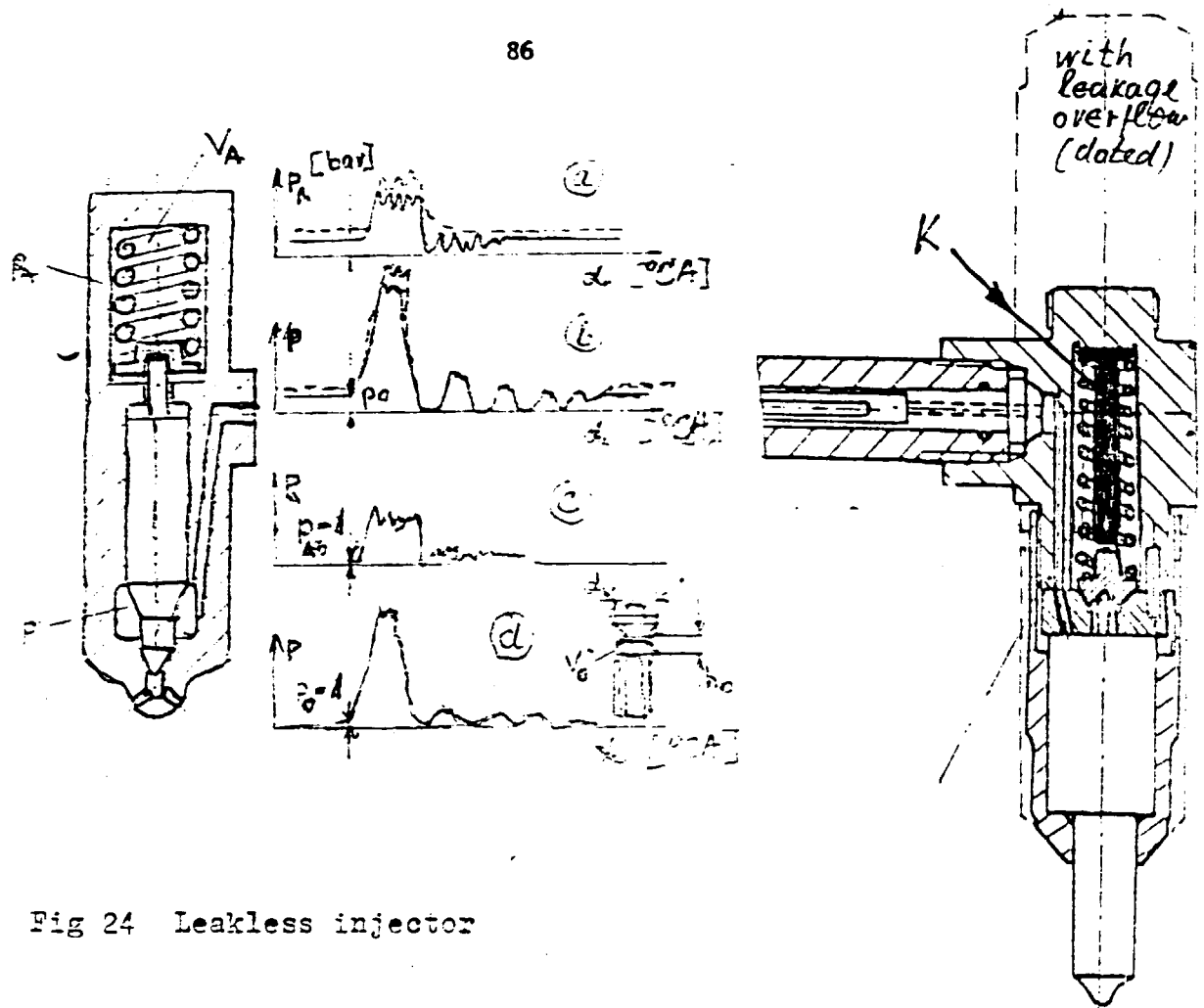


Fig 24 Leakless injector

With good matching (see c and d, Fig 24) a promising results are achieved. To decrease V_A as much as possible filler K was used.

6. Using experiments to define eff. leakage flow area μA vs. pressure p_{II} the calculation can be made for the all injection parameters wanted. It may be a small modul added to the overall injection fuel programme. It's to be suggested to use the 1st programme sent as much accurate one.

Is to be mentioned that wear increase with higher content of very fine dispersed dirtyness in diesel oil.

Shortcomings

The main drawbacks:

- change in fuelling
- unwanted change in residual pressure
- change in injection pressure
- unstable injection parameters at low speed-low load operation
- load dispersion at low speeds

The above cited results in :

- soot emission increase at low speeds
- poor torque back up
- nozzle hole cockings
- increase of fuel consumption rate
- unstable idling operation
- increase in CO emission at low speeds
- some decrease in power output

Inspection

The points mention in negotiations 1 - 5 said all about inspection. The most important are leakage flow measurements and pressure drop in time. Doing that Fig's 25 and 26 may be obtained.

Fig 25 shows the time elapsed in /s/ vs. diameter clearance Δd for pressure drop 350-300=50 bar. This diagram may be used for μA determination.

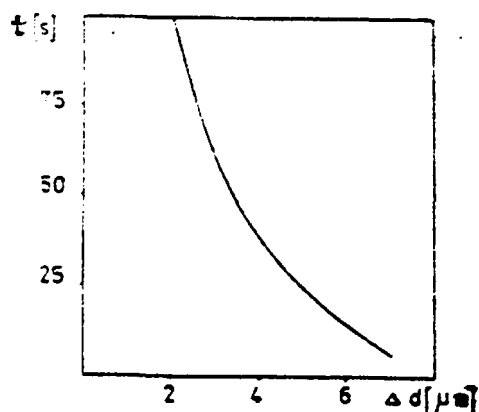


Fig 25 Time t elapsed for 50 bar pressure drop vs. diametrical clearance needle-nozzle body

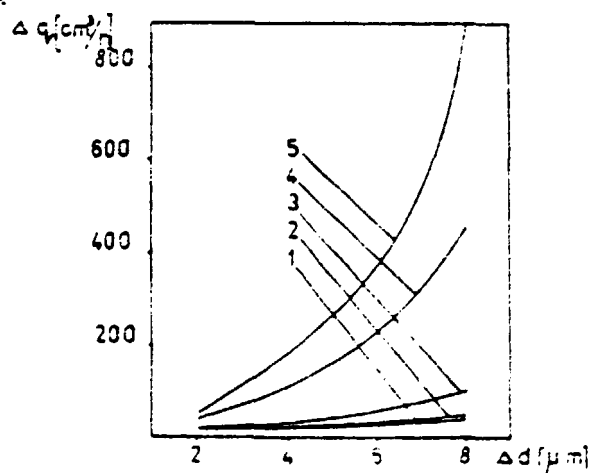


Fig 26 Relationship of fuel leakage in needle-nozzle assembly, against diametral clearance for various rotating speeds
 5 - 1100 rpm HP pump
 1 - 300 rpm HP pump

In the end, related to other types of injector wear, may be said; they are much more concentrated toward change of injector opening as well as closing pressure. If may effects the whole

injection events but also the timing.

However, related to engine performances, the largest impact may have decreased closing pressure of injector. With decreased pressure difference at the end of injection, fuel is poor dispersed and introduced in the very favourable ambient for cracking having no time to complete the combustion. Nozzle hole coking and a high soot emission are the results (see Fig. 27).

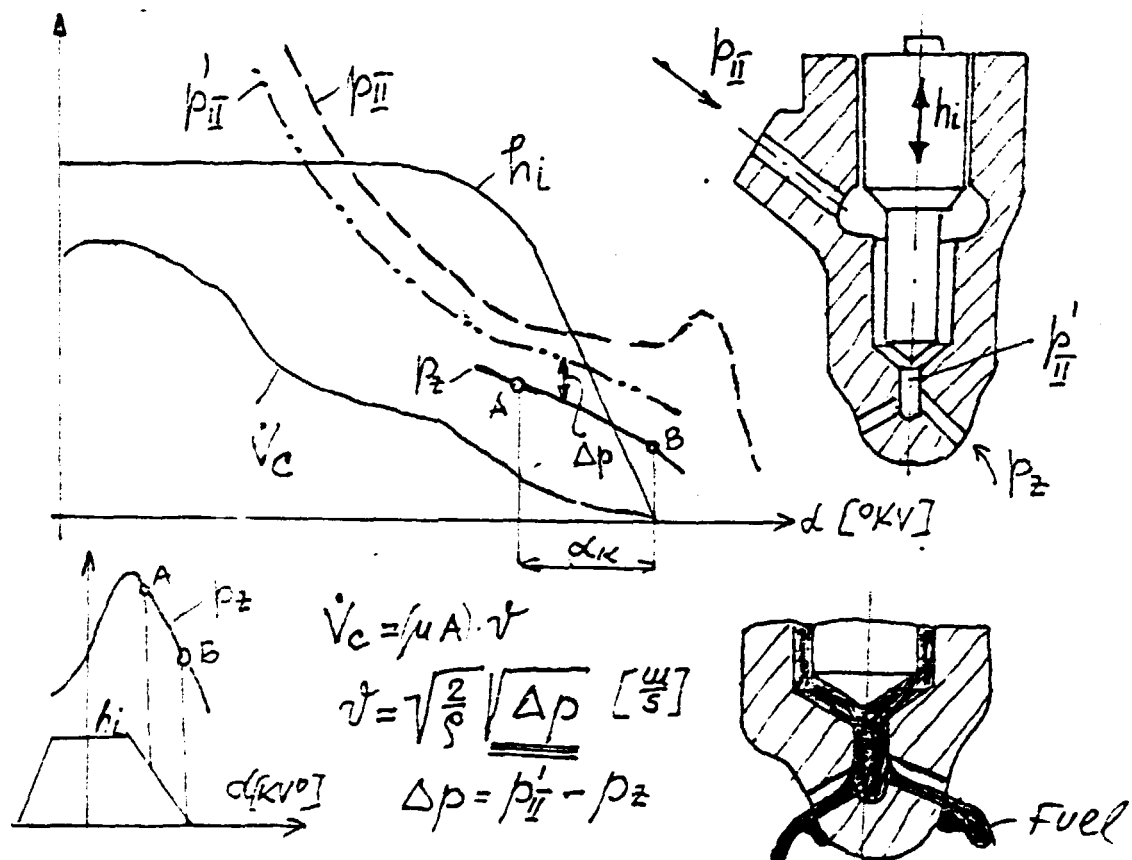


Fig 27 Poor dispersion of the fuel because of a low pressure difference at the end of injection (low closing pressure).

Is to be mentioned, that the decrease of injector opening (as well as closing) pressure may be effects by spring itself but the reason is often the wear on the spring on needle contact surfaces. The inspection is very easy to performe by checking the injector opening pressure change.

A short overview - system testings

In endurance tests the service life of fuel injection system under fuel load conditions may be determined depending

upon the main influencing factors of peak pressure and (constant) rotational speed.

However, in practice, it is the service life expressed in hours run (h) or in distance driven (km or miles) which is of interest. The prerequisite for determining the service life is the knowledge of data given the percentage in distribution of load during operation in field. A simple classification unit suitable for field-use, was taken to determine this load distribution. Using this method, a two-dimensional time distribution can be obtained for the control-rod travel/rotational-speed performance characteristics for all the possible applications of the pump.

Using load-collectives, and the theory of the linear failure accumulation according to Palmgren-Liner, a procedure was developed for determining the service life from the full-load life.

The relationship of service life to full-load life represents a characterization of the collective. Multiplication with the mean driven speed results in the so-called "fuel-load distance"

$$VZ \frac{\text{service /h/}}{\text{full load/h/}} = V_m \frac{(\text{km})\text{service}}{\text{service /h/}} = VS \frac{(\text{km}) \text{ service}}{\text{full load /h/}}$$

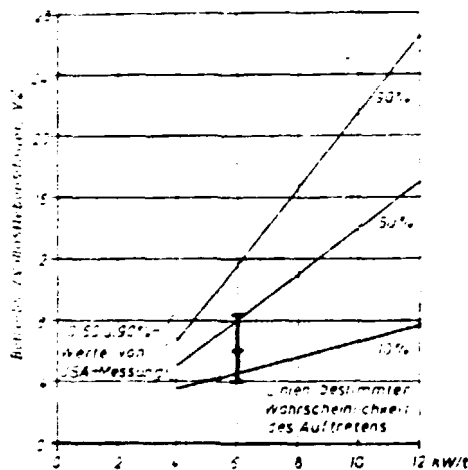


Fig 28 Relationship of service to full-load life VZ versus rated output total weight (statistical evaluation of 96 results with trucks).

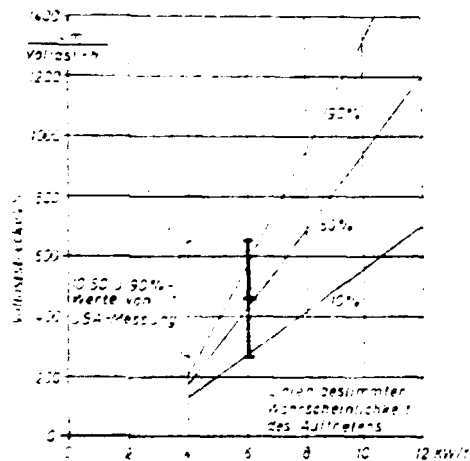


Fig 29 Full-load distance VS versus rated output/total weight

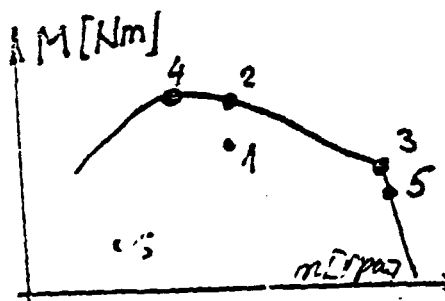
Example Truck 6 kW/t at 10% $V_{S10}=270$

Service life 500.000 km, testing for injection system

$$\frac{500.000}{270} = 1850 \frac{h}{km}$$

$V_{Z10}=4,5$ The method shown is more applicable for the pump. For the whole system we are using the next shown procedure 1000 h.

- | | | | | |
|----|-----|----------------|-----------------------|---------------------|
| 1) | 35% | $0,85 M_{max}$ | $n = 2/3 n_{n_{max}}$ | $+1/3 n_{P_{emax}}$ |
| 2) | 15% | full load | " | " |
| 3) | 15% | P_{emax} | $n_{P_{emax}}$ | |
| 4) | 20% | M_{max} | $n_{M_{max}}$ | |
| 5) | 5% | $0,8 P_{emax}$ | $1,03 n_{P_{emax}}$ | |
| 6) | 10% | idling | n_{min} | |



TOPIC 3Proposals related to:"Glow plug supported combustion
in neat methanol operation"1. CR- Compression ratio

In-cylinder peak pressure measured demonstrates very low values related to DI diesel engine operation; peak pressure reached hardly 50 bar at rated power. It means, besides of relatively low rated mean effective pressure, that in methanol operation compensation of CR drop was not applied.

Peak of compression pressure for CR=16,5 is quite enough high for diesel oil operation. However, converting to methanol, because of 10 times more energy needed for mixture formation than that in diesel oil operation, effective peak compression pressure will be considerably lower. This fact asks for CR compensation when CH_3OH is to be used as fuel. The more CH_3OH doped and mixed with diesel oil the larger CR compensation requirement. In the case of neat methanol CR compensation requirement reaches the max value (Fig 1).

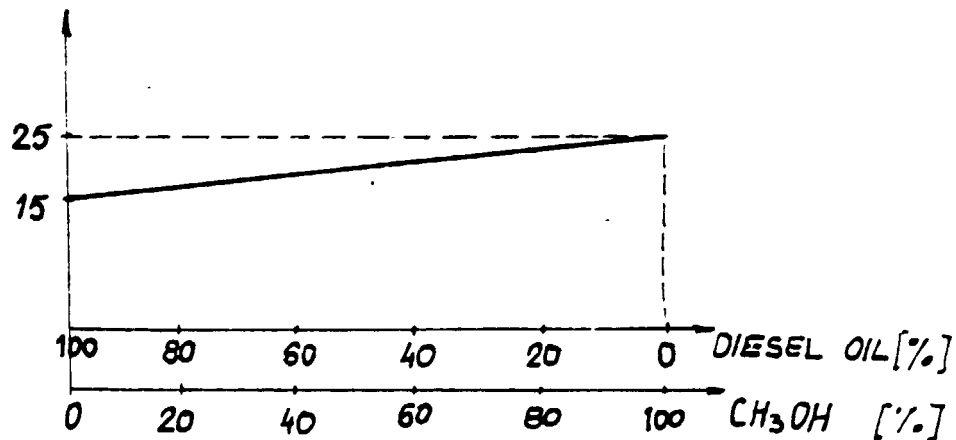


Fig 1 CR sufficient for stable ignition at starting when diesel oil- CH_3OH blends are used in diesel engine (without ignition improver)

Some disproportions may be noticed by peak in-cylinder pressure and neat peak compression pressure ratios.

A simple calculation may show that neat peak compression pressure amounts of about 40 bar at rated power. It means that oforementioned ratio amounts 1,25, what is pritty low for DI engine. Moreover, in-cylinder pressure history may be as shown in Fig 2.

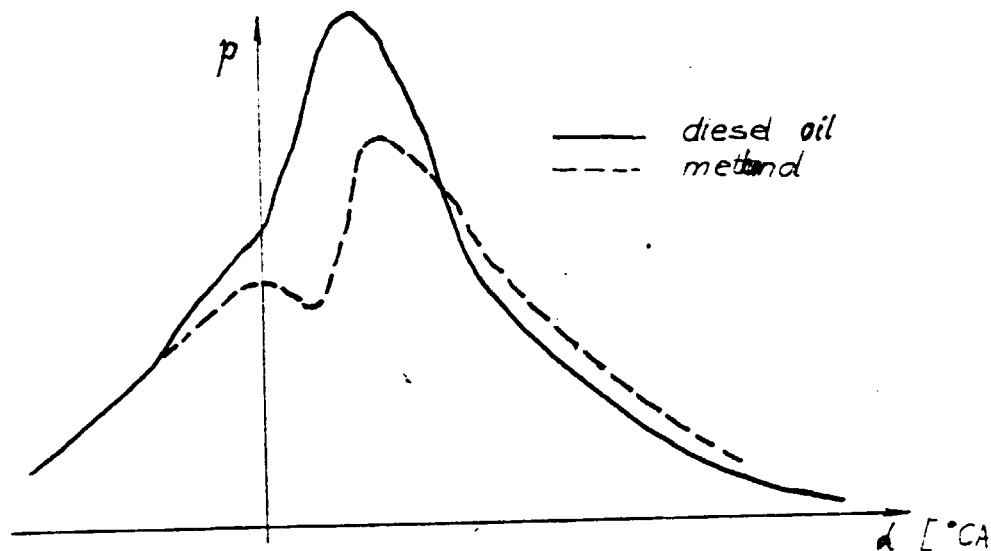


Fig 2 In-cylinder pressure diagrams:

———— diesel oil
 - - - - - methanol

The in-cylinder pressure diagrame for methanol combustion shown in Fig results in:

- late combustion
- small amount of $\int p x$
 (x - instanteneous piston velocity)
- unstable low load operation.

CR compensation is also required when using methanol in ST engines.

To demonstrate the later said, some VW experimental results are presented. VW used the both techniques with methanol: carburation and fuel injection. The results of both techniques mentioned as well as results for gasoline use are shown.

Piston temperature measurements were made with a 1,6 l VW gasoline engine. The engine was run on the test bed in different versions with regard to mixture formation according to the use of different fuels, such as gasoline (regular), CH_3OH , M 15 (15% CH_3OH + 85% gasoline) and ethanol.

It was found, that with M15 (only 15% CH_3OH was mixed) piston temperatures were about 10°C lower as compared to engine operation on gasoline, provided the engine build up was kept practically unchanged.

The temperature rise found with the carburetor version, when this engine was operating on CH_3OH fuel, is due to the increased compression ratio 12,5 compared to 8,5. As the piston temperature depends on combustion temperature being lower with alcohol fuels than with gasoline fuel, the influence of increased compression ratio is partially compensated.

A further increase of the compression ratio towards 13,4 was achieved using fuel injection version (5 points compared with gasoline operating on CH_3OH with ϵ increased, the thermal efficiency was evident. Comparing with gasoline 4,5 power output increase was measured.

Exhaust temperatures were $90 \pm 120^\circ\text{C}$ lower with CO emission increased.

The Fig's 3 and 4 show with gasoline engine also, that "last of compression" must be compensated. It's no use to fray CH_3OH application without CR compensation.

This appendix was presented only to demonstrate that the same happened with SI engine also related to CR lost by CH_3OH application in "existing engines".

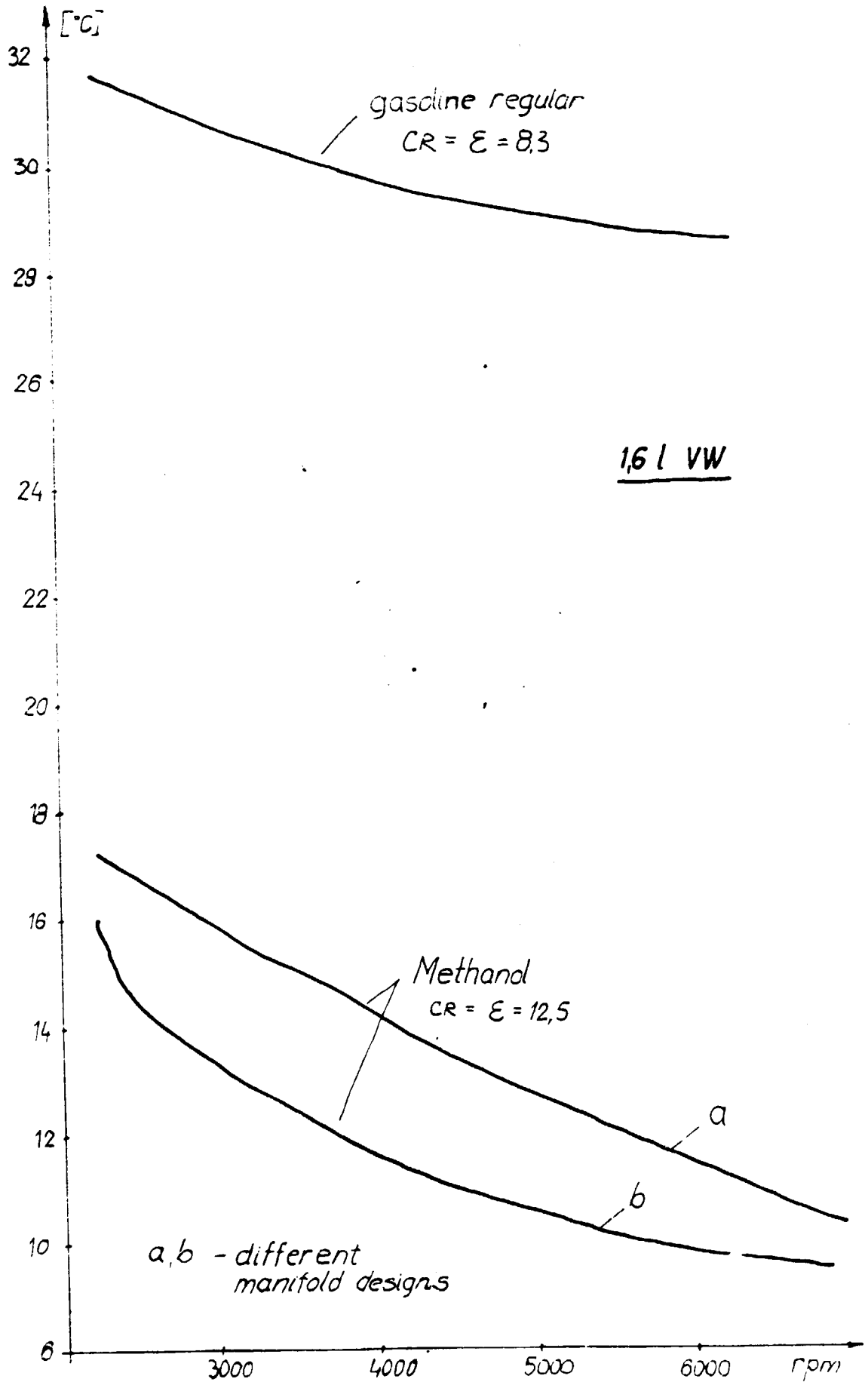
Although Fig 4 presents piston temperatures for SI engine, CR was increased by factor 1,6 in CH_3OH operation comparing with gasoline. Only with this increase top piston temperatures were the same for the both fuels.

With diesel engine in CH_3OH application factor 1,6 results in $\text{CR}=25,6$ for the same top piston temperatures (t_1) as in diesel oil operation. This very approximate comparison demonstrated the need for same CR compensation in methanol operation.

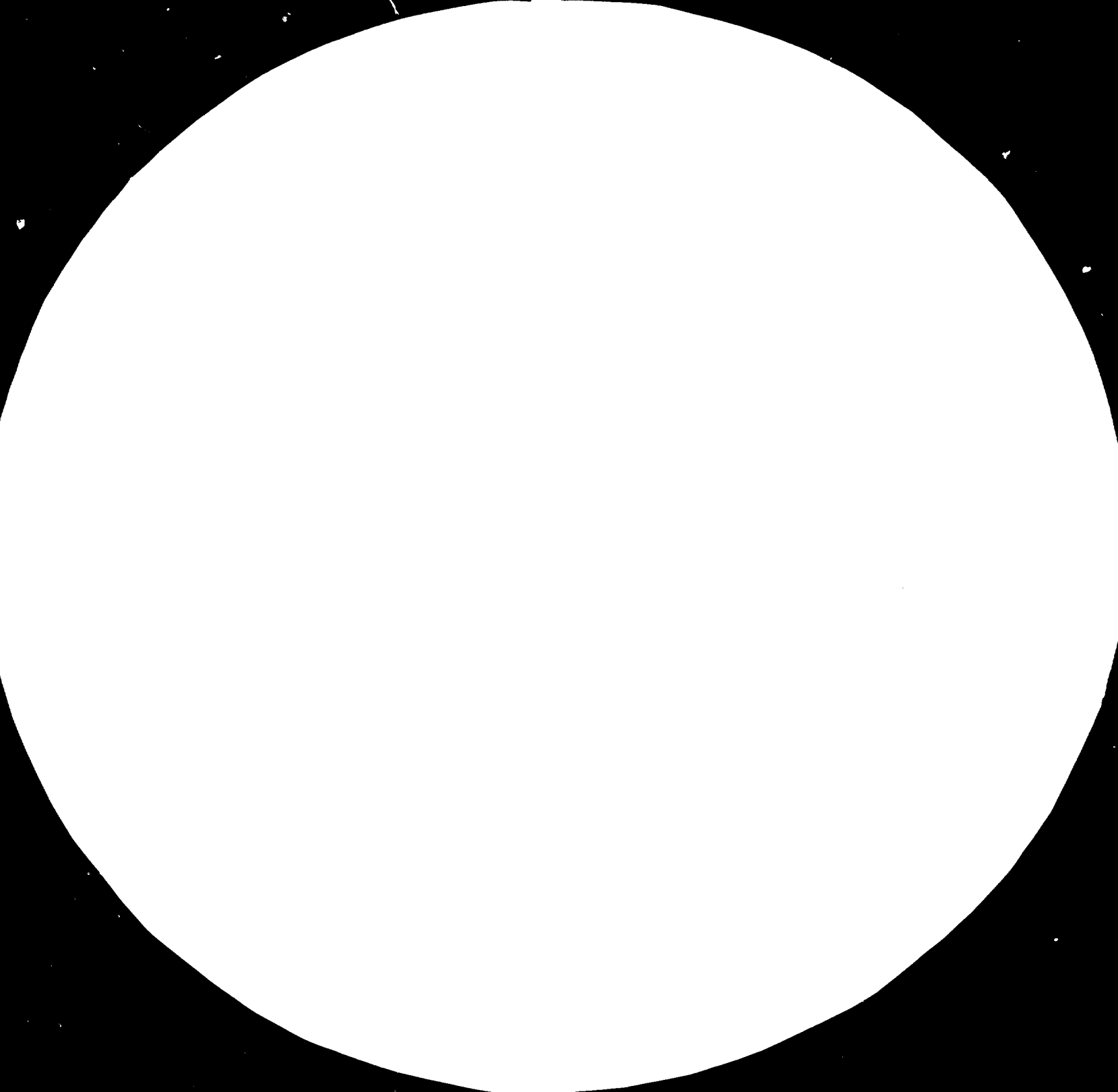
Proposal Converting to methanol CR ratio must be increased for 2 units if glow plug is to be used.

Increased CR ratio may help to:

- improve startability
- decrease operation of missfiring
- decrease fuel consumption rate
- decrease energy consumption of glow plug



— — —





28



32



36



40

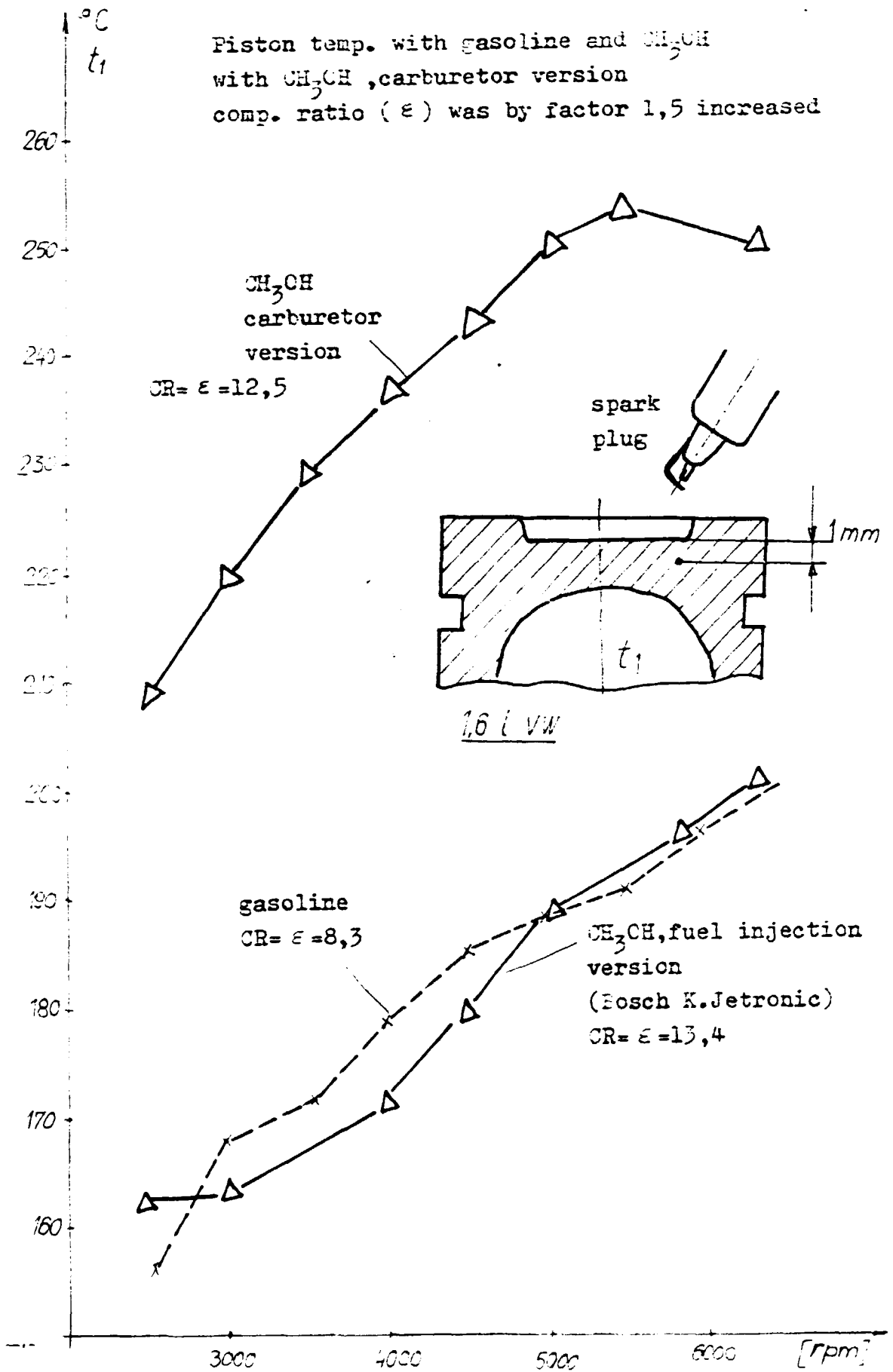


MICROCOPY RESOLUTION TEST CHART

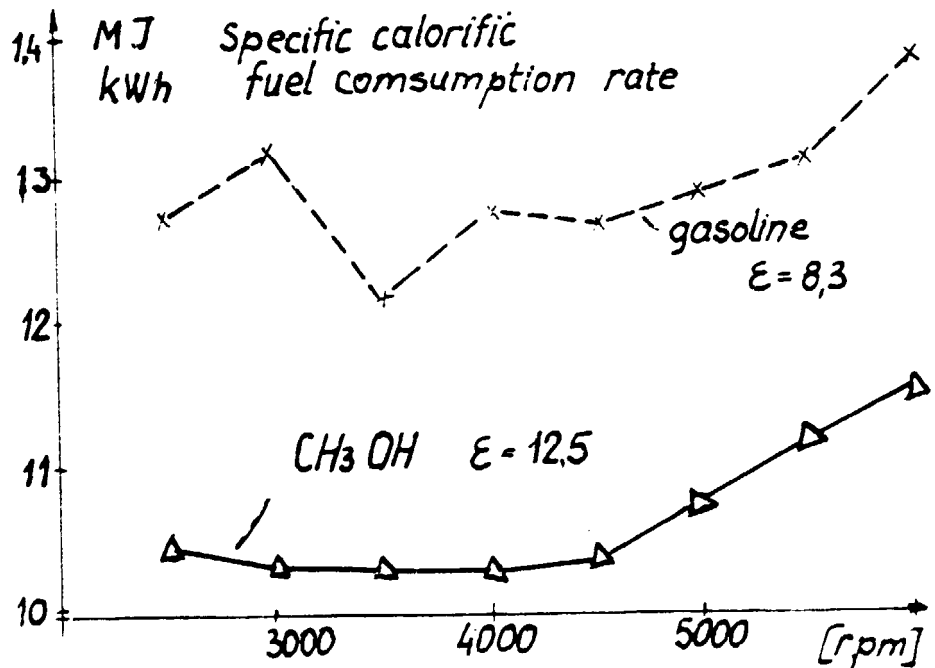
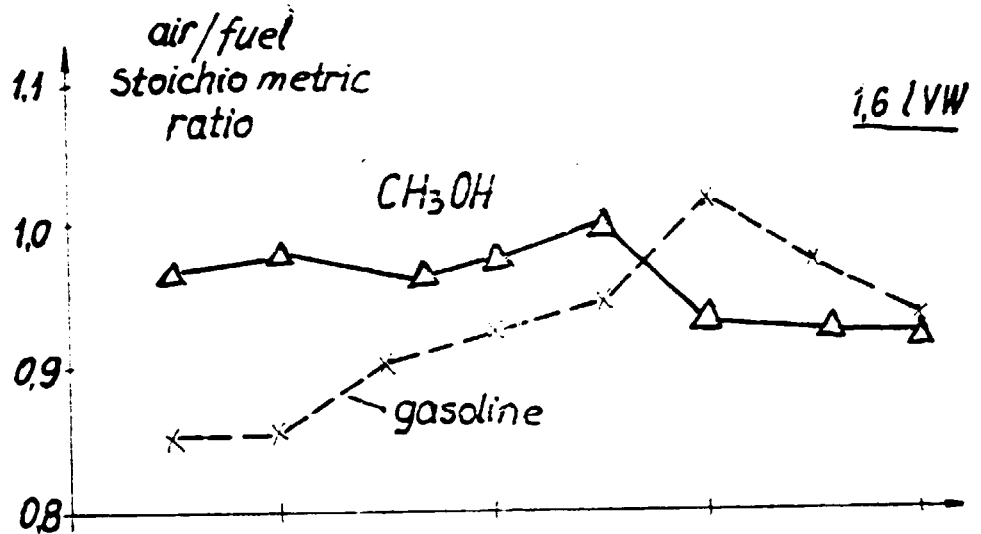
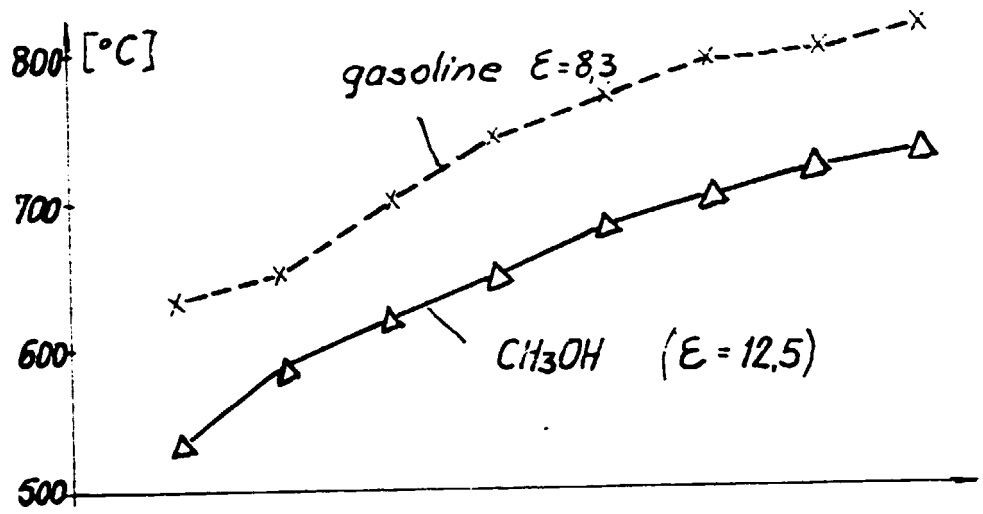
NATIONAL BUREAU OF STANDARDS

STANDARD REFERENCE MATERIAL NO. 1010

U.S. GOVERNMENT PRINTING OFFICE



Exhaust temperature



2. Injection

More advanced injection to ignite methanol is a consequence of:

- high ignition delay of methanol
- large quantity of fuel injected in the combustion chamber before ignition
- start of injection in less convenient conditions for ignition

The solution may be controlled injection as was yet explained in this report. Controlled injection is not so difficulty to realize using two injector springs or the injector with hydraulically controlled needle lift. The both systems are shown as well as explained in this report. Using controlled injection, the fuelling in the pre-ignition period decrease same docs in-cylinder temperature drop also. Thus, better ignition and improved low-load operation may be expected.

In this report, the system with single hole injector for controlled injection is shown also. However, to apply single hole nozzle swirl ratio and combustion chamber bowl must be matched. Using existing engine some of controlled injection effect may be realized with multi-hole nozzle also.

Number and distribution of nozzle holes have a great influence on diesel engine operation. This influence increases with energy for mixture formation increased, as is the case in CH_3OH operation. It's of interest to remember, that in methanol operation the best results were obtained when the same injection system was used as for diesel fuel injection. It means nearly by factor 2 prolonged injection period. This fact results in late combustion only. Converting to methanol the ground rule may be:

$$\alpha_{\text{diesel oil}} \text{ period of injec.} \approx \alpha_{\text{methanol}} \text{ period of injec.} \quad (1)$$

if no change in the mixture formation process.

In the most successful methanol diesel engine L9204FW (see p.232 "Neuen Krafftstolten out der Spur") MAF by first matching, doubled plunger dia. and nozzle hole cross-sec. area comparing with diesel fuel operation (engine L9204FM). Ricardo institute in "Ricardo news" reported, that converting to methanol the capacity of fuel injection system must be increased. For the mixture process unchanged, our experiments showed, that the optimum may be reached nearly for the condition given by Eq 1.

Thus injection rate must be increased comparing with diesel oil injection. However, the whole injection system must be matched, acc. to increased fuelling and injection rate (retraction volume, dead volumes, plunger pre-lift setting etc).

3. Swirl and scwish (SR and SQ)

With some combustion chambers high SR intensity produces a high heat transfer to the combustion chamber walls and with this unwanted cooling of compressed air. It decrease the startability as well as combustion stability in low load operations. Swirl intensity may be reduced in methanol operation because of higher velocity of flame propagation and combustion (non-sooty flame). But decrease of swirl may help to reduce the appearance of missfiring and to increase the combustion stability with load decreased.

As a rule of thumb, it may be suggested:

- converting to methanol SR may be reduced in amount of 20%.

4. Combustion chamber isolation

Cast iron instead of alu-alloy piston may help to conserve more heat into combustion chamber. Doing this, the next characteristics will be improved:

- startability
- low load operation
- reduction of fuel consumption because of additional heat returned to the combustion process.

The above propolsal may not be of any problem, namely "Kirloskor" reported, that just in the engine considered a new cast iron piston was applied (see Appendix sent).

About 3000 swiss franks costs ceramic overlay on the piston and on the cylinder head ("Plasma-Technik" Swiss), but is no use when any producer in India does'nt exist. However, it'll be of interest to collect information in India where plasma-technique has been practisized. If any, it's possibly to get much better isolation. To be mentioned, that some tool producers have been using ceramic plasma-coating to increase the service life of their tools.

5. Switching on technique

It's well established fact that using methanol the next points must be considered:

- starting
- low load operation
- cold operation
- transients

when methanol used in diesel engine.

Using mixing technique, the ignition quality of diesel oil decreases in the presence of methanol (because of cooling effect).

If extra good isolation of combustion space doesn't exist, using glow plug, stable starting and low load operation without misfiring couldn't be realized.

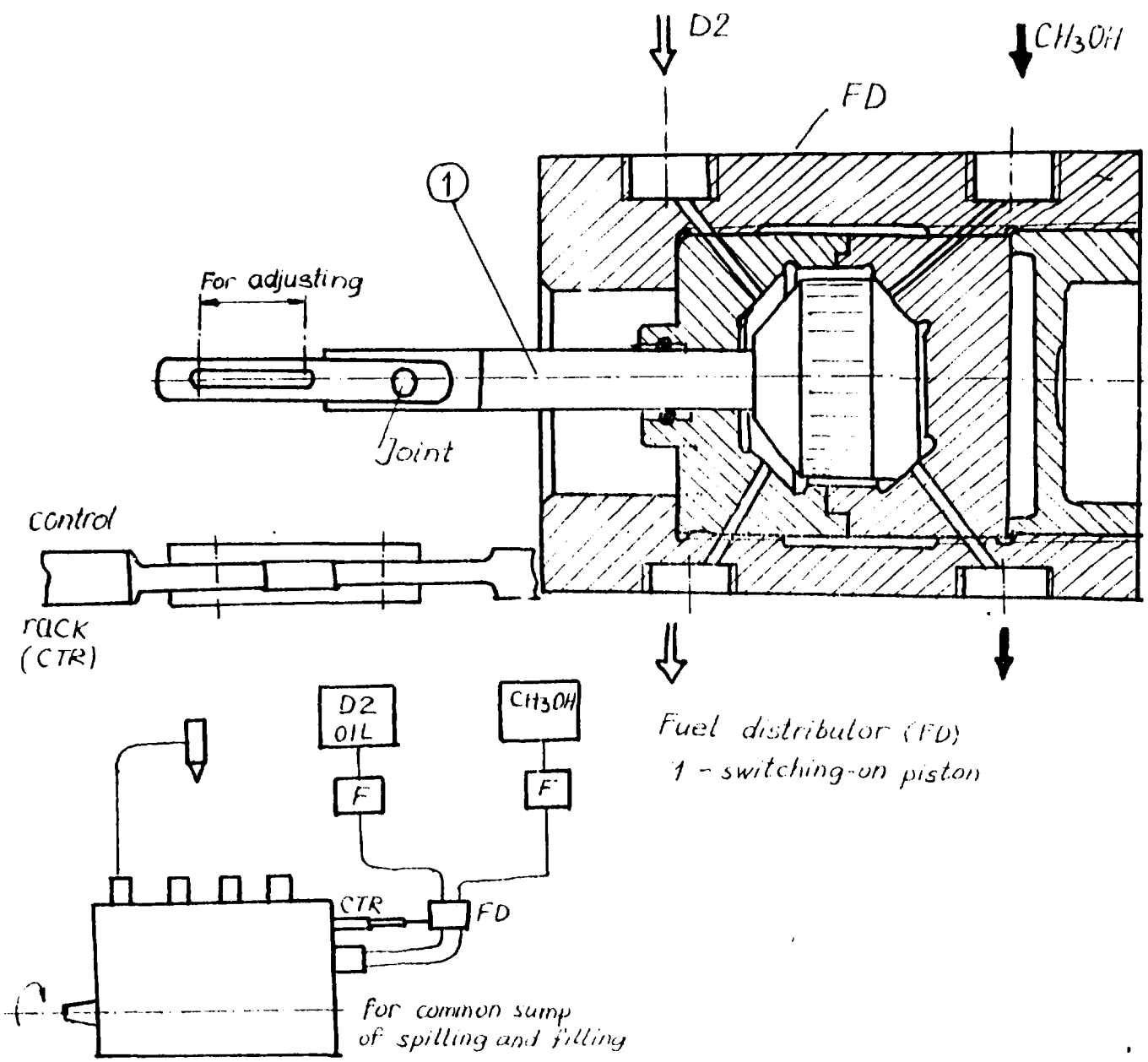
For good starting switching on technique may be proposed, although not for vehicular application. However, for example, for watering purpose it's still possible to apply switching-on technique. Switching-on technique enables during starting to use diesel oil only. In low load operation with load increased quantity of methanol doped increases also. In full load operation methanol only is injected. A diagrammatic sketch of switching-on technique is shown in Fig 6.

The piston 1 (see Fig 6) is connected with control rack of HP pump. The engine considered has a single governed speed, thus rack position is load dependent so does the piston 1 also. The fuel volume "closed" between the inlet of the pump sump and fuel distribution FD, must be as small as possible. When

sump of HP pump are good a very good mixing of fuels mixed may be obtained. This mixing is produced by filling and spilling process (Fig 7). Pressure diagrams shown in Fig 7 depicts that in the sump of HP pump a high fuel turbulence exists. However, the temperature in the sump must be low because of methanol presented. Misfiring may be produced by methanol cavities promotion in the sump also.

With the small single cylinder engine the low pressure pump wasn't use, but because of cavities formation, if high temperature, sump volume must be pressed. With low pressure pump and overflow valve, the fuel pressure in the pump sump may be kept over CH_3OH evaporation point. Overflow valve and short circuit

Fig 6 Switching-on technique



of low pressure system help in better mixing as well as in better colling.

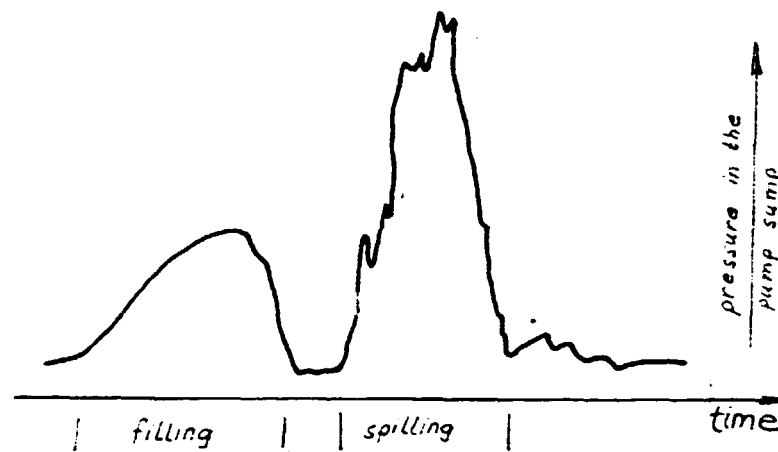


Fig 7

6. Valve timing

Timing fairly satisfactory for very slow speed, as for starting, would be theoretically that intake valve should open at top center and close at bottom center, whereas the exhaust valve should open at bottom center and close at top center. But with high speeds it is necessary to advance the opening of the exhaust valve and retard the closing for the intake valve in order to:

- reduce the work of exhaust
- induct more amount of air.

Overlapping of the closing of the exhaust and the opening of the intake valve makes possible:

- the scavenging of the clearance space
- the cooling of combustion space.

With single cylinder engine considered 1500 rpm is fairly low and timing optimized with overlopp decreased may produce :

- better starting
- more stable low load operation.

Is to be recommended to use calculat. programme for timing optimization at first.

7. Conclusions

1. Glow plug supported combustion, when burning methanol in diesel engine, could not be recommended for vehicular applications without ceramic isolated combustion chamber.
2. For diesel engines in watering application when fuelling with methanol, to obtain better startability and low load operations is to be recommended to:
 - increase CR in to 2 + 3 units
 - apply switching-on technique
 - apply cast iron piston
 - reduce swirl ratio for about 20%
 - optimize injection with increased methanol injection rate, for about 50%
 - optimize nozzle hole distribution using calculation programme related to spray tip - piston bowl wall time contact
 - estimate by calculation a potential benefit with overlapping decreased .
3. When good matched for diesel fuel operation, a small HP pump has no capacity to deliver two times more fuel or the pressure diagrams correspond to Fig 8

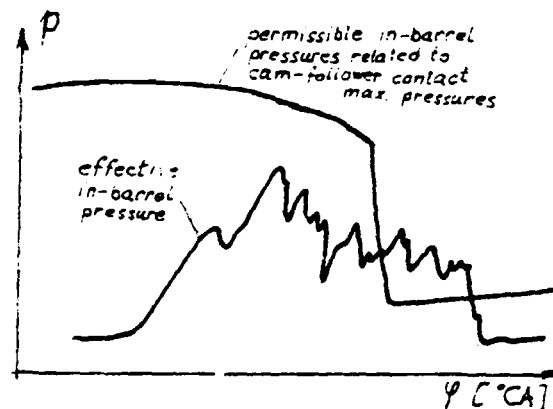


Fig 8 In barrel pressure diagrams

Thus, using separate modul in fuel injection calculation programme, with pre-lift and cam form given, the permissible in-barrel pressure diagram must be compared with effective one or to suffer from very fast cam-follower wear in the HP pump. When decreasing pre-lift, the mean fuelling rate will be additionally reduced and period of injection still more prolonged.

4. For any application after-injection phenomns must be abso-
lutly avoided. Again, calculation programme may solve this pro-
blem or needle lift measurements.

Permissible pressure contact

Acc. to Fig max. permissible pressure in the barrel of HP
pump may be calculated as follows:

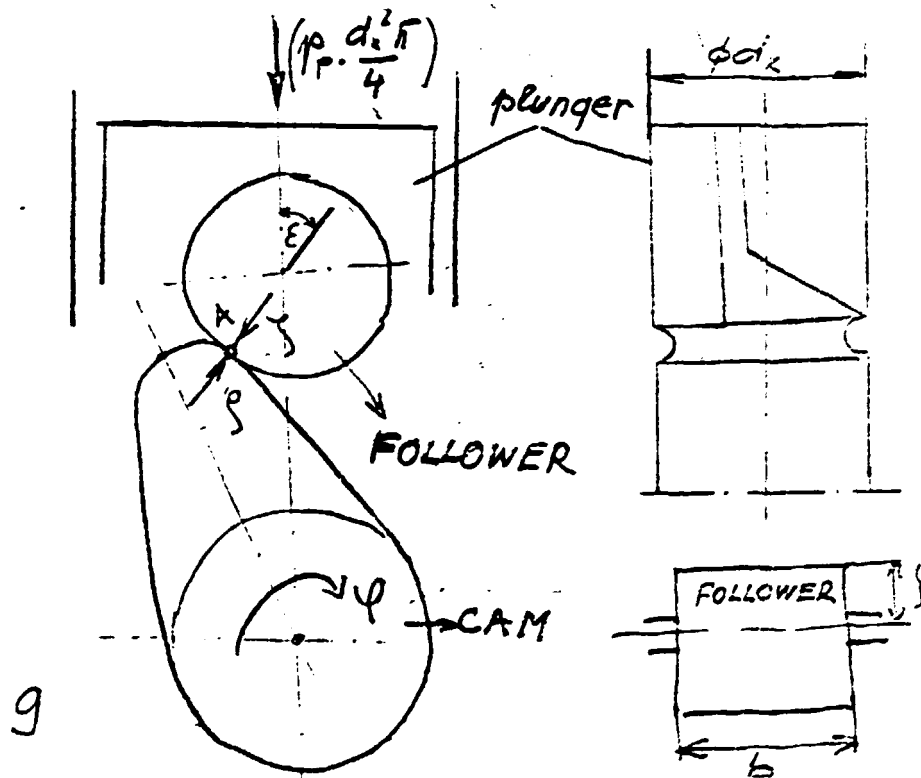


Fig 9

Expression (1) was derived from the work of Stipek T. (see
MTZ No 1 1980, MTZ No 5 1978) but using contact permissible
pressure of 1700 N/mm^2 in the every point A considered (see
Fig 9).

When calculating by Eq 1 for various angles ψ max. permissi-
ble in-barrel pressures may be obtained (Fig 10).

Using:

- effective in-barrel pressure diagraeme p_p obtained by calcu-
lation or by measurements after refraction valve (because of
simplicity)

- beginning of delivery known (pre-lift)
- period of delivery known.

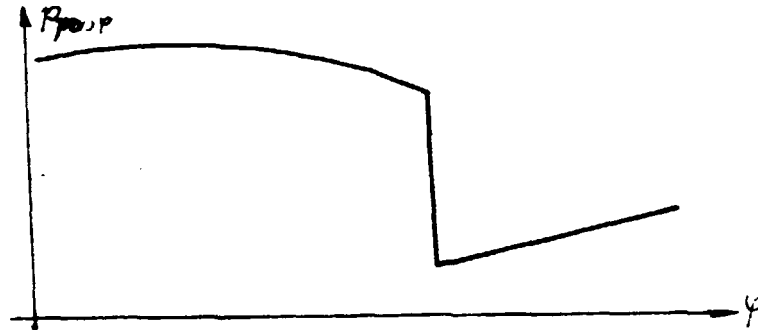


Fig 10 Max. permissible in-barrel pressure v.s. can angle

The next Fig 11 diagrams should be completed.

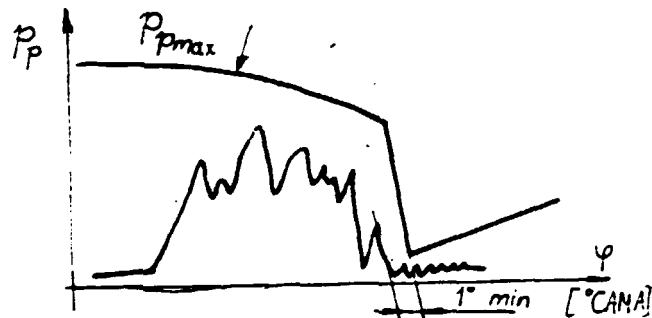


Fig 11

By injection matchings, particularly when fuelling increases for pre-lift given or/and pre-lift increases for fuelling given.

How to increase CR ?

- CR by existing engine may be increased by:
 - thinner cylinder head gasket, sometimes the problem because of small top clearance
 - or/and
 - piston with noufinished crown.

To do that piston producer must be contacted.

In Fig 12 not completely finished piston is shown, which has to be purchased. With thick line in Fig 12 nonfinished surfaces

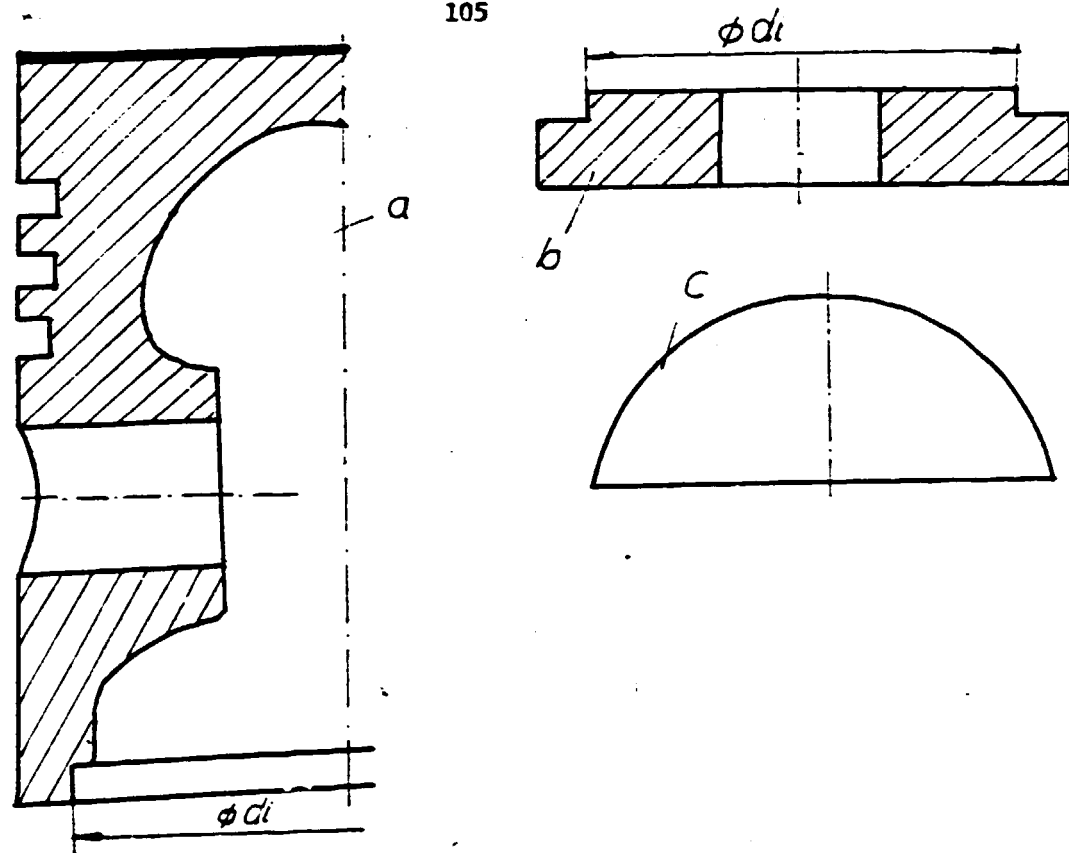


Fig 12

are shown ; ϕd_i serves for finishing in IIP workshop (see b and c in Fig 12). With primitive model c (thin sheet) every simple combustion chamber may be produced.

During our experiments per example we used (1978) comb. chamber volumes : 98, 100, 102, 104 and 106 cm^3 all of them produced as explained above.

How to avoid after - injection

Although needle lift transducer given operates, the needle lift events are hardy to follow, because of a bridge. This is specially the truth looking for after injection phenomenon.

After injection may after happend when:

- increasing fuelling without change of retraction valve
- increasing fuelling without increase of needle hloe dia.'s.

The simplest way is to calculate injection processor to follow experimentally needle lift diagrammes. Only at rated power the above experiments have to be performed.

After injection may be avoided by:

- increased retraction volume, but if decreases the capacity of

the HP pump

- or/and decreased dead volume (mainly decreasing HP tube inner dia.). It is to be recommended, inner dia to decrease on 1,5 mm (for the Kirlaskon engine). It may help to reduce a high influence of compressibility of methanol upon injection period as well as upon pressure drop at nozzle holes.

Increased TCE emission with mean effective pressure increased

Normally with p_e increased TCE exhaust emission decrease. The reason for that is higher temperature with p_e increased and with this better completion of combustion.

Is to be considered that, when late combustion happens although without *misfiring*, TCE may increase with loading increased. It may be still one evidence for late combustion. However, when TCE concentrations measured are not reduced at stoichiometric ratio, the later said may not be truth because of a very high dilution at low loads.

Generally about spray tip penetration, swirl intensity and loads - single controlled speed

With single cylinder engine SR intensity becomes constant and independent of mean effective pressure. SR promotes:

- heat release control with better mixing
- more cooling of charged air.

For the more deposited on the wall of piston bowl a high swirl intensity may control heat release rate only when temperature of the bowl sustains evaporation. With constant swirl intensity and fuelling decreased, wall temperatures also decrease becoming the lowest at starting conditions. When wall temperature drops under critical value for fuel used, deficit of fuel evaporized is evident and stable heat release is not more possible. More heat for evaporation need than released via combustion.

Generally more deposit of the fuel on the wall may be expected with:

- smaller cylinder dia.
- higher injection intensity
- low injection intensity

} Fig 13

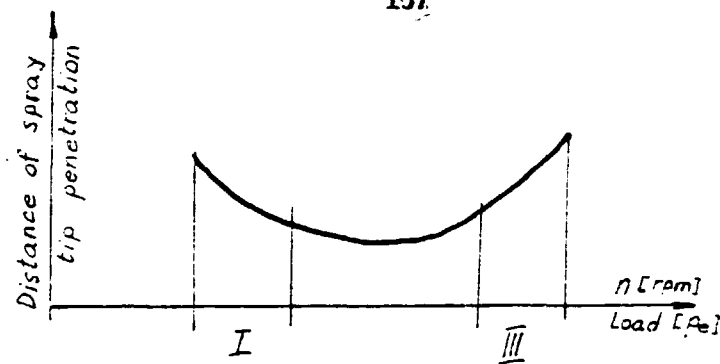


Fig 15

I because of dense core of the spray (bad dispersion), Sauter mean dia. becomes greater or \underline{mV} product increases although velocity \underline{V} is reduced.

III because of high intensity of injection, \underline{V} becomes higher and although d_{32} decreases, product \underline{mV} again increases.

The aforementioned was the reason for controlled injection. Namely, with controlled injection at low loads and starting more fuel is dispersed in air but at higher loads more fuel deposited on the wall of piston bowl.

Cavitation erosion on diesel injection pump

The wear by cavitation erosion is of importance for fuel injection systems, especially when operating with methanol as fuel.

Cavitation attack is mostly pronounced around spill port (plunger, barrel and wall of gallery). To prevent it the easiest way (although not always successful) may be the use of safety screw, see Fig 14. Having, per example, radioactive isotope P-59 and operating with methanol at rated power fuelling, it's possible, on a single way, to study the tendency of wear, using just the safety screw as a most subjected to cavitation attack.

Relevant investigations were performed in Graz (Austria) using the test circuit shown in Fig 15.

The experiments showed that, at the beginning the wear runs to mg quantities, however it was reduced by a factor of roughly 1000 after a run-in time, Fig 16. Fig 16 shows that, the wear reached 4 mg, in $1 \frac{1}{2}$ time interval after starting, approaching to only $2,5 \mu\text{g/h}$ after 25 hours of operation. In order to detect such a small quantity, fuel was poured out, the whole system 6 times washed out and the new active fuel tanked in (point

2 and 4).

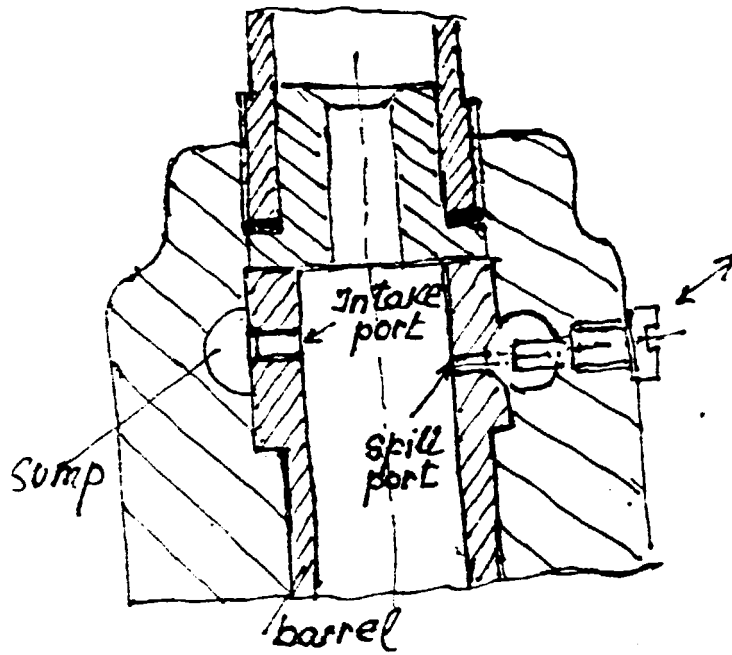


Fig 14 Safety screw apposite spill port

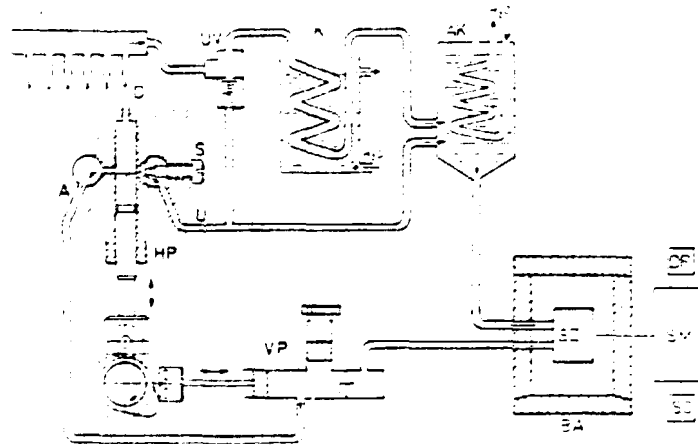


Fig 15 Test circuit for the diesel injection pump

- VP - low pressure pump
- HP - high pressure pump
- A - inlet duct
- D - pressure duct
- U - overflow duct
- S - radioactive screw
- UV - overflow pressure valve
- K - cooler

- AK - balancing tank and cooler
- SZ - scintillation meas. head
- SM - measuring device
- DR - printer
- SC - strip chart recorder
- BA - lead isolation

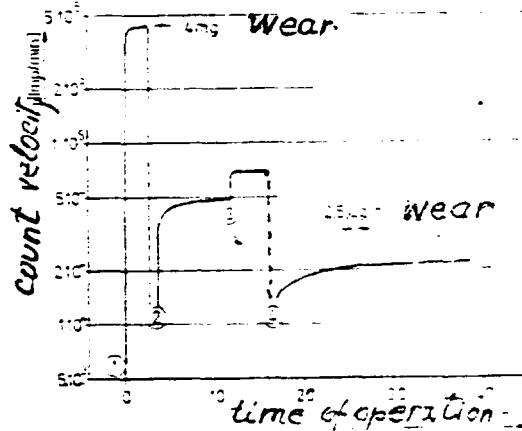


Fig 16 Time-dependent process of the wear by cavitation erosion on a safety screw of the injection pumps.

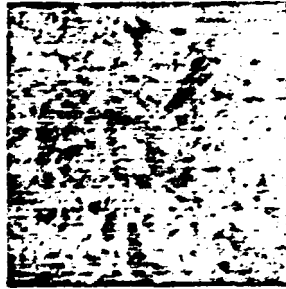


Fig 17

Fig 17 shows the section from the front of the polished safety screw after 44,5 h's of operation, which was subjected to cavitation. (For more information see the 1st Report)

Single cylinder engine in spark plug version and S/D ratio

The small engine considered has the ratio stroke/bore=1,375, mean piston velocity at rated power of 5,5 m/s and swept volume /surface cylinder ratio of 2 cm.

Simple calculation may show that, when using higher stroke max. in-cylinder pressure (for the same expansion pressure shape) must be increased (CR increased). CR increase, when spark plug is to be used, may not be necessary, but lower peak in-cylinder pressure in methanol operation results in poor efficiency asking for compensation of CR loss.

The existed small engine may be modified to use spark plug instead of glow plug. For the first experiments it may be changed only. After successful test related to ignition and low load operation finished the following improvements may be performed by matching:

- a) injection period
- b) spray penetration, distribution and atomization
- c) nozzle holes-arrangement and hole dia.'s
- d) CR ratio for better efficiency
- e) SR ratio for better volumetric efficiency
- f) cast iron piston application
- g) combustion chamber modification
- h) spark plug (position, spark duration)

Spark plug arrangement may not be more expensive than of glow plug offering bellow cited advantages:

- single fuel operation
- some engine for the both fuels, diesel oil and methanol as well as for their blends.
- smallest change when fuel changed
- reliable start under cold ambient conditions
- stable low load operations and transients with small TOR emissions.

In order to support abovecited APPENDIX XI is added (not in this report, for ITP only) related to "KOMATSU" experiments with spark ignition assisted diesel in multi-fuel operation (Automotive Engineering, November 1983).

TOPIC 5"Approach to piston bowl desing for
DI-Diesel engine"

Because of:

- many subjects considered
 - relevant background not brought with
 - anticipated long term visit of expert in combustion subject
- all in TOPIC 5 considered, may be done in very short version and by heart only. However, when need, additional in formations related to the subject 5 may be sent thereafter.

1. Swirl ratio - SR

Average swirl ratio is defined as the rotational speed of air at TDC of compression divided by the engine speed. It may be measured and calculated by averaging the swirl ratios obtained from a number (N) of swirl profiles at various axial locations.

$$\text{Swirl ratio} = \text{SR} = \frac{1}{R} \int_0^R \frac{\bar{w}}{r} dr \quad (1)$$

$$\text{Average swirl ratio} = \overline{\text{SR}} = \frac{1}{N} \sum_{i=1}^n (\text{SR}) \quad (2')$$

or average swirl ratio may be expressed as follows:

$$\overline{\text{SR}} = \frac{30 \sum_{i=1}^n \left| \int_0^R \frac{\bar{w}}{r} dr \right|}{N \cdot R \cdot n \cdot \pi} \quad (2)$$

where:

- \bar{w} - ensemble-averaged mean swirl velocity at radius r
- R - bowl or cylinder radius
- n - engine speed /rpm/

If it is assumed that air rotates like a solid body at TDC the equation above reduces to :

$$\text{Swirl ratio} = \overline{\text{SR}} = \frac{\text{vortex speed}}{\text{engine speed}} = \frac{\bar{w} \cdot 30}{R \cdot n \cdot \pi} \quad (3)$$

which has been used almost exclusively by many investigators due to the difficulty of obtaining detailed swirl velocity

profiles.

When measuring speed of the wheel n_w (rpm) see. to Fig 1

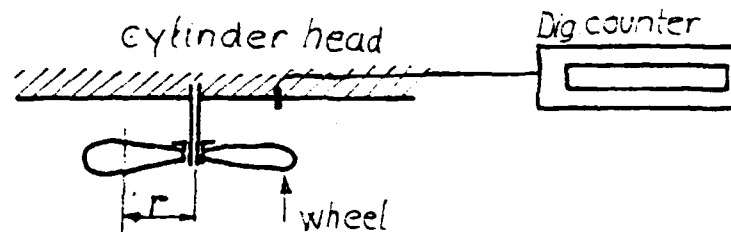


Fig 1

$$f \cdot \omega_{\text{wheel}} = \bar{w} \quad (4)$$

Substituting Eq 4 into Eq 3 results in:

$$\bar{SR} = \frac{n_{\text{WHEEL}}}{n_{\text{engine}}} \quad (5)$$

Thus, measuring n_w and dividing by n_e \bar{SR} may be obtained.

2. Fuel spray accommodation

In the first report as well as in this report many approaches are given related to calculation of fuel tip penetration. We used one shown in the 1st report (see Appendix and example shown). The whole procedure was explained as well as calculation in the listings sent. The whole programme consist of:

- calculation of injection parameters
- fuel injection system matching
- data for calculation of dispersion
- data for calculation combustion
- data for calculation of spray penetration
- data for calculation fuel deposition.

As may be seen in the diagrams shown (see the outputs, 1st report), time or angle fuel contact history of spray tip - wall of piston bowl was presented. In this way fuel deposited on the wall may be calculated in dependance of crank angle. Moreover, locations and areas of fuel deposition may be defined as well.

However, in the programme sent (1st report) swirl impact upon spray movement was not included, because of not existing \bar{SR} data. But fuel tip deviation may be calculated using Eq's of momentum. Related to swirl moment of momentum, it is calculated

as:

113

Angular momentum or
moment of momentum :
(per unit mass)

$$AM = \frac{2}{R^2} \cdot \int_0^R \bar{w} \cdot r^2 \cdot dr$$

Average angular momentum : $\overline{AM} = \frac{1}{N} \cdot \sum_{i=1}^N (AM)_i$

This calculation may be performed using one separate additional modul (was not sent in the 1st Report).

The calculation programme of fuel tip contact is most important one related to spray - bowl matching. It may be concluded that, many different comb. chambers are successfully used but only with spray history matched. Spray history matched understands:

- speed and load dependent matching
- injection period, beginning of injection
- injector holes pressure drop
- low of injection
- atomization
- contact areas on piston bowl v.s. crank angle.

By means of above matched and followed calculation of engine performances, is to be defined (for the combustion chamber chosen):

- nozzle hole distribution
- nozzle hole dia.'s
- position of injector (if not existed)
- injector open - and closing pressure
- retraction volume
- HP tube dia. and length
- plunger dia.
- effective plunger lift
- pre-lift setting
- swirl intensity, inlet (duct) port desing.

The above procedure described followed by some refinings by calculation is especially important when:

- piston bowl could'nt be properly designed because of existing stroke, l/r ratio and piston compression height.
- capacity of existing pump is limited but larger HP pump could'nt be used because of space on desposal.
- position of injector could'nt be changed because of existing cylinder head.

Only after abovecited procedure:

- rig test experiments
 - on engine experiments
- may be the following steps.

3. Combustion chamber shape

To change combustion chamber modifying the bowl shape is normally more difficulty than to desing a bowl for the new engine.

In the first case must be considered:

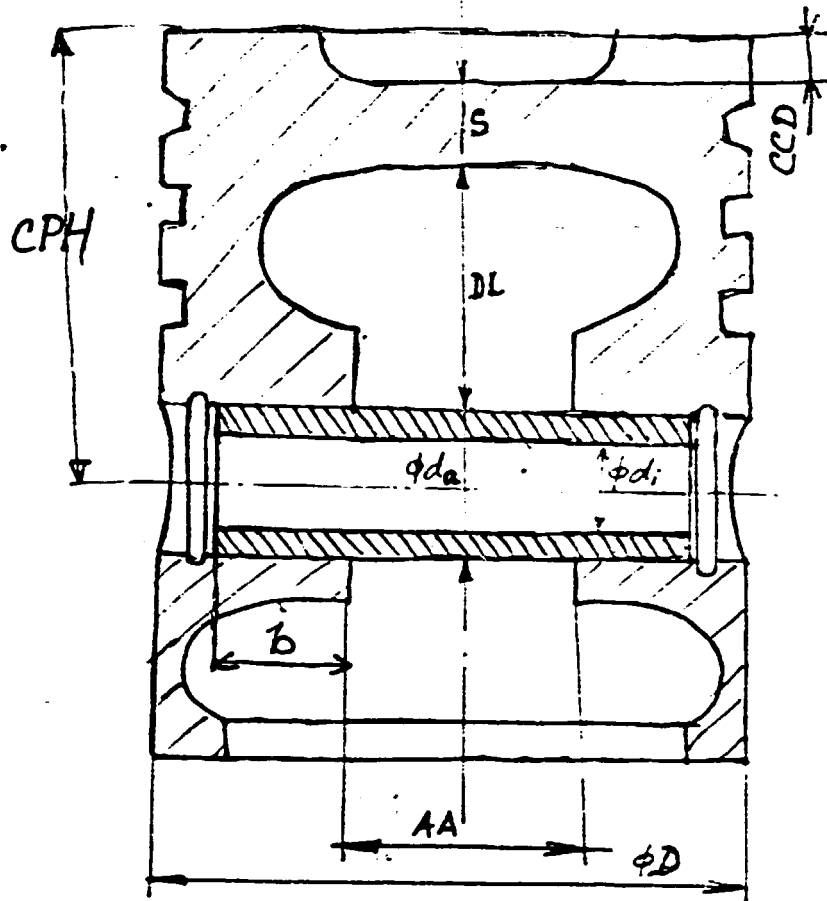
- existed CPH - see Fig 2
- existed r/l ratio see Fig 3,d
- accomodation height of piston (Fig 2 and Table 1)
- gudgeon pin outside dia. $\varnothing d_a$ (Fig 2)
- space for the balacing movement of conrad small end (Fif 3,d)
- piston crown thickness S (Fig 2)
- piston top clearance
- stroke and block of existing engine.

Thus, the depth of piston bowl CCD (Fig 2) for existing engine depends on many factors.

TABELE 1

Max.mean effective pressure /bar/	Max. specific piston loading $\frac{\text{max. power output} / \text{kW}}{\pi \cdot D^2 / 4 \text{ cm}^2}$	Accomodation height $DL = \frac{1}{3} D$
< 8	< 0,185	< 20
8 + 10	0,185 + 0,22	20 + 30
> 10	> 0,30	30 + 35

The bowl shape acc. to Fig 2a was suggested for neat met-hanol combustion. This combustion chamber is typical representation of combustion - fuel deposition on the wall - single hole nozzle - high swirl. The bowl has a high height CCD (see Fig 2) and may not be applied for existing engine. In this case modification must be performed acc. to Fig 2b. However, only accurate measurement now may show if single nozzle hole may be used. (Very after three holes are needed)



$$d_a = (0,32 D$$

$$AA = (0,33 D$$

$$DL = (0,12 D$$

min.

$$p_b = \frac{p_{max} \frac{\pi D^2}{4}}{2 b d_a}$$

$$d_i = (0,42 d_a$$

$$S \geq 0,10 D$$

$$p_b < 60 \text{ N/mm}^2$$

p_{max} - max. in-cylind. press.

Fig 2 Piston proportions for diesel NA-DI engine

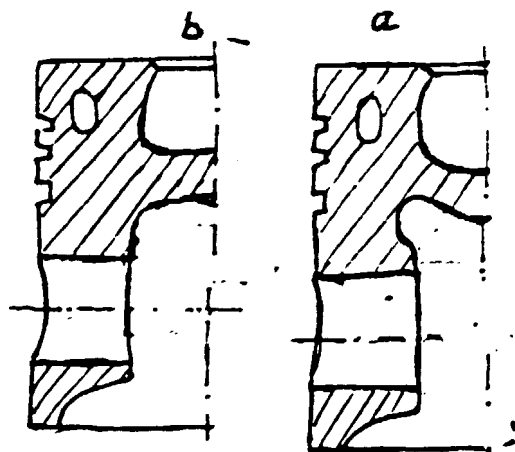


Fig 2a Spherical piston bowl

Fig 2b Semi spherical piston bowl

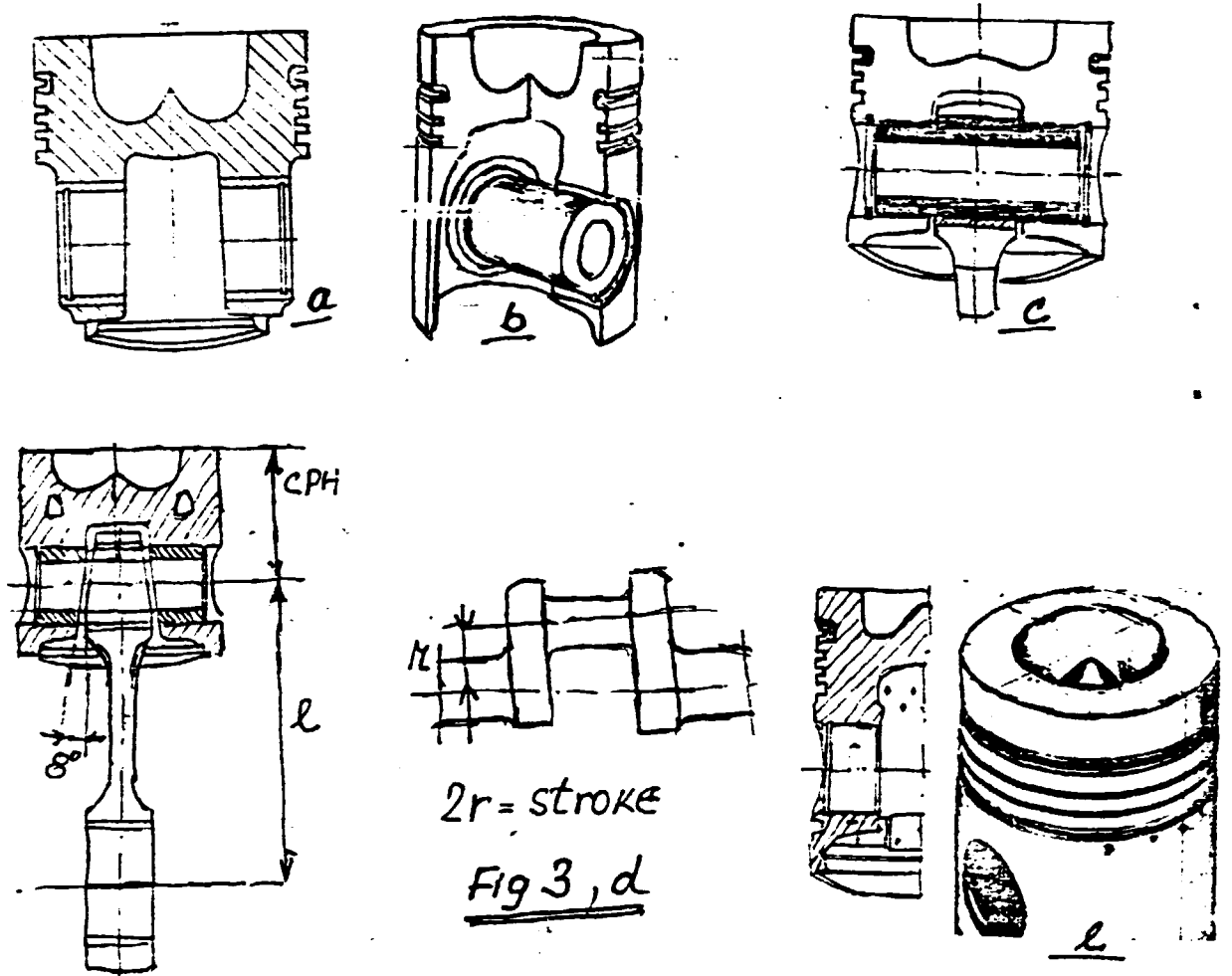


Fig 3

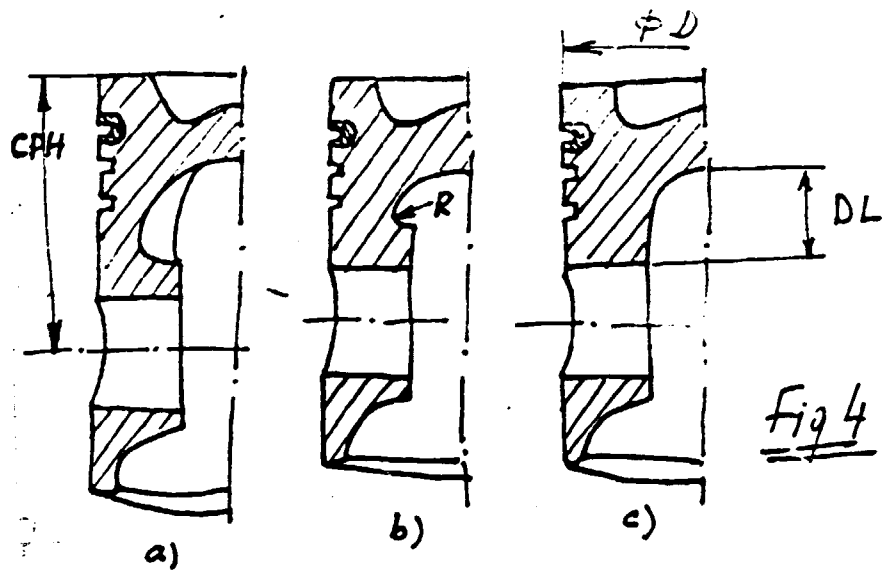


Fig 4

Fig 4

Generally is valid, the smaller piston dia. the deeper piston bowl, for the DI diesel engine.

Fig 3 shows the various versions of omega shaped bowls. All of them have been successfully applied but piston dia., nozzle holes as well as swirl ratio separately matched. For the bowls shown in Fig 3, b, c and d four nozzle symmetrically distributed holes are used. Swirl of middle intensity. Chamber Fig 3, d asks for some higher swirl and more fuel deposition on the wall. Chamber type b, was yet applied in methanol combustion but with the pilot ignition.

Very after, dependent of CPH given (see Fig's 2 and 4) inner shape of piston must be modified. In Fig 4, c was the smallest height CPH on disposal. Sometimes, design d Fig 3 may help to decrease the outside dia. of gudgeon pin and to obtain more freedom for the design of piston bowl.

To follow the effect of circular motion of air swirl intensity has to be changed. For the purpose of experiments masked inlet valve may be used. Masked valve may be produced very easily acc. to Fig 5.

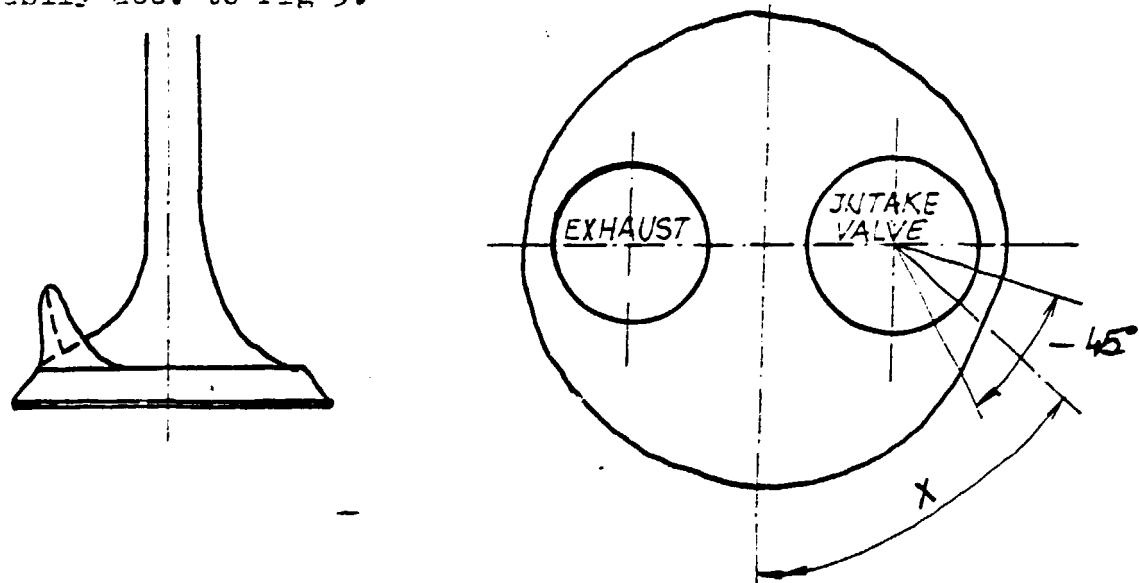


Fig 5 Masked inlet valve, angle x must be defined experimentally

The combustion of squish and swirl in the types of bowl Fig 2 and Fig 3, results in a toroidal air motion around the piston axis. Intensity of squish increases with the clearance of piston cyl. head decreased.

Fig 6 shows open DB new combustion chamber as a simplest one, but is more difficult to match the fuel injection system to it. Again one time, combustion chambers usually have a shape to conform to the spray form.

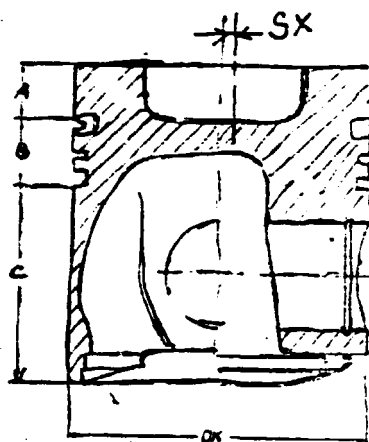


Fig 6

Till now open-combustion chambers were considered only. Open-chambers shown have the bowl dia.'s of about one half of piston outside dia.'s. The excentricity S_x (see Fig 6) must be experimentally defined related to swirl intensity desired and volumetric efficiency. Sometimes injector position existed and possibility of nozzle holes distribution effects the excentricity S_x also.

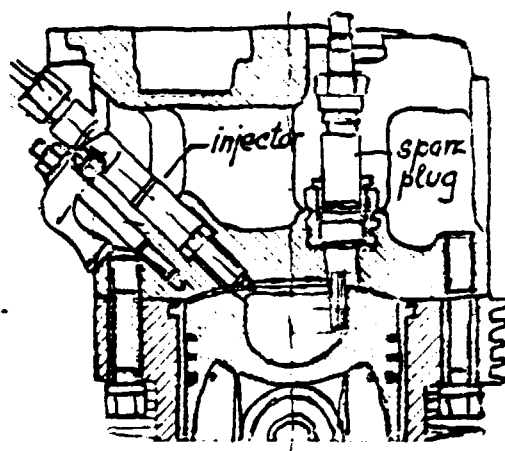


Fig 7 Comb. chamber of MAN engine L9204 FM

MAN combustion chamber shown in Fig 7 is of open type also. It has spherical bottom of the bowl other shown in Fig 3 toroidal bottom.

It may be interesting to compare till now shown and discussed with Komatsu combustion chamber (see Appendix XI, not in this report). The combustion chamber is of Mexican-hat type and Fig's 2 and 3 shown the whole arrangement for CH_3OH use in diesel engine. It may be still one time concluded that, many combustion chamber may be developed but every time, fuel spray history as well as swirl-squish interaction are decisive factors for the success.

It is of interest to mention that, the



Fig 3

both producers: MAN and KHD have the open combustion chamber but top of the piston is not flat. DB with cylindrical combustion chamber has a flat top of piston.

The newest developments of combustion chambers and pistons have been concentrated on saving the fuel and on increase of multi-fuel properties. The both mentioned means to save the heat or to reduce the heat loss. Ceramic components are still our future and investigations showed that, heat loss may be reduced with conventional materials also.

Per example:

MA-DI diesel engine, diesel fuel, swept volume $V_H = 1 + 2 \text{ dm}^3$, mean piston velocity $\dot{x}_{sr} = 8 + 10 \text{ m/s}$ at $p_e = 7 \text{ bar}$, specific fuel consumption rate may be correlated as:

for Alu-alloy piston:

$$b_e = (210 + n \cdot 0,0158) - 12,3 \cdot V_H \quad /g/kWh/$$

$n = /rpm/ , V_H /dm^3/$

for cast-iron piston:

$$b_e = (205 + n \cdot 0,0158) - 12,4 \cdot V_H \quad /g/kWh/$$

It's of interest to see the influence of heat loss reduction on combustion chamber and piston design. Moreover, the strivings are directed to change the combustion process and to accommodate the injection, but now toward reduction of heat losses.

Fig 9 shows the participation of corresponding piston areas on heat transfer (loss) at TDC position. Fig 10 shows that in cold operation volume V_1 (top land clearance) approachy 13%.

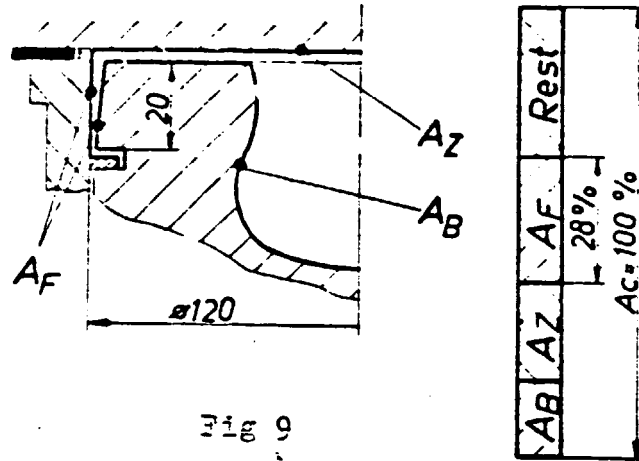


Fig 9

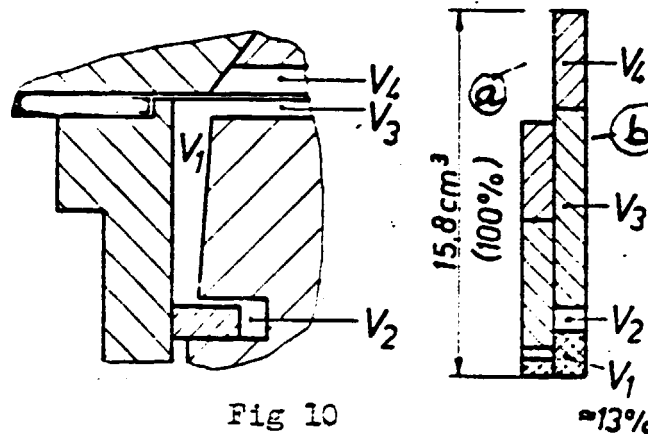


Fig 10

The investigations showed in Fig's 9 and 10 were evaluated related to fuel consumption and mean effective pressure. The results obtained were, more then of interest, what can be seen in Fig 11. Fig 11 depicts that top land clearance dead volumen has a largest influence upon the both:

- increase of fuel consumption rate Δb_e
- decrease of mean effective pressure Δp_p .

Further on, it may be also concluded that the both, heat isolation and combustion process with less heat transferred to the walls have a positive effect on engine performance figures. Doing above cited, engine will be effectively prepared for the use of alternative fuels also.

In Fig 12 are two pistons shown. Combustion chambers are developed for the less heat transferred to the wall of the piston bowl. The piston shown in the left is IFA MM production and ma-

materials is cast iron. The right piston presented is modern Elsbett piston made from cast-iron or from steel.

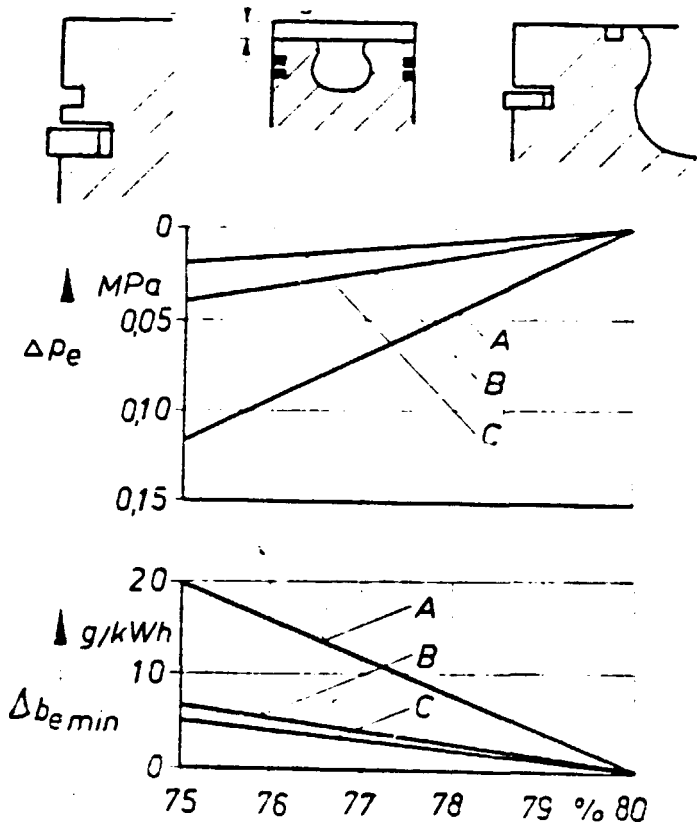


Fig 11

$$V_z = V_A + V_B + V_C$$

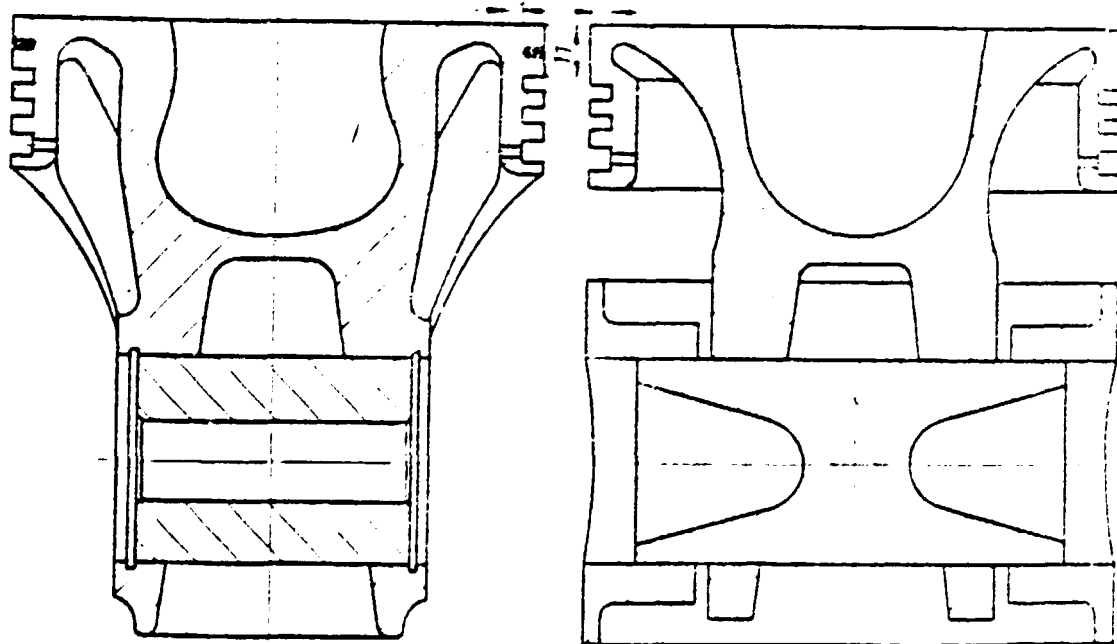


Fig 12 Cast iron IFA piston (left) and Elsbett steel piston (right)

Thus, we are now dealing with most modern combustion chamber of Elsbett. Fig 13 explains the combustion process of single jet combustion method for better heat isolation.

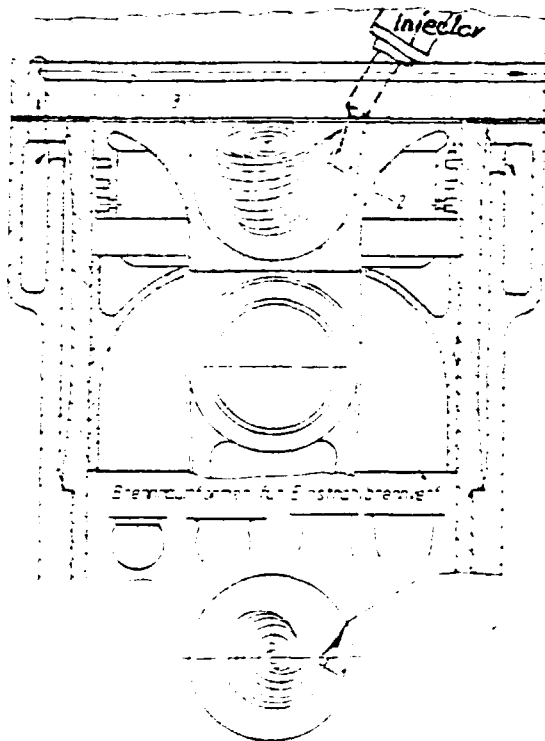


Fig 13 Single jet combustion method for better heat isolation (Elsbett)

- 1 - position of the jet
- 2 - piston (butts against the liner at 4)
- 3 - cylinder head without water pockets
- 4 - bore for coolant to the injection nozzle.

The combustion chamber is similar as for MAN but with Elsbett the spray exercises circular motion being introduced in the intense swirl (see page 1, Fig 13). The gases with lower specific mass are more collected around the bowl center but the air, not immediately taking part in combustion, will be forced toward the wall being acting as a "heat transfer hindrance". Air protection mantle around the bowl wall becomes thinner with fuelling increased. This is the reason for better fuel consumption figure at partial loads (comparing with other combustion process). It means that Elsbett process is the best at "cruise drive".

Fig 15 shows cross-section of oil-cooled Elsbett 3-cylinder car engine of $1,38 \text{ dm}^3$ swept volume. Piston dia. = $\varnothing 80 \text{ mm}$, stroke = 90 mm.

Fig 16 shows the combustion Elsbett chambers for truck application. Cylinder design enables the increase of piston diameter without increase of stress on cylinder head and engine block.

The whole design procedure may be seen in Fig 17.

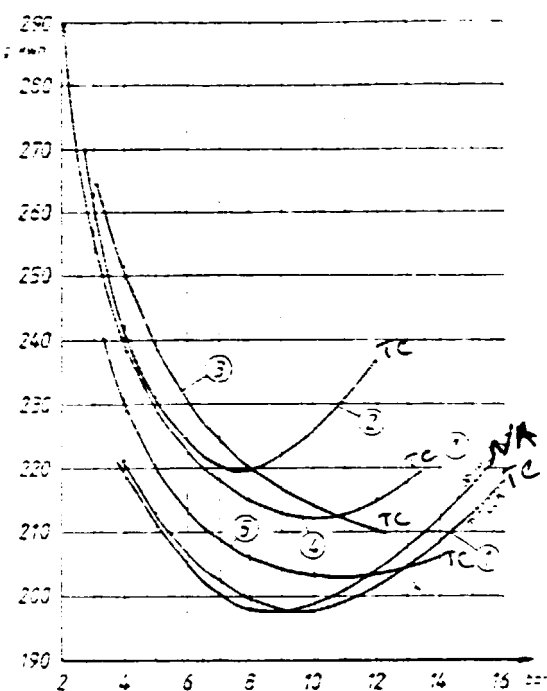


Fig 14 Part-load s.f.c. at
7,5 m/sec piston velocity

- 1 -heat isolated single jet
DI engine 15,5 dm³, 6 cyl.
- 2 -heat isolated single jet
DI engine 1,58 dm³, 5 cyl.
- 3 -single jet DI engine
cooled charging air
11,4 dm³, 6 cyl.
- 4 -Four jet DI engine,
without intercooling
9,6 dm³, 6 cyl.
- 5 -Four jet DI engine,
without intercooling,
with heat insulated engine
components, 9,6 dm³, 6 cyl.

TC - turbocharged NA - natural aspirated

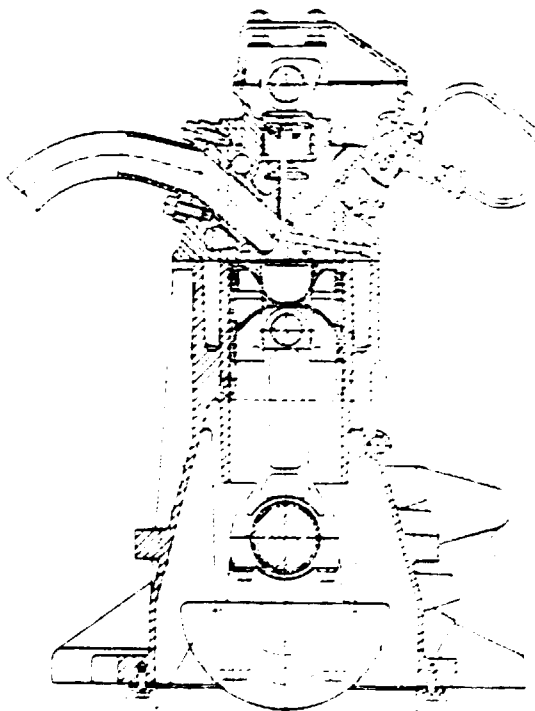


Fig 15 Cross-section of oil-cooled Elsbett 3-cylinder
car engine

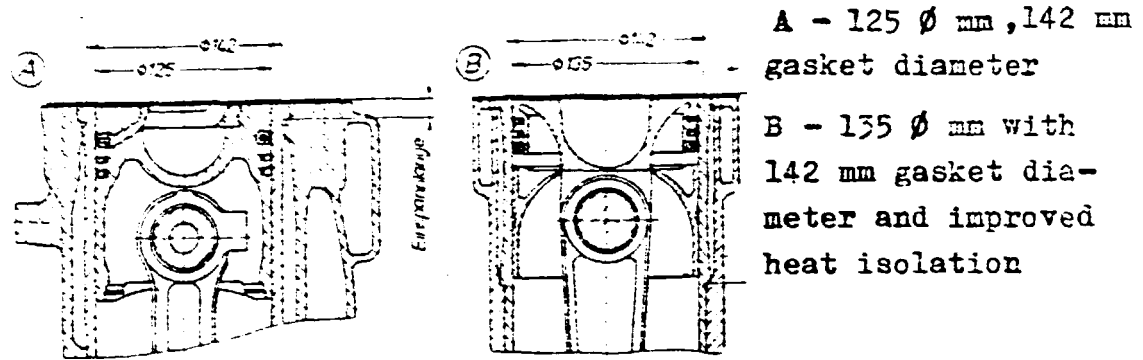


Fig 16 For truck application

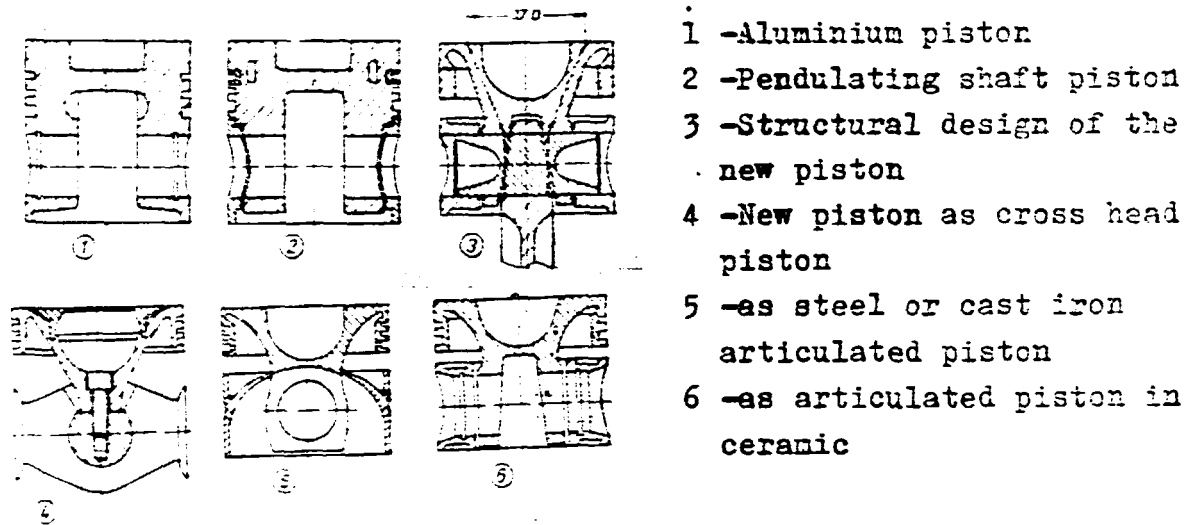


Fig 17

Heat saving achieved may be obtained by comparison of cooling requirements before and after conversion for improved heat isolation (Fig 18).

Thus:

- 1 -passenger car swirl chamber diesel engine
- 2 -passenger car DI engine after conversion
- 3 -truck engine before conversion
- 4 -truck engine after conversion, using water as coolant
- 5 -truck engine after conversion, using oil as coolant

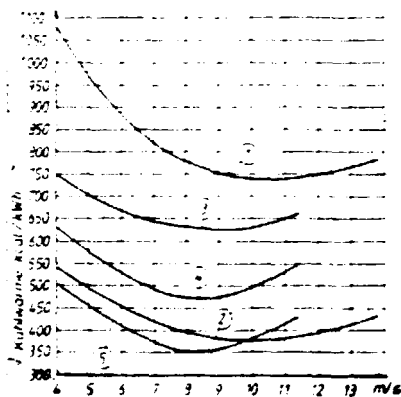


Fig 18 Cooling heat required /kcal/kW/ v.s. car velocity $\frac{m}{s}$

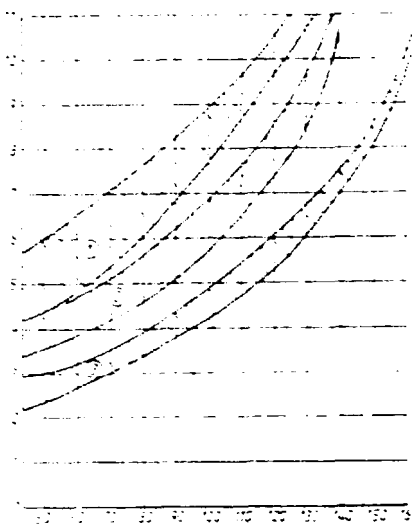


Fig 19 Fuel efficiency / l/100 km/ v.s. car velocity /km/h/ for passenger car of the 3 different combustion methods

As shown here developing the single jet combustion system further for improved heat insulation resulted not only in the best passenger diesel car engine concerning noise, fuel efficiency and power; it also demonstrated that practically all improvements in the heat balance of the engine at the same time made the engine less expensive.

Re-entrant bowls claim for the inside turbulence. Namely, turbulence inside the bowl increases considerably to those generated early in the intake stroke. In the absence of swirl (see "Steyr"-Wien, "Famos"-Sarajevo) and with the re-entrant bowl configuration (acc. to Arcoumains-Bicen-Whitelaw), the squish induces a similar axial flow structure to that in the cylindrical bowl but of stronger nature. (See Perkins squish-lip). With re-entrant bowl squish is more pronounced. The addition of swirl, however, results in the formation of two vortices rotating in opposite directions (see Fig 20). The swirling motion exhibited spiralling characteristic at the entry plane of the bowl and solid body type of rotation near the bowl base.

For the case of the cylindrical piston-bowl (open combustion chamber) and in the absence of swirl, a squish-induced toroidal vortex occupies the whole bowl space at TDC of compression. Interaction of swirl with compression-induced squish, however, results in the formation of a counter-rotating vortex in the axial plane in addition to the near solid body rotation of the fluid in the tangential plane (see Elsbett combustion chamber). The squish, in

In the end it's interesting to see differences in fuel consumption figure but now in field. Fig 19 depicts that passenger car with Elsbett 3-cyl. engine may have average fuel consumption of about 4 l/100 km.

- 1 -Gasoline engine
- 2 -IDI diesel engine
- 3 -single jet diesel engine

the presence or absence of swirl, does not alter the overall turbulence levels which remain comparable to those obtained with the flat piston. This swirl profile at 180° of compression

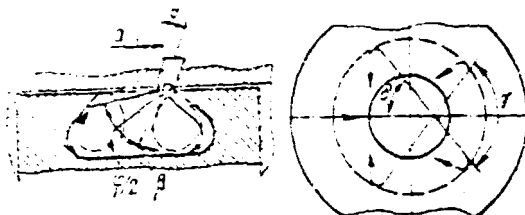


Fig 20 CHBI-re-entrant bowl with new nozzle holes distribution (5 holes). $a=10,7 \text{ mm}$, $\epsilon=24^\circ$, $\beta=15^\circ$, $\gamma=2\delta$, $\varphi/2=75^\circ$

depends more on piston-bowl geometry rather than on the intake swirl field which is better reflected on the final angular momentum of the bowl contents (Ar.-Bic.-Whit.).

Practically considered re-entrant bowl is prone to operate at the top rim of the bowl and in more difficulty to control the combustion process. With this combustion chamber 4 or more holes are needed and fuel is macro-distributed by nozzle holes. With Elsbett and MAN as well as partly with D process (MHD) air motion is mixture controlling. Re-entrant bowl produces more combustion noise with higher pressure rise. Peak in-cylinder pressure is normally higher than that with open combustion chamber. However, re-entrant bowl, if good matched, may show a good fuel consumption figure.

Comparing the both, open and re-entrant combustion chambers may be concluded that open piston bowl offers more benefit than re-entrant one. We may also conclude that, the swirling motion inside the cylindrical bowl is closed to solid body rotation while re-entrant bowl gives to complex flow patterns. Equally, in the presence or absence of swirl, does not augment the turbulent energy inside the cylindrical and open bowls contrary to re-entrant configuration where turbulence generation may be observed.

Having more complex flow pattern of introduced air, re-entrant bowl is less suitable related to control of:

- fuel spray patterns
- time-space history of mixture formation
- heat release rate
- heat transferred to the wall.

Open cylindrical combustion chamber with deep spherical bo-

ttom may be suggested for methanol combustion in diesel engine. Fuel spray pattern may be more like Elsbett or more like MAN. Otherwise, using controlled injection at partial loads, MAN new engines, have more fuel distributed in air also (like Elsbett). At higher load is a large difference related to fuel spray patterns between MAN and Elsbett. Further on cast iron piston and CR=18 may be suggested also (for CH_3OH combustion).

As yet mentioned, sometimes is not so easy to apply deep combustion chamber in existing engine. Three piston rings (1st keystone, 2nd tapered compression ring 90°, 3rd spring supported oil ring) is a standard today (in diesel engines). Top land may be only at 10% Dk. But above said does not help for deeper combustion chamber location because of:

- stroke given
- gudgeon pin dia.
- piston compression height given
- connecting rod small end
- min. bottom thickness of the bowl needed.

However, some compensation up to 5 mm may be obtained on a primitive way.

Controlling the temperature during forging the conn-rod may be manufactured with shorter length l (see Fig 21), let say up to 2 mm. Moreover, very often happens in series production

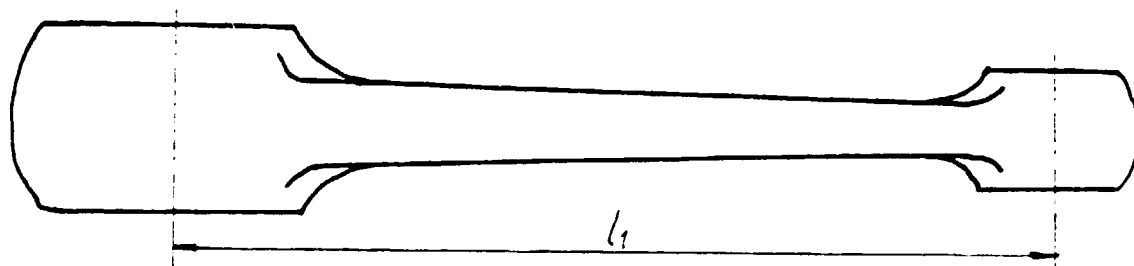


Fig 21

also that some of conn-rod forged become yet shorter and have to be refused. We've been using just refused conn-rods without special order.

The distance between the centers of conn-rod holes may be manufactured shorter also in the work-shop; let say up to 1 mm shorter (see Fig 22).

When counterbalance weights at BDC may come to contact with piston, it may be reworked-out acc. to Fig 23 or/and counter weights may be field out, Fig 24. Because of shorter distance l

(see Fig 22) $\beta_{\max} = \arcsin \frac{r}{l}$ becomes greater and the conn-rod may come to contact with cylinder liner. In this case the windows have to be made in liner, see Fig 25.

After matching in engine experiments, new connecting-rod may be fabricated properly.

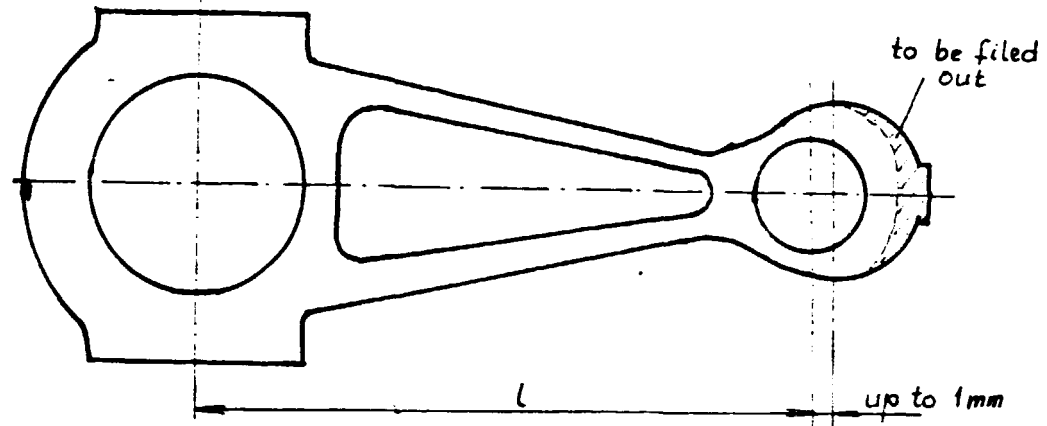


Fig 22

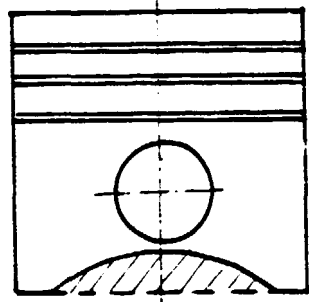


Fig 23

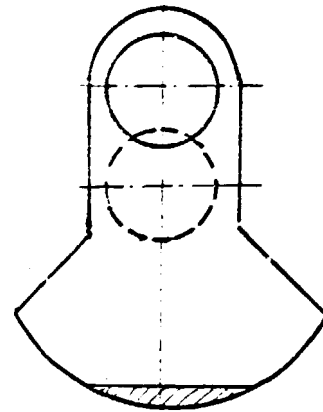


Fig 24

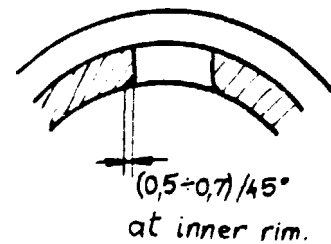
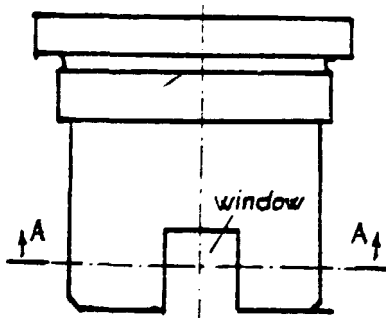
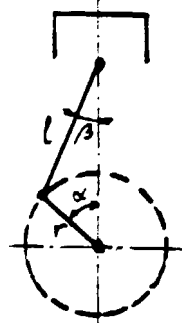
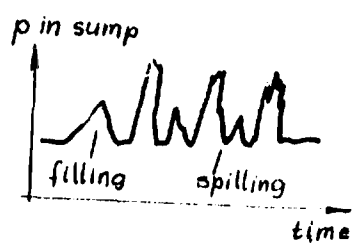


Fig 25

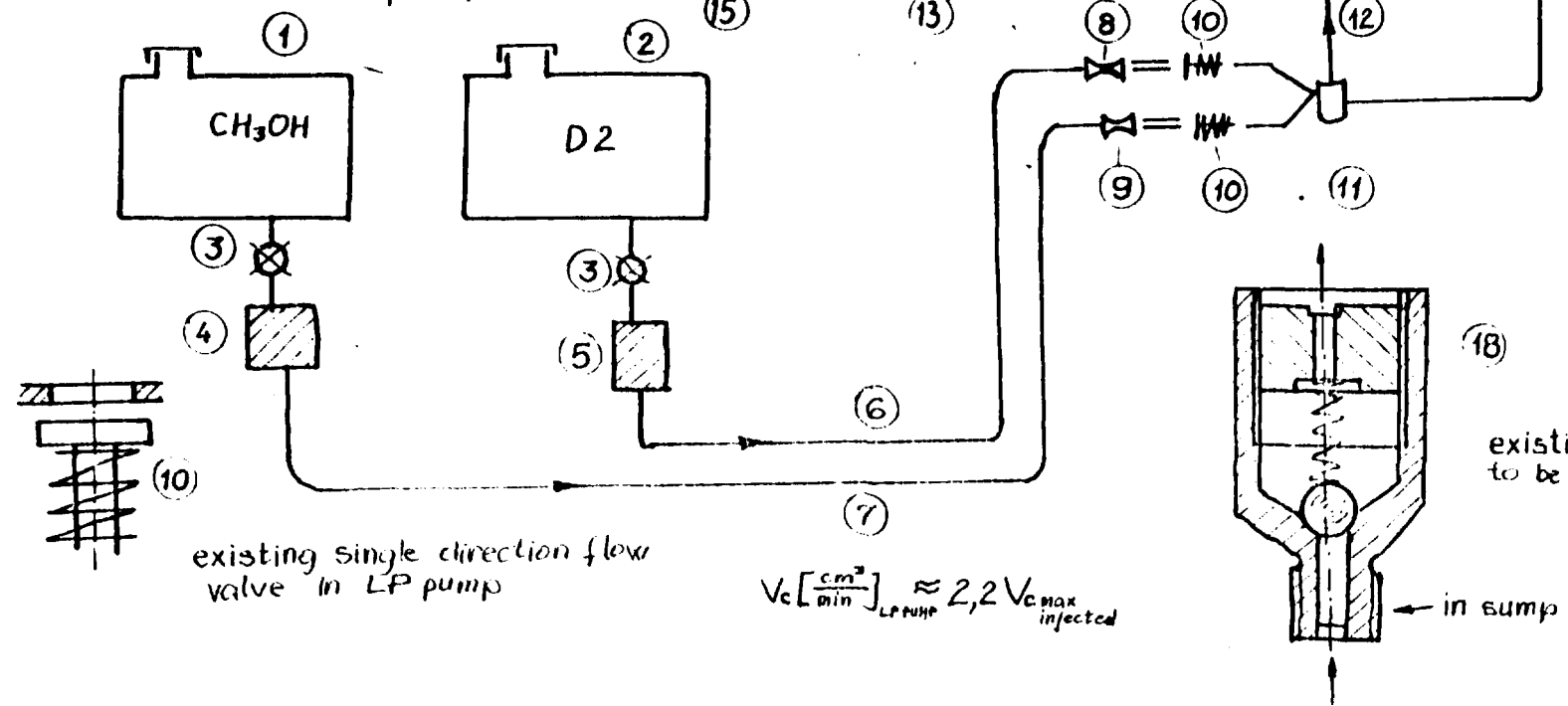
- 1-2 fuel tank
- 3 simpk valve
- 4-5 fuel filter
- 6,7 supply tube
- 8-9 doping
- 10 single direct valve
- 11 conection
- 12 supply tube
- 13 LP pump
- 14 inlet tube
- 15 HP pump
- 16 common sump
- 17 realise screw
- 18 spring valve
- 19 mixing tube

81-91 instead of 8-9 in swithing-on application as was yet explained

Leakless barrel must be used (contact MICO)



- Mixing by:
1. Overflow of filling
 2. Overflow of spilling
 3. Overflow of LP pump
 4. Injection by pos. 18



existing single direction flow valve in LP pump

$$V_c \left[\frac{cm^3}{min} \right]_{LP\ pump} \approx 2,2 V_{c, max\ injected}$$

existing filter valve to be set at 0,5 bar

Fig 1

Appendix X 2 related to the TOPIC 2

In argument with suggestions given in the TOPIC 2 the relevance experiments were performed using D_2+CH_3OH blend as fuel. TATA in-line engine was used and A-type pumps $\varnothing 7 \times 8$ mm was applied. 20% by volume methanol was doped to diesel oil and with external constantly stirred homogeneity unstable mixture was prepared. Additionally internal mixing was applied acc. to the Fig 1. Positions from 1 to 11 were replaced with stirring technique in this experiments. It was done purposely in order to check very fast:

- starting
- low load operation
- knocking
- full load operation and transient.

The experiments were performed on 27 August 1964. Cold start was not completed because of conditions on desposal.

Starting, under ambient lab conditions was without any problem as well as for low load operation. Fuel load was observed at 2800, 2000, 1500 and 1000 rpm. Exhaust temperatures measured were in error because of instrumentation on desposal. Transients observed were as usual, taking into account dynamometer-inertia and resistance coupled.

Completing successfully first provisional testing of engine reactions related to blend used, the bellow cited step of experiments may be suggested.

Using the arrangement shown in Fig 1 the engine performances have to be observed, but now much more in detail. Doping quantity of methanol may be expected up to 30% by volume, it means, that for same power output, the fueling must be properly corrected.

Instead of very primitive flow doping pos. 8 and 9 (Fig 1) fuel distribution may be used (see pos. 81 - 91, Fig 1) as was yet explained in detail.

Doing above mentioned up to 12% of diesel fuel may be replaced by methanol.

Although the princip of mixing may be successful, it should be estimated the all change needed, to obtain as much of their benefits as is economically worthwhile.

ONLY TO MENTION :

The recent rapid application of the Diesel turbocharged engine to railroads has been brought about by the need for better performance and overall economy.

The main goods applying turbocharging were to:

- increase $\rightarrow \frac{\text{kW output}}{\text{dm}^3 \text{ swept volume}}$
- decrease $\rightarrow \frac{\text{m}^3 \text{ engine box volume}}{\text{kW output}}$
- decrease $\rightarrow \frac{\$}{\text{kW}}$ in the first cost
- decrease $\rightarrow \frac{\text{g}}{\text{kWh}}, \frac{\text{l}}{100 \text{ km}}$ fuel consumption rate (let say about 10%)
- decrease \rightarrow engine exhaust emission
- decrease \rightarrow engine noise emission
- simplify \rightarrow engine production by reduction of engine types.

Although, these principles are still valid, NA engines should be modified also to obtain as much of their benefits as is economically worthwhile. Reducing, per example, the fuel consumption rate by NA version, is of benefit for later turbocharging also. Thus our attention must be paid to fuel saving by NA engine at first.

It may be mentioned, that combining turbocharging and CH_3OH as fuel further fuel saving may be obtained and thus in a very simple way.

TOPIC 9Exhaust gas on-line analysis1. THC - THCO

Dealing with methanol as fuel, especially at low load, in cold operations and transients some correction must be used in FID outputs, when as CH_3OH equivalent calibrated. It may be done by calibration itself or approximately by:

$$C_{\text{THC measured}} \cdot \frac{2}{2} = C_{\text{THC evaluated}}$$

In the case of calibration we are using the procedure acc. to Fig 1.

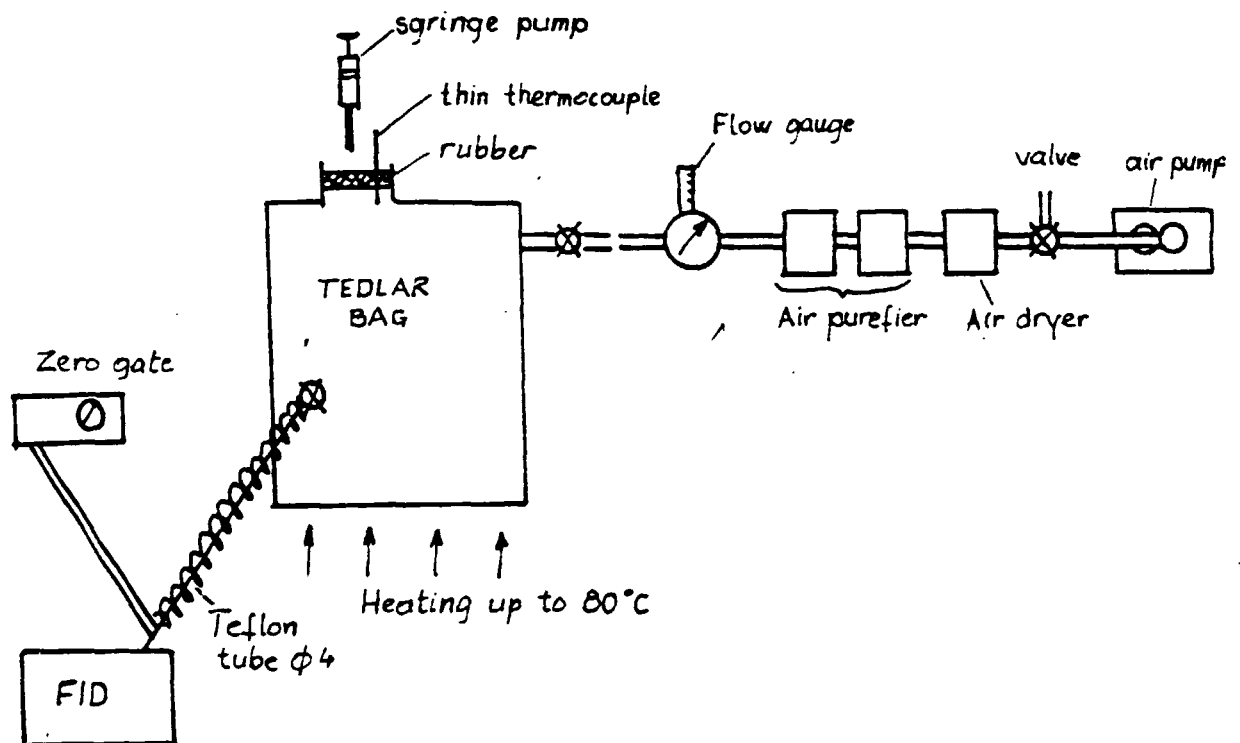


Fig 1 With pump CH_3OH of known volume should be injected

We are using air instead of N_2 when dealing with diesel engine. The reason for that:

- at low load operation excess air is very high, thus stoichiometric ratio may be exceeded six times
- just at low loads THC concentration are important

Having O_2 in excess our sample gas changes character of hydrogen envelope flame into more prexined one. Changing character of diffusion flame ionisation effect will be changed

and so does FID output also. To compensate that the best way is to use the purified air as dilution gas (see Fig 1). The same has to be used by C_3H_8 dilution. On the contrary dealing with SI engine we've been using H_2 as "carrier gas".

For THC equivalent C_3H_8 calibration and diesel exhaust analysis we use the procedure acc. to Fig 2.

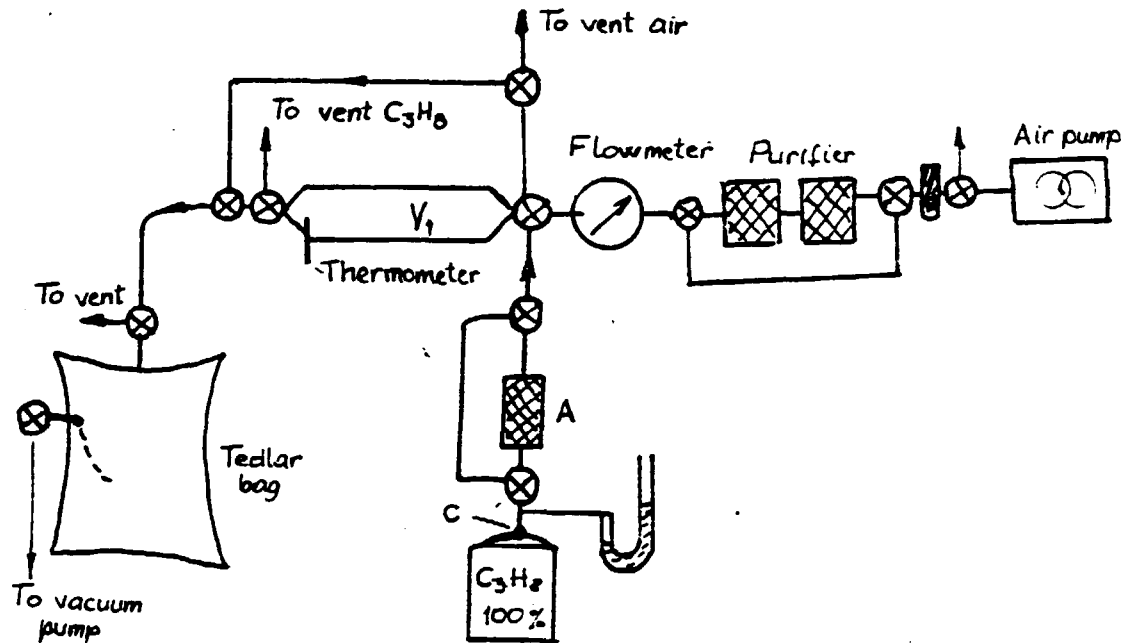


Fig 2 Preparation of C_3H_8 span gas

C_3H_8 % must be checked by gas chromatography. We use commercial C_3H_8 for industrial application. According to the impurities presented we choose the purifier - A (see Fig 2).

Volume V_1 is C_3H_8 trop, which must be precisely measured in before hand. Tube B is very long stretching out of lab. After purifying the volume V_1 with C_3H_8 , valve C must be closed to wait about 30' for ambient pressure accommodation in V_1 .

We use the our special very simple anregement to check the accuracy of floweters, what is very important for calibration gases.

CO_2 calibration gas we prepare in the same way using Kipp apparatus ($CaCO_3 + H_2SO_4$). To remove the water one drying column may be used. However, because of very low pressure by CO_2 production, case must be taken related to resistances and time for trop spilling setting longer (NDIR-calibration).

CO is produced using anticacid+water. Very slowly only some water droplets are added and the temperature of acid is to be observed $40 \pm 60^\circ C$. Again, because of low pressure core must be

taken related to resistances (NDIR calibration).

Because of very high carbon particulates content in diesel exhaust gases, some filtration must be applied. However, THC emission is only of interest at very low load, where the soot emission is very low also. It means that, only two glass filters may be applied by heated up to 205°C . We use ϕ 4 mm teflon tube and heating technique the same as shown in Fig 1. In order to measure concretely combustion air is cleaned over two columns

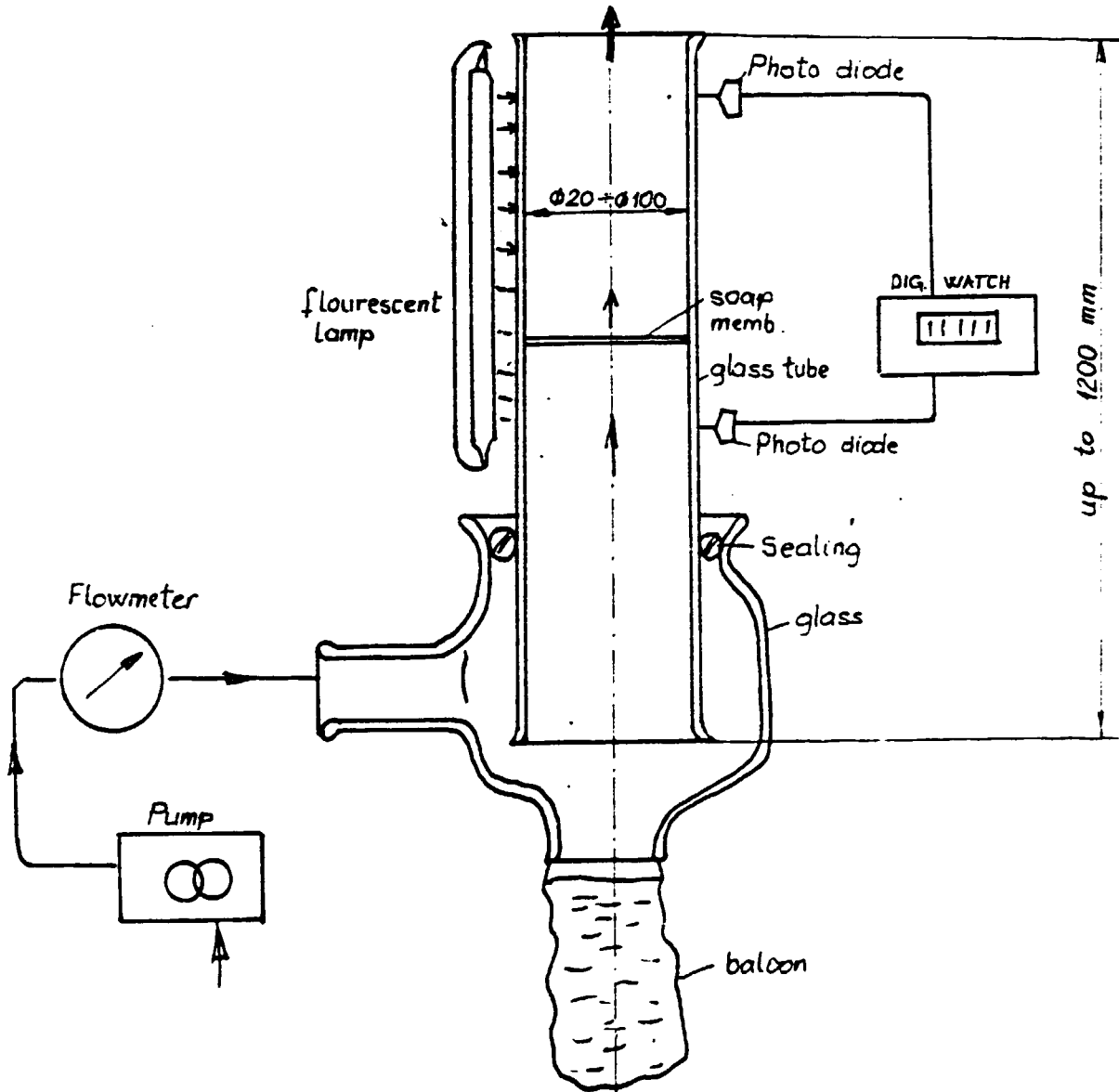


Fig 3

(separate air generation). To find plateau increasing H_2 flow rate is practically impossible with some apparatuses. Therefore is the best way to keep about 80% of max. value and calibrate it the same H_2 flow rate.

Background can be depressed only if clean air is to be used.

With H_2 low pressure setting oscillations of diffusion flame may be observed and variation in the data measured also.

Data measured must be reduced at stoichiometric ratio and expressed as emission index

$$\frac{(g) \text{ TCO}}{(g) \text{ fuel burnt}} = \frac{(g) \text{ C}_x\text{H}_y}{(g) \text{ fuel burnt}}$$

Only in this way analysis is possible.

2. NO_x measurements

One of the very difficult analysis is on-line NO_x measurements in diesel engine exhaust gas. The arguments may be mentioned:

1. NO_x is of interest at highest loads but the soot emission is also high
2. NO_x may be absorbed, destroyed and converted by: soot collected, high surface to volume ratio of sample line and material used.
3. Converter efficiency decreases with time
4. Partially clogged capillaries in the chemiluminescent analyses
5. Optical filter of photo multiplier soiling
6. High vacuum needed in reaction chamber
7. Span gas change with time (NO/NO_2)
8. Sample flow rate decrease because of soot collected on filters
9. NO_2 loss in water trap.

In our lab praxis we use the scheme shown in Fig 4.

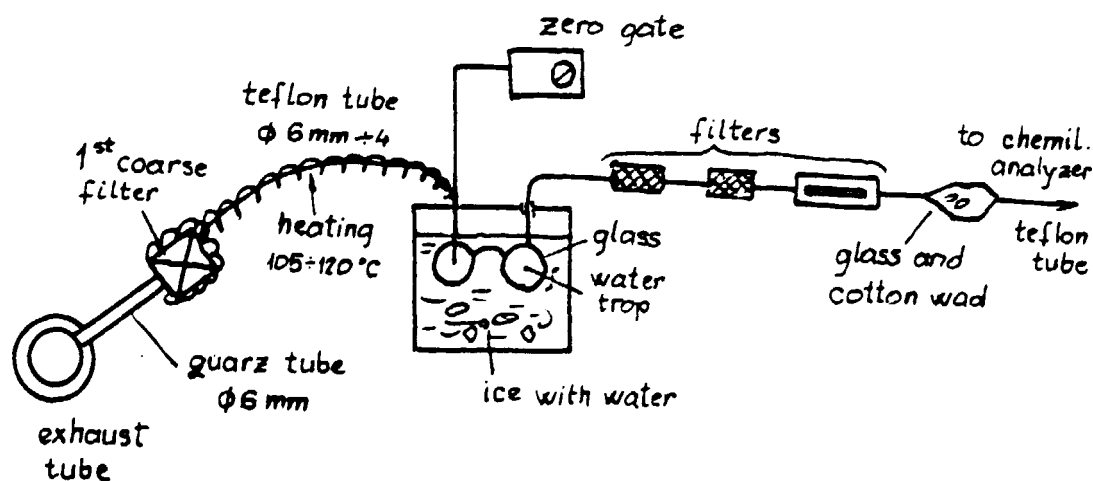


Fig 4 NO_x on-line measurements

Filters shown in Fig 4 are explained in the 1st Report already.

The first part of sample line is heated to avoid condensation of water in the teflon tube (surface/volume high). The length of heated tube approaches 1 - 1,5 m only. Fast condensation of water but in smallest surface/volume ratio (two spherical glass traps).

At temperatures less than 100°C soot collected absorbs NO_x and at higher than 250°C starts NO_x destruction. At 900°C and with reasonable sample flow rate, soot collected in a column of about 500 mm length, destroys NO_x completely.

Therefore, care must be taken about temperatures and amount of soot collected. However, in on-line measurements first sign is sample flow drop and decrease of analyzer outputs. It is to be noticed that, sample flow rate has to be kept the same as for calibration.

NO/N_2 high span calibration gas may be deluted by N_2 but, two "Oxisorb" column must be used to purify N_2 and to avoid $\text{NO} \rightarrow \text{NO}_2$ conversion (calibration in error and bottle attack).

To check converter efficiency or calibration gas being long-lasting in the bottle, self made converter ($\text{NO}_2 \rightarrow \text{NO}$) may be used acc. to Fig 5.

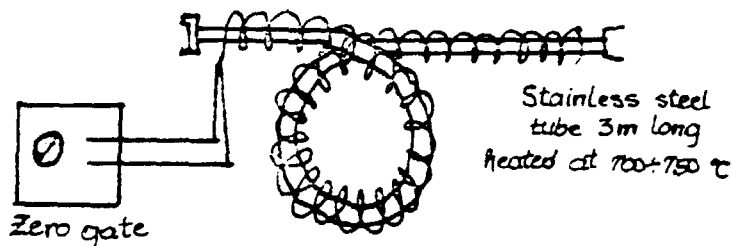


Fig 5 Converter $\text{NO}_2 \rightarrow \text{NO}$

Continuously doping O_2 in NO/N_2 mixture unstable calib. gas NO_2/NO may be produced of known concentration. However, dynamically produced NO_2/N_2 span gas must be in on-line technique continually used.

TOPICDynamic

During mission two engineers have been trained related to piston-mechanics and balance. One booklet (66 pages) was presented and translated into english. The whole subject was considered in the way of computer application and calculation of:

- $x, \dot{x}, \ddot{x}, \rho, \dot{\rho}, \ddot{\rho} \rightarrow f(\alpha)$

- K, I, K_x, K_y, K_z instanteneous inertia loading

-Balancing

- $K, K', K'', K''', K_1, K_2, K_3, K_4, P_1, P_2, P_3, P_4$ instanteneous whole loading

- $M_e = M - (M'' + M''' + M''')$ instanteneous torques

- $M''' = M'''_1 + M'''_2 + M'''_3 + M'''_4 + M'''_5$ instanteneous torques of friction

-fly wheel calculation

-torsional vibration problem, calculation of eigen frequencies, resonant state only.

Some examples are given related to application. Per example using Eq. for M' the whole starting process may be studed, of interest for CH_3OH use as fuel.

ICEIC 5High - pressure injection

Efficiency of diesel engine combustion depends mostly on fuel-air mixture formation. Mixture formation depends in:

- fuel pressure drop in nozzle holes
- fuel spray direction relative to air movement
- beginning of injection (timing)
- period of injection
- law of injection
- atomization of fuel injected
- stoichiometric ratio
- swirl and squish
- combustion chamber or piston bowl
- air temperature
- pressure of air.

The all above factors mentioned are location and time dependent and have to be optimised via compromise between:

- fuel consumption
- exhaust emission-combustion noise
- mechanical loading
- thermal loading.

As mentioned already, decisive factor is time-volume history of mixture formation in a very narrow space during a very short period of time.

With diesel engine the both, air and fuel take part in mixture formation. Thus, the energy E_R needed for combustible mixture formation may be expressed by:

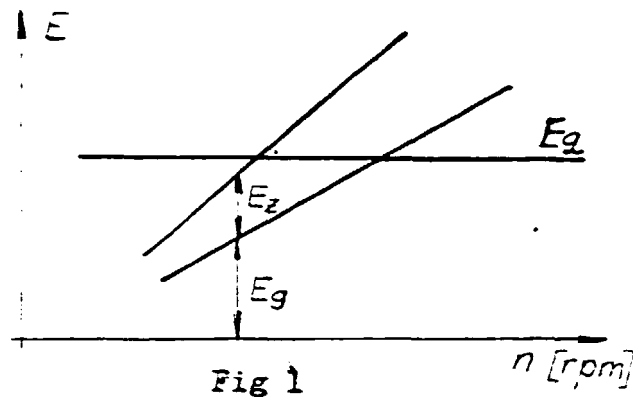
$$E_R = E_q + E_z \quad (1)$$

where: E_q - part of E_R given by fuel injection
 E_z - part of E_R given by air motion.

A logical hypothesis may be : the higher E_z the lower E_q .
 But higher E_z means:

- lower volumetric efficiency with NA engines
- higher thermal loading of the parts forming combustion chamber
- higher heat loss
- bad cold startings.

The drawbacks mentioned were the impetus to increase the part E_1 or to apply high-pressure injection (HPI). However, it's not the whole philosophy of HPI, still one point must be considered. Namely, with conventional fuel injection system (CJI) using of the same time E_1 as well as E_2 for mixing, we experienced speed dependent dis. proportions related to the mixture quality (Fig 1).



E_2 (see Fig 1) may be considered as constant with vehicular diesel engine at full load operations because of nearly constant fueling. Meanwhile, the both E_1 as well as E_3 are increasing with speed (n) increased (see Fig 1); thus at higher speeds we have surplus but at lower speeds deficit of energy needed for good mixture formation (soot, bad torque back up).

Using theoretically only E_1 for mixture formation results in a high pressure drop Δp at nozzle holes. The question arises, what's then with spray tip penetration related to small piston dia.'s? Spray penetration getting longer and so doing fuel deposition on the wall when absence of swirl combustion may be poor. However, depending of nozzle hole geometry we may have a dense high penetrated spray or finer dispersed short penetrated, which supports faster transformation of liquid phase into gaseous one and better homogenisation of combustible mixture.

Thus, we are asking not for high penetration, on the contrary, the more intense spray must be better atomized only under all speeds. Here is the second point of HPI philosophy which accents: not only HP injection but independent of speed also.

With much better atomization HPI claims for better combustion history which results in increase of thermal efficiency and reduction of soot emission. Moreover, when swirl intensity reduced engine volumetric efficiency increases and "unnecessary" heat transferred to walls will be reduced also.

However, it must be noticed that fast combustion can not be applied when accompanied with a high in-cylinder pressure rise (Fig 2) $dp_z/d\alpha$.

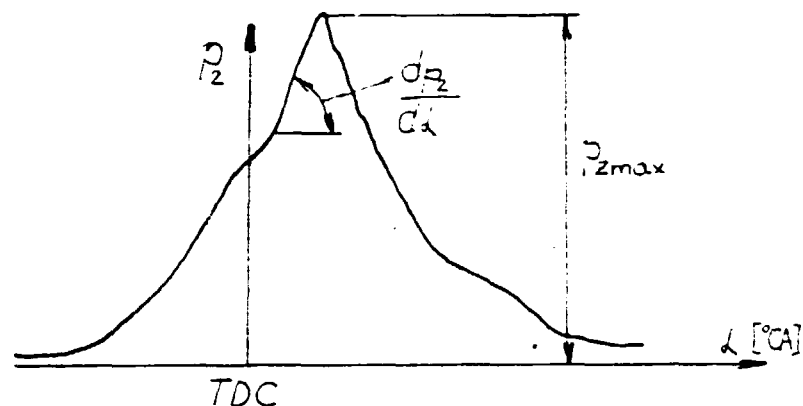


Fig 2

Otherwise, a faster combustion may be of benefit when timing retarded. Namely, retarded timing and fast combustion may result in $dp_z/d\alpha$ decrease as well as p_{zmax} reduced; but only if engine reacts.

Years long (acc. to Parker) we connected HPI with shorter injection period (α_{ub}).

a) Converting some engines to HPI, shortening α_{ub} without change of timing we experienced

- $dp_z/d\alpha$ increase
- combustion noise increase
- p_{zmax} increase
- NO_x increase
- soot emission decrease
- specific fuel consumption decrease
- exhaust temperature decrease

b) HPI, shorten injection period (α_{ub}) and retarded timing resulted in

- specific fuel consumption increase
- max. in-cylinder pressure decrease
- $dp_z/d\alpha$ decrease
- exhaust temperature increase
- soot emission increase
- noise emission decrease.

a) and b) above are the general tendencies. The case b) speculates:

1. Timing decreased \rightarrow better conditions for ignition
2. Faster ignition \rightarrow faster combustion.

However, case b) gave very often disappointing results because of engine unexpected reactions. Thus we compromise in-between: fuel consumption figure, emission, mechanical and thermal loadings. Here is the question: why many engines have not been reacted according to case b) speculations?

Some dilemmas about noncorresponding engine reaction may be discussed as follows ;

x - HPI application increases the pressure in the whole HF system (retractive valve cap, HF tube, injection holder) but HPI means a high pressure drop (Δp) at nozzle holes only. When, for example, any where too high elasticity exists or/and too much resistances a high pressure produced by pump may be considerably lost and then it's not HPI at all.

y - the more intense pressure drop at nozzle holes may be used for:

- (1) - better fuel atomization
- (2) - longer spray penetration
- (3) - the both (1) and (2)

In the case (2) we experienced too much fuel deposited on the wall and in the absence of intense swirl homogenization of mixture deteriorates.

In case x or/and y we increased fuel consumption only. More energy used for injection and because of p_{zmax} timing was retarded , thus the both directed to fuel consumption increase.

Coming back to the points a and b let show the typical diagram we know (Fig 3).

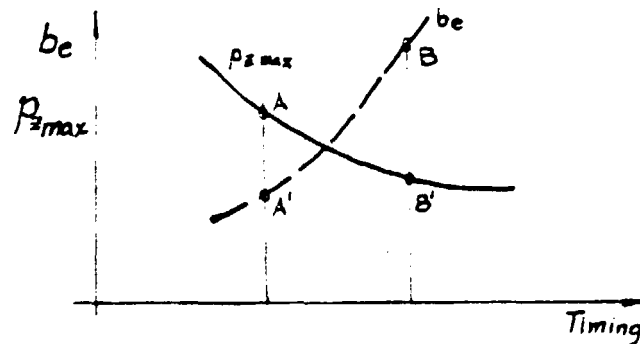


Fig 3

Fig 3 is a typical representation of HPI of of higher Δp application but accompanied by shorter period of injection. It was the essence of our HPI understanding because we applied HPI with shorter injection period only (acc. to Parker). May be not too short? It was practically only geometrical redistribution acc. to Fig 4.

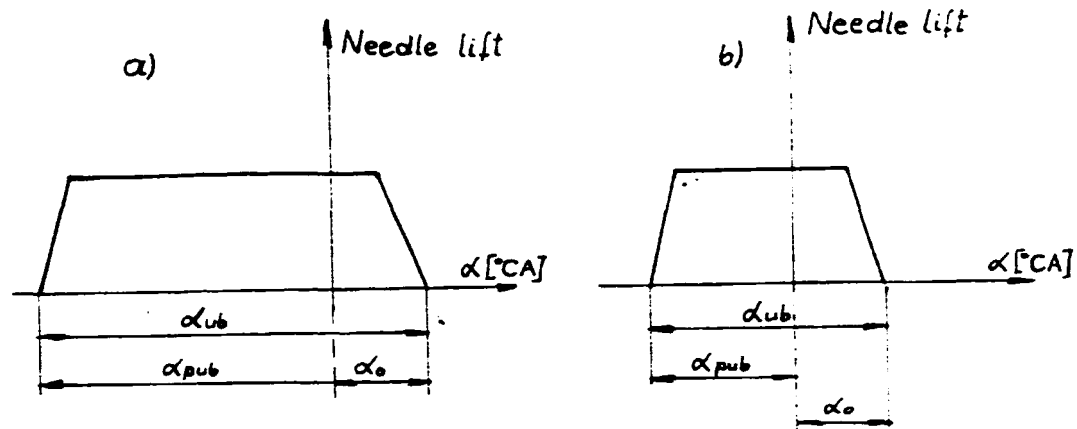


Fig 4 a) conventional injection system
b) HPI system

Let's remember that, about 3 years ago Daimler Benz (DB) - Bosch investigated HPI in cylindrical DB combustion chamber. Injection pressure was increased successively up to 2000 bar, but they concluded that cylindrical DB bowl may not be fit related to HPI. However, we may comment their results as:

"spray penetration was unfavourable for the combustion chamber and swirl chosen when pressure drop in nozzle holes increased." Was the Parkers philosophy a wrong one?

When dealing with HPI still two points have to be considered:

1. When fast injected instantaneous fuel concentrations per unit volume of combustion chamber increase, what may result in droplet coagulation.
2. Very fast plus very fine dispersed fuel requires a lot of energy. For example: 50 mm³ fuelling only but dispersed uniformly in 2 μm required 55 kW. Therefore, CRIDEC system may be a solution related to energy need. Only to mention that W. Ball (Ricardo) calculated (for conventional system) energy need about 1% of engines power output.

On 24 June 1984 in TH - Karlsruhe the newest results were reported related to HPI (Heinrich and Drescher, IFA - München).

The essence of the report was:

- when bad shorter than finer atomized but with the same duration of injection as for conventional system. Increased pressure drop in nozzle holes was used to increase atomization only.

We may anticipate the next step of HPI development in combustion:

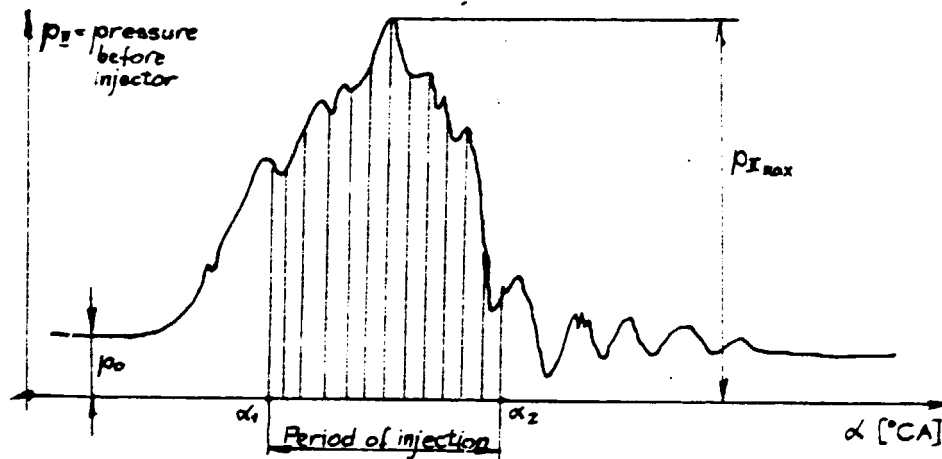
- shorter duration
- finer atomization

but the both matched to the swirl, squish, bowl, outputs and speeds.

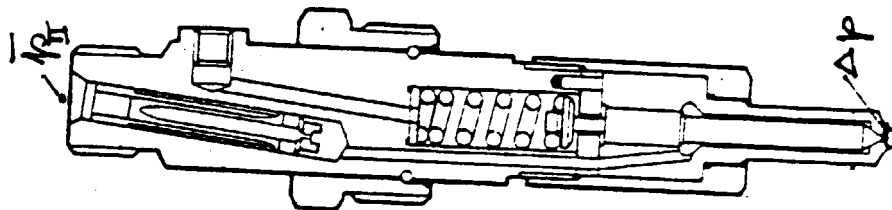
For the purpose of experiments F. and P used one modern (closed design) conventional pump made possible $P_{II\max}$ up to 1500 bar.

Is to be noticed, that HPI doesn't mean a high $P_{II\max}$ only. Moreover, the mean effective pressure during effective injection \bar{P}_{II} must satisfy the conditions:

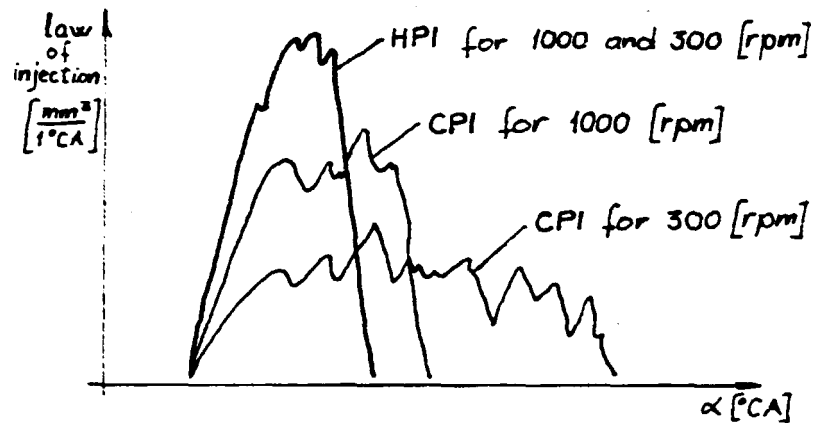
1. $\bar{P}_{II} \geq 0,6 P_{II\max}$



2. \bar{P}_{II} increased, used for Δp increase only



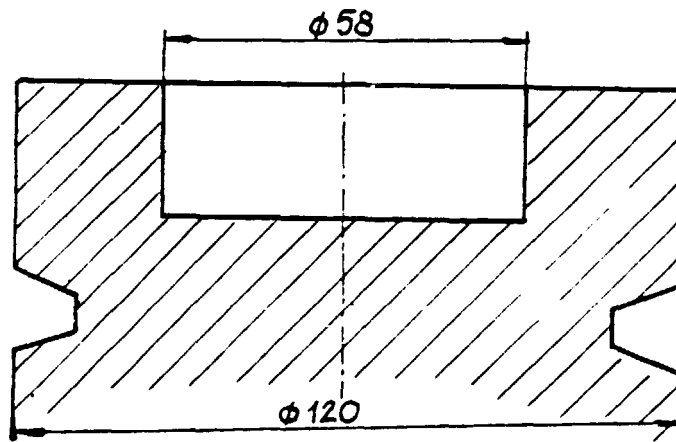
3. \bar{P}_{II} does not depend of n /rpm/



The shorter injection period the less important shape of injection law. At very short injection law of injection becomes one pulse only.

For the purpose of experiments Heinrich and Prescher (H&P) used DB single cylinder research NA engine; $V_H=1,8 \text{ dm}^3$, $\phi 128 \times 140 \text{ mm}$, rated speed 2200 rpm, CR=17,4. Related to fuel consumption figure, combustion chambers as well as swirls were separately optimised for CPI- and HPI system. Experiments II in this Report.

For the purpose of analysis of mixture for motion and combustion single cylinder air cooled engine was used; $\phi 120 \times 140 \text{ mm}$, rated speed 2300 rpm, $\epsilon = 19,5$; piston bowl $\phi 58 \text{ mm}$.



Injection system used:

CPI

HP pump BOSCH PESIFM $\phi 10 \text{ mm}$, prelift 2,8 mm.

Retraction $V_R = \text{const.} = 50 \text{ mm}^3$

HP tube $\phi 2 \times 925 \text{ mm}$

Injector DLLA 150S/86, 4 holes, $\mu f = 0,27 \text{ mm}^2$

Injector open. pressure 175 bar
 Fuelling up to 150 mm³/cycle was used

HPI

HP pump BOSCH PE6ZM140, ϕ 15mm, prelift 1,5 mm

HP tube ϕ 1,6x1180 mm

Retraction $p_0 = \text{const.}$ (const. residual pressure)

Injector DILL 145 PV, 4 holes

Injector $\mu f = 0,11 \pm 0,18 \text{ mm}^2$

Injector opening pressure 500 bar

With HPI effective cross-sectional nozzle holes flow area (μf) was varied in order to keep the same period of injection as for CPI. Injector opening pressure was extreme high. However, TAI-Mar-ibor has one export engine with 270⁺⁸ bar opening pressure.

Here is a new approach in H&P work. With pressure increased we usually increased up to shorten period of injection, but they kept injection period the same (with reduced μf) as for CPI - better atomization.

In Fig 5 are \bar{p}_{II} presented for the both CPI and HPI system. It may be seen that:

$$\bar{p}_{II}(\text{HPI}) \approx 3 \cdot \bar{p}_{II}(\text{CPI})$$

approaching to 1500 bar at rated power.

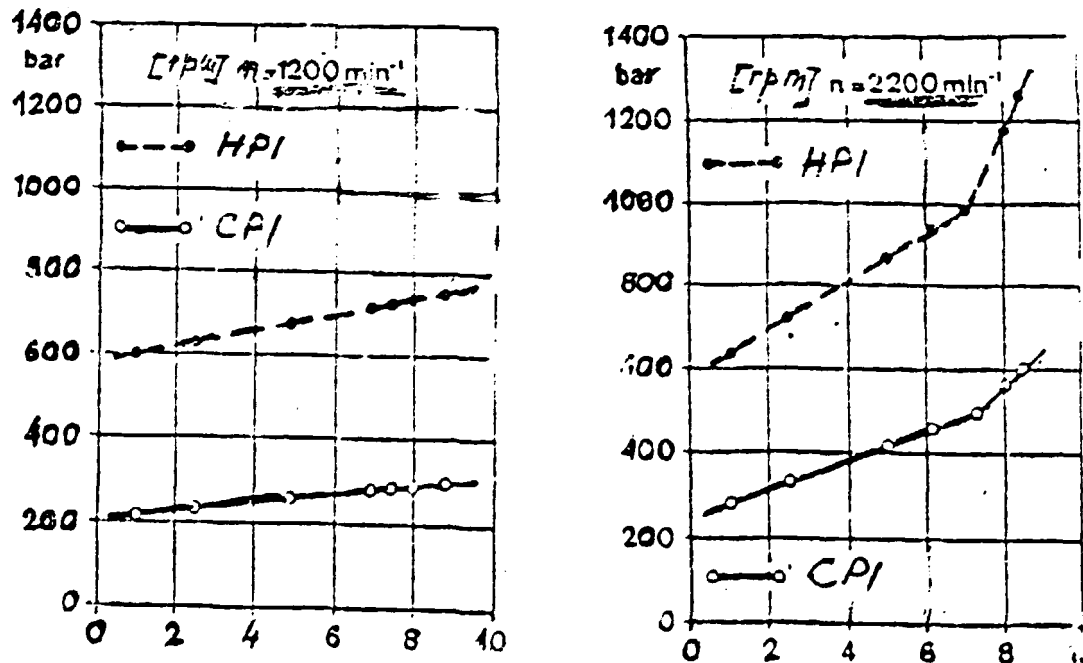


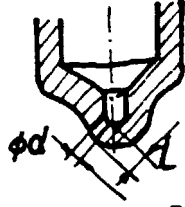
Fig 5

In order to follow spray events in I experiments 3 nozzle holes were plugged and fuelling reduced on $V_{\text{cyl experim. spray}} = \frac{1}{4} V_{\text{cyl experim. engine}}$.

It means results obtained may be used qualitatively only.

Photograph taken were evaluated for the both systems being operating under conditions:

- same start of injection bBDC=15/°CA/
- same l/d of nozzle hole



- same fuelling at 20 mm³/cycle
- without swirl.

Fig 6 depict the results.

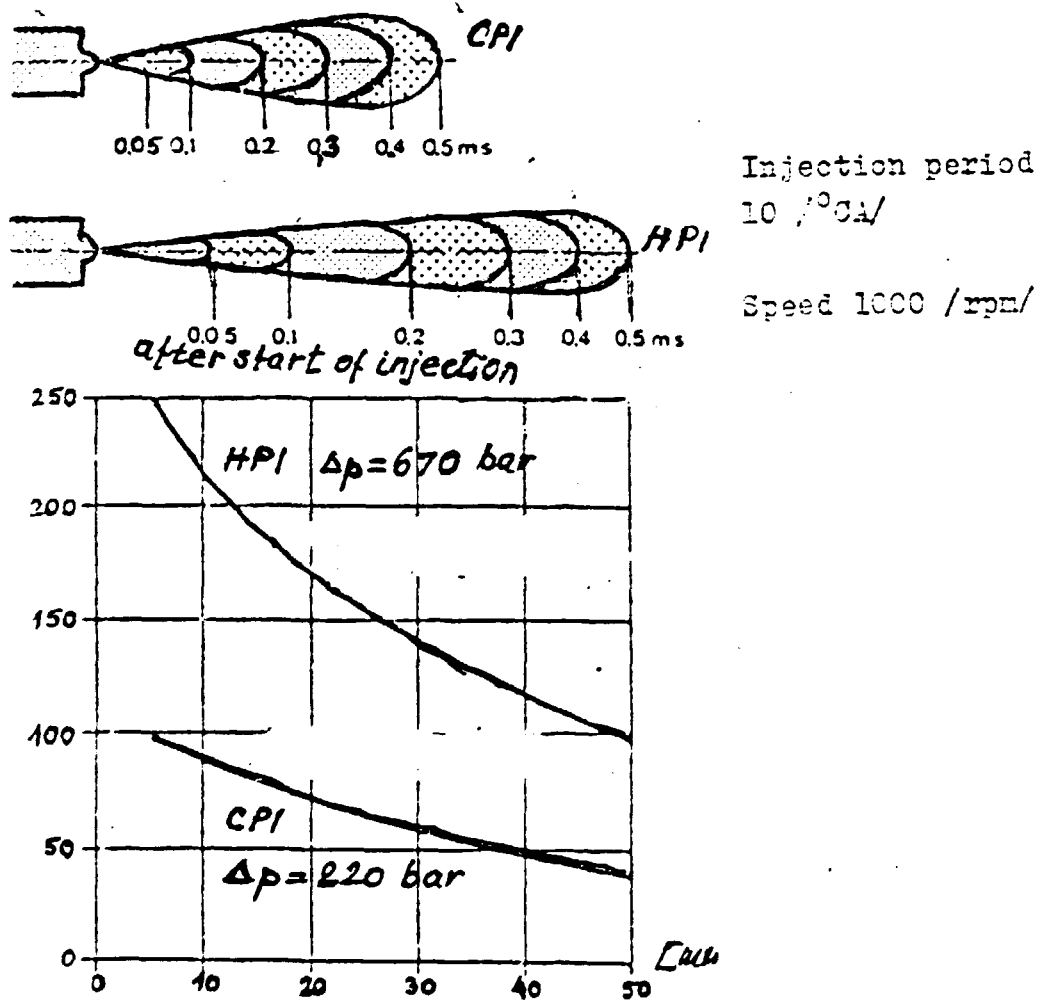
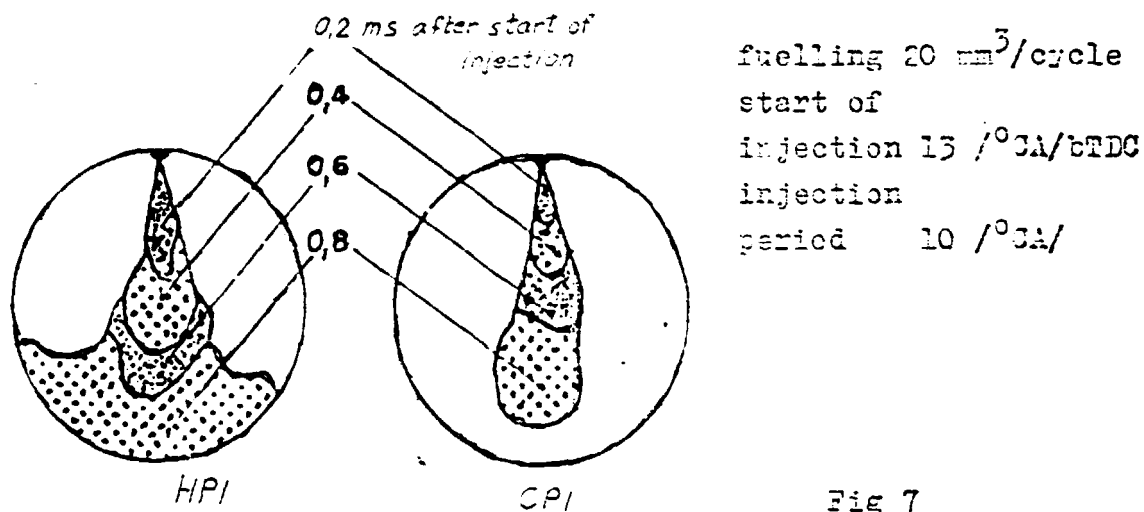


Fig 6

With HPI fuel spray got more narrow and its tip velocity was nearly by factor 2 higher than of CPI. HPI formed earlier the fuel vapour phase and in larger quantity, see Fig 7.



With CPI, vapour phase is mostly around spray but HPI vapour phase may be observed into the spray also.

With HPI liquid phase converts faster into vapour one. Despite vapour penetration in the front of spray, its tip penetrates longer and more early reaches the combustion chamber wall.

With the both CPI and HPI, when swirl of middle intensity combustion started at the same α /°CA/ supposing the same instant of beginning of injection. It means that with the both, CPI and HPI ignition delay was the same, Fig 8.

When HPI, combustion starts abruptly in the larger part of bowl volume and the spray front. When CPI combustion starts around the spray. With HPI after stable start of combustion, vapour phase doesn't develop any more, it means better homogenization and shorter period of combustion, Fig 9. It's in agreement with our investigations. We retarded for 4 + 7 /°CA/ the timing, when HPI. Fig 10 shows the result of HPI.

Fuelling 20 mm³

Start of injection 15° bTDC

Injection period 10° CA

Swirl: middle intensity

■ liquid phase, ▨ vapour, □ flame

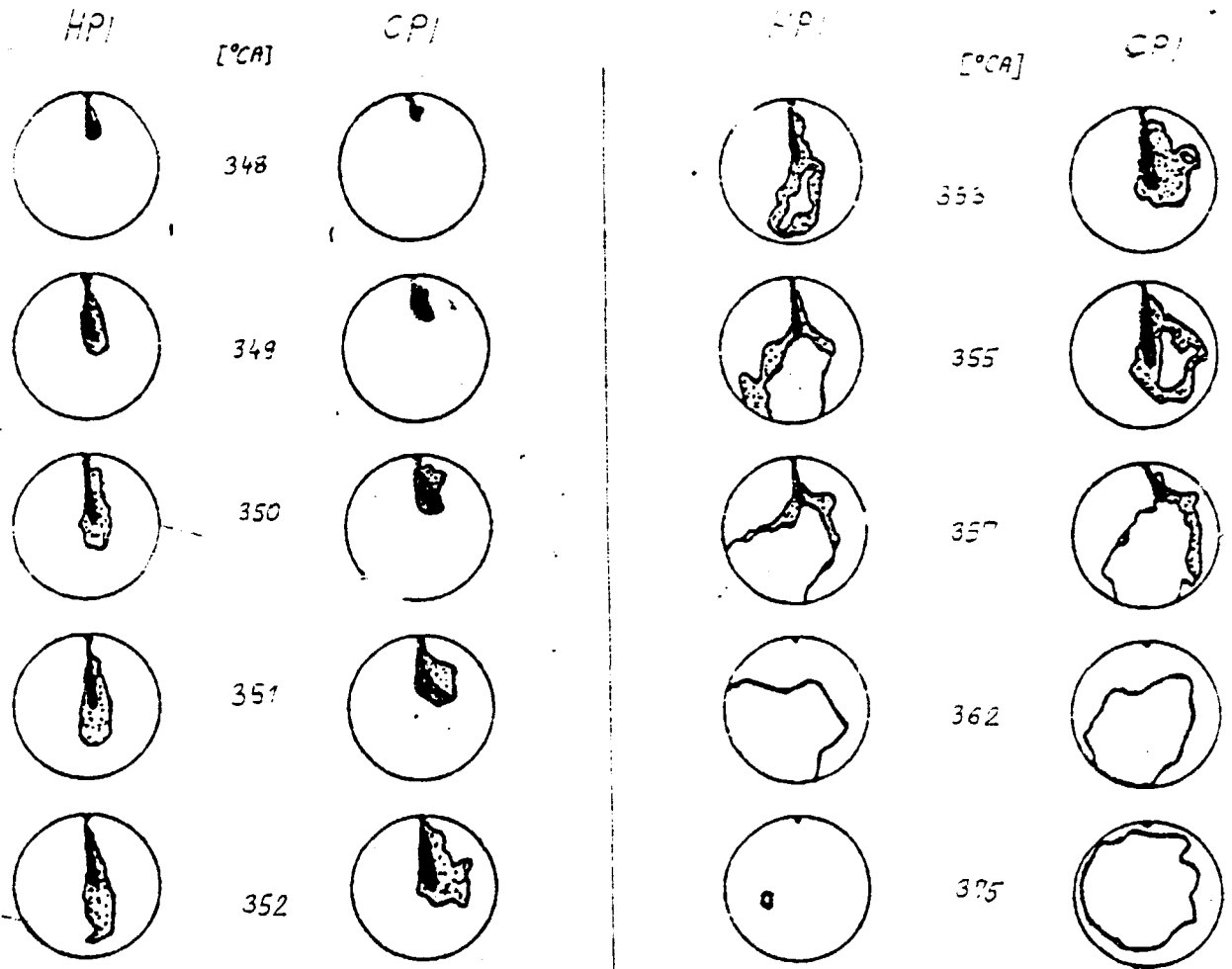


Fig 8 HPI - flame extinction at 375 °CA

CPI - flame extinction at 430 °CA

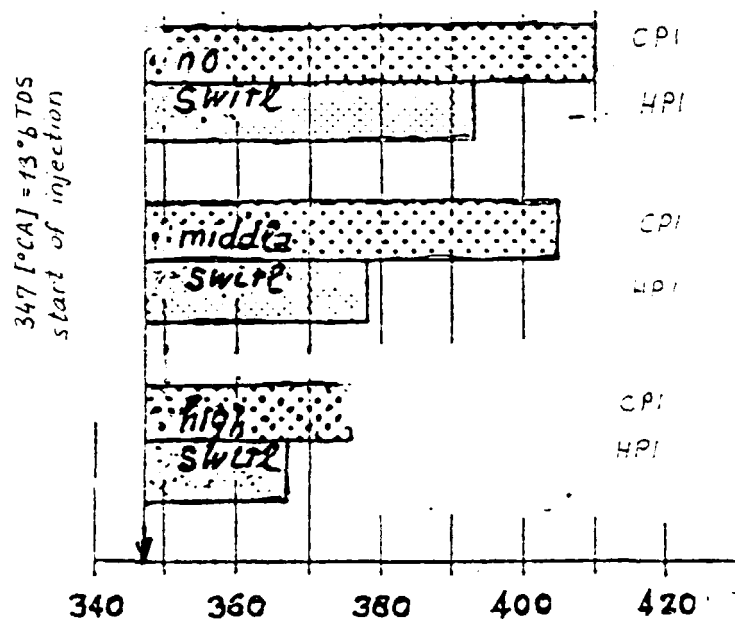


Fig 9 Duration of combustion
 Fuelling 20 mm³
 start of injection 15 °CA bBDC, injection period 10 °CA

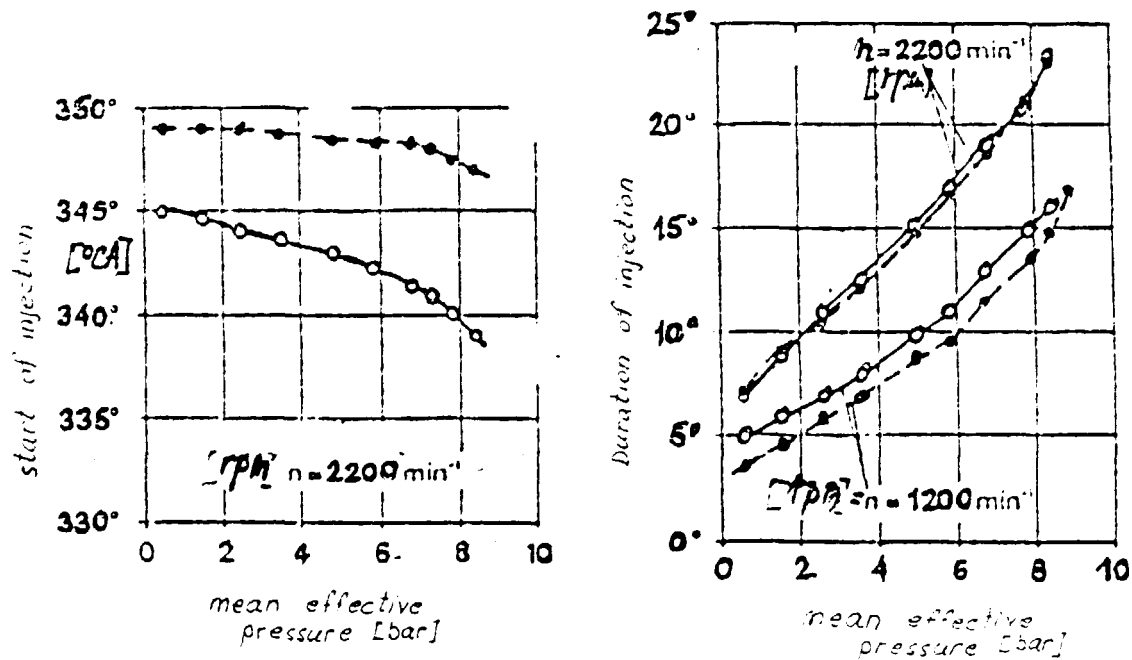


Fig 10

The results of experiments II

The both, HPI and CPI system were tested with 3B single-cylinder engine. However, piston bowl and swirl were matched separately from CPI, but injection period was the same.

As was yet mentioned, the ignition delay was the same the both systems, see Fig 11.

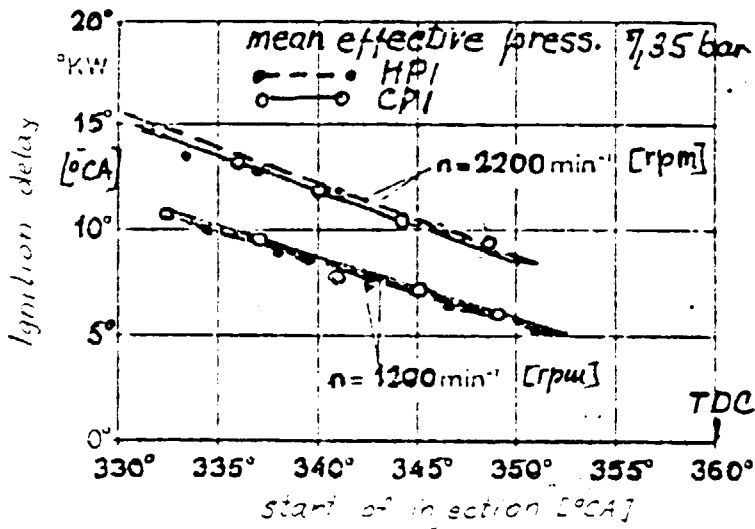


Fig 11 Start of injection was optimized related to fuel consumption in Fig 12

HPI had a high influence on soot emission, see Fig 12.

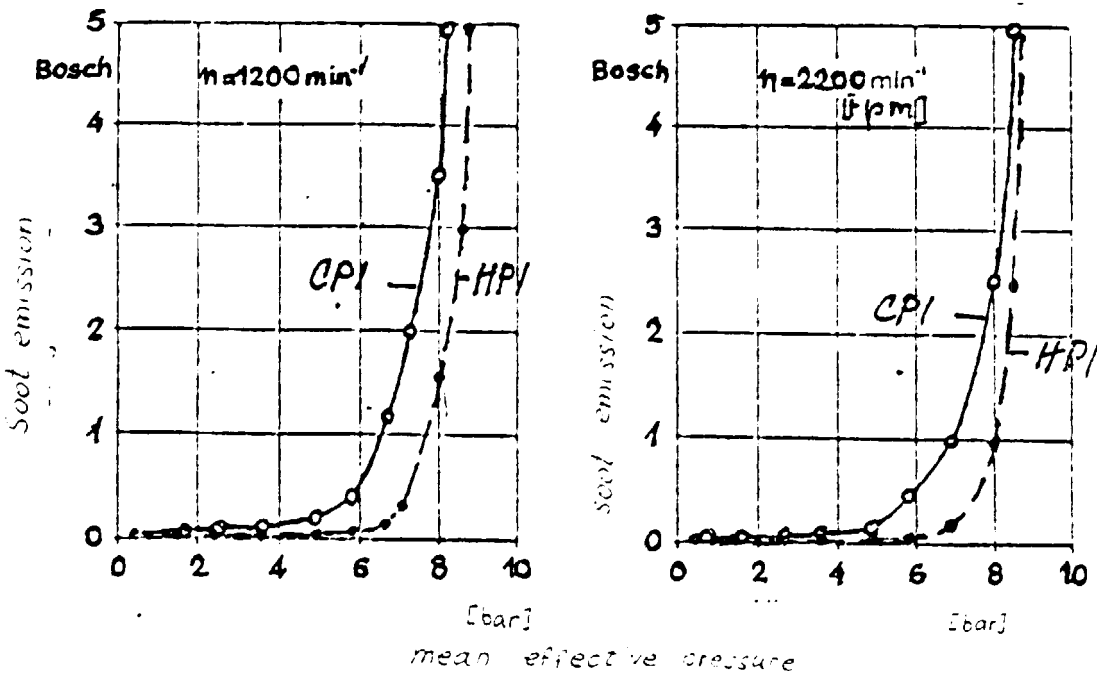


Fig 12

When limited soot emission at 2 BOSCH units, max. effective pressure with HPI was greater for one bar than that with CPI, see Fig 13.

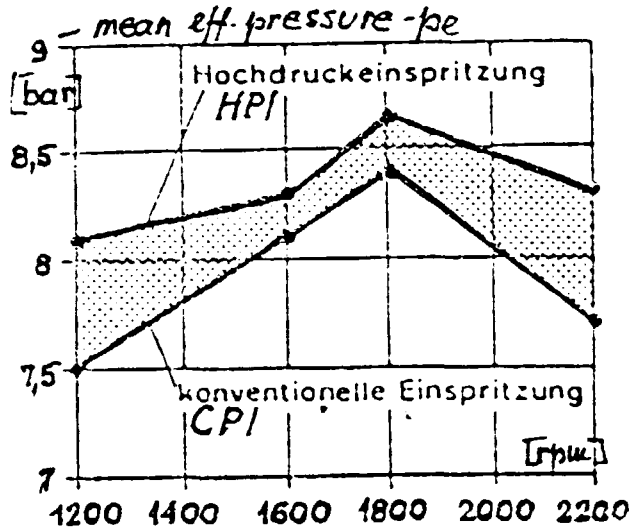


Fig 13

Similarly, when soot limited at full load with CPI, application of HPI, for the same power outputs as for CPI, resulted in lower soot emissions for 0,5 + 1,1 Bosch units, see Fig 14.

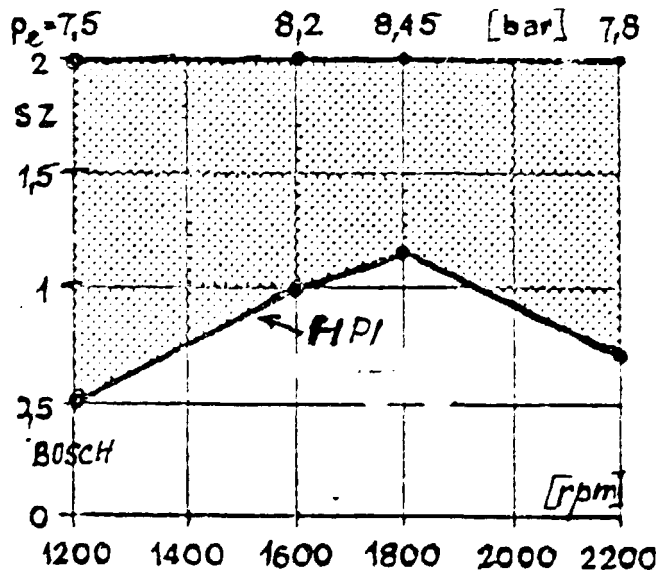


Fig 14
HPI and CPI - the same power outputs

Fig 15 depicts THC emissions for the both injection systems investigated but optimized related to fuel consumption.

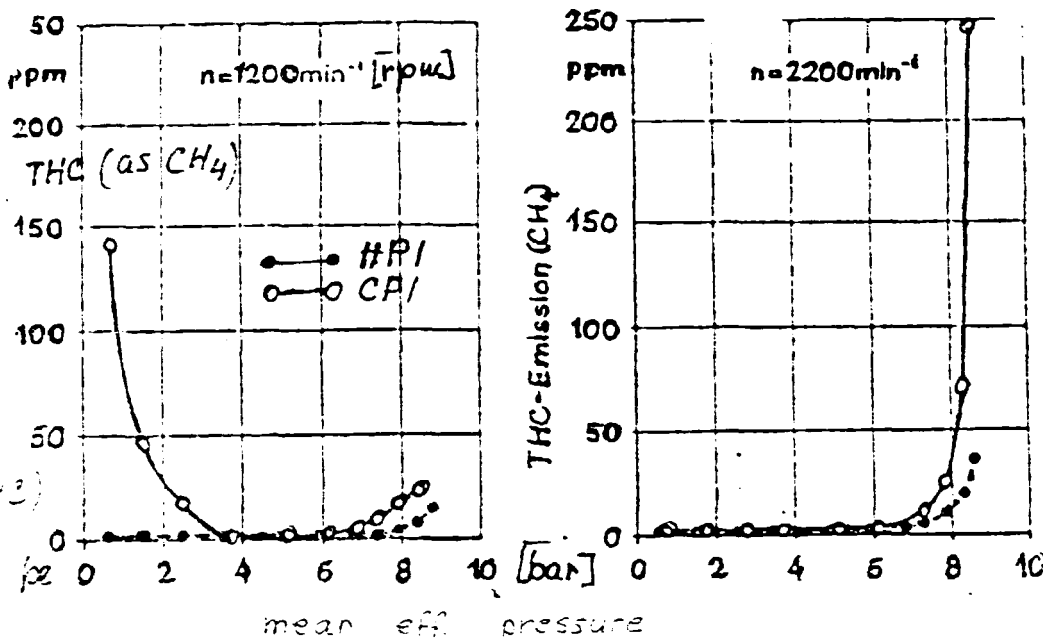


Fig 15

Typical NO_x dependences for diesel engine shows Fig 16.

Notably:

- strong dependence on loading
- weak dependence on speed.

NO_x emission was nearly the same for the both injection system used.

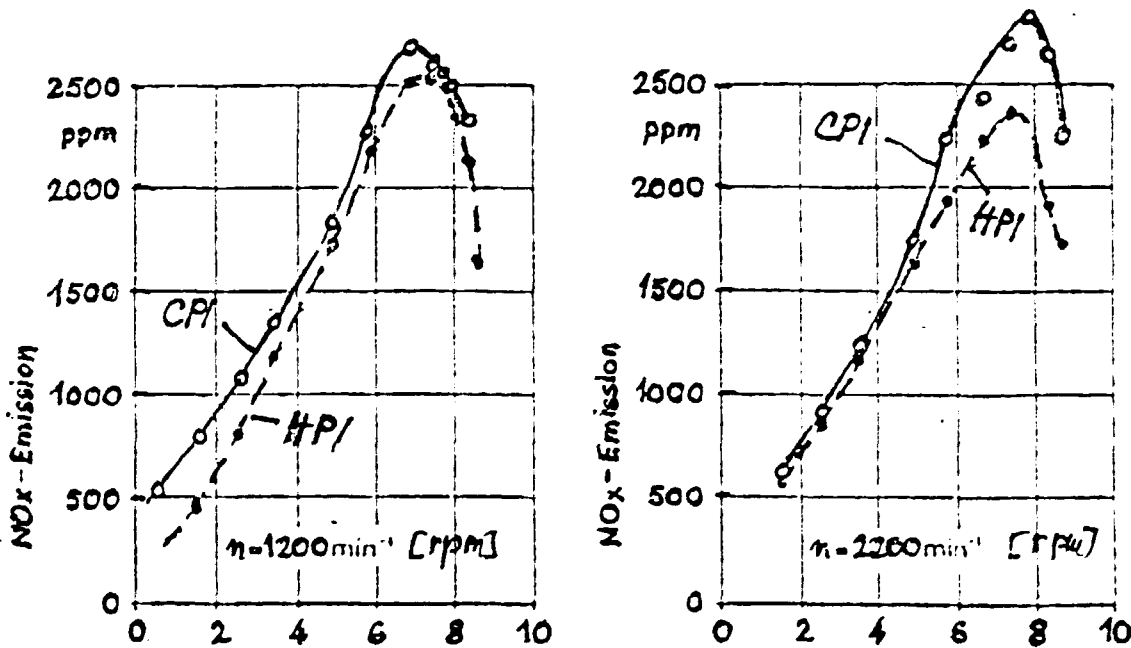


Fig 16 NO_x emission, timing optimized related to fuel consumption

Fig 17 shows that fuel consumption was nearly the same for the both injector systems investigated.

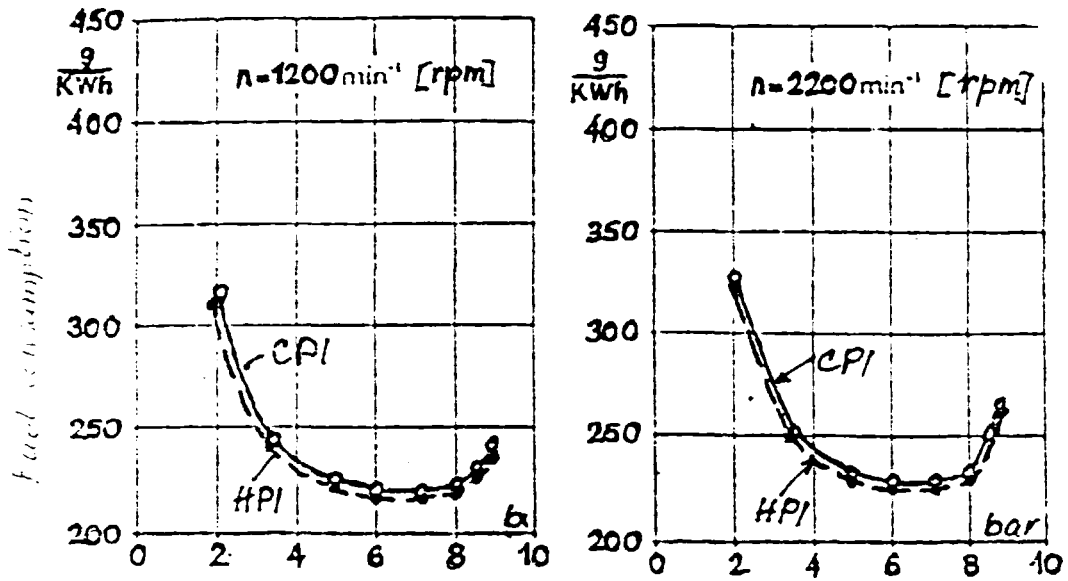


Fig 17

However, Fig's 18 and 19 depict that pressure rise and heat release rate became higher with HPI, although max in-cylinder pressures were lower. The above said produced higher combustion noise than that with CPI system. Despite of timing retarded (15° BTDC), HPI showed (see Fig 19) a high increase of heat release at TDC. It may be probably decreased by better matching of injection law.

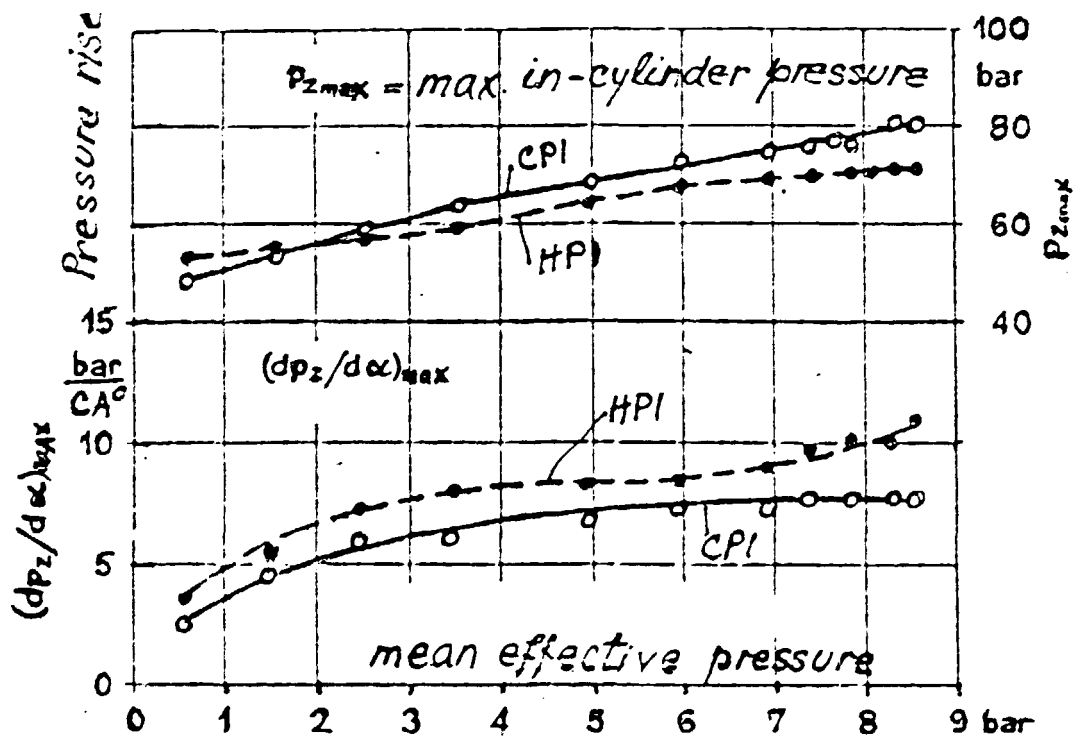


Fig 18

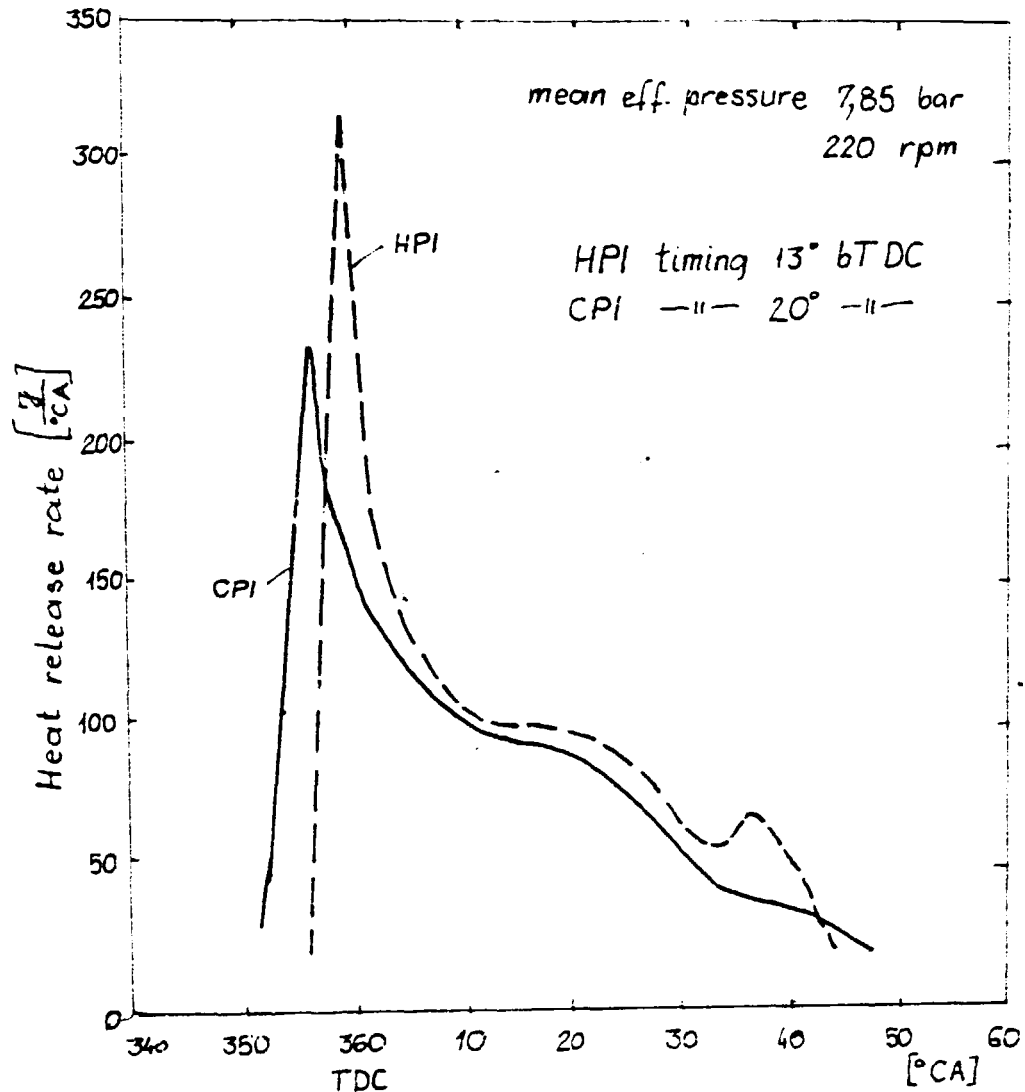


Fig 19

Heinrich - Prescher's conclusions:

- when $\Delta p = 670$ bar instead of 220 bar at nozzle holes, the velocity of fuel spray tip increases by factor 2, so does fuel vapour also
- at const. timing, combustion delay does'nt depend on pressure drop in nozzle holes (in the range investigated)
- when Δp higher, timing may be retarded and with this, ignition delay may be shorter
- with HPI the first appearance of the flame is around the flame front. Besides that, high temperature radiation drop faster and the combustion period becomes shorter.
- soot emission decreases with Δp increased.

Matsouka, Kamimoto and Kobayashi, as well as Kahn earlier, showed the "flame figure" when fuel spray penetrated to the wall of

piston bowl, Fig 20.

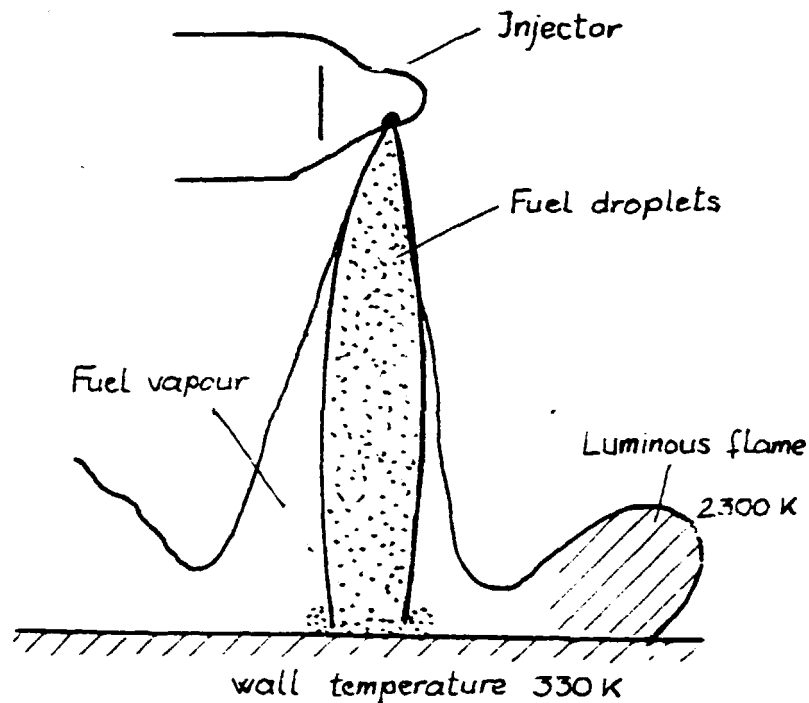


Fig 20

It's obviously clear that, having a larger nozzle hole dia., swirl intensity must be higher because of larger deposition of the fuel. It means to disperse more in air, smaller nozzle hole has to be applied or for less intense swirl, fuel must be finer dispersed in air.

Unavoidable shortage of CPI is a long spray distance at low and high speed operations. However, CDI (MAN) system claims to solve this problem, as was yet explained.

To disperse finer asks for higher pressure drop at nozzle holes. Here is to be mention.

1. $\bar{P}_{II}/P_{II\max}$ satisfied must be obtained at a high $P_{II\max}$.
 2. Increasing $P_{II\max}$, resistances and elastic deformation of HP tube increase also. Thus, HPI may be applied when the corresponding stiffness of the whole injection system exists.
 3. a high $\bar{P}_{II\max}$ we need for high Δp at nozzle holes only.
- The expression for a part of fuel injected ΔV in a time Δt may be expressed as follows:

$$\Delta V = \mu f \sqrt{\frac{2}{\rho}} \sqrt{\Delta p} \cdot \Delta t$$

$$\Delta V = \mu f \sqrt{\frac{2}{\rho}} \sqrt{\Delta p} \cdot \frac{\Delta \psi}{6n}$$

$$\Delta V = \text{const} \cdot \mu f \cdot \Delta p^{1/2} \cdot \Delta \varphi \quad \text{for } n = \text{const [rpm]}$$

where : μf - flow cross-sectional area of nozzle holes
 Δp - pressure drop at nozzle hole
 $\Delta \varphi$ - duration in $^{\circ}\text{CA}$ for the injection of volume ΔV

Thus:

- $\Delta \varphi$ may be shorten with increased - shorter period of injection.
- Still shorter period of injection may be obtained combining a higher Δp with μf increased - a larger hole dia.
- When decreased μf and increased Δp ; $\Delta \varphi$ may be kept unchanged - finer dispersion.
- Every time is possible to combine μf and Δp for optimum $\Delta \varphi$

In order to increase Δp the below cited may be used:

- increase of plunger dia.
- decrease of μf
- increase of plunger pre-lift
- new shape of the cam in HP pump

but:

- after injection
- too high wear of cam-follower
- leakage at connection retraction valve cap-pump body
- cavitation wear

have to be avoided.

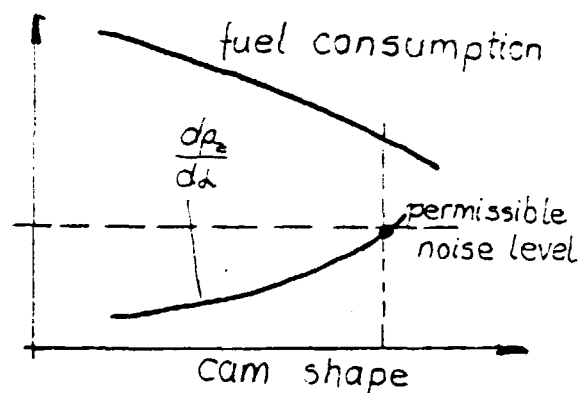


Fig 21

Fig 21 explains cam shape matching $dp_z/d\alpha$ = in-cylinder pressure rise.

In DI-NA diesel engine may be of benefit to accelerate the combustion within 10 - 15 °CA aTDC, let say for about 2 kcal/°CAm³. It may be done by:

- reduction of nozzle hole dia.'s
- application of nozzle design acc. to Fig 22.

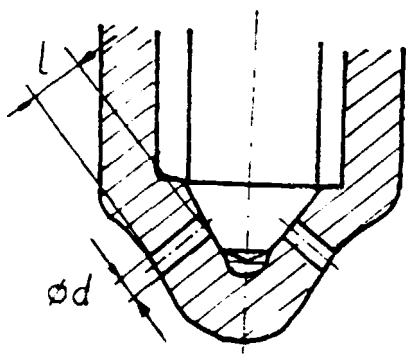


Fig 22 Sackless nozzle

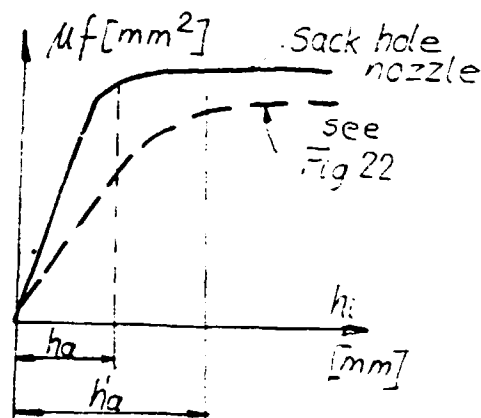


Fig 23

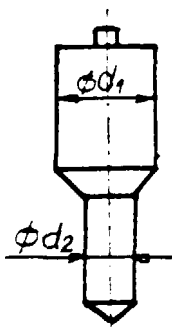
Sackless nozzle offers some advantages:

- less fuel injected in the period of ignition because of retarded increase of effective flow area of nozzle (μf) in dependence of needle lift (h_i), see Fig 23. (of interest for CH₃OH also).
- THC emission may be drastically reduced.

Potential drawbacks:

- reduced service life of nozzle
- nonuniform fuel distribution of nozzle holes with multi-hole injector
- 1/d more difficulty to match.

With HPI injector opening pressure has to be increased. Doing that injector closing pressure increases also. Sometimes reduced hydraulic ratio of needle helps to obtain higher opening pressure. Doing that closing pressure decreases but



$d_1 = \phi 6 \text{ mm}$
 $d_2 = \phi 4,5 \text{ mm}$
Usvali
 $d_2 = \phi 3,5 \text{ mm}$

Fig 24

it may be not of importance when injected faster (see Fig 24). One practical example of toward HPI application shows Fig 25 as the influence on engine characteristics. As for engine: $\phi 120 \times 140 \text{ mm}$, 6 cyl. in-line, water cooled, combustion chamber of ω type (see Fig 3 b, page in this report), production "Steyr".

- A_c / mm^2 / increases (or lead volumes of the system)
 - M_T / mm^2 / decreases
 - more steeper cam shape
 - pre-lift increases
 - n / rpm / increases
 - plunger dia. increases ($\pi d_p^2 / 4 = A_p$)
- V_T increases

above expression):
 HP tube. tendency to alter injection increases when (see the
 nozzle hole flow area, A_n - cross-sectional flow area of
 at the end of delivery, v - velocity of sound (1520 m/s),
 where: A_p - cross-sectional area of plunger, V_T - plunger velo-

$$A_p V_T \leq 5 \cdot a \cdot (M_T) \cdot V_T$$

tion without number valve the next expression must be used:
 valve may be applied (see the 1st report). To avoid after inje-
 However, after injection may be the problem, to avoid, number
 engine output.

- increasing plunger dia.
- increasing plunger dia. (injection pre-lift possible)
- injection velocity increased and it had positive effect upon

It may be seen that:

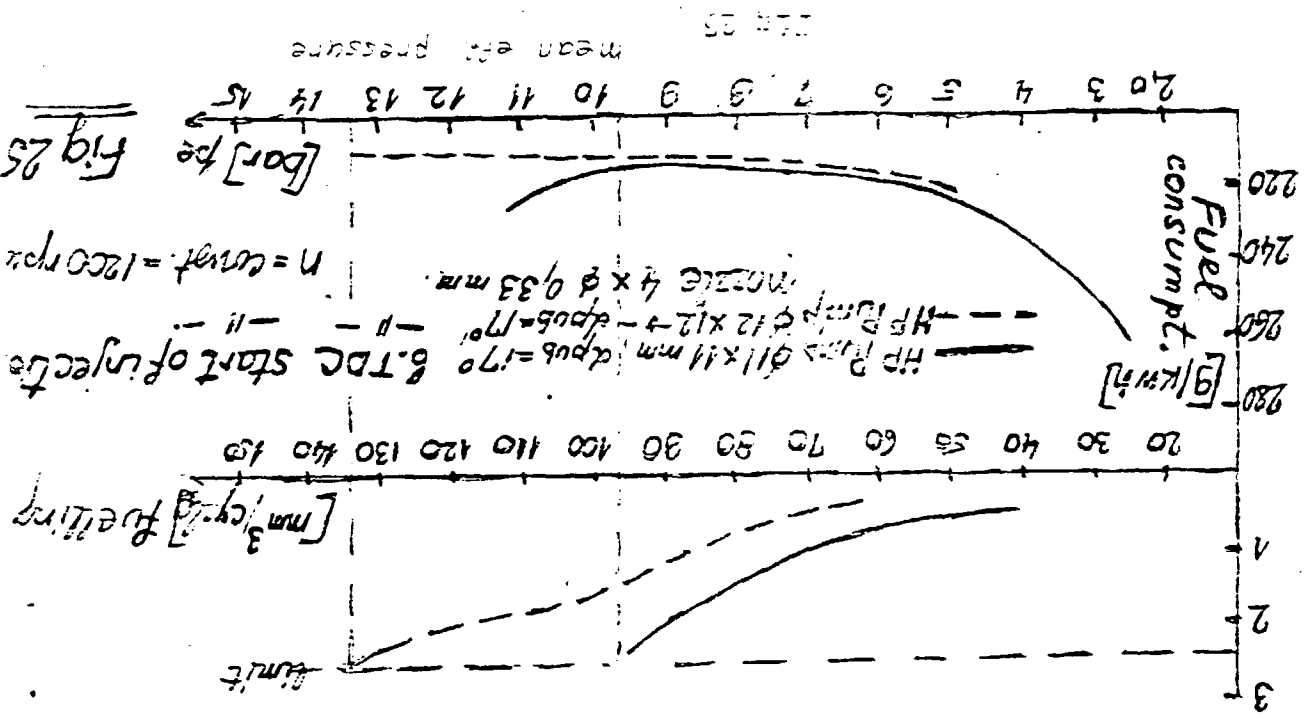


Fig 25

Appendix II 3 related to subject 5

During discussion related to subject 5 were informations were desired but concerning deeper cylindrical piston bowl as well as fuel arrangement.

Fig 1 shows hyperboloid combustion chamber (HPA) with three possibilities related to single hole directions of nozzle.

In-cylinder pressure diagrams shown on the right in Fig 1 correspond to spray arrangement 1, 2 and 3. Spray marked with number 3 offers more multi-fuel tendency.

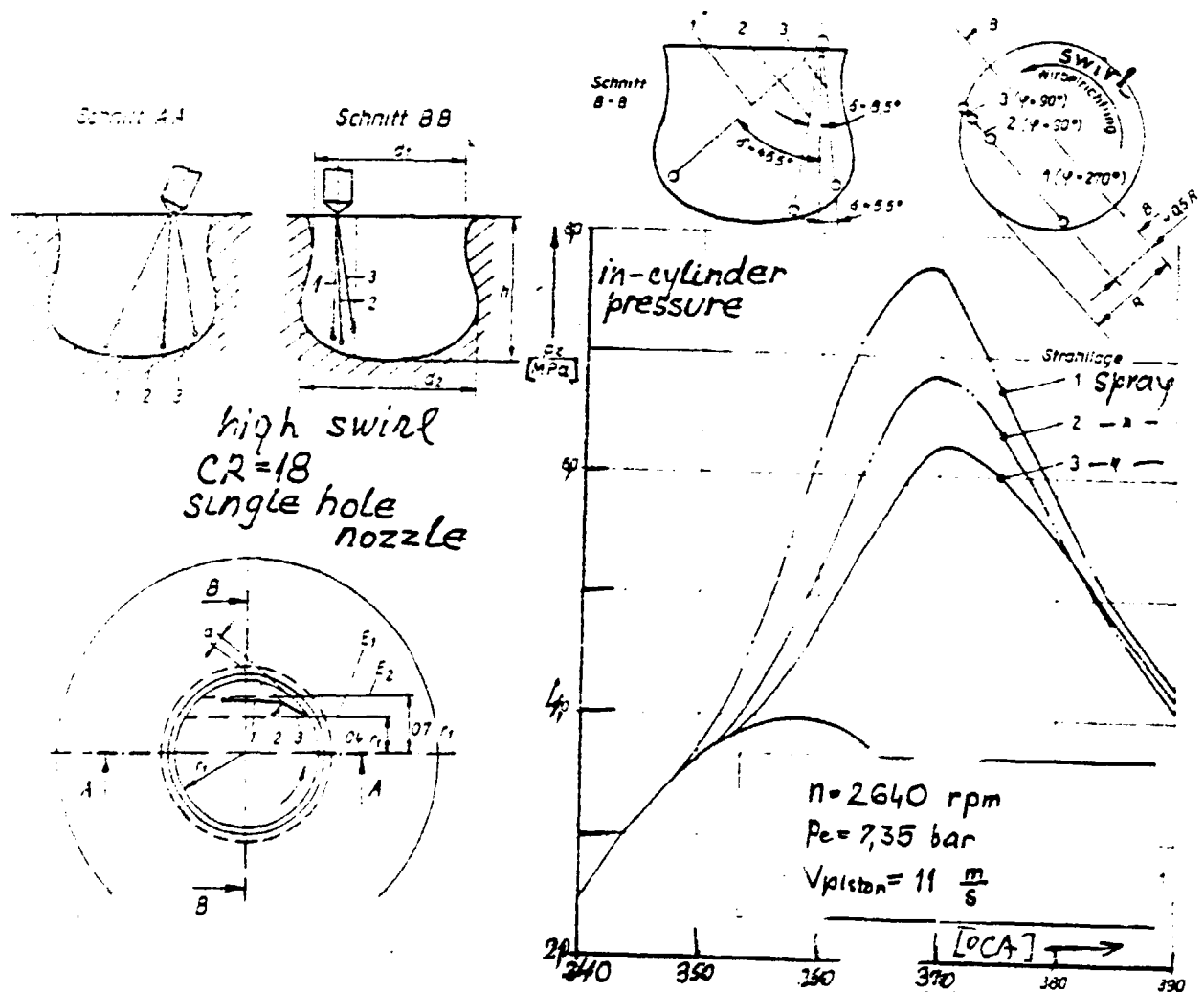


Fig 1

However, in-cylinder pressure diagram when gasoline, depicts characteristics figure of late combustion, see Fig 2, on the right. Is to be mentioned that missfiring was not experienced but late combustion produced a bad fuel consumption figure. Thus this combustion chamber with nozzle arrangement 3 (Fig 1) also asks for spark plug to control combustion. Otherwise, hyperboloid combustion

chamber as well as Elsbett are suitable for benzene combustion also, without any modifications.

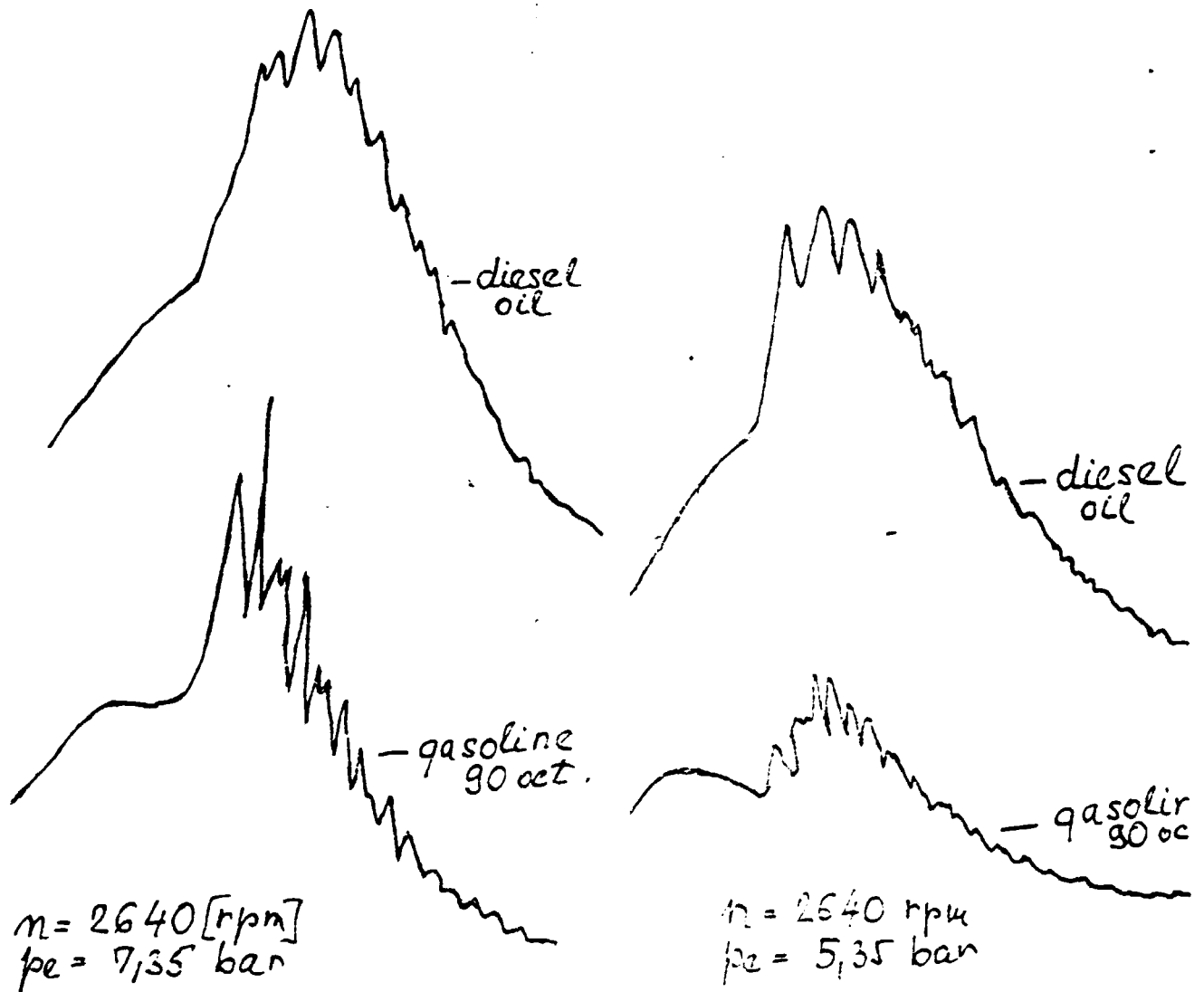


Fig 2 In-cylinder pressure diagrams

As was yet said, spark plug is unavoidable not only because of late combustion in low load operation with gasoline or for better starting. Moreover, spark plug must control combustion when fuel with low cetane number. It's known that heat release rate in amount of $120 \text{ kJ/kg}^\circ\text{CA}$ results in knocking. Using gasoline 95 and hyperboloid combustion chamber (arrangement 3, Fig 1) without spark plug, max. heat release rate approaches $270 \text{ kJ/kg}^\circ\text{CA}$ what is by factor 3,5 higher than in the case of diesel oil combustion. Fig 3 shows peak in-cylinder pressure, pressure rise $dp_z/d\alpha$ and fuel consumption v.s. mean effective pressure at rate speed. The both, gasoline and diesel oil were tested in hyperboloid combustion chamber (arrangement 3, Fig 1) without spark plug. It may be

seen that, with gasoline peak in-cylinder pressure increases at higher loads because of knocking. At low load operation, fuel consumption increase because of late combustion, when gasoline used as fuel. Knocking tendency may be seen from $dp_p/d\alpha$ traces.

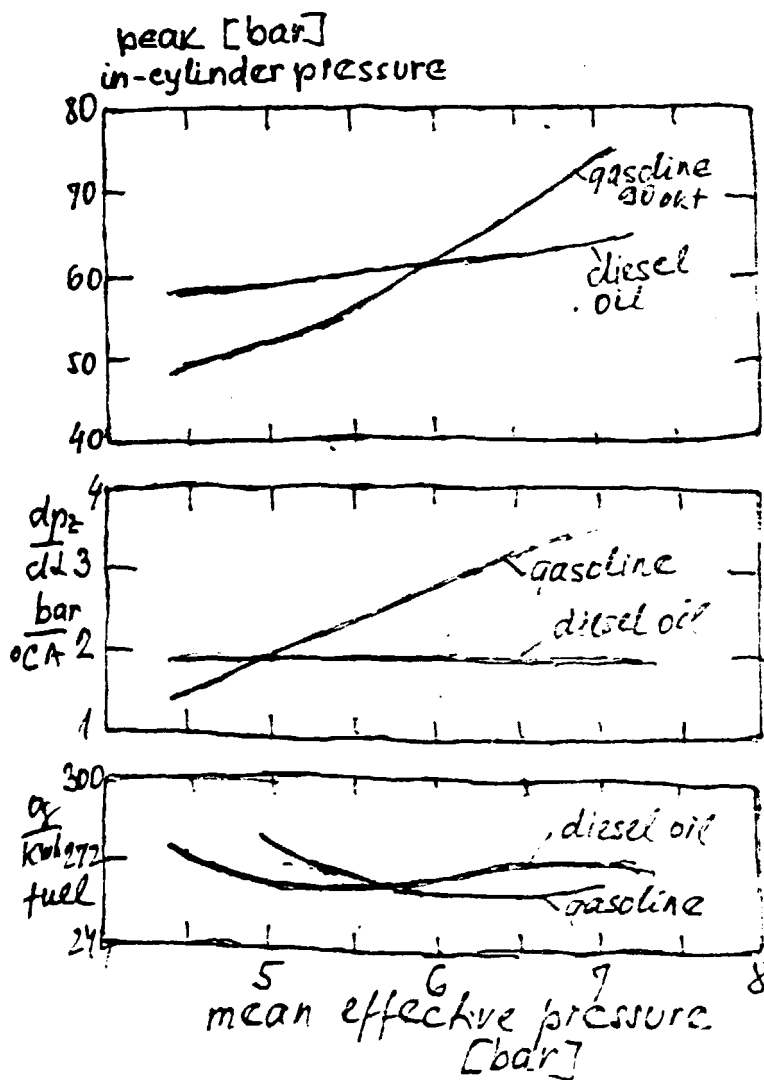
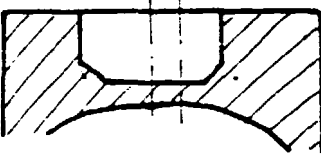
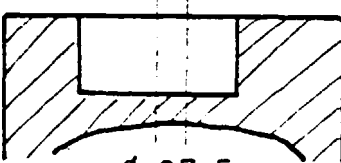


Fig 3

Still one evidence that without spark plug, fuels with low cetane number may not be used in diesel engine operation.

Appendix K 4 Miscellaneous subjects

1. Mixed diesel oil- CH_3OH was used in TATA engine (see Topic 2). However, data collected showed that fuel consumption demonstrated a high rate with diesel fuel also. It was the reason to compare existed TATA engine with one of new DB engines series CM 366.

	<u>TATA engine</u>	<u>DB, CM 366</u>
engine type	6 cyl., 4 stroke in line, water cooled, vehicular application, NA	the same
Type of comb. chamber (nearly the same)		
<u>Piston dia.</u> mm	ϕ 92	ϕ 97,5
Stroke mm	120	133
CR	17	17
Rated power /kW/	82	100
Rated speed /rpm/	2800	2800
Swept volume / cm^3 /	4786	5958
Specific rated power output $\frac{\text{kW}}{\text{dm}^3}$	17,13	16,78
Mean piston velocity at rated power/m/s/	11,2	12,4
Max. torque /Nm/	?	402
Speed at max. torque /rpm/	1800	1400
Engine weight /kg/	?	445
Specific weight /kg/kW/	?	4,5
Number of piston rings	5	?
Inlet duct	?	Resonant matched
Injector number of nozzle holes	4	4

Injection pump (ECSCE)	A		A
Min. fuel consumption rate /g/kWh/	265	←+25%→	212
Fuel consumption rate at rated power/g/kWh/	~ 294	←+25%→	235
Comparison between NA-TATA and OM366LA version at rated power /g/kWh/			
	294	←+33,6%→	220
at n_{max} position	265	←+33,6%→	198

OM366LA is TC-IC version of OM366 NA version.

As was yet suggested in the 1st Report, before CH₃OH application fuel consumption must be reduced with diesel fuel at first. Here is a many reasons to do that. For example capacity limit of injection pump, etc.

Without to change to much fuel consumption figure may be better and at the same time engine less expensive.

It's known that about 75% of neat friction loss belongs to piston/piston rings - cylinder sliding. Simple calculation may show, that replacing existed piston ring set with only 3 piston rings (1st keystone, 2nd tapered , 3rd spring supported elastic oil ring) neat friction loss may be decreased for about 12% at rated power and so does fuel consumption rate also. Wear and oil consumption not to mention.

Thus with very small change:

- inlet duct matched
- cylindrical combustion chamber
- injector and pump better matched
- 3 piston rings and shorter piston skirt

fuel consumption in diesel operation may be reduced for about 20%.

Reached a good fuel consumption figure with diesel fuel at first it's reason to apply methanol as replacing fuel, but with spark plug ignition control.

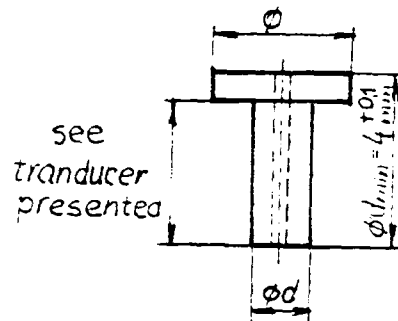
(For DB-OM366 engine see ATZ 4(April)1984., Arthur Mischke and Dietrich Kopenhöfer. May 1984 we tested OM366 (4 cylinder)

and found data given were correct).

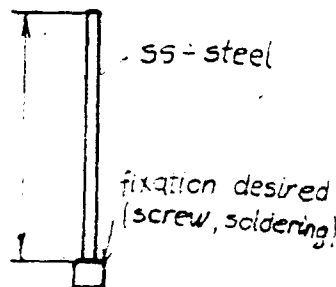
2. Proforma invoice was desired for our inductive transducers and bridge-needle lift measurements.

To do that need:

- official letter
- dimensions of transducer body



- dimensions of transducer needle



3. For CH_3OH application as well as for H_2 system testings - F&M P7 pump may be used. When asked, we may contact F&M and purchased for JJP P7 pump gratis for the time of six months.

Official letter and all data of existing Bosch pump are needed. When Bosch original type indication any other data are unnecessary.

4. As was explained during commons experiments, IATA engine has not timer at all (when correct informed). Reaching 2800 rpm any diesel engine must have time advancer for the better fuel consumption figure, better torque back-up and lower neck loading.

We apply timing advancer when

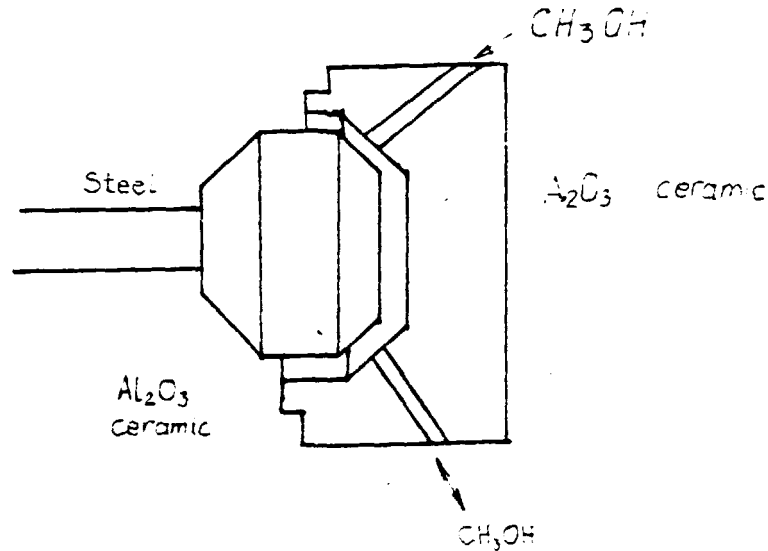
$$n_{\text{rated}} \geq 2400 \text{ rpm}$$

5. In some experiments with methanol we decreased the flow of cooling water and improved low-load operation.

6. As was yet mentioned calculation technique is to be recommended for matchings. Many programmes are today on disposal. For the optimisation matchings, calculation may not be avoided. Thus, we use for matching the calculation at first accompanied

by experiments after. If any need some of the programs may be sent to IIP as well as expert for practical application.

7. Fuel distributor suggested in Fig 6, page 33 as well as its connection in Appendix K 2, Page 116 may be made from two different materials. Namely, where methanol ceramic may be used.



It is to be noticed that leakage of methanol in the pump may produce:

- a high wear at pump bearing
- a high wear at cam and follower
- very fast deterioration of lubricant when integrated oil circuit

Service life of plunger, barrel, retraction valve, nozzle body and needle could not be a long one when neat methanol used. Therefore in any way, some lubricant to methanol must be added. It is to be mentioned, the higher pressure in the pump the better lube property of the liquid. Sulphurous components exhibit a good lube property when stable mixed without separation.

"Estimation of Wiebe's Heat-Release Parameter"

(Bulaty - Glanzmann, MTZ 86 (1984) 7/8)

Elaborated by:

Černej Anton

Filipović Ivan

Gebert Krešimir

Maribor, september 1984.

Based on kinetic, Wiebe law of combustion enables, when proper matched, the accomodation of law of heat release to the various conditions in engine operation. Thus, Woschni showed the re-calculation of Wiebe parameters $(m, \Delta\varphi_v)$ from one to another conditions.

$$\frac{dQ_B}{d\varphi} = \frac{Q_B}{\Delta\varphi_v} a (m+1) \gamma^m e^{-a\gamma^{m+1}} \dots (1)$$

$$\gamma = \frac{\varphi - \varphi_{VA}}{\Delta\varphi_v}$$

where:

Q_B - integrated input heat

$\Delta\varphi_v$ - period of combustion

a - const (for 99,9 % of combustion $a=6,905$)

m - shape parameter

γ - relative instanteneous period of combustion

φ_{VA} - beginning of combustion

However, problem appears to define Wiebe-equivalent law of combustion when usual test bench results on desposal without in-cylinder pressure diagrams. We used "trial and error" method as time consuming and unaccurate one. Here is one basic method described to estimate Wiebe's heat-release parameters by means of systematic cycle calculations (Thomas Eulaty and Walter Glanzmann).

Basic methode

Experimental data:

- b_e - fuel consumption
- $P_{z,max}$ - peak in-cylinder pressure
- P_{me} - mean eff. pressure

have to be reproduced by systematic cycle calculation as accurate as possible.

In some examples by cycle calculations low pressure events (LW - gas exchange process) remain unchanged. Thus, high

pressure part of working cycle (HD) may be independently calculated supposing the connection points of the both parts (HD and LW) known (Fig 1). The connection points may be approximately defined as shown in Fig 1, point ac and ex. The end points of HD part of cycle in BTC (UTP) are connected by line of isentropic change of state with ac and ex.

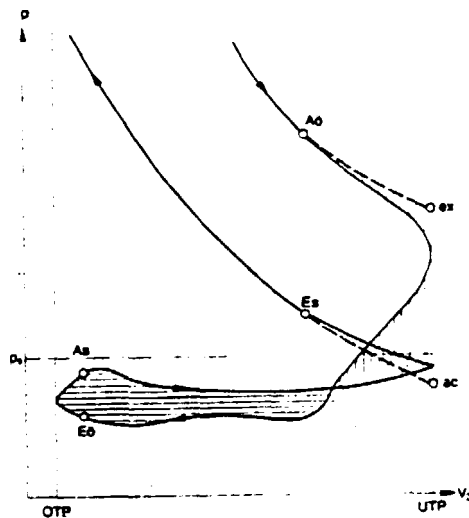


Fig 1 Connection of gas exchange process to high pressure part of working cycle of four stroke engine

p_s - scavenging pressure

A0 - exhaust opens

As - exhaust closes

E0 - intake opens

Es - intake closes

ex - end of expansion

ac - start of compression

Solid line: real pressure curve

broken line: isentropic change of state

State in point ac depends on:

- state in scavenging receiver (p_s, T_s)

- typ of engine

- valve timing

When no LW calculation performed p_{ac} and T_{ac} may be estimated approximately as follows:

$$\left. \begin{aligned} p_{ac} &= (0,96 \div 0,985) p_s \\ T_{ac} &= 0,833 \cdot T_s + 86 \end{aligned} \right\} \dots (2)$$

Thus, for calculation of HD part of working cycle we have on desposal:

- starting point or ac introduced by fuel
- upper limit of calculation given by peak in-cylinder pressure.

The area of in-cylinder pressure diagram of the working part of cycle (HD, Fig 1) without gas exchange process (p_{iOLW}) may be estimated by means of:

- mean eff. pressure (measured) p_{me}
- supposed friction of engine p_{mr}
- gas exchange δ_{piLW} acc. to Eq 3.

$$p_{mi} = p_{iOLW} + \delta_{piLW} = p_{me} + p_{mr} \dots (3)$$

Now, with one reasonable value of start of combustion chosen (γ_{vA}) (per example $\gamma_{vA} = 714$ °CA with middle speed four stroke engine) systematic calculations may be performed, acc. to Eq 1. For three periods of combustion chosen ($\Delta\gamma_{vA,B,C}$) at $\gamma_{vA} = \text{const}$ three shape parameters ($m_{A,B,C}$) are supposed. Thus, we have nine combinations on desposal and for every case $m, \Delta\gamma_v$ at $\gamma_{vA} = \text{const}$. HD diagram has to be calculated. The selection of shape parameter is explained in Fig 2a. Cross-sections A, B, C of each peak in-cylinder pressure curve and line $p_{z,max}$ soll given, correspond to the shape parameters $m_{A,B,C}$.

At the same time the mean pressures p_{iOLW} vs. shape parameters are presented in Fig 2b. Again, the points A, B, C are defined by means of shape parameters in Fig 2a. The line A-B-C in Fig 2b satisfies the condition. $p_{z,max}$ soll but only the point R satisfies the second condition also p_{iOLW} soll (given). Point R defines the shape parameter m_R demanded. Using Fig 2c the second Wiebe parameter $\Delta\gamma_{vR}$ may be defined.

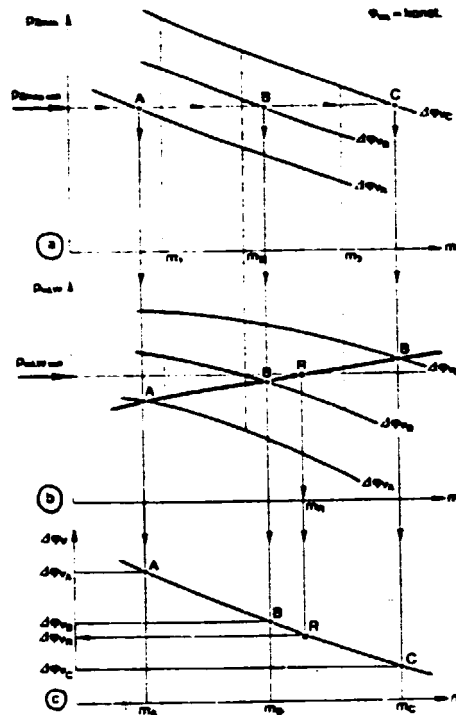


Fig 2 Graphical representation of basic method

Thus we have:

$$\varphi_{VA}, m_R \text{ and } \Delta\varphi_{VR}$$

under condition given:

- fuel consumption
- peak in-cylinder pressure ($p_{Z,max}$)
- mean pressure ($p_{iOLW \text{ soll}}$)
- start, point ac (Fig 1).

The corresponding combinations of $m, \Delta\varphi_v$ (see Fig 3 and Table 1) is possible to define for almost every start of combustion and typ of engine given.

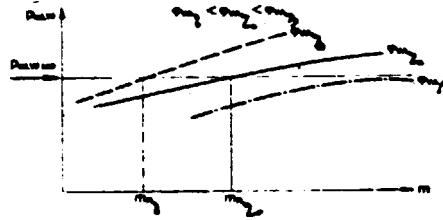


Fig 3 Dependence of m.e.p. on shape parameter at different timings of heat release

Table 1 Results of estimation of the heat-release parameters for different heat-release timing and parameter conversion along propeller operation line

P_e NW	n min ⁻¹	P_{30} bar	T_{30} K	Q_{30} KW	Q_{30} KW	m	P_{30} bar	P_{30} bar	P_{30} bar	T_{30} K	Q_0 kJ/AS	L_0
727.6 100%	430	3.385	340.3	710.95	82.11	1.108	24.612	126.927	11.557	1122.3	372.4	2.049
				714.34	80.66	0.901	24.828	126.880	11.557	1122.3	372.4	2.049
				717.02	80.11	0.736	24.630	126.846	11.559	1122.6	372.4	2.049
582.1 80%	399.2	2.753	336.5	710.99	80.58	0.690	20.990	115.091	9.402	1115.6	314.2	1.987
				714.34	79.18	0.728	20.977	113.886	9.421	1117.8	314.2	1.987
				716.99	78.61	0.594	20.944	112.782	9.438	1119.9	314.2	1.987
436.6 80%	362.7	2.102	337.1	711.19	79.67	0.660	17.168	99.313	7.321	112.99	257.2	1.863
				714.47	78.45	0.541	17.142	97.164	7.348	1134.0	257.2	1.863
				717.08	77.89	0.444	17.114	95.355	7.378	1136.7	257.2	1.863
291 40%	316.8	1.500	335.7	711.70	77.93	0.449	13.048	79.910	5.315	1141.4	198.0	1.733
				714.84	76.58	0.370	13.066	77.592	5.351	1149.2	198.0	1.733
				717.38	76.03	0.305	13.072	75.569	5.391	1157.7	198.0	1.733
145.5 20%	251.5	1.144	335.1	711.50	82.41	0.356	8.358	62.719	3.424	980.0	126.4	2.07
				714.58	81.33	0.294	8.363	60.486	3.447	975.4	126.4	2.07
				717.07	80.89	0.243	8.431	58.728	3.482	985.5	126.4	2.07

Concerning that gravity centre of combustion of every combination remains nearly unaffected, the shape parameter m increases with earlier start of combustion, see Fig.4

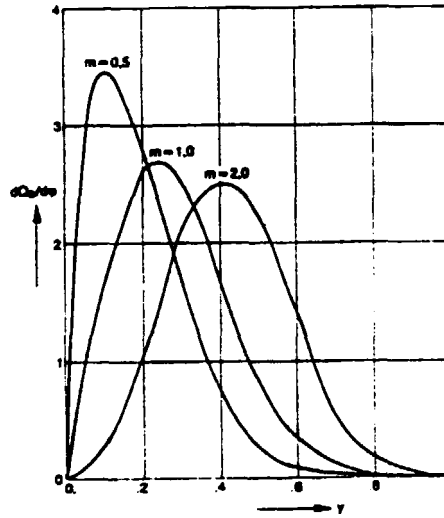


Fig 4 Different heat-release patterns depending on shape parameter \underline{m} (see Eq 1)

When start of combustion too early (per example ψ_{VA1} - Fig 3) desired mean eff. pressure can not be reached although extreme high value of \underline{m} may be applied.

